Baculovirus as a gene delivery and expression vector in mammalian cells

Elisabetta Locanto (2014)

Baculovirus as a gene delivery and expression vector in mammalian cells

Elisabetta Locanto

A thesis submitted in partial fulfilment of the requirements of Oxford Brookes University

for the degree of

Doctor of Philosophy

OXFORD BROOKES UNIVERSITY

July 2014

Abstract

The interior homeostasis of a solid organ, such as a kidney, is greatly altered during the surgical removal, storage and transplantation process from donor to recipient. Consequently, normal organ function may be delayed or prevented following transplantation. The main injury that organs have to withstand often occurs subsequent to the restoration of blood flow; this injury is known as ischaemia reperfusion-injury (I/R injury) and is associated with hypoxia, free radical formation and organ failure.

Viral gene therapy, such as BacMam gene transfer technology (Baculovirus-based expression in mammalian cells) is an attractive option for reducing I/R injury due to its high safety profile compared to mammalian viruses. However, limiting factors, including the requirement of high-doses of viral vector and low transgene expression levels are still a hurdle for the successful use of this technology. Therefore, the initial objectives of this study were to develop and validate a number of methods for concentrating BacMam along with the use of a number of chemical compounds to improve BacMam gene delivery in kidney cells. Amongst all the approaches screened, high-speed (for small volumes) and low-speed (for large volumes) centrifugation methods were the most effective for concentrating BacMam virus ($4x10^9$ and $1x10^{10}$ pfu/ml, respectively). Transduction of HEK cells was improved between two- to 10-fold in the presence of sodium butyrate or hydroxyurea alone and significantly improved *egfp* (enhanced green fluorescence protein) expression (~40-fold) when both chemicals were used in combination.

Subsequently, in the second part of this study an *in vitro* culture model was developed and evaluated for assessing ischaemic injury in kidney cells using antimycin A in combination with 2-deoxyglucose. It was shown that *sod-2* and *bcl-2* overexpression in injured kidney cells improved the effect of I/R injury by enhancing the recovery of ATP post-reperfusion

Furthermore, to examine the possibility of reducing injury associated with cold preservation, an *ex vivo* hypothermic perfusion system of porcine kidney was established and validated using reporter and protective genes. Importantly, for the first time, BacMam has been used to transfer *ex vivo* a protective gene (*sod-2*), into kidneys which appeared to provide protection against hypothermic preservation-associated injury by improving the recovery of cellular ATP.

Publications and Presentations

Publications

Hitchman RB, **Locanto E**, Possee RD, King LA., (2011). Optimizing the baculovirus expression vector system. Methods. Sep;55(1):52-7.

Hitchman RB, Murguía-Meca F, **Locanto E,** Danquah J, King LA., (2011). Baculovirus as vectors for human cells and applications in organ transplantation. J Invertebr Pathol. Jul;107 Suppl:S49-58.

Poster and oral presentation

Locanto, E., Hitchman, RB., King, LA., (2013). Methods for enhancing BacMam gene delivery into solid organs. Postgraduate Research student Symposium at Oxford Brookes University, Oxford, UK (poster).

Locanto, E., Hitchman, RB., King, LA., (2012). BacMam; a novel delivery vector for ischaemia. First International Meeting on Ischemia Reperfusion Injuries in Transplantation Poitiers, France (poster).

Locanto, E., Hitchman, RB., King, LA., (2012). BacMam a novel gene delivery vector for ischaemia. British Society for Gene Therapy annual conference –UCL Institute of Child Health, London, UK (poster).

Locanto, E., Hitchman, RB., King, LA., (2012). BacMam a novel gene delivery vector for ischaemia. Postgraduate Research student Symposium at Oxford Brookes University, Oxford, UK (oral presentation).

Locanto, E., Hitchman, RB., King, LA., (2011). Baculovirus as a gene delivery vector for ischaemia reperfusion injury. ESGCT and BSGT Collaborative Congress - Brighton, UK (poster).

Locanto, E., Hitchman, RB., King, LA., (2011). An ischaemia reperfusion injury model for baculovirus gene delivery : XLIV Annual Meeting of the Society for Invertebrate Pathology Halifax, Nova Scotia, Canada (poster).

Locanto, E., Hitchman, RB., King, LA., (2011).Human embryonic kidney cells as a model to improve baculovirus transduction London Cell Cycle Club –University College London (Invited speaker).

Acknowledgments

I would like to thank my supervisor Professor Linda A King for all her support and guidance during my PhD. I am very grateful for the opportunity she gave to me to develop my research and intellectual skills. Professor Robert Possee, thank you for all your advice and support, and for providing me reagents and viruses when I needed them. I would like to thank both Dr. John Runions and Dr. Sarah Irons for training and advice in immunofluorescence confocal microscopy and for always being there when I had a technical question or problem; Dr. Daniel Read (CEH) for training and helping me with the flow cytometer.

I would like also to thank all the members of the Insect Virus Research Group and Oxford Expression Technologies Ltd, past and present, for all your help and advice during the last four years. I am especially grateful to Farheen and Olga for all the fun we had and for always being there when I needed lab help or moral support.

Yet more invaluable contribution has come from my family, especially my parents; thank you for teaching me what hard work and dedication are and where those attributes will take you in life. A big thank you to my sister Anna, you were always there for me, no matter what. A special thanks to Christine Hitchman for giving me costant love and encouregment.

My most sincere thanks go to my Richard, for being very supportive throughout the past three years, for cheering me up whenever I was stressed or sad and for enduring all my negative emotions during frustrating moments. I couldn't have done this without your support. I am so lucky to have you by my side; "thank you Love". Finally, to my sweet potato Lucy and to my big boy, Joseph, I say a big thank you for all your love and patience during my writing up.

List of Figures

List of Tables

List of Abbreviations

ADP:	Adenosine diphosphate
AKI:	Acute kidney injury
AMP:	Adenosine monophosphate
ARF:	Acute renal failure
ATP:	Adenosine triphosphate
AVV:	Adeno-assocated virus
BAC:	Bacterial artificial chromosome
BCIP:	5-Bromo-4-Chloro-3'-Indolyphosphate p-Toluidine
Bcl-2:	β-cell lymphomas gene
BEVS:	Baculovirus expression vector system
BP:	Base pairs
BSA:	Bovine serum albumin
BV:	Budded virions
cDNA:	Complementary DNA
CHO:	Chinese hamster ovary
CMV:	Cytomegalovirus immediate early promoter
CO_2 :	Carbon dioxide
CRF:	Chronic renal failure
CT:	Computed tomography
Cyt c:	Cytochrome c
Cu/Zn:	Copper/zinc
CV:	Concentrated virus
Da:	Dalton
DAF:	Decay accelerating factor
DIP:	Defecting interfering particle
DMF:	Dimethylformimide
DMSO:	Dimethylsulphoxide
DNA:	Deoxyribonucleic acid
dNTP:	Deoxynucleotide triphosphate
Dpi:	Days post infection
E. coli:	*Escherichia coli*
EGFP:	Enhanced green fluorescent protein
FBS:	Foetal bovine serum
FP:	Few polyhedral
GP64:	Baculovirus glycoprotein 64 kDa
GSH-Px:	Glutathione peroxidise
GV:	Granulovirus
H_2O_2:	Hydrogen peroxide
HDACis:	Histone deacetylases inhibitors
H&E:	Hematoxylin and eosin staining
HEK293:	Human embryonic kidneys cells clone 293
HK-2:	Human kidney 2
HSPG:	Heparan sulfate proteoglycans
HIV:	Human immunodeficiency virus

Hpi: Hour post-infection
Hpp: Hour post perfusion
hpt: Hours post-transduction
I/R: Ischaemia/reperfusion
KSFM: Keratinocyte serum-free
IVRG: Insect Virus Research Group
LDH: Lactate dehydrogenase
LB: Luria Bertani broth
LLC-PK1: Porcine kidney cells
Mn: Manganese
MOI: Multiplicity of infection
mPTP: Mitochondrial permeability pore
MW: Molecular weight
NBT: Nitro Blue tetrazolium
NCBI: National Centre for Biotechnology Information
NICE: National Institute for Health and Care Excellence
NIH: National institute of health
$NO^{\bullet}$: Nitric oxide
NPV: Nucleopolyhedrovirus
NRK: Normal rat kidney cells
O_2: Oxygen
$O_2^{\bullet-}$: Superoxide anion
ODV: Occlusion derived virions
OH•: Hydroxyl radical
$ONOO^-$: Peroxynitrite
ORF: Open reading frame
OV: Original virus
PAS: Periodic acid-Schiff staining
PBS: Phosphate buffered saline
PCR: Polymerase chain reaction
Pfu: Plaque forming units
Polh: Polyhedrin gene
RAC: Recombinant DNA advisory committee
RLU: Relative luciferase units
RNS: Reactive nitrogen species
ROS: Reactive oxygen species
RSV: Rous sarcoma virus promoter
Rpm: Rotations per minute
SDS: Dodium dodecyl sulfate
SDS-PAGE: Sodium dodecyl sulfate polyacrylamide gel electrophoresis
Sf-9: *Spodoptera frugiperda*
Sf-21: IPLB-SF-21 cell line
siRNAs: Small interfering RNA
Sod: Superoxide dismutase gene
SOD-1/3: Copper/zinc superoxide dismutase
SOD-2: Manganese superoxide dismutase
TGF-$^{\beta}$1: Transforming growth factor-beta1
VP39: Baculovirus capsid protein 39 kDa

VSV-G:	Vesicular stomatitis virus-G protein
UW:	University of Wisconsin
UV:	Ultraviolet

"The road of life twists and turns and no two directions are ever the same. Yet our lessons come from the journey, not the destination."

Don Williams, Jr.

To the loves of my life

Richard, Joseph & Lucy

Table of Contents

Chapter 1

Introduction

1.1 Baculovirus

1.1.1 INTRODUCTION

Many invertebrate viruses are insect-specific pathogens which mainly infect arthropods in both terrestrial and marine ecosystems (Miller, 1997). Amongst these, members of the *Baculoviridae* have received the greatest attention. Baculoviruses are rod-shaped, enveloped, DNA viruses with a large circular and supercoiled genome which encodes for 100-200 predicted proteins (Miller, 1997). Members of this family contain a number of genes that are unique to individual baculovirus species as well as a group of genes conserved in all fifty-three baculoviruses sequenced to date (Oliveira *et al.,* 2013).

The baculovirus life cycle involves several sequential steps, including entry of the virus into the host, early and late gene expression, DNA replication, morphogenesis and the release of two distinct virion phenotypes (Miller, 1997). In an infected cell, the progeny egress from the nucleus and then bud through the cytoplasmic membrane where they acquire a lipid-containing envelope and membrane-bound glycoproteins before becoming mature budded virus (BV). In the very late phase of infection a second progeny is formed, the occlusion-derived virus (ODV); these nucleocapsids are retained in the nucleus to be enveloped and occluded in a paracrystalline matrix, polyhedrin, forming an occlusion body (OB).

Although baculoviruses exhibit a high degree of host specificity towards the order *Lepidoptera*, they are capable of infecting more than six hundred insect species from the orders *Hymenoptera, Diptera, Coleoptera* and *Trichoptera*, predominantly during the larval stages (Miller, 1997; Miller & Lu, 1997). Due to this narrow host range, they were initially studied as a biological control agent to regulate insect pest populations (Bonning & Hammock, 1992).

The discovery during the 1980s of a strong promoter, which drives the expression of one of the virus very late genes (*polyhedrin*, *polh*), led to the development of baculovirus as tool for biotechnological research (Miller, 1988). Recombinant baculovirus were constructed by placing a foreign gene under the control of the *polh* promoter and used to infect insect cells in culture to produce recombinant protein. This baculovirus expression vector system (BEVS) soon became extensively utilized by the biopharmaceutical industry (Gentilomi *et al.,* 2006; Wu *et al.,* 2012; Teng *et al.,* 2013). In particular, two baculovirus species have been used for foreign gene expression: *Autographa california* multicapsid nucleuopolyhedrovirus (AcMNPV) and to a lesser extent *Bombyx mori* NPV (BmNPV).

1.1.2 BACULOVIRUS TAXONOMY

Originally baculoviruses were classified based on OB morphology into two genera (Figure 1.1): nucleopolyhedroviruses (NPVs) and granuloviruses (GV; reviewed by Blissard and Rohrmann, 1990). Members of the genus NPV have been isolated from the order *Lepidoptera*, *Hymenoptera* and *Diptera*; they produce a large OB between 0.15 to 15 µm occluding many ODV in a polyhedrin matrix. Whereas, GVs were isolated only from *Lepidoptera* and show small OBs, 0.13 to 0.50 µm, containing a single virion enclosed in granulin (Rohrmann, 1992). However, the two crystalline protein matrix structures have the same function, protecting the embedded ODV outside of the host *e.g.,* against UV light and desiccation (reviewed by Blissard & Rohrmann, 1990).

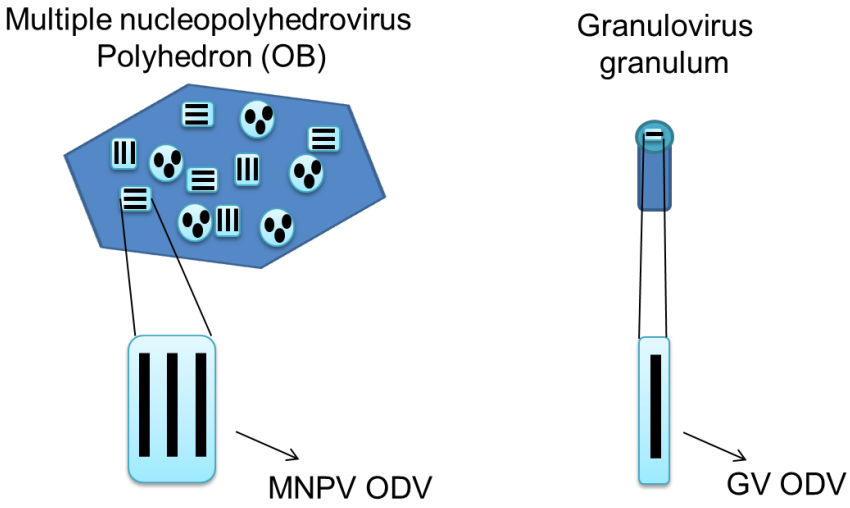

Figure 1.1. Schematic representation of baculovirus OBs. MNPV polyhedral section and ODVs (left) and GV granulum and ODV (right).

In 2004, the increasing number of sequenced baculovirus genomes and the development of sophisticated phylogenetic analysis models led to a different classification and nomenclature for the *baculoviridae* family (Jehel *et al.,* 2006). The current classification system is based on phylogenetic, biological and morphological characteristics and comprises four genera: *Alphabaculovirus, Betabaculovirus, Gammabaculovirus* and *Deltabaculovirus* (Figure 1.2; Jehel *et al.,* 2006). *Alphabaculovirus and Betabaculovirus* include lepidopteran-specific NPV and GVs, respectively, (Jehle *et al*., 2006). Furthermore, the *Alphabaculovirus* can be separated into two subgroups I and II depending on the type of envelope protein incorporated in the BV (Jehle *et al.,* 2006). The envelope fusion protein used by the group I baculoviruses is GP64 and a furin-cleaved (F) protein is utilized by the group II baculoviruses (Herniou & Jehle, 2007).

Gammabaculovirus comprise the hymenopteran-specific NPVs, whose genomes are typically smaller and do not contain genes coding for envelope proteins suggesting that BV may not be produced (Jehle *et al*., 2006). Finally, the *Deltabaculovirus* include the diptera-specific baculoviruses whose OB protein shows no homology to polyhedrin or granulin proteins (Jehle *et al*., 2006).

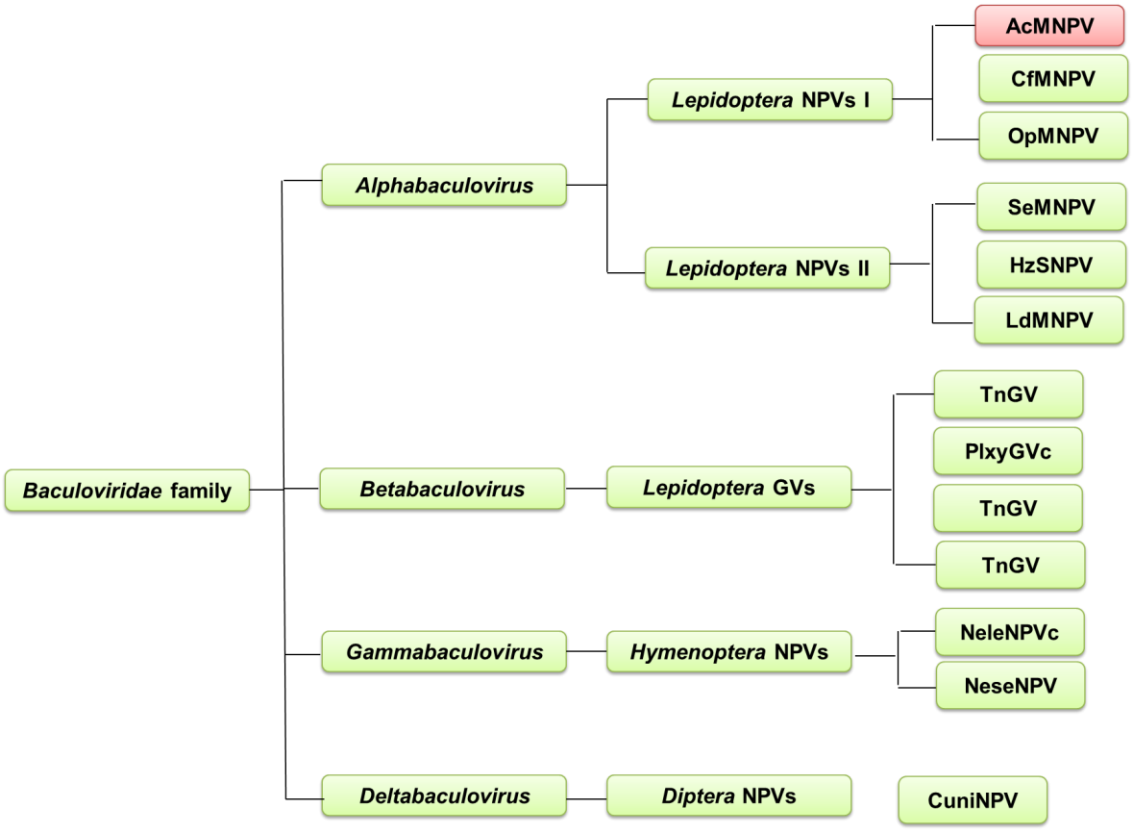

Figure 1.2. Baculovirus phylogeny. Baculovirus evolutionary tree based on the amino acid alignment of 29 baculovirus core genes. The family *Baculoviridae* consists of 4 major genera: *Alphabaculovirus*, *Betabaculovirus*, *Gammabaculovirus*, and *Deltabaculovirus.* Only subsets of characterized species within each group are shown. Figure modified from Au *et al.* (2013).

1.1.3 BACULOVIRUS REPLICATION CYCLE: FROM INSECT HOST TO CELL CULTURE

The most studied baculovirus is AcMNPV, isolated in 1971 from the Alfalfa looper (Vail *et al.,* 1971). It was the first baculovirus to be sequenced and was found to be 134 kbp with 154 predicted open reading frames (ORFs; Ayres *et al.,* 1994). AcMNPV belongs to the *Alphabaculovirus* genus (section 1.1.2) and has been shown to be able to infect at least forty species within the order Lepidoptera (reviewed by Bonning, 2005). The virus used for the experiments in this thesis was derived from AcMNPV strain C6 (Ayres *et al.,* 1994) and the following sections describe this virus.

AcMNPV utilizes a biphasic life cycle which is characterized by the production of two distinct forms of viral progeny, BV and ODV, which are subsequently occluded to form OBs (Figure 1.3; Blissard & Rohrmann, 1990). The roles of these two phenotypes, produced at different locations in the cell and at different times, differ significantly. BVs are produced in the late phase of infection and acquire their envelopes by budding through the host plasma membrane. They are responsible for spread of the infection cell-to-cell within the host or when the virus is amplified in cell culture. In contrast, ODVs are produced in the host cell nucleus, in the very late phase of infection and are enveloped in an occlusion matrix protein, polyhedrin, forming the OBs. ODVs mediate secondary infection and are also responsible for horizontal transmission between insect hosts (reviewed by Rohrmann, 2008).

BVs are composed of a single nucleocapsid enclosed by an envelope membrane containing a glycoprotein at one end, GP64 (Figure 1.3 A). GP64 exists as a disulphide-linked trimer of which each protein contains a signal peptide at the N-terminal and an anchor domain at the C-terminal. GP64 is essentially required for efficient viral budding and cell-to-cell transmission (Oomens & Blissard, 1999). In contrast to BV, the ODV envelope is more complex with five or more envelope proteins (Figure 1.3 B). Examples include ODV-E66, ODV-E25, ODV-E18 and several *per os* infectivity (PIF) proteins such as P74, localised on the outside of the ODV membrane. P74 was identified to play a crucial role in ODV entry into cells and may be involved in the fusion process (Faulkner *et al.* 1997).

Despite the difference in lipid and protein components of their envelope membranes, BV and ODV share similar capsid compositions (Figure 1.3; reviewed by Funk *et al.,* 1997). The major capsid proteins are represented by VP39 which is randomly distributed over the surface (Russell *et al.,* 1991), P80 (Lu & Carstens, 1992), P24 and the essential structural protein ORF1629, located downstream from the polyhedrin gene (reviewed by Funk *et al.,* 1997). However, ODV-EC27 has been found in ODV but not in BV capsids (reviewed by Funk *et al.,* 1997). This protein has a distinct functional characteristic; it acts as a multifunctional cyclin regulating the host cell cycle during baculovirus infection (Belyavskyi *et al.,* 1998).

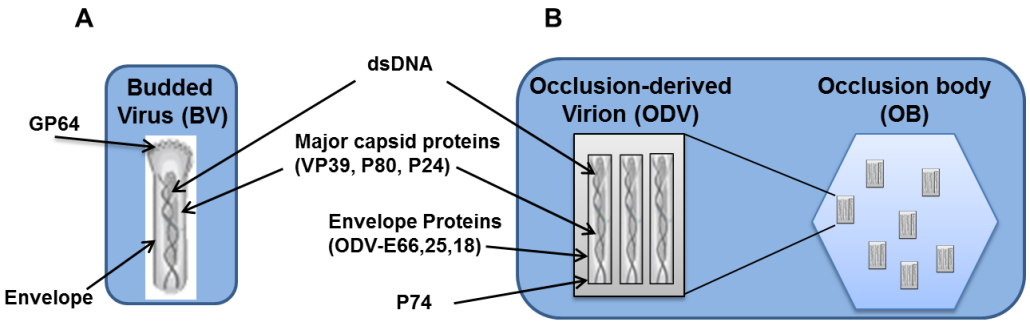

Figure 1.3. Schematic representation of the two baculovirus phenotypes and their structural proteins. (**A**) Budded virus (BV) and (**B**) occlusion-derived virions (ODV) occluded in the occlusion body (OB).

I. Early and late stages of larval infection

In the natural environment baculoviruses are found as OBs on plant surfaces and in the soil (reviewed by Rodriguez *et al.,* 2012). The infection begins when an insect larva ingests food contaminated with OBs (Figure 1.4; Keddie *et al.,* 1989). Upon ingestion, the high alkaline conditions in the midgut of the host cause dissolution of the OBs and the released ODV penetrate the midgut peritrophic membrane at the apical ends of the microvilli (Federici, 1997). The infection progresses with the ODVs entering the midgut epithelial cells, by clathrin-mediated adsorptive endocytosis (Long *et al.,* 2006). In the cytoplasm, the virions are quickly unpackaged and from here nucleocapsids can have one of two destinations (Figure 1.4). Virions either exit immediately from the columnar epithelial cells into the haemolymph initiating a systemic infection within the host (Washburn *et al.,* 2003) or are transported into the nucleus where viral transcription and replication occur immediately after the viral DNA is uncoated (reviewed by Rohrmann, 2008). In the nucleus, the early viral genes are transcribed by host RNA polymerase II (Fuchs *et al.,* 1983). The resulting early proteins are essential for regulation of early transcription, viral DNA replication and inhibition of apoptosis, a defence mechanism activated by the infected host. Immediate-early (*ie*) genes such as *ie-0*, *ie-1*, *ie-2* and *pe-38* are the first to be expressed and their promoters can drive transcription in non-infected insect cells (reviewed by Prikhod'ko, 1999). In particular, the principal trans-regulator of baculovirus gene expression is *ie-1*, expressed in both early and late phases of infection. IE-1 is a multifunctional transcriptional regulatory protein, trans-activating a number of delayed-early genes and a small number of late genes such as the late capsid protein gene (*vp39*) and the very late *polh* gene (Guarino & Smith, 1990; Passarelli *et al.,* 1993).

The replicated DNA is then packaged to form new progeny capsids. The nucleocapsids bud first through the nuclear membrane and then through the cell membrane where they

obtain a lipid envelope containing the glycoprotein GP64. The BVs are then ready to propagate the infection from the midgut, through tracheal cells, to almost all of the larval tissues via the haemolymph, referred to as the secondary infection (Federici, 1997; Volkman, 1997).

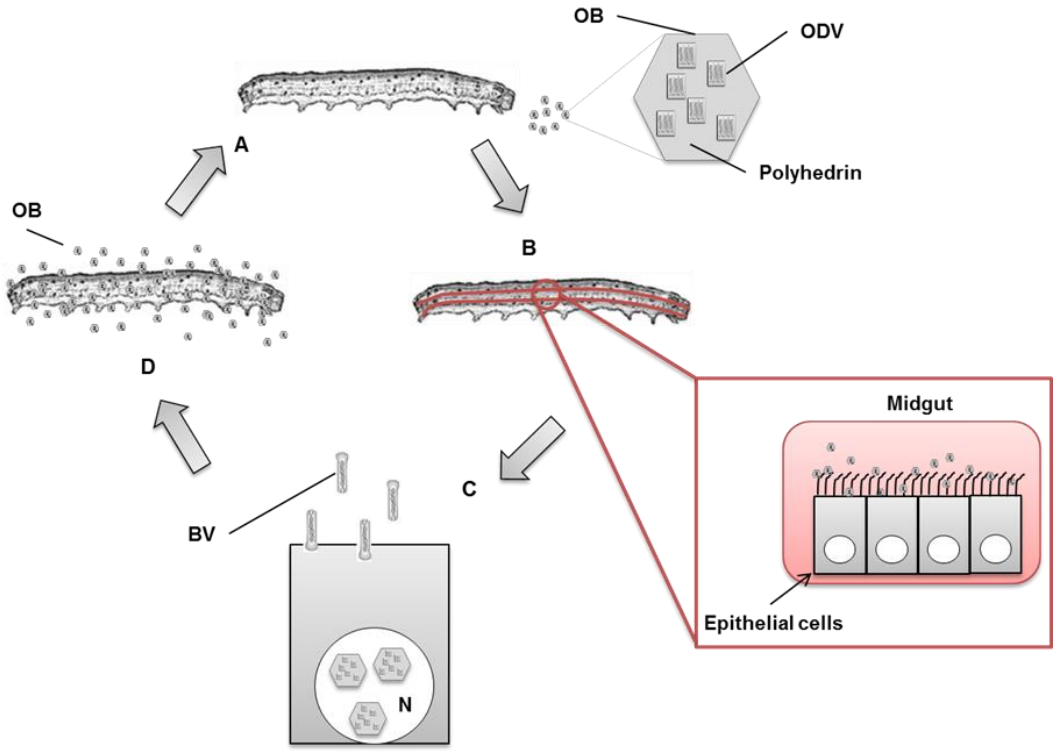

Figure 1.4. Baculovirus life cycle *in vivo*. (**A**) Infection is initiated by the ingestion of a virus occlusion body (OB). (**B**) The OB is dissolved and occlusion-derived virions (ODV) are released initiating the primary infection in the midgut epithelial cells. (**C**) From the cell cytoplasm nucleocapsids are transported to the nucleus where viral transcription and replication begin. Two virus phenotypes are produced, budded virus (BV) and ODV occluded inside a polyhedrin matrix. (D) Late stages of virus infection trigger liquefaction of the host and release OBs into the environment.

From approximately 24 hours post-infection (hpi), BV production declines and there is a shift to ODV/OB formation. ODV are produced when nucleocapsids become enveloped with viral-induced membranes in the intranuclear ring zone of the nucleus, referred to as the peristromal space (Summers & Volkman, 1976). In the nucleus, the enveloped ODVs are occluded inside the proteinaceous matrix polyhedrin to form polyhedra. Each polyhedron is further covered by an envelope or calyx, which is predominantly formed from carbohydrates and a phosphoprotein, PP34 (Whitt & Manning, 1988; Gombart *et al.,* 1989).

In the very late stages of infection, OBs begin to be accumulated into tissues causing enlargement, weakening the basal lamina of the infected insect. The infected insect

eventually dies and liquefies within 5-10 days and the accumulated OBs are released into the environment where they can be ingested by more larvae (Blissard & Rohrmann, 1990). The terminal liquefaction is accomplished by the coordinated activity of two late-expressed virus genes, *chiA* (chitinase) and *v-cath* (cathepsin) (reviewed by Volkman, 1997).

II. Baculovirus replication in cell culture

The *in vivo* and *in vitro* life cycles of baculovirus are very similar to each other. However, cultured insect cells need to be directly infected with BVs (Figure 1.5) because the ODV are approximately a thousand times less infectious (Lynn, 2003).

The host insect cell lines most commonly used for AcMNPV studies are those derived from *Spodoptera frugiperda* IPLB-Sf21-AE (Sf21), *S. frugiperda* (Sf-9) and *Trichoplusia ni* BTI-Tn-5B1-4 (Tn-5). Sf21 cells were isolated from *S. frugiperda* pupal ovarian tissue (Vaughn *et al.,* 1977) and the Sf9 cell line is a clonal isolate of the Sf21 cells. The Tn-5 cells were derived from the cabbage looper *Trichoplusia ni* (McIntoh & Ignoffo, 1989; Granados *et al.,* 1994; Patterson *et al.,* 1995).

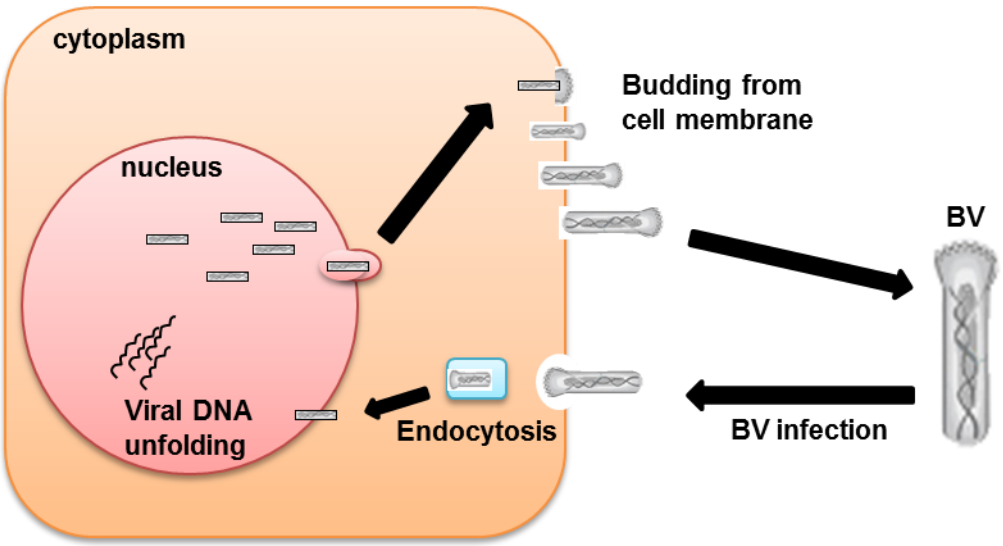

Figure 1.5. Baculovirus *in vitro* replication. For insect cells growing in culture, infection begins when BV enter by endocytosis. The nucleocapsid is then transported into the nucleus where new progeny BVs are produced. BVs bud through the cell membrane to infect adjacent cells. BV: budded virus.

In cell culture, infection begins when at least one virus particle has entered the cell and has successfully started its replication cycle. The first step of BV infection is to bind to the

cell surface of the target cells, a process mediated by the envelope glycoprotein GP64 (Okano *et al.,* 2006). Subsequently, following attachment, the virus enters the target cells via clathrin-mediated adsorptive endocytosis (Long *et al.,* 2006). Endocytosis is rapidly followed by multistep processes which include vesicular transport, endosomal escape, intracytosol transport of the nucleocapsids to the nucleus, nuclear entry and capsid disassembly (Charlton & Volkman, 1993; Plonsky *et al.,* 1999). Inside the nucleus, the baculovirus genome uncoats and viral gene expression initiates. These sequences of events ultimately lead to the production of new progeny BVs (see section 1.1.3-I).

Different parameters are important for a successful baculovirus infection in cell culture. These include (1) the ratio between BV and cell number, referred to as multiplicity of infection (MOI; Licari & Bailey, 1991). High MOI results in a synchronous infection, where BVs simultaneously infect all the cells in the culture; low MOI leads to asynchronous infection which is characterized by different cell populations, comprising both infected and healthy cells; (2) cell cycle phase. Generally, BV infection of insect cells causes cell cycle arrest in the G2/M phase (reviewed by Monteiro *et al.,* 2012).

Lynn and Hink (1978) showed that infecting cells at either G1 or S phase resulted in a higher percentage of cells infected than cultures infected at the G2 phase. Later, Kioukia and colleagues suggested that baculovirus infection of Sf9 cells is very efficient in S phase (Kioukia *et al.,* 1995). This was also confirmed by Saito *et al.* (2002) who showed an increased infection yield in cells at G1/S phase compared to cells infected at G2/M phases; (3) serial passage of baculovirus in cell culture, which can cause the development of a mutant form of virus (Cheng *et al.,* 2013).

In general, this mutant form is associated with the production of few polyhedra (FP) within the nucleus. The FP phenotype produces hypertrophied nuclei and larger plaques. It has been reported that the development of this phenotype is correlated to mutations in the *fp25k* gene (Fraser *et al.,* 1983; Carstens, 1987). In addition to the formation of this baculovirus phenotype in cells, *fp25k* mutations lead to higher titres of BV in the cell culture medium, offering a selective advantage over the normal BV phenotype (Fraser *et al.,* 1995; Cheng *et al.,* 2013).

1.1.4 BACULOVIRUS EXPRESSION VECTOR SYSTEM (BEVS)

The first successful use of BEVS dates back to 1983 when Smith and colleagues used AcMNPV strain C6 as an expression vector to produce human β-interferon in insect cells

(Smith *et al.,* 1983). During the last thirty years, BEVS has been developed into one of the most effective methods for expression of recombinant protein in insect cells (reviewed by Hitchman *et al.,* 2011; reviewed by Li *et al.,* 2012). Furthermore, BEVS has been successfully employed in surface display, gene therapy and vaccine production (reviewed by Sokolenko *et al.,* 2012; Kawahara & Takaku, 2013; Yeh *et al.,* 2014).

I. Development of the BEVS

Originally, many time-consuming and technically difficult steps such as the identification of a recombinant baculovirus and its subsequent isolation by plaque purification were required. Brief overviews of the main studies that have contributed to the evolution of a system are summarized in Table 1.1.

The *flash*BAC system was used in this project and is described in more detail. *Flash*BAC was based on BacPAK6 vector, however, it lacks *chiA*, part of the essential gene *orf1629* and the *polh* coding region, which were replaced by a BAC replicon (reviewed by Hitchman *et al.,* 2011). The essential gene deletion precludes virus replication within insect cells while the BAC replicon allows the viral DNA to be maintained and propagated in bacterial cells. A recombinant baculovirus is produced by co-transfecting insect cells with circular *flash*BAC DNA (there is no need to linearize the virus) and a transfer plasmid containing the foreign gene of interest. Homologous recombination in insect cells restores the function of the essential gene, allowing the virus DNA to replicate and at the same time inserting the foreign gene of interest under the control of the *polh* promoter replacing the BAC sequence. As it is not possible for parental virus to replicate there is no requirement for a selection system.

Table 1.1. Overview of BEVS major improvements

Year	Discoveries	Reference
1980	Development of a chemically-defined media for the growth of insect cell lines *S. frugiperda*	Wilkie *et al.,* 1980
1990	A substantial improvement was achieved when insect cells were co-transfected with linear baculovirus DNA for recombination with a transfer plasmid containing the recombinant gene .	Kitts *et al.,* 1990
1991	Generation of defective interfering particles (DIPs) of AcMNPV in bioreactors helped to better understand the genetic alteration of baculovirus during continuous passaging in insect cells.	Kool *et al.,* 1991
1992	The discovery of repeated replication origins distributed in the AcMNPV genome led to enhance virus replication efficiency.	Pearson *et al.,* 1992
1993	The BEVS system was further enhanced by introducing a restriction enzyme site, *Bsu361*, which deleted *polh* and inactivated the essential *orf 1629*. *Orf 1629*, was then restored, following recombination with a transfer plasmid, with the gene of interest, producing nearly 100% recombinant virus. This system is now commercially available as BacPAK™ (Clonthech), BaculoGold™ (BD Bioscience). A bacterial artificial chromosome (BAC) was inserted into the AcMNPV genome which allowed recombinant virus DNA to be produced and maintained in bacterial cells . This system is currently marketed as Bac-to-Bac™ (Invitrogen).	Kitts and Possee , 1993 Reviewed by Hitchman *et al.,* 2011; Luckow *et al.*, 1993
1998-2013	A number of BEVS have been developed and are commercialised under the name of: BacVector-3000 (Novagen); ProEasy™ and ProFold™-C1 (AB vector); MultiBac, licensed to Redbiotech AG (Switzerland); *Flash*BAC™ (Oxford Expression Technologies Ltd).	Suzuki *et al.,* 1998. US Pat. No.5753220 Belyaev , 2007. US Pat. No.7226781. Berger *et al.,* 2004; Barford *et al.,* 2013 Possee and King, 2008. US Pat. No.7413732)

This one-step technology makes *flash*BAC very amenable to high throughput robotics, allowing production of multiple viruses and expression screening in multi-well plate format. *flash*BAC™ has been further modified by the deletion of *v-cath* to produce *flash*BACGOLD™. This has improved the efficacy of the secretory pathway and enhanced the yield of secreted or membrane targeted proteins (reviewed by Hitchman *et al.,* 2011). The development of *flash*BACULTRA™ has taken the technology a step further by the deletion of three more genes, *p10*, *p74* and *p26* from the viral genome, further increasing protein yield and stability (Hitchman *et al.,* 2010).

II. BEVS *vs.* other recombinant protein expression systems

BEVS offers several advantages compared to bacteria, yeast and mammalian expression systems, these are summarised in Table 1.2.

Table 1.2. Advantages of BEVS compared to other gene delivery systems.

Advantages	Reference
Biosafety. Baculovirus are considered safe since they are unable to replicate in mammals and plants .	Volkman & Goldsmith, 1983; Chen *et al.,* 2011
High yields of recombinant protein . High transgene production enabled by strong very late gene promoters, *polh* and *p10*, which are highly transcribed during the very late phase of infection but not essential for the baculovirus life cycle in cell culture.	Smith *et al.,* 1995 Palomares *et al.,* (2006)
Easy to scale up. Insect cells are relatively simple to maintain in suspension culture compared to mammalian cell lines and they can be easily grown in bioreactors.	Elias *et al.,* 2000; Weber *et al.,* 2002
Capable of large DNA insertions, of up to thirty-eight kilobase (kb) .	Cheshenko *et al.,* 2001
Complex co- and post-translational modifications, insect cells are able to perform *i.e.* proteolytic processing, O- or N-linked glycosylation, phosphorylation, signal peptide cleavage, acylation and amidation all necessary for the production of functional proteins of eukaryotic origin.	Gout *et al.,* 1992; Altmann *et al.,* 1999; Hassan *et al.,* 2009; Geisler & Jarvis, 2010

Recently, due to the differences between mammalian and insect protein glycosylation patterns, concern over the use of BEVS for the production of recombinant therapeutic glycoproteins has been raised (reviewed by Geisler & Jarvis, 2010).

Mammalian cells produce complex N-glycans containing terminal sialic acids while, insect cells generally produce simpler N-glycans with terminal mannose residues (Figure 1.6).

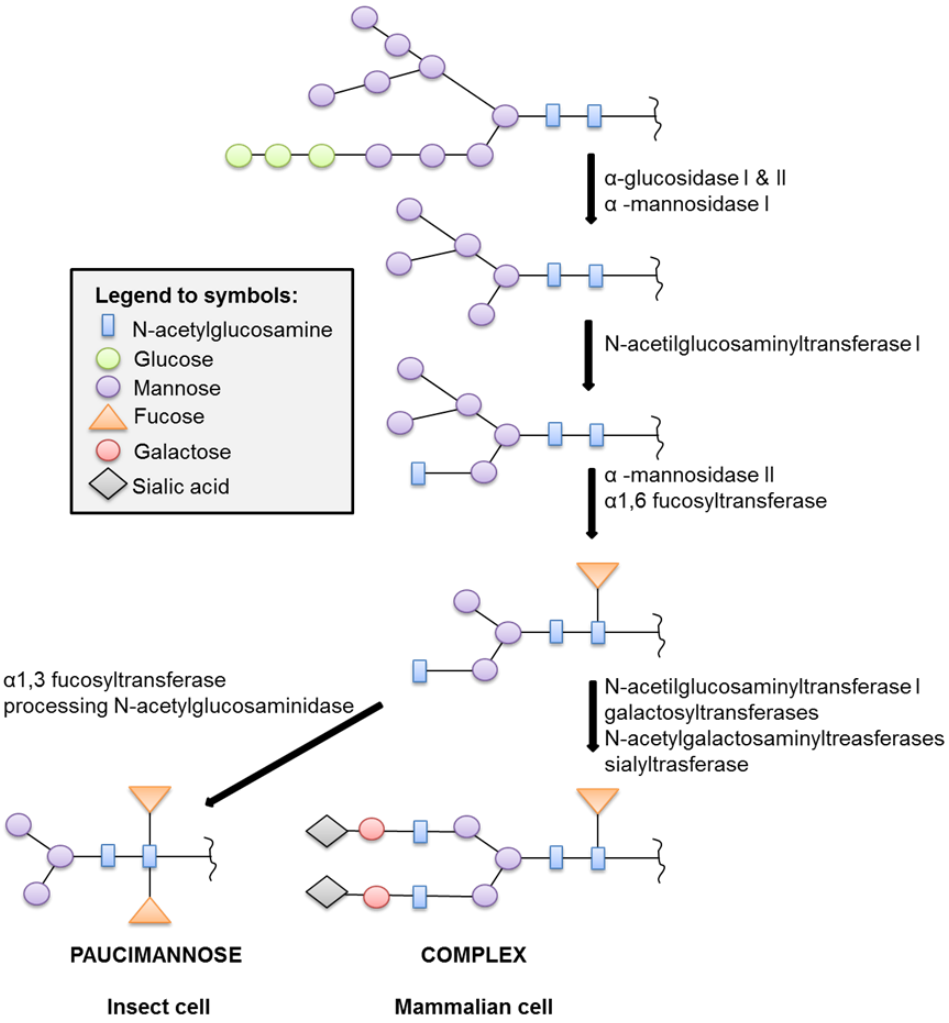

Figure 1.6. N-glycosylation pathways, mammalian cells *vs* insect cells. The N-glycosylation pathway of a new protein begins with the binding of a preassembled glycan. Generally this is followed by a number of reactions that produces a common intermediate. In insect cells this intermediate is further trimmed to paucimannose, while in mammalian cells it is elongated to produce complex N-glycans. Symbolic representations are shown in the legend. Modified from Geisler & Jarvis (2009).

This structural difference can potentially induce allergenic reactions in humans, compromising the biomedical importance of recombinant glycoproteins produced using this system (Harrison & Jarvis, 2006). Reports have detailed that either the lack of terminal sialic acids or the presence of core α1,3-linked fucose residues on glycoproteins produced by BEVS negatively impacts their pharmacokinetic behaviour and limits their safety and therapeutic application (reviewed by Hillar & Jarvis, 2010).

In contrast, a different study suggested that the presence of mannose residues on recombinant glycoprotein vaccines, produced using BEVS, positively impacted their efficacy by modulating the mammalian immune system (Hervas-Stubbs *et al.,* 2007).

III. BEVS for pharmaceutical production

The BEVS technology has been used for the production of pharmaceutical proteins and vaccines. Five different vaccines for human and veterinary use are commercially available and many others are progressing to clinical trials, these are summarized in Table 1.3 (reviewed by Cox, 2012).

Table 1.3. Baculovirus based vaccines.

Vaccine	Description
Porsilis® Pesti (Intervet, Netherlands)	This is the first baculovirus-based animal vaccine for classical Swine Fever and received European market approval in 2000.
Porcine circovirus 2 (Merck & B. Ingelheim)	Vaccines PCV2 was approved for commercial use in 2007
Cervarix® (GSK, Rixensart, Belgium)	This bivalent human papillomavirus virus-like particle (VLP) vaccine (against cervical cancer) Was the first human vaccine produced using baculovirus in insect cells. It was approved by the European Medicines Agency in September 2007 and the United States Food and Drug Administration (FDA) in October 2009.
Provenge® (DENDREON Corp.)	Provenge® vaccine is produced by exposing patient's white blood cells to the prostate surface antigen (PSA) protein which is produced using BEVS technology. It was approved by the FDA in 2010.
Diamyd® (Diamyd MedicalAB, Sweden)	A therapeutic vaccine for the treatment of type-I diabetes mellitus, currently in phase III trials (2012).
FluBlok® (Protein Sciences Corp. USA)	FluBlok® is formed of three full-length of recombinant haemagglutinin proteins against seasonal flu. Recently completed phase III of clinical studies and received approval by the FDA in January 2013.

1.2 Gene Therapy

1.2.1 GENERAL OVERVIEW

In the last two decades, rapid progress in biotechnology has driven gene therapy to the forefront of medical research. Gene therapy (the use of genes as medicines) comprises a broad approach for the treatment of pathological conditions caused by a single recessive gene, acquired genetic diseases and viral infections (reviewed by Misra, 2013). Generally, there are two types of gene therapy, germ line and somatic. In germ line therapy, the germ cells are modified by the introduction of a therapeutic gene which is integrated into the genome; therefore, any changes due to the therapy will be passed to the next generation (Matthews & Curiel, 2007). In contrast, somatic gene therapy is when the gene is inserted into target cells and any modifications are restricted to the patient being treated, *e.g.* they are not inherited by the next generation (Bank, 1996). The difference between these two approaches is important since to date only gene therapy on somatic cells has been allowed due to ethical reasons (reviewed by Wirth *et al.,* 2013).

Both viral and non-viral vectors have been used for gene therapy. However, there are still many limitations with these vectors and their safe use is still a major concern. Some of these issues include lack of tissue specificity, their inability to cross transport barriers and rapid clearance after systemic circulation in targeted tissues (Bone, 2007). Another major limitation of using delivery vectors is the activation of the host immune response which inhibits the effect of the delivered therapeutic protein (reviewed by Giacca & Zacchigna, 2012). For these, and other reasons, much effort is now being put into the development of safer and more efficient vectors.

1.2.2 HISTORICAL PERSPECTIVES – FROM FIRST STEPS TO CURRENT STATUS

The milestones during the history of gene therapy are shown schematically in Figure 1.7. The foundations for gene therapy were first laid by Griffith's in 1928; he observed a non-virulent pneumococcal bacteria type transforming into a virulent type by mixing living non-virulent bacteria with heat-inactivated virulent bacteria. These findings were subsequently confirmed by McCarty and colleagues which demonstrated that deoxyribonucleic acid (DNA) triggered this transformation (Avery *et al.,* 1944). Few years later, in 1952 Lederberg and Zinder discovered that certain bacteria can transfer genetic material by mating and also described the acquired resistance to the same antibiotic (reviewed by Wirth *et al.,* 2013).

From there, DNA became a topic of great research interest and many important findings and in 1953 first Wilkins and Franklin then Watson and Crick developed the helix structure model of double stranded DNA. This discovery allowed the isolation of genes from DNA which escalated the knowledge of the molecular and genetic basis of human disease.

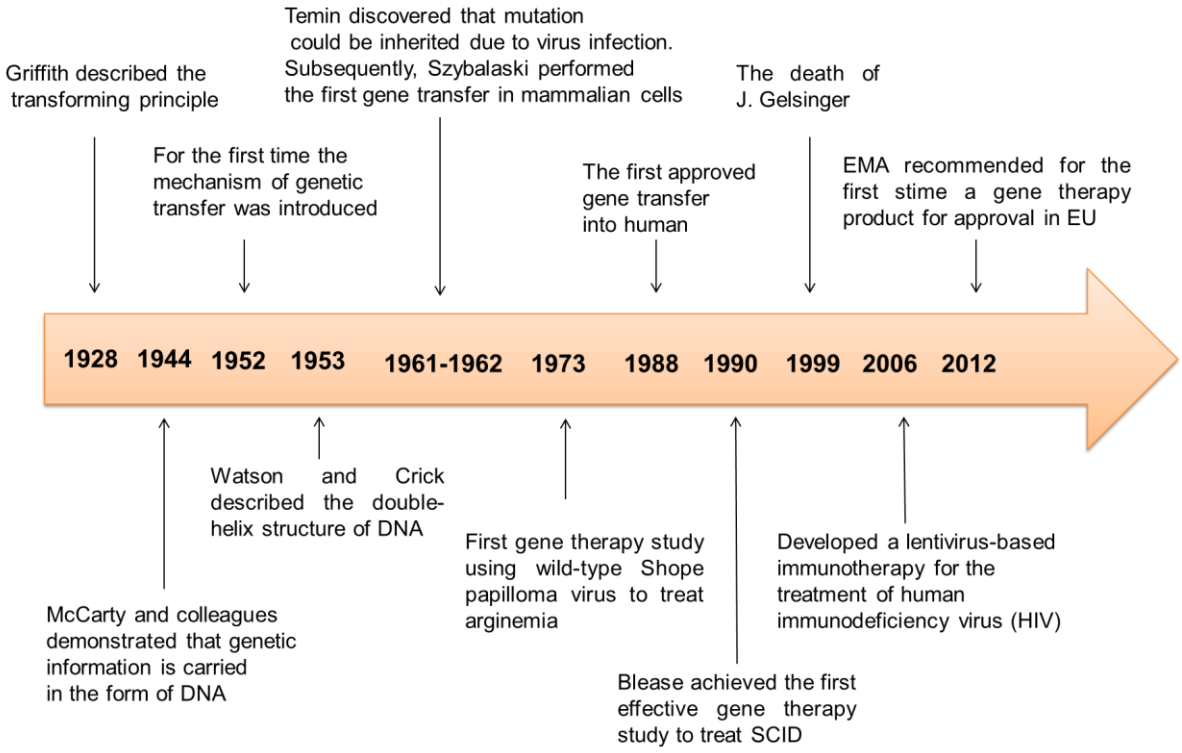

Figure 1.7. Timeline highlighting some of the main milestones in the gene therapy history. Modified from Wirth *et al.* (2013).

Temin observed that chicken cells infected with the Rous sarcoma virus inherited mutations of viral specific genes (Temin, 1961). Motivated by this finding, Rogers and Pfuderer in 1973 performed the first human gene therapy trial on two sisters suffering from arginemia (a urea cycle disorder). In this trial the wild-type Shope papilloma virus was injected into the sisters with the intention of delivering the arginase gene. However, the therapy was unsuccessful as their arginine levels remained unchanged (Rogers *et al.,* 1973). In 1988, the US Recombinant DNA Advisory Committee (RAC) officially approved the introduction of foreign genes into humans in the form of naked-DNA. Rosenberg and co-workers traced the movements of tumour-infiltrating blood cells confirming that tumours do not grow at the injection site (Rosenberg *et al.,* 1990; and 1993).

Furthermore, Blease achieved the first effective gene therapy study (Blease *et al.,* 1995) using white blood cells to cure a rare genetic immune system disorder. Only one of the two patients exhibited a successful and temporary response after the start of the therapy.

In 1999, an 18 year old boy, Jesse Gelsinger, died during a clinical trial for ornithine transcarbamylase deficiency (a rare metabolic disorder) at the University of Pennsylvania Philadelphia; as a consequence, the FDA placed a temporarily ban on all gene therapy trials using virus in human subjects. Important issues were identified and new rules, aimed to protect patient's safety, were put into place after a public three-day investigation was carried out by the National Institute of Health (NIH) (reviewed by Cavazzana-Calvo *et al.,* 2004). More recently, in November 2006, a group of scientists from the University of Pennsylvania developed a lentivirus-based immunotherapy for the treatment of human immunodeficiency virus (HIV). This was the first human clinical trial evaluating a lentiviral vector where patients showed stable and increased immune response against HIV antigens over the course of the treatment (Levine *et al.,* 2006).

At present more than 1900 gene therapy studies have been approved and conducted worldwide. The most commonly used gene therapy vectors are adenovirus, retrovirus and naked plasmid DNA (reviewed by Wirth *et al.,* 2013). Table 1.4 summarised the main gene therapy products for clinical use.

1.2.3 BACMAM: AN INSECT VIRUS FOR GENE DELIVERY

The first evidence of baculovirus entering vertebrate cells (including human cells), was reported during studies on its safety as a biological control agent (Volkman & Goldsmith, 1983). In these experiments, many different vertebrate cells internalized wild-type baculovirus particles, although no viral replication was observed. It was concluded that only the population of cells exposed to virus were transduced, whereas the cells not in contact with the virus were unaffected (Tjia *et al.,* 1983; Groner *et al.,* 1984).

Carbonell *et al.* (1985) used recombinant baculovirus carrying marker genes under either the Rous sarcoma virus long terminal repeat promoter (RSV) or the very late *polh* promoter to evaluate virus entry and gene expression in dipteran and mammalian cells.

The infections/transductions failed to produce detectable levels of chloramphenicol acetyltransferase and β-galactosidase gene expression in both cell lines. This study suggested that the gene promoter plays a crucial role in baculovirus mediated gene expression in non-permissive cells.

Table 1.4. Gene therapy product for clinical use.

Product	Description	Reference
Gendicine™ (SiBiono Gene Tech Co.),	A non-replicative adenovirus, approved in China in 2003 for the treatment of head- and neck-squamous cell carcinoma.	Reviewed by Peng, 2005
Oncorine™ (Sunway Biotech Co. Ltd)	A temporarily replicative adenovirus used in combination with chemotherapy in the late-stage of refractory nasopharyngeal cancer. This was approved in China in 2005.	Reviewed by Yu & Fang, 2007
Cerepro® (Ark Therapeutic)	A gene based medicine for malignant brain tumour which completed a phase III clinical trial in 2008.	Wirth *et al.,* 2009
Glybera (UniQure)	An adeno-associated virus modified to express lipoprotein lipase for the treatment of acute lipoprotein lipase deficiency. Its approval was endorsed by the European Medicine Agency (EMA) in 2012.	Reviewed by Ylä-Herttuala, 2012 Reviewed by Wirth *et al.,* 2013
ProSavin® (Oxford BioMedica)	A gene-based therapy for Parkinson's disease which uses LentiVector® gene delivery. In 2012, ProSavin® successfully completed phase I/II clinical trials.	Palfi *et al.,* 2014

In the mid-1990s, first Holfmann, and then Boyce with their respective co-workers, outfitted AcMNPV with a mammalian expression cassette, containing either cytomegalovirus immediate early promoter (CMV) or RSV to drive the expression of reporter genes. Using these viruses they were able to detect transgene expression in a range of cell lines derived from human, rabbit, and mouse. Hepatocytes in particular were transduced very efficiently (Holfmann *et al.,* 1995; Boyce & Bucher, 1996). These pioneering studies increased interest in baculoviruses as novel non-human viral vectors for gene therapy application. Subsequent researchers have confirmed the safety of these vectors and high-levels of expression have been observed in vertebrate cells, including cells of non-hepatic origin, up to fourteen days post-transduction (Condreay *et al.,* 1999; reviewed by Chen *et al.,* 2011).

The list of cells susceptible to baculovirus transduction is extensive and still growing but includes cells derived from monkey, porcine, rat, feline, hamster, fish, avian, frog, and shrimp tissues (reviewed by Kost *et al.,* 2005), also primary and progenitor cells, and more recently human embryonic stem cells and mesenchymal stem cells (Bak *et al.,* 2011; Lin *et al.,* 2011). Baculovirus-based vectors for expression in mammalian cells are generally referred to as BacMam. Therefore, the same nomenclature will be used in this thesis.

The exact molecular mechanism of BacMam entry into mammalian cells still remains poorly characterised and initially was thought to involve electrostatic interactions, heparin sulphate and phospholipids (Duisit *et al.,* 1999; Tani *et al.,* 2001). Other studies demonstrated that virions can be taken up by clathrin-mediated endocytosis, macropinocytosis (Matilainen *et al.,* 2005; Long *et al.,* 2006) and phagocytosis (Laakkonen *et al.,* 2009). Specific binding sites for baculovirus uptake have also been proposed (Wang *et al.,* 1997). Furthermore, the role of GP64 in BacMam attachment on the cell surface has been investigated and it was shown that the virus can enter cells through direct fusion (Kaname *et al.,* 2010; Kataoka *et al.,* 2012). More recently, Makkonen *et al.* (2013) investigated the role of heparan sulfate proteoglycans (HSPG), subfamily syndecans, during BacMam entry in a number of mammalian cells. Makkonen and colleagues demonstrated that BacMam interacts with 6-O and N-sulfated chains of HSPG and most importantly, binds specifically to the receptor syndecan-1 which mediates the internalization of BacMam in vertebrate cells.

1.2.4 APPLICATIONS OF BACMAM IN PRE-CLINICAL STUDIES

Numerous experiments in animals have been performed using BacMam; in particular studies have been carried out in mice, rat and rabbit and have revealed that the brain, eyes and testis are immunoprivileged areas (reviewed by Airenne *et al.,* 2010; 2013). These sites showed an intrinsic ability to prevent the activation of adaptive and innate immune responses to antigens (reviewed by Kaikkonen *et al.,* 2011). Although pre-existing immunity is not a concern for BacMam mediated gene delivery (Strauss *et al.,* 2007), both alternative and classical complement pathways may limit BacMam clinical evaluation (Hofmann & Strauss, 1998; Georgopoulos *et al.,* 2009). For this reason the first pre-clinical study using BacMam as a gene delivery vector in an *in vivo* context was unsuccessful (Sanding *et al.,* 1996). Although previous studies showed high transgene expression levels in primary cultures they failed to transduce *in vitro* liver tissue from rat and mice.

Following the Sanding *et al.* (1996) study, more investigations were conducted and a few years later Hofmann and colleagues confirmed that gene transfer *in vivo* was hampered by the inactivation of BacMam via the complement system (Hofmann & Strauss, 1998).

Many strategies have been developed over the last decade to solve complement related problems and relevant examples included the use of complement inhibitors such as cobra venom factor (Hofmann & Strauss, 1998), a soluble complement receptor type 1 (Hofmann *et al.,* 1999). The use of a silastic collar device, to avoid complement attack, allowed the carotid arteries of New Zealand white rabbits to be successful transduced by BacMam (Airenne *et al.,* 2000). Complement resistant BacMam have also been produced by fusing the CD55/decay accelerating factor (DAF) to GP64 (reviewed by Kaikkonen *et al.,* 2011). The functional domain of the human DAF was genetically fused to the envelope protein GP64 and the fusion protein was efficiently displayed on the surface of BacMam. This modified BacMam showed strong complement resistance in *in vitro* assays and successfully mediated *in vivo* gene delivery in neonatal rat liver (Huser *et al.,* 2001). Other approaches included the use of inhibitors for proteases that activate the complement system (Tani *et al.,* 2003).

Studies on cartilage and bone tissue engineering investigated potential approaches to exclude the complement effect. Chen and colleagues used a BacMam vector to transduce chrondrocyte cells before seeding them into a polymeric scaffold and culturing for three weeks (Chen *et al.,* 2008). The transduced cells/scaffold developed cartilage like tissues and eight weeks after implantation into osteochondral defects of New Zealand white rabbits, hyaline cartilages were regenerated and efficiently integrated with adjacent host tissues (Chen *et al.,* 2008). The potential use of BacMam in cartilage tissue engineering was also investigated by Chuang and co-workers who used a BacMam to genetically engineer human bone marrow stem cell. They demonstrated that BacMam transduction led to osteogenesis of bone marrow mesenchymal stem cells (BMSCs). In addition, they observed ectopic bone formation in nude mice and repair of calvarial bone in immunocompetent rats (Chuang *et al.,* 2010). Other approaches used compstatin, a highly potent and selective C3 inhibitor (Georgopoulos *et al.,* 2009) and positively charged polyethylenimine to coat the BacMam surface (Yang *et al.,* 2009).

More recently, the effect of DAF, factor H-like protein-1, C_4b-binding protein, and membrane cofactor protein were investigated for protection of BacMam vectors from complement-mediated inactivation (Kaikkonen *et al.,* 2010). These complement regulatory proteins were displayed on the vector surface as fusions to the membrane anchor of the vesicular stomatitis virus-G (VSV-G) protein.

Virus vectors exhibited complement resistance *in vitro* and intraportal delivery of DAF-displaying BacMam led to increased survival and enhanced gene expression in immunocompetent mice. Macrophages treated with DAF-displaying BacMam produced lower levels of inflammatory cytokines compared to control virus. These data suggested that DAF-display can protect BacMam against complement inactivation and reduce complement-mediated inflammation injury (Kaikkonen *et al.,* 2010). Recently, Paul *et al.,* (2013) generated a nanohybrid baculovirus, using cationic polyamidoamine dendrimer synthetic nanoparticles, encapsulated within poly (lactic-co-glycolic acid) microspheres. The study showed successful protection of baculovirus from the host immune system as well as enhanced transduction *in vivo*.

Although the complement system mediates inactivation of BacMam vectors in a *in vivo* context, a significant angiogenic response has been reported in immunocompetent rabbit skeletal muscle and rat heart after intramuscular and intramyocardial delivery, respectively (Paul *et al.,* 2011; Heikura *et al.,* 2012). This immunogenicity has been advantageous for cancer therapy (Heikura *et al.,* 2012). BacMam harbouring suicide genes, tumour suppressor genes, pro-apoptotic genes, immune-potentiating genes, and anti-angiogenesis genes have been tested *in vivo* in animal tumour models (reviewed by Wang & Balasundaram, 2010; Luo *et al.,* 2012). Data from cancer immunotherapy studies using mice vaccinated with baculovirus exhibited protection against tumour cells (Hervas-Stubbs *et al.,* 2007). BacMam transduction of antigen-presenting dendritic cells produced encouraging results for melanoma therapy (Zeng *et al.,* 2012).

The new millennium started with two successful BacMam studies. Firstly Airenne *et al.* (2000) showed that BacMam was able to mediate efficient periadventitial gene delivery into rabbit carotid arteries. This was followed by another study where Sarkis *et al.* (2000) tested the ability of a BacMam vector containing a green fluorescent protein (GFP) expression cassette to transduce neural cells *in vitro* and *in vivo*. They concluded that various neuroblastomal and non-neuronal cell lines, as well as three human neural primary cultures, were efficiently transduced by the vector. Moreover, direct injection of the BacMam into rat and mouse brain allowed *in vivo* transduction, predominantly in glial cells (Sarkis *et al.,* 2000). Recently, a bio-distribution experiment was performed by Räty *et al.* (2007) using Wistar rats. BacMam vectors coated with ^{99m}Tc-labelled polylys-ser-DTPA-biotin peptide were administered to rats (intrafemoral, intramuscular, intracerebroventricular and intraperitoneal) before being imaged by microSPECT/computed tomography (CT) *in vivo*. Results suggested that BacMam spread through the rat's lymphatic system which impacted transduction and its bio-distribution in the body.

Additionally, extensive expression was seen in kidneys and spleen after intraperitoneal administration. This study showed that administration of BacMam via the peritoneum might offer a new way to target kidney diseases (Räty *et al.,* 2007). BacMam viruses have also been demonstrated to efficiently deliver genes in human embryonic stem cells (Zeng *et al.,* 2007; 2009) and transduction did not compromise genome stability or pluripotency of stem cells (Yan *et al.,* 2009). Moreover, they demonstrated the potential use of these vectors in assisting neural transplantation.

More recently, BacMam, carrying the herpes simplex virus thymidine kinase (a suicide gene), was used to transduce mesenchymal stem cells before ganciclovir drug administration. Bak and colleagues observed inhibition of tumour growth and significantly prolonged survival of animals, suggesting BacMam was an attractive option as a targeting vehicle for systemic cancer therapy (Bak *et al.,* 2011). Studies carried out by the Insect Virus Research Group (IVRG) at Oxford Brookes University suggested that baculovirus can up-regulate the immune response *in vitro* and no evidence of cellular injury or reduction in cell viability was observed in porcine kidneys transduced *ex vivo* (Hitchman *et al.,* 2011; Murguía-Meca *et al.,* 2011).

1.3 Renal Ischaemia reperfusion-injury

1.3.1 KIDNEY

I. Structure and function

Kidneys are paired bean-shaped organs situated in the retroperitoneum space and are highly specialized organs. Their main function is to maintain whole-body homeostasis. They also regulate acid-base balance, fluid electrolyte concentration and excrete metabolic waste products like urea, creatinine, uric acid, as well as foreign chemicals. In addition, the kidneys have a vital endocrine function by secreting renin, the active form of vitamin D, and erythropoietin. Both hormones are important for maintaining blood pressure, calcium metabolism and synthesis of erythrocytes. Owing to the overwhelming genetic similarity between pigs (porcine) and humans, pigs represent an important model for biomedical research.

In this study porcine kidneys (Figure 1.8 A) were used as a model to study I/R injury. Therefore, the porcine kidney will be described in this section. The coronal plane section of a kidney shows two distinct areas; an outer region known as the cortex and an inner region, the medulla (Figure 1.8 B). The medulla is divided into several striated conical masses named renal pyramids. The base of each pyramid is positioned at the corticomedullary boundary which extends towards the renal pelvis to form a structure called papilla. The surface of each papilla contains small openings from which urine droplets pass. This represents the distal ends of the collecting ducts or ducts of Bellini.

The renal pelvis characterizes the extended portion of the upper urinary tract where two or three major calyces extend outward (Figure 1.8 C). Each major calyx is composed of several minor calyces that extend to the papillae. The major calyces function is to drain the urine produced by each pyramidal unit (Durben & Gerlach, 1979). From the lower region of the renal pelvis originates the ureters. Renal pelvis, calyces and ureters are formed of smooth muscle that contracts rhythmically to expel the urine to the bladder (Constantinou & Hrynczuk, 1976).

In pigs as well as humans and most other mammals, the vascular flow is provided by the renal artery which originates directly from the aorta artery. The renal artery enters the hilar region of the kidney and divides to form an anterior and a posterior branch. The anterior branch is subsequently divided in three segmental or lobar arteries and supplies the upper, middle and lower regions of the anterior surface of the kidney. Instead, the posterior artery perfuses the posterior region and is formed by small apical segmental branch. The venous network is divided into a series of veins leading to the renal vein and the inferior vena cava.

II Renal histology

Histologically, the renal parenchyma is formed by glomeruli, tubules, interstitium and blood vessels (Figure 1.9). The cellular morphology of the different cell types forming the nephron correspond to their specific role in kidney functions (see Section 1.3.2). The tuft of capillaries is formed by unique endothelial cells perforated by fenestrae, held together by the mesangium that is formed by mesangial cells.

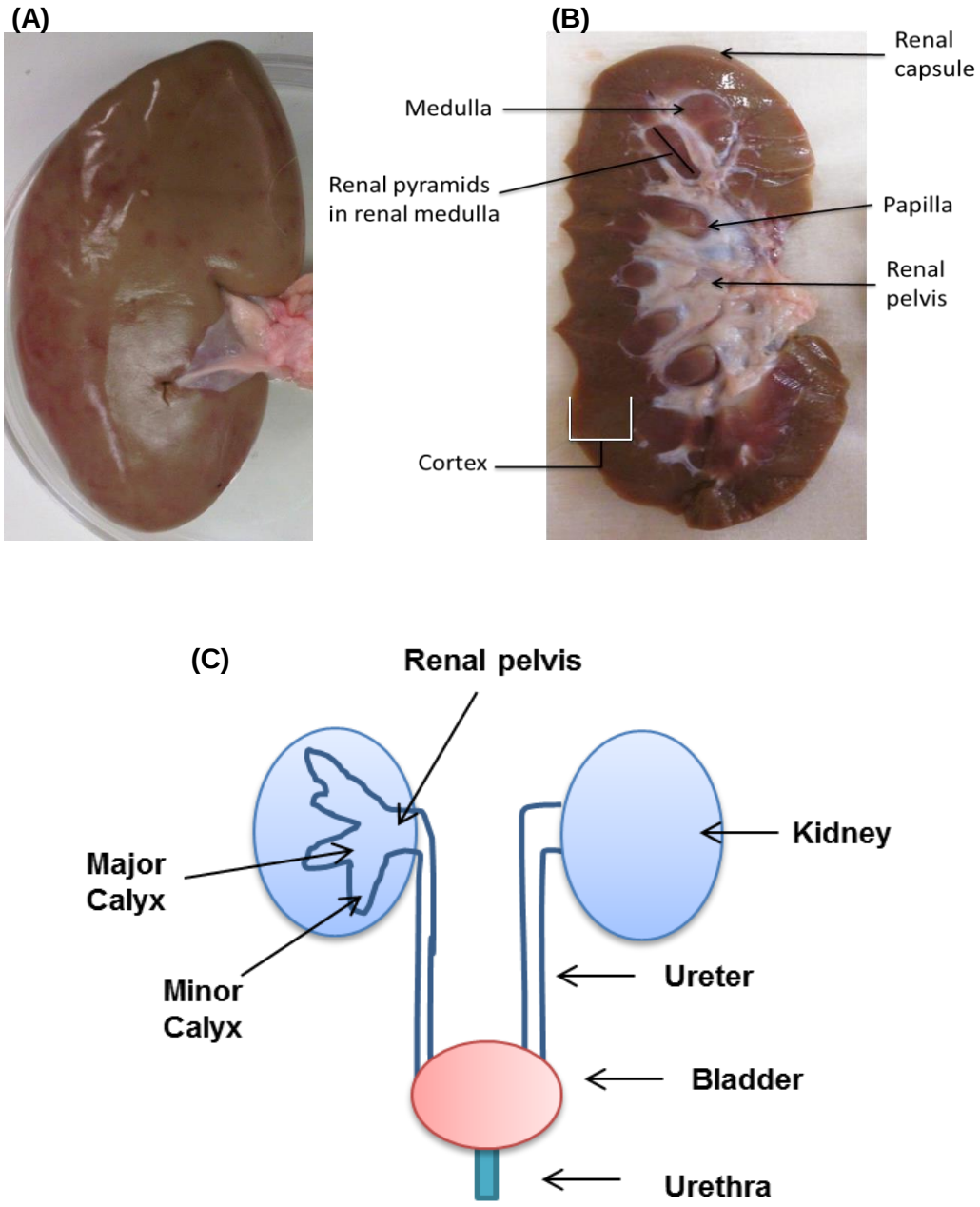

Figure 1.8. Porcine kidney anatomy. (**A**) Whole kidney, (**B**) coronal plan section highlights the outer cortex, the medulla and the renal pyramids where the collecting ducts drain off urine droplets in the central pelvis. (**C**) Schematic diagram of the upper urinary system; the renal pelvis divides into two or three major calices, each of which subdivides into several minor calices.

The mesangial cells, containing contractile microfilaments, are responsible for maintaining structural integrity and, due to their similarity to smooth muscle cells, regulate blood flow by relaxation or contraction movements (Michael *et al.,* 1980; Davies, 1994). Surrounding the capillaries tufts, are podocytes and parietal epithelial cells, which play a major role in glomerular filtration. However, it has been hypothesized that podocytes may function as structure-stabilizing cells by stabilizing the folding pattern of the tuft through linking neighbouring capillary loops to each other (Kriz *et al.,* 1994; 1995).

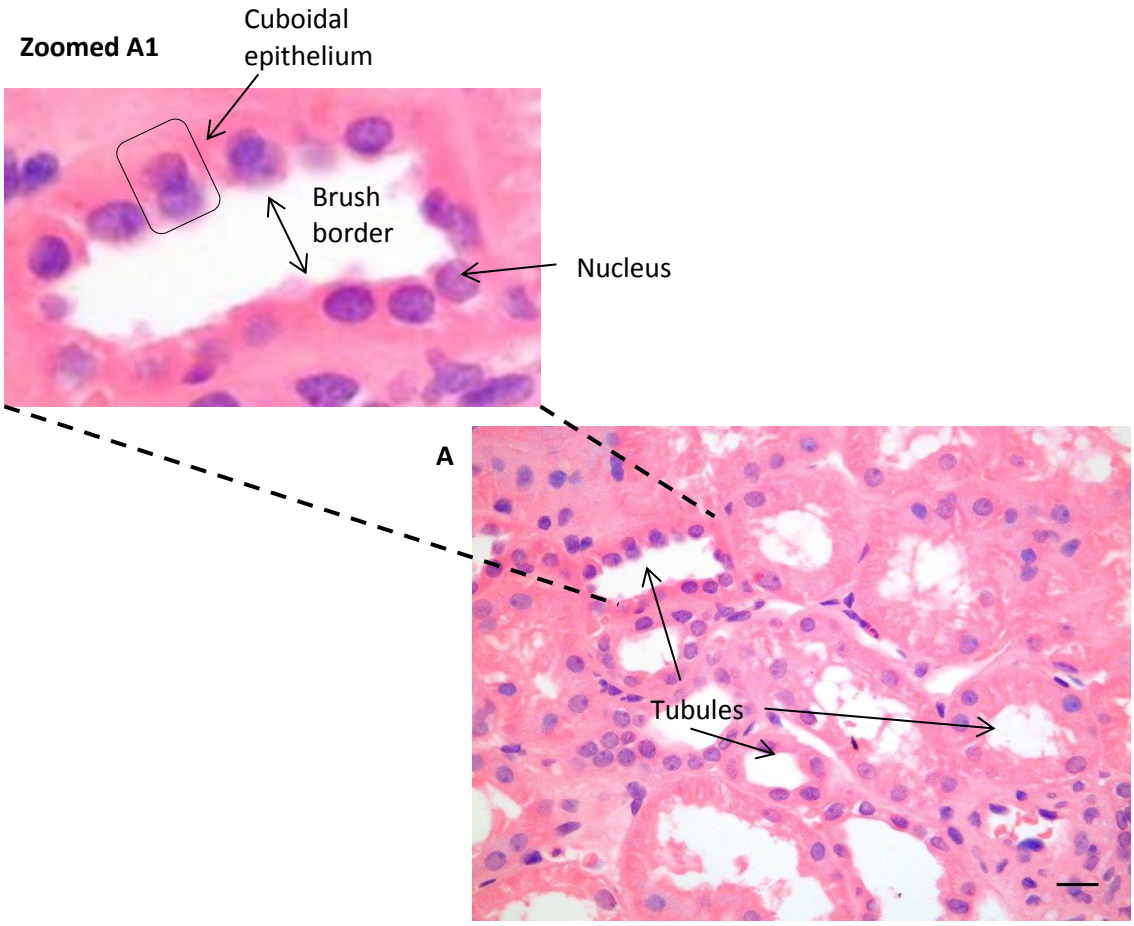

Figure 1.9. Normal histology of human kidney tissue. (**A**) Section of renal tubules (arrows) stained with hematoxylin–eosin staining (magnification x200). (**A1**) Zoomed renal tubule; the section shows simple cuboidal epithelium cells, cell nuclei and intact brush border. Scale bar = 20 µm. Image obtained from Prof I. Roberts (Department of Cellular Pathology, John Radcliffe Hospital, Oxford, UK).

The proximal tubules are characterized by specialized cubdoidal cells (Figure 1.9), essential for active fluid transport. Similar cells, but with less complex morphology, are present in the thick descending loop of Henle. The descending and ascending limbs are formed by four different types of epithelial cells.

The distal tubules and collecting ducts are formed by simple epithelial cells with a cuboidal morphology that do not display the deeply acidophilic, granular cytoplasm characteristic of the proximal tubule (Figure 1.9). The interstitium space contains specialized interstitial cells and connective tissue elements. The larger renal blood vessels are structurally similar to those in other body sites.

1.3.2 The nephron

The kidney's basic functional unit is the nephron, a blood plasma filter (Rashidi & Khodarahmi, 2006; Derossi & Cohen, 2008). The nephron's essential components are: glomerulus surrounded by Bowman's capsule, the proximal and distal tubules, the thin descending and ascending limbs of the loop of Henle and the collecting tubule (Figure 1.10). Blood enters the kidney through the renal artery and passes through a series of small arteriole branches before arriving into the capillary system of the nephron to be filtered. Water and solutes are reabsorbed into the bloodstream during the transition of the filtrate from the nephron to the collecting tubes; the filtered fluid is then emptied into the bladder through the ureters.

I. The glomerulus

The basic filtration units of the kidney are glomeruli (Figure 1.10 A), formed of a unique capillary network surrounded by endothelium (Figure 1.10 B). The different cell types are separated from each other by a glomerular basement membrane into which the filtrate is collected (reviewed by Jarad & Miner, 2009). This membrane plays a key role in the ultra-filtration of blood plasma by acting as charge-selectivity barrier (reviewed by Goode *et al.,* 1996; and Miner, 2012). The collected ultra-filtrate from the Bowman's space enters the proximal tubules at the urinary pole of the glomerulus (Figure 1.11 A).

II. The proximal tubule

During glomerular filtration, the filtrated fluid moves to the proximal tubules where about 80% of the ultra-filtrate is reabsorbed (Guyton, 1991). The proximal tubules are formed of a convoluted region, known as *pars convoluta*, followed by a straight portion named *pars recta*. However, morphologically they are divided in three distinct segments: S1, S2, and S3 as shown in Figure 1.12 (reviewed by Christensen *et al.,* 2012).

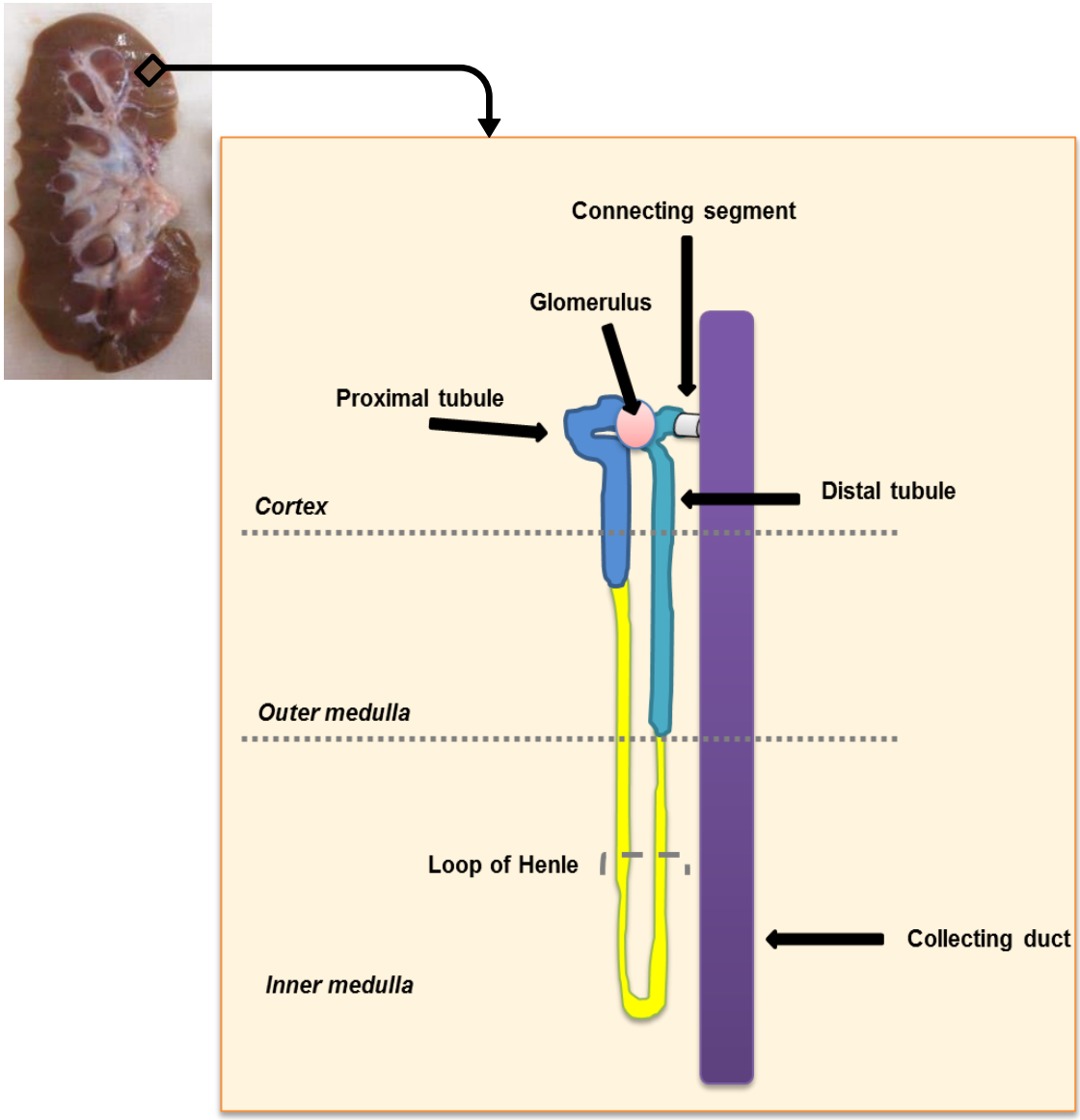

Figure 1.10. Schematic representation of a kidney nephron.

The S1 segment forms the initial portion of the proximal tubule which originates at the glomerulus pole. The end region of the *pars convoluta* together with the initial portion of the pars recta forms the S2 segment, while the S3 segment represents the last portion of the proximal tubule localized between the cortex and the outer medulla (Maunsbach, 1966).

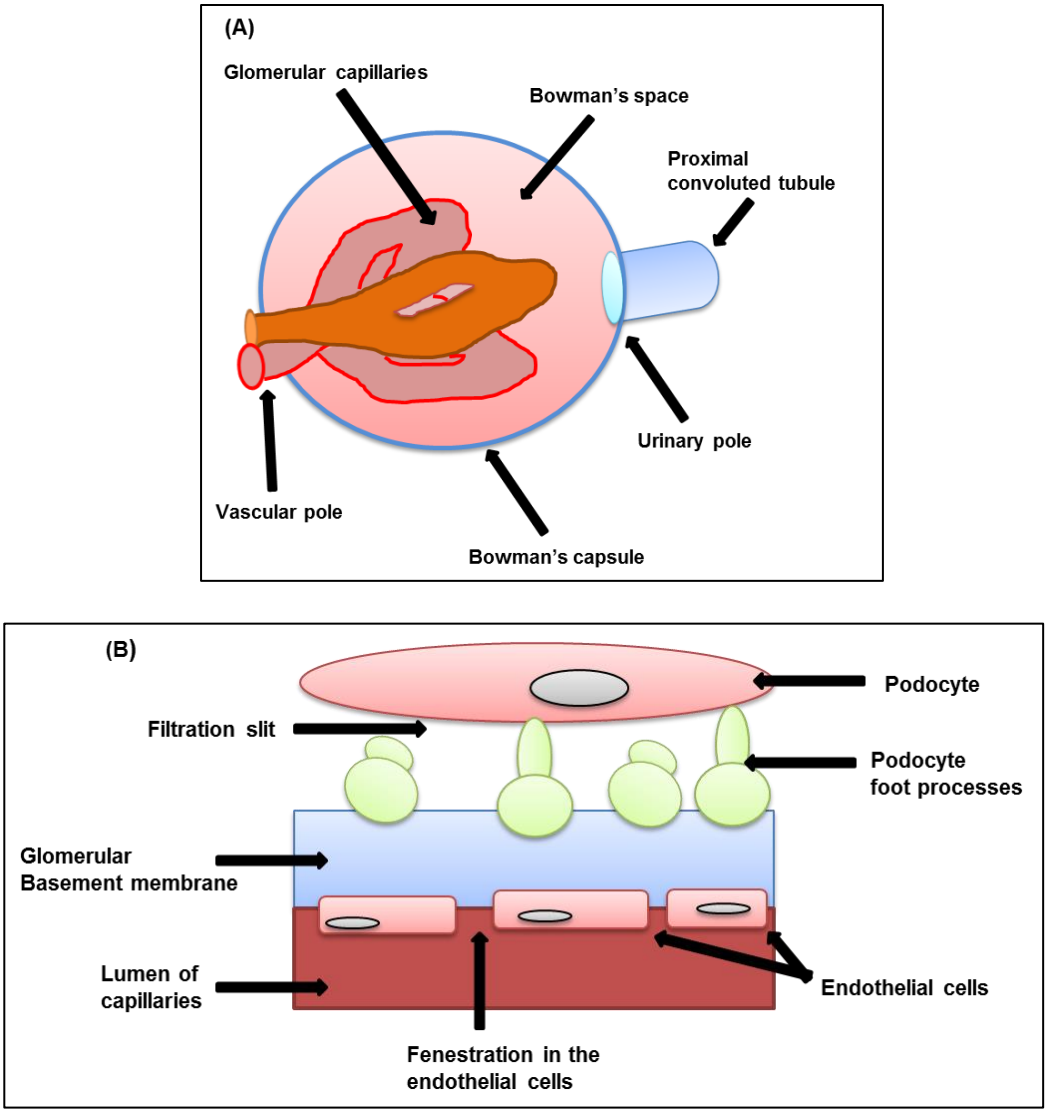

Figure 1.11. Diagram of glomerulus (A) and glomerulus filtration barrier (B).

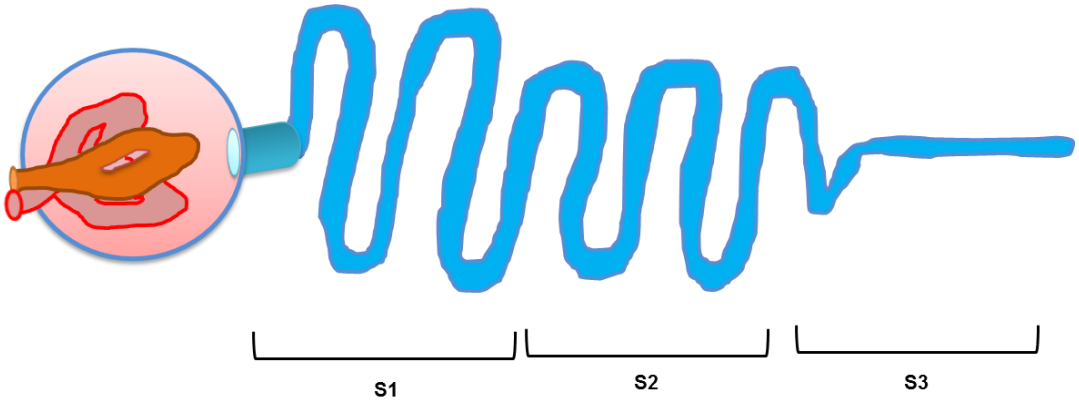

Figure 1.12. Diagrammatic representation of the proximal tubule. The proximal tubules are morphological divided in three segments, S1, S2 and S3. S1 and S2 are localized in the cortex while the S3 segment represents the proximal tubule portion between the cortex and the outer medulla.

Besides a reabsorption function, the proximal tubules are responsible for the excretion of drugs, toxins and other organic compounds; they are involved in a number of important metabolic functions (Wright, 2005) and it has been proposed that they might have immune-modulatory functions by acting as specific target cells during allograft rejection (Yard *et al.,* 1992; Van Dorp *et al.,* 1993). Nevertheless, due to their vast spectrum of functions it is not surprising that several inherited and acquired kidney disorders are closely linked to the proximal tubules (reviewed by Nakhoul & Batuman, 2011). Therefore, in light of this, the *in vitro* work carried out in this thesis was based on an immortalized proximal tubule epithelial cell line, human kidney-2 (HK-2; Ryan *et al.,* 1994).

III. The loop of Henle

The loop of Henle is composed of two segments: the thin descending limb which is a continuation from the proximal tubule S3, and the thin and thick ascending limb (Figure 1.13). The descending limb is mainly permeable to water (Kokko, 1970), whereas the ascending limb become impermeable to water and permeable to ions (Greger, 1985). The main function of the loop of Henle is to regulate the current exchange mechanism for the ionic compound sodium chloride (NaCl) between the filtrate and the interstitial fluid surrounding the loop (Thomas, 1998).

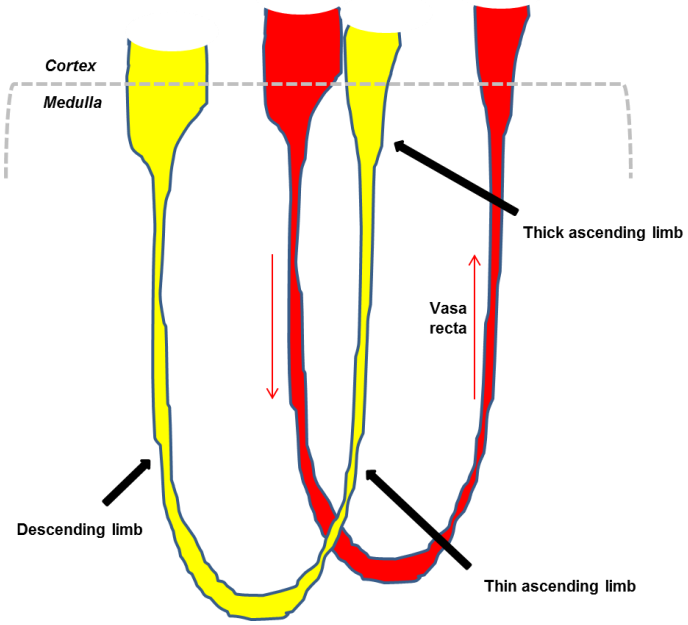

Figure 1.13. Loop of Henle. The loop of Henle limbs are localized at the medullar region. The thin descending limb, the thin and thick ascending limbs are parallel to the vasa recta vessels.

IV. The distal tubule and collecting ducts

The cortical distal tubular portion is defined as the region between the macula densa and the collecting duct. This can be morphological divided into distal convoluted tubule and connecting tubule. The filtrate is collected from numerous distal tubules into the connecting tubule, a tubular segment that connects the collecting ducts system, at the cortical region, with the distal tubules. The ultra-filtrate is then drained from the connecting segment into the collecting ducts. The collecting ducts represent the final control of the urine composition and based on their location they are divided in cortical, outer medullary and inner medullary collecting ducts (reviewed by Muto, 2001). In addition, this portion of the kidney is almost completely impermeable to water and for this reason any excess will be lost in the urine (reviewed by Berridge, 2012). The urine from the medullary collecting ducts is excreted into the renal pelvis before being transported into the urinary bladder.

1.3.3 RENAL FAILURE

Renal failure is a well-known medical condition in which kidneys are unable to reabsorb water and solute and fail to remove waste products from the blood. Kidney failure can be divided into two main categories, acute renal failure (ARF) and chronic renal failure (CRF). ARF causes are grouped into three categories, pre-renal, intra-renal and post-renal, whereas, CRF occur when kidneys are not able to recover after one or more episodes of ARF (reviewed by Lameire *et al.,* 2013). ARF has emerged as the most common renal disease in hospitalized patients producing serious morbidity and mortality and prolonged hospitalisation (Mehta *et al.,* 2004). This thesis focused on one of the most common causes of intra-renal ARF, namely ischaemia reperfusion-injury (I/R injury) (Sheridan & Bonventre, 2001; Giraud *et al.,* 2011).

The term ischaemia is referred to as a progressive condition from a hypoxic state where interrupted blood flow causes intracellular oxygen depletion. Although ischaemia induces cell damage, the real injury is manifested after restoration of the blood flow and tissue oxygenation. The main mechanisms triggering the injury are reactive oxygen species (ROS), excessive inflammatory response and rapid electrolyte shifts (Cai *et al.,* 2006; Zhu *et al.,* 2007). I/R injury often occurs following kidney transplantation, due to the obligated interruption of blood flow during the transplant period. Two types of ischaemia may occur during renal transplantation, warm and cold ischaemia. In particular, warm ischaemia is further divided into donor warm ischaemia either after circulatory death or after brain death and recipient warm ischaemia.

In donors, the warm ischaemia starts from the time of asystole until the organ is preserved in a cold perfusion solution. While, in recipient warm ischaemia begins with the removal of the organ from ice up until the start of the reperfusion (reviewed by Halazum *et al.,* 2007). Cold ischaemia occurs when kidneys collected from living donors are directly preserved in cold preservation solution. However, both types of ischaemia have a significant impact on short and long-term transplant outcome (Peters *et al.,* 1995). It can lead to primary non-function of the transplanted organ (<5% of recipients), delayed allograft function, which occurs in up to 50% of recipients (Abu Jawdeh & Rabb, 2011; Ghadiani *et al.,* 2012) and multiple organ dysfunction (Yassin *et al.,* 2002; Park *et al.,* 2012).

1.3.4 PATHOPHYSIOLOGY OF RENAL ISCHAEMIA REPERFUSION (I/R) INJURY

The pathophysiology of I/R injury is complex and multifactorial affecting both the renal tubular epithelium and renal microvasculature (Bonventre & Weinberg, 2003). The key manifestation of ischaemia is a rapid decrease in the level of adenosine triphosphate (ATP) followed by mitochondrial dysfunction and enhanced production of ROS (Feldkamp *et al.,* 2004). Decreased levels of ATP, which depend on the severity and duration of the blood flow interruption to the organ, can initiate a number of critical metabolic consequences (Figure 1.14; Devarajan, 2005).

I. Ionic imbalance

Following oxygen deprivation, epithelial cells are unable to maintain sufficient intracellular ATP levels for essential processes. This rapid degradation of ATP to adenosine diphosphate (ADP) and adenosine monophosphate (AMP) is recognised as the first consequence of ischaemia. AMP is further metabolized into adenine nucleotides and then into hypoxanthine which contributes to the generation of ROS. Furthermore, ATP depletion induces loss of cell membrane integrity followed by derangement of cellular ion homeostasis and, if severe enough, cell death by necrosis and apoptosis (Bonventre & Yang, 2011). Provision of exogenous adenine nucleotide or thyroxine, in order to stimulate ATP re-generation, has been studied in animal models (Wagener *et al.,* 1995), however, this approach failed in a trial to treat human acute renal failure (Acker *et al.,* 2000).

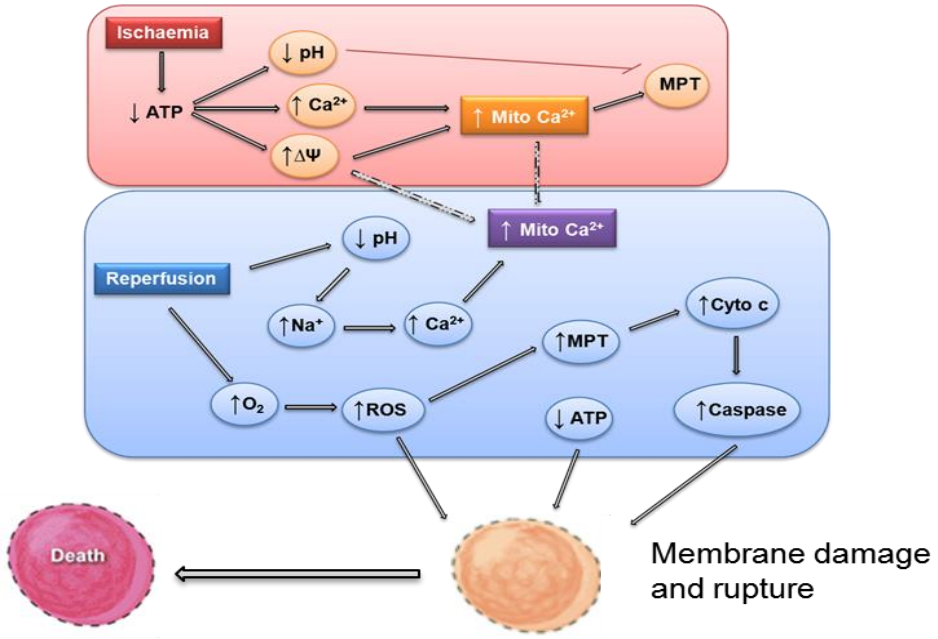

Figure 1.14. Pathways leading to cell death in I/R injury. During ischaemia the decline of ATP levels results in a decreased pH, increased cytosolic calcium (Ca^{2+}) and mitochondrial membrane potential (Δψ). This leads to increased mitochondrial Ca^{2+} (Mito Ca^{2+}) which results in the activation of the mitochondrial permeability pore (MPT). However, acid pH inhibits MPT. At the reperfusion stage, the re-introduction of O_2 leads to the generation of ROS and activation of the MPT. Altogether, loss of ATP, ROS and MPT activates the apoptotic pathway causing a rapid loss of plasma membrane integrity and cell death. Modified from Murphy & Steenbergen (2008).

Following ATP depletion, positively-charged protons accumulate in the cytoplasm, activating the Na^+/H^+ (sodium/hydrogen) exchanger (Figure 1.15 A). The Na^+/K^+ ATPase pump, which regulates Na^+ levels in the cytoplasm, is unable to function due to the lack of ATP and consequently cells are loaded with excessive levels of Na^+. As a result, Na^+/Ca^{2+} (sodium/calcium) antiporter activity is enhanced, which leads to an increased concentration of cytosolic and mitochondrial Ca^{2+}. As shown in Figure 1.15 (B), at the reperfusion stage the combinations of high Ca^{2+} levels, ROS and decreased hydrogen ion potential (pH) activate the mitochondrial permeability pore (mPTP). The conformational change of the mPTP causes further ROS production, depletion of ATP and rupture of the mitochondrial membrane releasing cytochrome c (cyt c) into the cytoplasm. Ultimately, these processes lead to cell death (Murphy & Steenbergen, 2008; Halestrap & Pasdois, 2009).

.

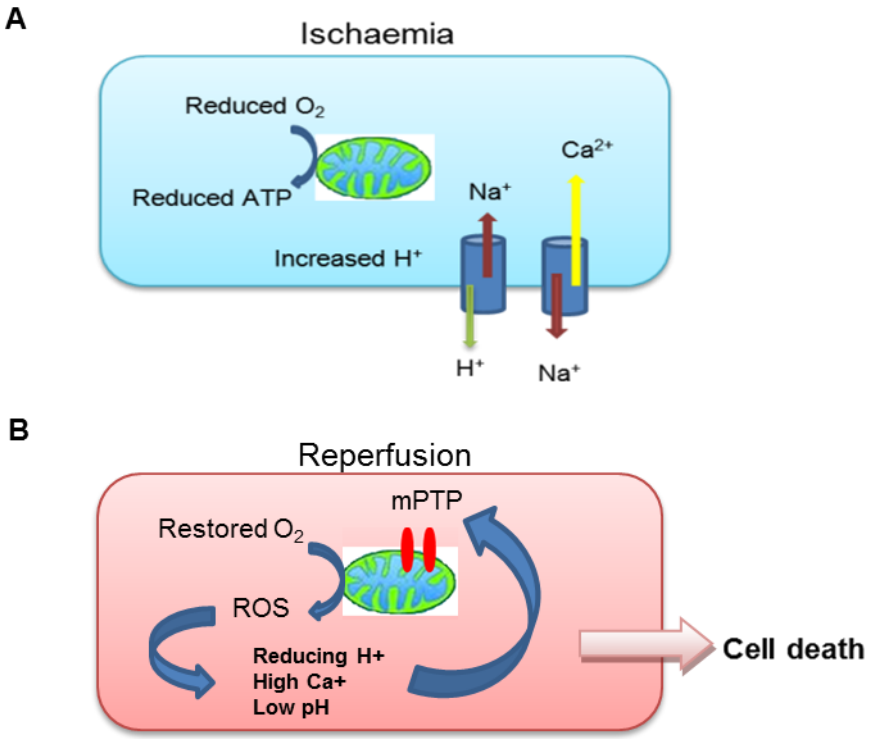

Figure 1.15. Cellular response to ischaemia and reperfusion. (**A**) The ATP deletion during ischaemia leads to increased intracellular hydrogen ion (H^+) and calcium (Ca^{2+}). (**B**) Following reperfusion the generation of reactive oxygen species (ROS), changing pH and Ca^{2+} induce the conformational change of the mitochondrial permeability pore (MPP); this lead to cell death. Modified from Kharbanda (2010).

II. Oxidative stress

Within minutes following reperfusion, several factors contribute to renal tissue injury; the molecular oxygen (O_2) reacts with the accumulated hypoxanthine generating xanthine and ROS (Chan, 2001). ROS can be generated by different systems, however the mitochondrion represents the major site of production (Greene & Paller, 1992; Nath & Norby, 2000). ROS are produced under normal cellular conditions to accomplish physiological roles (Nose, 2000) and are degraded by antioxidant enzymes, *e.g.,* superoxide dismutase, glutathione peroxidase and catalase (Droge, 2002; Trachootham *et al.,* 2008). However, during I/R injury an excessive production of ROS together with reduced antioxidant defences may cause a range of cellular damage, such as DNA strand breaks, lipid peroxidation and reduction of protein sulfhydryl bonds (Nath & Norby, 2000; Goswami *et al.,* 2007).

Following re-oxygenation the O_2 molecule is quickly reduced by one-electron. This produces a relatively stable intermediate named superoxide anion ($O_2^{\cdot-}$) (Figure 1.16).

The $O_2^{\cdot-}$ represents the precursor of most ROS generated in cells; its dismutation can occur either spontaneously or through a reaction catalysed by the superoxide dismutase enzyme (SOD) and produces hydrogen peroxide (H_2O_2). As shown in Figure 1.16, H_2O_2 is then further reduced via catalase or glutathione peroxidise (GSH-Px) into water (Becker, 2004) or partially reduced to a hydroxyl radical (OH•) via the Fenton reaction (Mao *et al.,* 1993; Liochev & Fridovich, 1999). In addition, $O_2^{\cdot-}$ can react with nitric oxide ($NO^{\bullet}$) producing peroxynitrite ($ONOO^-$) a very powerful oxidant from the group of reactive nitrogen species (RNS) (Beckman & Koppenol, 1996; Radi *et al.* 2002).

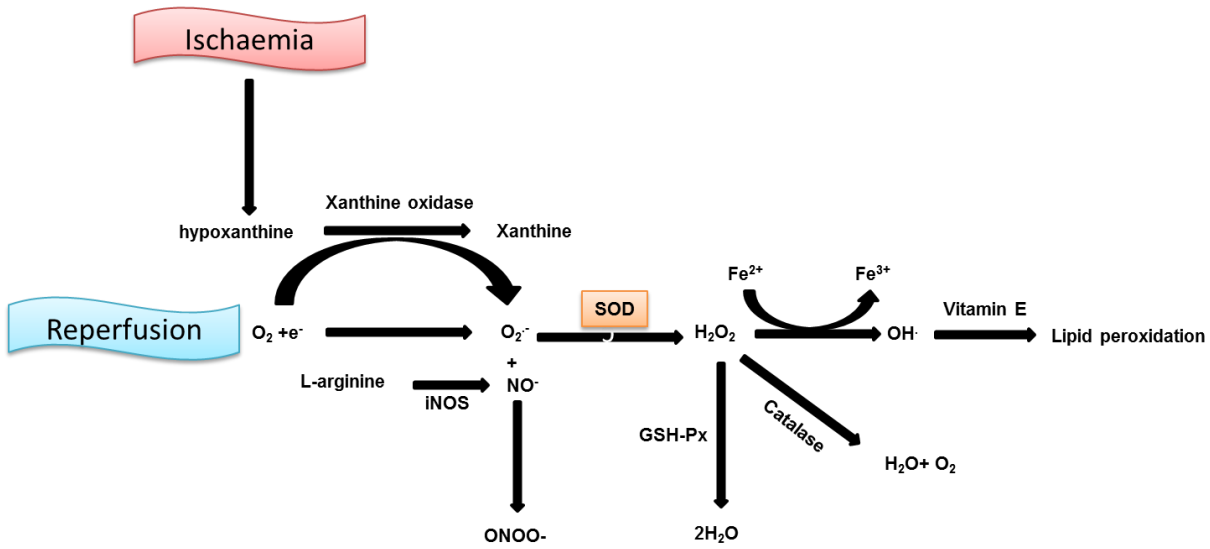

Figure 1.16. Generation of ROS in I/R injury. O_2 reacts with an impaired electron (e-) to form $O_2^{\cdot-}$. $O_2^{\cdot-}$ is converted in H_2O_2 by the enzyme SOD. H_2O_2 undergoes spontaneous conversion to $OH^{\cdot}$. Alternatively, it can be detoxified via glutathione peroxidase (GSH-Px) or catalase to H_2O and O_2.

The primary cellular antioxidant defence system is the SOD family. The catalytic activity of SOD enzymes was first discovered in bovine erythrocytes by McCord & Fridovich (1969). In the years following this discovery a number of SODs have been identified that are characterized by their metal group and cellular localization. They have been found in both prokaryotic and eukaryotic cells including copper/zinc- (Cu/Zn, SOD-1/3), manganese- (Mn, SOD-2), nickel-, iron- and iron/zinc- enzyme (Yost & Fridovich, 1973; Steinman *et al.,* 1974; Whittaker *et.al.,* 1998). Although they have some distinction, all SODs catalyse the dismutation of $O_2^{\cdot-}$. In human tissues three isoforms are present, SOD-1, SOD-2 and SOD-3 (Johnson & Giulivi, 2005).

Mn-SOD or SOD-2, localized in the mitochondrial matrix (Zelko *et al.,* 2002), was the isoform utilized in the work described in this thesis. It exists as a homotetramer with a molecular weight of approximately 23 kDa (Barra *et al.,* 1984) and contains one Mn atom per subunit. It cycles from Mn(III) to Mn(II) and then back to Mn (III) during the two step dismutation reaction. Many reports have shown that SOD-2 plays a key role in attenuating injury or death under conditions of enhanced oxidative stress (Kasahara *et al.,* 2005; Fukui & Zhu, 2010; Aguirre & Culotta, 2012) and SOD-2 deficiency in mice leads to prenatal lethality (Huang *et al.,* 2001). For this reason many researchers have aimed to up-regulate SOD-2 activity. Different studies have provided conclusive evidence that overexpression of SOD-2 protects against I/R injury (Cruthirds *et al.,* 2005; Usui *et al.,* 2011). Moreover, several other studies have demonstrated the beneficial effects of pharmacological approaches in preventing excessive ROS formation during I/R injury *e.g.,* administration of xanthine oxidase inhibitor such as allopurinol (Hu *et al.,* 2012); exogenous administration either *in vivo* or *in vitro* of antioxidant mimetic enzymes *e.g.,* SOD mimetics such as Tempol (Thomas & Sharifi, 2012).

Recent studies support the hypothesis that ROS-mediated injury may occur several hours after reperfusion begins. Kulah *et al.,* (2007) measured the accumulation of an oxidative stress biomarker, ox-LDL, in rat kidney tissue during I/R injury. They observed that the plasma ox-LDL levels did not increase significantly at twenty-four hours following the reperfusion. However, a peak and a decline of biomarker levels were observed at forty-eight and seventy-two hours post I/R injury. In conclusion, Kulah and colleagues (2007) identified long term complications in addition to the immediate cellular damage of reperfusion as things to be considered in future strategy development.

III. Apoptosis

During I/R injury, the endogenous antioxidant system becomes inadequate to control ROS concentration and in this pathological scenario the increased oxidative stress/damage eventually leads to apoptotic cell death. The term apoptosis refers to programmed cell death and is used by the cell to eliminate redundant or damaged cells (Hoeberichts & Woltering, 2003). A schematic representation of apoptosis is shown in Figure 1.17. It can be activated by either extracellular signals including toxins, hormones, growth factors and nitric oxide (Popov *et al.,* 2002; Brüne, 2003) or intracellular signals. Cells initiate intracellular apoptosis in response to stress such as oxidative stress (reviewed by Ozbek, 2012). Under normal cellular homeostasis a number of anti-apoptotic factors inhibit the conformational change of mPTP, and consequently they prevent mitochondrial disruption and the release of cyt c (Cory & Adams, 2002).

However, an excessive formation of ROS in mitochondria triggers the activation of the intracellular apoptosis pathway. Cyt c released from mitochondria to the cytoplasm, together with the apoptotic protease activating factor 1 (Apaf-1) form a complex named the apoptosome (Chernyak, 1997). The apoptosome activates a cascade of proteolytic reactions that lead to cell death by cleaving cytoskeletal, metabolic and cell signalling proteins (Namura *et al.,* 1998).

BCL-2 proteins are the main regulators of apoptosis (Figure 1.17). Members of this family are classified into two groups: anti- and pro-apoptotic. The first anti-apoptotic gene was discovered in non-Hodgkin's follicular B-cell lymphomas, known as B-cell lymphoma 2 (*bcl-2*), between chromosomes 14 and 18 t (14; 18) (Bakhshi *et al.,* 1985). Identification of BCL-2 as an inhibitor of apoptosis prompted the discovery of other members of this family. In particular, three members with protective function were characterized: *bcl-x*, *mcl-1* and *a1* (Boise *et al.,* 1993, Kozopas *et al.,* 1993). Additionally, other proteins were identified that interact with BCL-2 such as BAX which promotes apoptosis rather than protecting against cell death (Oltvai *et al.,* 1993). Subsequently more pro- and anti-apoptotic proteins were characterized such as pro-apoptotic protein BIK, and the anti-apoptotic BCL-Xs (Aouacheria *et al.,* 2001).

In mammals, BCL-2 is related at least to twenty members, all of which share one or more conserved BCL-2 homology domains (reviewed by Cory & Adams, 2002) and regulate apoptosis through protein-protein interactions (Cory *et al.,* 2003). Deletion of pro- or increased expression of anti-apoptotic proteins have been shown to reduce I/R injury mediated cell death (Hochhauser *et al.,* 2003). In particular, overexpressing the anti-apoptotic enzyme BCL-2 has been shown in a number of studies to reduce total cell death and apoptotic cell death following I/R injury in different organs (Suzuki *et al.,* 2008). Saikumar *et al.* (1998) demonstrated that BCL-2 prevented hypoxic injury in kidney proximal tubule cells by inhibiting mitochondrial release of cyt c. Similarly, Isaka and colleagues showed that BCL-2 augmentation protected renal tubular epithelial cells from I/R injury by suppressing autophagosomal degradation of injured mitochondria (Isaka *et al.,* 2009).

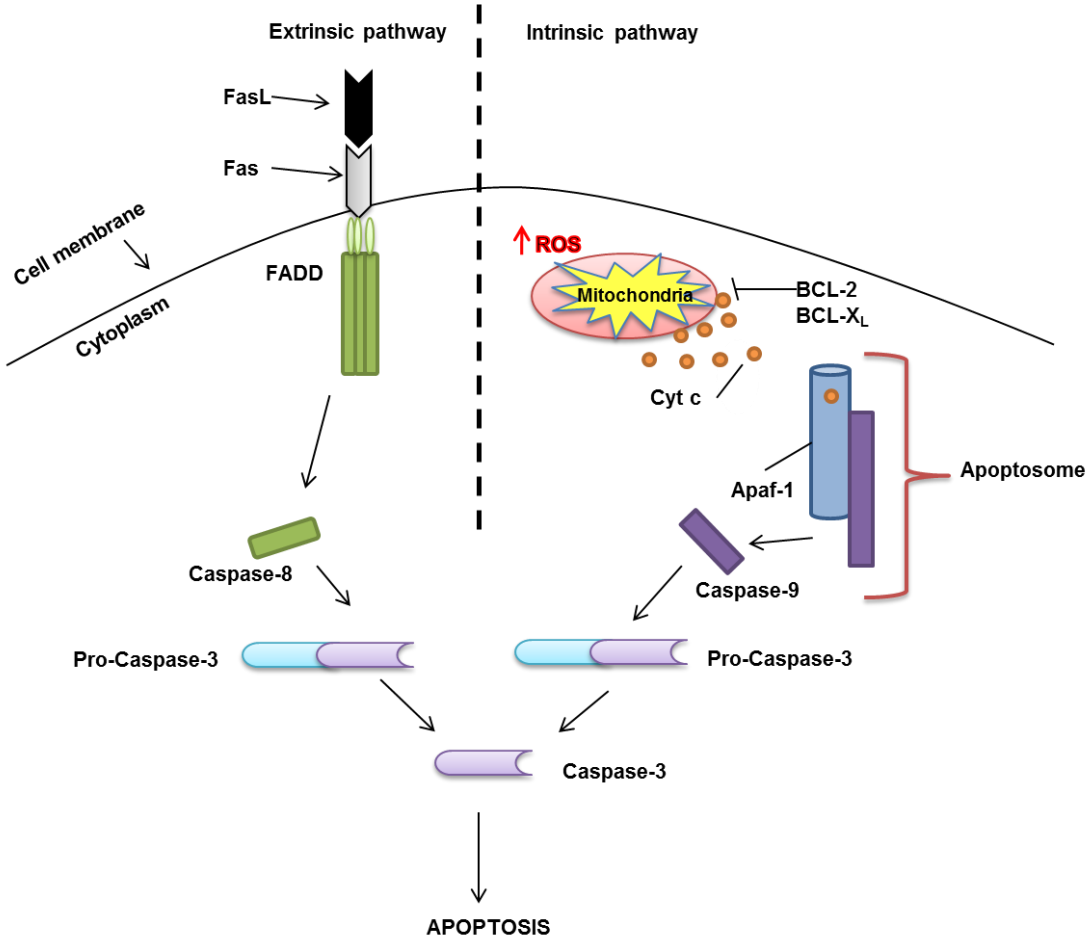

Figure 1.17. Apoptosis pathways. In the extracellular pathway, the binding of the ligand, FasL, to the receptor, Fas, results in the activation of caspase-8. In the intrinsic pathway, the intracellular signal e.g. high concentrations of ROS, induces the release of cyt c, formation of apoptosome and the activation of caspase-9. Caspase-8 and -9 activate caspase-3 which leads to cell death. BCL-2 and BCL-X_L play an important role in inhibiting cyt c release from mitochondria; this prevents the apoptosis activation. Modified from Berrou *et al.* (2012).

1.3.5 HISTOLOGICAL CHANGES DUE TO I/R INJURY

As described in Section 1.3.4, a number of mechanisms are implicated in the process of I/R injury that cause changes in the renal histology. A photomicrograph of a human renal biopsy with signs of ischaemic tubular necrosis is shown in Figure 1.18. Increase in ROS production, depletion of intracellular ATP and elevated Ca^{2+} levels interfere with normal metabolic processes. Under these conditions, ischaemic cells lose their actin cytoskeletal integrity, their membrane polarity changes which disrupts tubular transport function and they detach from the basement membrane. Histologically, these changes occur mainly in the renal tubules (Figure 1.18).

Renal tubules appear with sloughing of the brush border membrane into the lumen or invagination into the cytoplasm, which leads to the redistribution of integrins and Na^+/K^+ ATPase to the apical surface (Lameire & Vanholder, 2004). Furthermore, ischaemic tubules are characterized by the epithelium flattening, tubular dilatation and loss of cell nuclei (Figure 1.18).

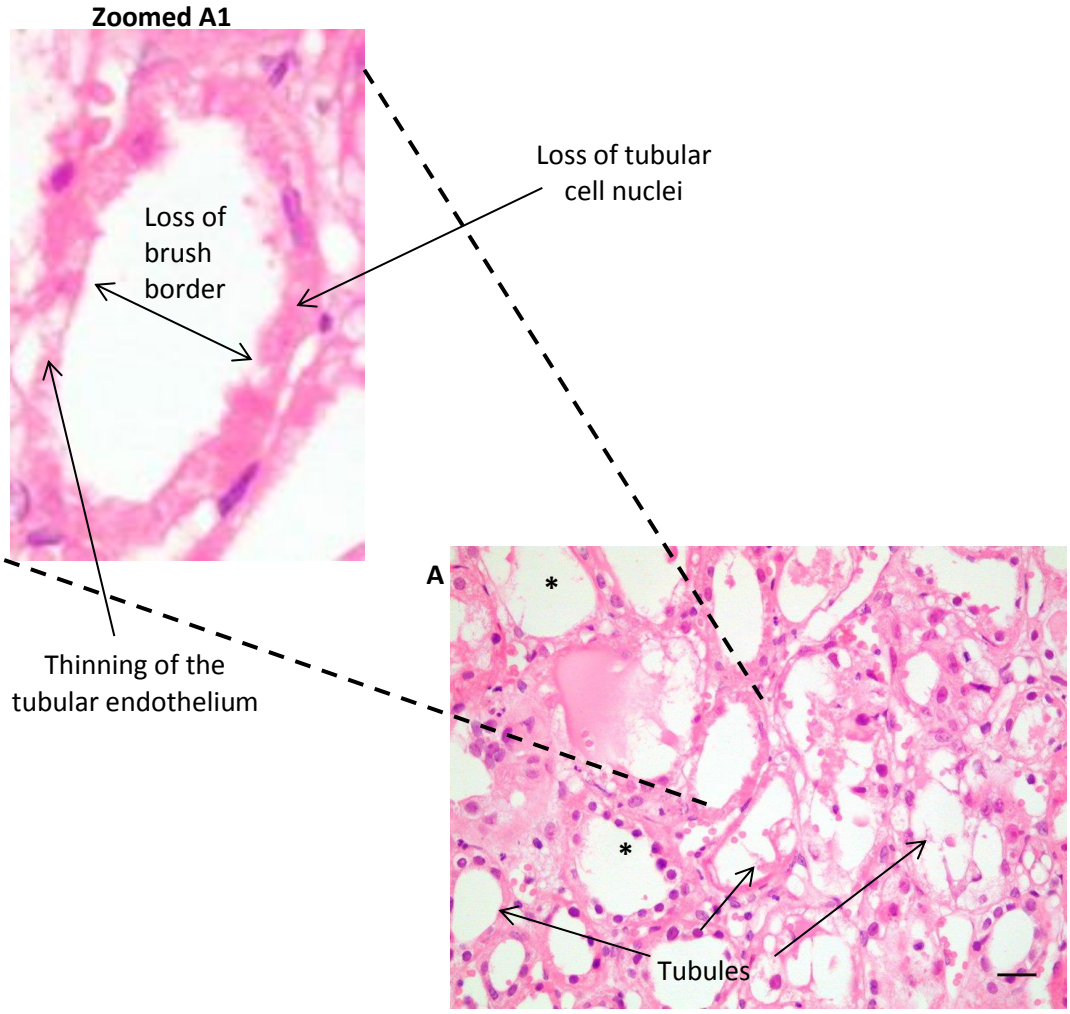

Figure 1.18. Representative image of human renal biopsy showing ischaemic tubular necrosis. (**A**) Section of renal tubules (arrows) stained with hematoxylin–eosin (magnification x200). (**A1**) Zoomed renal tubule; the section shows loss of brush border, loss of cell nuclei and thinning of the tubular endothelium. Asterisks indicate dilated tubules. Scale bar = 20 µm. Image obtained from Prof I. Roberts (Department of Cellular Pathology, John Radcliffe Hospital, Oxford, UK).

1.3.6 EXPERIMENTAL MODELS

Over the past decade numerous experimental models have been developed to explore the pathophysiology mechanisms of renal I/R injury. Various conditions have been used including animal models for *ex vivo* / *in vivo* studies as well as *in vitro* models such as oxygen and glucose deprived cultures of renal cells (Lee & Emala, 2002).

These models have enhanced our understanding of renal diseases and played an important role in the search for adequate therapeutic treatment for I/R injury. Although animal experimentation is subject to legal and ethical restrictions, animal-based experimental models are crucial in renal I/R injury studies. Indeed, pre-clinical animal studies play a central role in either testing medical devices or assessing the efficacy of therapeutic treatment before their use in human patients.

I. *In vitro*

In vitro models are generally used to study molecular mechanisms, specific pathways involved in cellular damage and/ or death caused by I/R injury events. These experimental models can be performed using either primary cells or immortalized cell lines. The most frequently used cell lines are porcine kidney cells (LLC-PK1) which have a proximal tubular cell phenotype (Hull *et al.,* 1976) and HK-2 cells which are proximal tubular cell (PTC) line derived from normal human kidney. The major areas of I/R injury investigation have included overexpression of protective genes, enhancing enzyme activity and suppressing the expression of genes that activate the cell death pathway. A wide variety of techniques that mimic I/R injury *in vitro* have been developed and are generally classified as either: (1) external cellular environment alteration such as the *in vitro* model of mineral oil immersion (Hitchman *et al.,* 2011); (2) cellular metabolism manipulation using chemicals *e.g.,* mitochondrial inhibitors such as antimycin A (Doctor *et al.,* 1994). Over the past decade, a number of *in vitro* renal studies used antimycin A in combination with a non-metabolizable glucose analog, 2-deoxyglucose, to induce mild/severe intracellular ATP depletion (Iwata *et al.,* 1995; Xie & Guo, 2006; Kumar *et al.,* 2009).

More recently, encouraging results have been achieved with pre- and post- conditioning approaches (Bon *et al.,* 2012; Yuan *et al.,* 2012). Murry *et al.* (1986) were the first to show that brief episodes of ischaemia decreased the extension of myocardial infarct induced by subsequent prolonged injury. This phenomenon named “ischaemia preconditioning” appears to be a body defence mechanism to an acute stress. However, its clinical use remains limited since it must be instituted before the ischaemia episode begins (reviewed by Selzner *et al.,* 2012). In 2003 a new model was developed (ischaemia post-conditioning) to overcome this limitation, by rapid and irregular interruption of blood flow during the initial phase of reperfusion.

II. *In vivo / ex vivo*

In vivo whole animal and *ex vivo* organ models are crucial due to the limitations of *in vitro* models. Various animal models of ischaemia have been developed and currently two types of I/R injury models are mainly used, warm and cold ischaemia (Section 1.3.3). A number of research studies used rodents as I/R injury models, due to their availability, easy manipulation and because of their small size (Susa *et al.,* 2009; Chen *et al.,* 2012; Wei & Dong, 2012). Experimentally, mice or rat I/R injury is induced by temporarily clamping one of the arteries such as celebral or renal, followed by reperfusion (Willaam *et al.,* 2006; reviewed by Kennedy & Erlich, 2008; Chen *et al.,* 2012). This model allowed scientists to better understand the pathophysiological mechanisms of renal injury. The pigs (porcine) renal anatomy and vascular system is very similar to humans. Moreover, the pig genome showed high sequence homology with humans (reviewed by Kuzmuk & Schook, 2011). For these reasons pigs are an ideal model for studying I/R injury.

Transplantation represents the only available treatment for patients with end-stage renal failure; however kidney graft is limited by a shortage of organ donors. During clinical practise cold-buffered solutions, reducing cold storage times and *ex vivo* perfusion have been adopted to reduce I/R injury (Moers *et al.,* 2009). In particular, *ex vivo* graft preservation is an essential approach due to the specific set of injuries associated with it (reviewed by Bon *et al.,* 2012).

During the last thirteen years a number of genes have been identified for overexpression via *ex vivo* therapy during transplantation (van der Wouden *et al.,* 2004). RNAi represents an novel strategy to reduce I/R injury and two recent *ex vivo* studies have demonstrated efficient silencing of proteins after administration of small interfering RNA (siRNAs) into the preservation solutions used for mouse cardiac grafts and pig kidney grafts (Yang *et al.,* 2011). More recently, Nicholson & Hosgood (2013) announced a novel method of *ex vivo* preservation based on normothermic perfusion. This method restored circulation and allowed the pig kidney to recover function before begin transplanted.

1.4 AIMS OF THE THESIS

1.4.1 Research background

Renal transplantation represents the only choice of therapy for many patients in the end-stages of renal disease; however, complications such as I/R injury present a significant hurdle to overcome during this procedure. The longer a kidney is exposed to an obligated interruption of blood flow the higher the risk of acute damage after transplantation due to reperfusion injury. Thus, minimizing or preventing I/R injury can lead to an improvement of short- and long-term graft survival. A number of viruses have been identified for use as gene therapy vectors (reviewed by Ghosh *et al.,* 2002; Lin *et al.,* 2010; Huang & Kamihira, 2013); amongst these vectors, BacMam virus vectors possess many beneficial features and a number of *in vivo* gene delivery studies have demonstrated their therapeutic potential (reviewed by Airenne *et al.,* 2010; and by Chen *et al.,* 2011).

Of particular relevance for this thesis was a pilot study carried out by Murguía-Meca and colleagues in the Insect Virus Research Group, Oxford Brookes University. They used BacMam to deliver a reporter gene into porcine kidneys *ex vivo* during a hypothermic static cold preservation study. Twelve kidneys from large pigs were perfused with University of Wisconsin (UW) solution containing BacMam virus carrying enhanced green fluorescence protein (*egfp*); viral particles were detected in transduced kidneys at different times and no evidence of additional injury or reduction in cell viability was observed between transduced organs and controls (Murguía-Meca *et al*., 2011).

1.4.2 Research objectives

Therefore, the overall objective of this thesis was to further develop the work initiated by Murguía-Meca *et al.* (2011) ultimately to demonstrate the utility of BacMam as a vector to deliver “protective” genes to reduce I/R injury in an *ex vivo* kidney model. Achieving this goal required a number of challenges to be overcome, including the development of BacMam-specific *in vitro* and *ex vivo* porcine kidney I/R models.

A brief description of the aims and objectives for each thesis chapter are detailed below:

- Transduction of large organs is likely to require high amounts of virus, preferably concentrated in low volumes for ease of handling and improved transduction efficiency. High levels of BacMam expression are often correlated with increasing virus concentration. Therefore, the aim of the work described in Chapter 3 was to compare different concentration methods, both for small scale and large scale culture volumes, and identify the optimal method for future studies.
- The aim of the work described in Chapter 4 was to evaluate the feasibility of using chemical compounds for improving BacMam gene expression and/or delivery *in vitro*, initially in different mammalian cells using reporter genes. Candidates showing potential would be optimised and tested further using protective genes in an *in vitro* model, as described in Chapter 5.
- Having generated BacMam viruses and optimised their concentration, expression and delivery in previous chapters, the work described in Chapter 5 focused on using BacMam to ameliorate I/R injury *in vitro*. To do this required the development of a BacMam-specific *in vitro* model of I/R injury in HK-2 cells.
- The aim of the work described in Chapter 6 was to develop an *ex vivo* cold kidney preservation model of I/R injury and then use the learning gained from previous chapters to reduce the injury, by BacMam delivery of protective genes.
- Chapter 7 contains a summary and discussion of all of the results chapters, including future work.

Chapter 2

Materials and Methods

2.1 MATERIALS

2.1.1 CHEMICALS AND GENERAL REAGENTS

All chemicals were supplied by Sigma-Aldrich Co. Ltd and given as weight/ volume (w/v) unless otherwise stated (Tables 2.1 and 2.2). Solutions were sterilised by autoclaving at 15 pounds pressure per square inch or by filtration through 0.45 µm or 0.2 µm filters supplied by Thermo Fisher Scientific Inc. Foetal bovine serum (FBS) was supplied by Lonza Group Ltd and heat inactivated at 56°C for 30 min.

Table 2.1. Chemical compounds used as transduction enhancers

Chemical Compounds	Description	Stock solution prepared in
Butyrate	Histone deacetylase inhibitor	1M in PBS*
Etoposide	Topoisomerase II inhibitor	0.01 M in DMSO**
Hydroxyurea	DNA synthesis inhibitor	1 M in PBS
Protamine	Polycationic molecule	50 mg/ml in dH_2O***
Cyclohexamide	Protein biosynthesis inhibitor	50 mg/ml in DMSO

* PBS: phosphate buffered saline
** DMSO: dimethyl sulfoxide
*** dH_2O: distilled water

Table 2.2. Reagents used in western blot analysis (method 2.2.27)

Chemical ID	Stock solution	Working volume	Supplied by
5-Bromo-4-Chloro-3'-indolyphosphate p-toluidine (BCIP)	50 mg/ml in dH_2O	33 µl	Fermentas, Thermo Fisher Scientific Inc.
Nitro blue tetrazolium (NBT)	50 mg/ml in 70% DMF*	66 µl	Life Technologies Ltd

* DMF: dimethylformamide

2.1.2 MOLECULAR BIOLOGY REAGENTS

Molecular biology reagents such as restriction enzymes, DNA polymerase and T4 ligase were purchased from New England Biolabs Ltd. Appropriate buffers were supplied with each enzyme (Table 2.3). DNA purification kits were purchased from MACHEREY-NAGEL, Thermo Fisher Scientific Inc. and Qiagen.

Table 2.3. Restriction enzymes

Enzyme ID	Recognition sequence	Buffer
Bgl II	A/GATCT	NEBuffer 3.1
Eco R I	G/AATTC	NEBuffer 2.1 or NEBuffer EcoR I
Not I	GC/GGCCGC	NEBuffer 3.1
Sph I	GCATG/C	NEBuffer 2.1
Xba I	T/CTAGA	NEBuffer 2.1
Xho I	C/TCGAG	NEBuffer 2.1 or NEBuffer 3.1

2.1.3 PLASMID DNA AND BACULOVIRUS TRANSFER VECTORS

All plasmids used were stored at -20°C until required (Table 2.4).

Table 2.4. Plasmid DNA and transfer vectors

Name	Description	Source
pBAC-1	AcMNPV transfer plasmid containing the full length *polh* promoter	Novagen®, Merck Millipore
pCI-neo	Mammalian expression vector carrying the CMV-IE promoter	Prof. I. Bermudez-Diaz (Oxford Brookes University)
pBAC-1_CMV40	AcMNPV transfer vector. The *polh* promoter was replaced with the mammalian CMV-IE promoter	Generated by E. Locanto
pMA_SOD-2	Plasmid DNA carrying *sod-2*	GeneArt®, Life Technologies Ltd
pSOD-2	Transfer vector carrying *sod-2*	Generated by E. Locanto
pMA_BCL-2	Plasmid DNA carrying *bcl-2*	GeneArt®, Life Technologies Ltd
pBCL-2	Transfer vector carrying *bcl-2*	Generated by E. Locanto
pGFP	Transfer vector carrying the enhanced green fluorescence reporter gene (*egfp*)	Generated by E. Locanto
pHM840	Mammalian expression vector carrying the reporter gene *lacZ*	Addgene, USA
pLAcZ	Transfer vector carrying the reporter gene *lacZ*	Generated by E. Locanto

2.1.4 TRANSFECTION REAGENTS

Transfection reagents used in this study are summarised in Table 2.5. The concentration used (5µl) per transfection was prepared according to the manufacturer's protocol.

Table 2.5. Transfection reagents

Transfection reagents	Description	Supplied by
Lipofectin	cationic liposomes	Life Technologies Ltd
***baculo*FECTIN**	positively charged polymer embedded into a porous nanoparticle	Oxford Expression Technologies Ltd

2.1.5 VIRAL DNA

*flash*BAC ULTRA™ DNA (Oxford Expression Technologies Ltd) was used to generate BacMam viruses. A number of BacMam viruses were produced for the purpose of this study and are listed in Table 2.6.

Table 2.6. BacMam viruses generated and used in this study

Virus name	Modification/Description
AcCMV_NULL*	AcCMV with no transgene inserted
AcCMV_EGFP	AcCMV expressing *egfp*
AcCMV_LacZ	AcCMV expressing*LacZ*
AcCMV_SOD-2	AcCMV expressing *sod-2*
AcCMV_SOD-2•6His	AcCMV expressing*sod-2* with histidine-tag at the C-terminal
AcCMV_Bcl-2	AcCMV expressing *bcl-2*

* AcMNPV with CMV promoter replacing the fully deleted polyhedrin promoter; this was named AcCMV.

2.1.6 ANTIBODIES

In Table 2.7 the primary antibodies used in this thesis are listed including their origin and working concentrations. Alkaline phosphatase-conjugated secondary antibodies were used for the detection of proteins. All secondary antibodies used were obtained commercially from Sigma-Aldrich Co. Ltd and are listed in Table 2.8.

Table 2.7. Primary antibodies used for immunofluorescence and western blot analysis

Antibody target	Antibody source species	Supplied/ produce by	Catalogue number	Working dilution (immune-fluorescence)	Incubation time (minutes)	Working dilution (Western Blot)	Incubation time (minutes)
anti-GP64 (AcMNPV)	Mouse	Gift from Dr. L. Volkman (University of California, USA)	-	-	-	1:200	30
anti-VP39 (AcMNPV)	Mouse	Gift from Dr. T. Ohkawa (University of California, USA)	-	-	-	1:1000	30
anti-SOD-2	Rabbit	Santa Cruz Biotechnology Inc.	SC30080	1:100	60	1:500	60
anti-Bcl-2	Mouse	Santa Cruz Biotechnology Inc.	SC492	1:100	60	1:800	60
anti-histidine	Mouse	AbD Serotec Ltd	MCA1396	-	-	1:1000	40
anti-EGFP	Rabbit	Abcam®	AB290	1:200	60	1:1000	60

Table 2.8. Secondary antibodies used for immunofluorescence and western blot analysis

Antibody target	Antibody source species	Conjugate	Supplied/ produce by	Catalogue number	Working dilution	Incubation time (minutes)
anti-mouse IgG	Goat	Alkaline Phosphatase	Sigma-Aldrich Co. Ltd	A3562	1:20000	60
anti-rabbit IgG	Goat	Alkaline Phosphatase	Sigma-Aldrich Co. Ltd	A3687	1:20000	60

2.1.7 CELL LINES AND MEDIA

I. Insect cells

The host cell lines susceptible to AcMNPV used in this study are listed in Table 2.9. Sf-21 cells were maintained in suspension culture in a stirred flask; whereas, Sf-9 cells were grown in shaking flasks. Both insect cell lines were cultured at 28°C.

Table 2.9: Insect cell lines

Cell line	Description	Source	Media	Source of media	Reference
Sf-21	*Spodoptera frugiperda* IPLB-Sf21-AE	Invitrogen™, Life Technologies Ltd	TC100 medium*	GIBCO, Life Technologies Ltd (13055-025)	Vaughn *et al.*, 1977
Sf-9	A clonal cell line isolated of IPLB-Sf21-AE		Sf9-S2 medium EX-CELL® 420 medium	PAA Laboratories Ltd (E15-875) Sigma-Aldrich Co. Ltd (14419C)	Luckow & Summers, 1988

*Media was supplied with 10% (v/v) FBS (Lonza Group Ltd).

II. Mammalian cells

Mammalian cell lines used in this thesis and their culture conditions are listed in Table 2.10. All cell lines were grown as monolayers and maintained at 37°C, 5% carbon dioxide (CO_2).

Table 2.10: Mammalian cell lines

Cell line	Description	Source	Media	Source of media	Reference
HEK293	Human embryonic kidney	SIGMA 85120602	Dulbecco's Modified Eagle Medium*	GIBCO, Life Technologies Ltd	Graham *et al.*, 1977
CHO	Chinese hamster ovary	Gift from Dr. S. Botchway (STFC Central Laser Facility, Oxford, UK)	Dulbecco's Modified Eagle Medium*		Tjio & Puck, 1958
HK-2	Human kidney 2	ATCC® CRL-2190™	Keratinocyte Serum Free		Ryan *et al.*, 1994

*Media was supplied with 10% (v/v) FBS, 100 U/ml penicillin (GIBCO, Life Technologies Ltd) and 100 µg/ml streptomycin (GIBCO, Life Technologies Ltd).

III. Bacterial cells

The *Escherichia coli* (*E. coli*) strain, XL-1 Blue (*genotype (endA1 gyrA96 (nal^R) thi-1 recA1 relA1 lac glnV44 F'[::Tn10 proAB$^+$ lacI^q Δ(lacZ)M15] hsdR17(rK$^-$ mK$^+$)* was used in this study for DNA amplification and cloning (Section 2.2.11). XL-1 Blue cells were grown either in liquid LB (Luria-Bertani) medium (per Liter: 5.0 g yeast extract, 10.0 g Bacto-trypton, 5 g NaCl, pH 7.2) or on LB agar plates containing 15 g/L bacto agar.

2.1.8 PORCINE KIDNEY ORGANS

Experiments were performed in accordance with the principles and procedures of the Oxford Brookes University Ethics Committee. Porcine kidneys were obtained from a local slaughterhouse. Organs were collected within 10 minutes (min) after slaughter (22 week old large white pigs) and flushed *in situ* with SOLTRAN kidney perfusion fluid (0.86% w/v potassium citrate, 0.82% w/v sodium citrate, 3.38% w/v mannitol and 1% w/v magnesium sulphate; http://www.ecomm.baxter.com). Kidneys were then placed in a plastic bag surrounded by ice packs and immediately transported to the laboratory for analysis.

2.2 METHODS

2.2.1 MOLECULAR BIOLOGY TECHNIQUES

2.2.1.I Designing primers

All of the oligonucleotide primers required were designed using gene sequences from the human genome, available from the National Centre for Biotechnology Information (NCBI) website (www.ncbi.nml.com). All forward primers were designed as shown in Figure 2.1 (A). The 5' end of each forward oligonucleotide contained "spacer" bases, the chosen restriction enzyme sequence and the kozak sequence, GCACC (G: guanine; C: cytosine; A: adenine). These were followed by the start codon, ATG (T: thymine) of the leader strand (Figure 2.1 A). The "spacer" bases were used to increase the restriction enzyme efficiency whereas the Kozak sequence was included to enhance translation efficiency of the mRNA (Kozak, 1987). Similarly, the 5' end of each reverse primer was designed to contain the "spacer" bases, a restriction enzyme sequence and a stop codon, TAA (Figure 2.1B). All primers were supplied lyophilised by Eurofins MWG Operon and dissolved following the manufacturer guidelines.

2.2.1.II Polymerase chain reaction (PCR)

Polymerase chain reaction was carried out using a SureCycler 8800 Thermal Cycler (Agilent Technology).

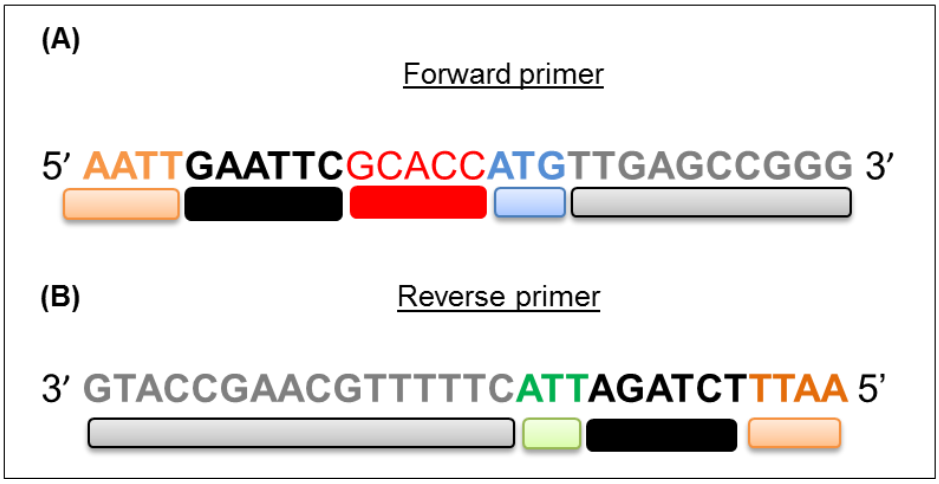

Figure 2.1. Design of forward and reverse primers. (A) Forward and (B) reverse primers. Spacer bases (orange), enzyme sequence (black), Kozak sequence (red) start codon (blue) gene sequence (grey) and stop codon (green).

Taq DNA polymerase (New England Biolabs) was used for analytical PCR and high fidelity Herculase II Fusion DNA Polymerases (Agilent Technologies) was used to amplify sequences for cloning. PCR reactions were prepared in a final volume of 50 µl in thin walled 0.2 ml PCR tubes. Each reaction consisted of DNA template (1-30 ng DNA), deoxynucleotide triphosphate mix (25 mM each dNTP), forward and reverse DNA primers (0.25 µM each primer), 1X reaction buffer and 1 unit (U) of polymerase enzyme. The conditions used for PCR are shown in Table 2.11. The optimal annealing temperature for each set of primers was determined using the temperature gradient option on the SureCycler 8800 Thermal Cycler.

2.2.1.III Purification of PCR products

Amplified PCR products were purified using a NucleoSpin® Extract II kit following manufacturer guidelines (MACHEREY-NAGEL). All buffers were supplied with the kit. The purified DNA was eluted in 20 µl of milli-Q H_2O.

2.2.1.IV DNA gel electrophoresis

Agarose gel electrophoresis was generally used to separate and identify DNA fragments which were then visualized by staining with ethidium bromide. For this project, 1% agarose gels were prepared in 1X TAE buffer (stock solution 50X, per litre: 242 g of Tris, 57.1 ml of glacial acetic acid and 100 ml of 0.5 M EDTA pH 8.0) containing 0.5 µg/ml of ethidium bromide (Severn Biotech Ltd). 2 µl of 6X loading dye (30% (v/v) glycerol and 0.25% (w/v) bromophenol blue) was added to each DNA sample.

A DNA ladder (New England Biolabs Ltd) was used to determine the size of the separated DNA fragments. The electrophoresis apparatus was set to run at a 100 Voltage (V) for approximately 1 h. The stained gel was analysed and documented using a UV trans-illuminator (Ingeneous system supplied by Syngene Bio Imaging).

Table 2.11. Optimised cycling conditions for amplification of specific DNA fragments

Amplified fragment	Denaturation	Annealing	Extension
SV40 Poly A	1 cycle: 95°C 5 min	30 cycles: 95°C 1 min 55°C 30 sec 72°C 2 min	1 cycle: 72°C 10 min
EGFP	1 cycle: 94°C 30 sec	30 cycles: 94°C 30 sec 61°C 60 sec 68°C 1 min	1 cycle: 68°C 5min
SOD-2	1 cycle: 94°C 30 sec	30 cycles: 94°C 30 sec 64°C 60 sec 68°C 1 min	1 cycle: 68°C 5min
BCL-2	1 cycle: 94°C 30 sec	30 cycles: 94°C 30 sec 61°C 60 sec 68°C 1 min	1 cycle: 68°C 5min
RT-PCR (Section 2.2.17)	1 cycle: 94°C 2 min	35 cycles: 94°C 30 sec 57°C 30 sec 72°C 30 sec	1 cycle: 72°C 5min

2.2.1.V Gel extraction and purification of DNA fragments

DNA fragments to be purified were run on a 1% (w/v) agarose gel containing ethidium bromide (Section 2.2.1.IV). DNA migration patterns were visualised using an ultraviolet (UV) trans-illuminator and fragments were then excised from the gel using a sterile scalpel and weighed (Mettler PE360 Delta Range Balance). DNA samples were purified using NucleoSpin® Extract II kit (MACHEREY-NAGEL) following the manufacturers guidelines. The purified DNA was then eluted from the silica membrane using milli-Q H_2O.

2.2.1.VI Restriction enzyme digestion

Restriction digestions were carried out in a final reaction volume of 20 µl. Each reaction consisted of 500-1500 ng of DNA, 1-2 units (U) of restriction enzyme, 1X buffer as supplied by the manufacturer and if required 2 µl of 10X bovine serum albumin (BSA). Reactions were routinely left to incubate at 37°C for 1-2 h and analysed by ethidium bromide-stained agarose gels (Section 2.2.1.IV).

2.2.1.VII 5' end dephosphorylation

Following restriction digestion, the 5' end of DNA plasmids were dephosphorylated using shrimp alkaline phosphatase following the manufacturers guidelines (Promega). This treatment prevented relegation of the linearized plasmid. Treated samples were purified as described in Section 2.2.1.V.

2.2.1.VIII DNA ligation

A number of ligation reactions were set up to clone digested DNA fragments into digested and SAP treated plasmid DNA. T4 DNA ligase (New England Biolabs Ltd) was used according to manufacturer's guidelines. A control sample containing vector DNA only was also prepared to test the restriction enzyme digestion efficiency. 2 µl of ligation reaction was then used to transform 100 µl competent bacteria cells (section 2.2.1.IX).

2.2.1.IX Transformation of bacteria with plasmid DNA

Competent bacteria cells (section 2.1.7.III) were transformed following the heat-shock protocol (Sambrook & Russell, 2001). 100 µl of cells were defrosted slowly on ice and 5 µl of the ligated product (section 2.2.1.IX) was added. Transformed cells were then plated onto LB agar plates (section 2.1.7-III) containing ampicillin antibiotic (stock solution: 50 mg/ml in dH_2O; working concentration: 50 µg/ml) and grown overnight at 37°C.

2.2.1.X Screening bacteria for recombinant plasmids

Cracking screening was used to screen bacteria colonies for the presence of recombinant DNA. Individual colonies (Section 2.2.1.IX) were picked using a sterile tooth pick and diluted into 25 µl of sterile dH_2O by pipetting. 2 µl of the dissolved bacteria were then further diluted into 300 µl of LB media containing the appropriate antibiotic. 25 µl of cracking buffer (0.02 M NaOH, 10 mM EDTA, 1X SDS and 10% (v/v) glycerol) was then added to the 25 µl of distilled water (dH_2O) containing bacteria cells. The reaction was quickly mixed and loaded on a 1% agarose gel (Section 2.2.1.IV). Two negative controls were included; a self-ligated control and circular parental plasmid DNA.

Samples were analysed under UV light for positive colonies as determined by the correct band size. Colonies corresponding to the correct DNA size were used to inoculate 5 ml bacteria cultures.

2.2.1.XI Purification of plasmid DNA

a. Small scale purification (mini-prep)

Plasmid DNA purification was carried out using GeneJET™ plasmid miniprep kit following the manufacturer's guidelines (Fermentas, Thermo Fisher Scientific Inc). The purified DNA was eluted from the columns using milli-Q H_2O.

b. Medium scale purification (midi-prep)

100 ml of bacteria culture were purified using a midi-prep kit supplied by Qiagen. This methodology was similar to the plasmid DNA mini-prep described above. The plasmid DNA was eluted and precipitated using 0.7 volumes of isopropanol; DNA pellets were then air-dried at room temperature and resuspended in 100 µl of milli-Q H_2O.

2.2.1.XII Plasmid DNA sequencing

Cloned DNA fragments were sequenced by Geneservice Ltd, Oxford to confirm their identity and integrity. Appropriate sequencing primers were designed or obtained from Geneservice Ltd. Sequence data was analysed using Gene Doc software V 2.7 developed by K. Nicholas (http://www.nrbsc.org/gfx/genedoc/).

2.2.1.XIII Quantitative gene expression analysis

Complementary DNA (cDNA) synthesis was performed in a two-step reaction using Cells-to-cDNA II Kit (Ambion, Life Technologies Ltd) according to the manufacturer's protocol. For reverse transcription a two-step RT-PCR protocol supplied by the manufacturer was followed. PCR amplification was performed using 5 µl of RT reaction and carried out as described in Section 2.2.1.II. The resulting PCR product was then analysed on a 1% agarose gel (Section 2.2.1.IV).

2.2.1.XIV RT^2 profiler™ PCR array

RT^2 Profiler™ PCR array (Arikawa *et al.,* 2011), supplied by SABiosciences, Qiagen (PAHS-052), was used to analyse *in vitro* cellular response to baculovirus transduction. Total RNA was extracted using a mirVana miRNA isolation kit (Ambion®, Life Technologies Ltd) following the manufacture guideline.

The isolated RNA was quantified by measuring its absorbance at 260 nm using a spectrophotometer (DU® 730; Beckman Coulter, Inc.) and RNA quality was assessed by non-denaturing agarose gel electrophoresis. Briefly, 1X agarose gel (Ambion) was dissolved in 1X northern buffer (Ambion) previously treated with diethylpyrocarbonate (DEPC)-water. RNA was converted into cDNA using RT^2 First Strand kit following the manufacturer's guidelines (SABiosciences, Qiagen).

The cDNA was loaded into a human innate and adptive immune response 96 well plate supplied by SABiosciences, (Qiagen) and amplified using an Applied Biosystems ABI 7500 cycler. Data was analysed using the manufacturer's data analysis software (http://pcrdataanalysis.sabiosciences.com/pcr/arrayanalysis.php).

Relative gene expression was calculated using the standard $\Delta\Delta C_t$ method:

$$\Delta\Delta C_t = \Delta C_t \text{ (experimental)} - \Delta C_t \text{ (control)}$$

The fold-change in gene expression was calculated as: $2^{(-\Delta\Delta Ct)}$.

2.2.2 CELL CULTURE TECHNIQUES

2.2.2.I Insect cell culture

Sf-9 and Sf-21 cells were maintained at 28°C in Erlermeyer flasks (Corning®) and glass Spinner flasks respectively. Sf-9 cells were agitated at 125 rpm using an orbital shaker (CERTOMAT® S II, Sartorius Ltd) and Sf-21 cells were cultured in a spinner shaker (MCS-104S, Bibby Scientific Ltd). Cell lines were passaged before reaching their stationary phase using appropriate medium (Section 2.1.7-I). The seeding density and cell viability was determined by trypan blue (0.2% solution) dye exclusion staining using a Countess® Automated Cell Counter (Life Technologies Ltd).

For long term storage, insect cells were frozen in liquid nitrogen. Cells were pelleted by centrifugation for 10 min at 500 *xg* (Heraeus™ Fresco 21, Thermo Scientific). Cells were then re-suspended at a final density of 10^6-10^7 cells/ml in the required media (Section 2.1.7-I) supplemented with 20% (v/v) FBS and 10% (v/v) DMSO. Subsequently, 1 ml aliquots of the cell suspension was dispensed into cryovials and placed into an isopropanol container for controlled cooling (rate 1°C/min; Mr. Frosty, Nalgene). The container was then placed into a -70°C freezer overnight. Cryovials containing the cells were then transferred to a liquid nitrogen storage tank. For recovery, insect cells were removed from the liquid nitrogen tank and rapidly thawed in a water bath at 28°C.

Cells were diluted into 10 ml of suitable media (Section 2.1.7-I) and pelleted by slow speed centrifugation (10 min at 500 *xg*). Re-suspended cells were dispensed into a T75 tissue culture flask (Sarstedt Inc.) and incubated at 28°C.

2.2.2.II Mammalian cell culture

All mammalian cell lines were adherent and maintained at 37°C, 5% CO_2 in 100 mm cell culture dishes (Sarsted Ltd). Cells were passaged when cell density reached 80% of confluence. Briefly, cell culture media was removed and cells were washed using 1X PBS. Cells were then incubated with 1X of 0.05% trypsin-ethylenediaminetetraacetic acid (GIBCO, Life Technologies Ltd) at 37°C for 5 min. Subsequently, pre-warmed medium was added to inactivate trypsin and remove EDTA. Cells were centrifuged at 500 *xg* for 5 min and re-suspended in fresh media. At this stage cells were distributed into a new cell culture dish for sub-culturing or counted and aliquoted for future experimental analysis.

For long term storage mammalian cells were frozen in liquid nitrogen. Cells were pelleted by centrifugation for 10 min at 500 *xg* (Heraeus™ Fresco 21, Thermo Scientific). Cell pellets were re-suspended in 70% (v/v) of medium (section 2.1.7-II), 10% (v/v) DMSO and 20% (v/v) of FBS. Cells were aliquoted in cryovials and placed in an isopropanol container for controlled cooling (rate 1°C/min at -70°C freezer for 24 hours (h). For permanent storage the cryovials were transferred to a liquid nitrogen storage tank. Cells were recovered by thawing the cryovials at 37°C. Subsequently, cells were washed, centrifuged and then re-suspended into a 100 mm dish containing 10 ml of warm complete medium (Section 2.1.7-II).

2.2.2.III Growth and storage of *E. coli* cells

XL-1 Blue competent cells were generated using the calcium chloride (CaCl) method (Sambrook and Russell, 2001) and stored at -70°C in aliquots of 100 µl. When required, XL-1 Blue competent cells were thawed on ice and used to inoculate LB media. Bacterial cultures were grown overnight at 37°C in a shaking incubator in the presence of the ampicillin antibiotic (stock solution: 50 mg/ml in dH_2O; working concentration: 50 µg/ml). For short term storage, cultures were stored at 4°C whereas for long term storage, bacterial cultures were stored at -70°C as glycerol stocks as follow: 590 µl of bacteria cultures were added to 160 µl of 80% glycerol in a 1 ml cryovial and gently mixed.

2.2.3 STANDARD BACMAM TECHNIQUES

2.2.3.I Transfection of cells with DNA

Transient gene expression and virus generation were carried out in insect cells using the liposome formulated transfection reagent Lipofectin® (Invitrogen). Transfections were carried out using the protocol supplied by the manufacturer.

a. Transient gene expression in insect and mammalian cells

1 µg of DNA was diluted in 100 µl of TC100 media (without FBS) in a 1.5 ml microfuge tube. Similar, 5 µl of lipofectin reagent was diluted in 100 µl of TC100 media in a separate microfuge tube. Subsequently, DNA and lipofectin were mixed together and left at room temperature for 30 min. 800 µl of TC100 was added to the lipofectin-DNA complex mix and applied to the cells to be transfected. After the transfection mix was applied to the cells, they were incubated for 5 h at 37°C before 1 ml of the relevant media was added to the transfected cells.

The gene copy number of transiently transfected cells was calculated using the following formula:

$$\text{Number of copies}^{1} = \frac{(\text{amount of DNA in ng}) \times (6.022\times10^{23}\ \text{molecules/mole})^{*}}{(\text{length of template in bp}) \times (\text{ng/g})^{**} \times (\text{weight of a bp})^{***}}$$

* Avogadro's number
** ng/g= 1 parts per billion (ppb) = $1X10^{9}$
*** The average weight of a base pair (bp) is 650 Daltons
[1] free-access copy number calculator developed by Staroscik, 2004

b. Virus generation in insect cells

BacMam viruses were generated by homologous recombination between viral DNA (Section 2.1.4) and a transfer vector DNA. Sf-9 insect cells were co-transfected with viral DNA (*flash*BAC ULTRA™ and transfer vector DNA following the manufacturer guidelines (Oxford Expression Technologies Ltd). The virus containing supernatant was then harvested and stored at 4°C. FBS (5% v/v) was added to the inoculum to improve stability during storage**.**

2.2.3.II Virus amplification

Virus stocks were amplified in Sf-9 cells as described in King and Possee (1992). The virus containing supernatant was aliquoted into sterile tubes, supplemented with 5% (v/v) FBS and stored at 4°C.

2.2.3.III Virus titration

a. Plaque assay

BacMam stocks were titrated by plaque assay as described by King and Possee (1992). Plaques were visualized by the addition of 1 ml of neutral red (0.5% neutral red stock solution was diluted in 15ml 1X PBS). Stained cells were incubated for 5 h at 28°C. The liquid overlay was then removed and dishes inverted in the dark to allow the dissipation of the colour. Plaques were counted and the virus titre determined using the calculation below.

Plaque forming unit (pfu)/ml = average plaques counted X Dilution factor X10

b. Quantitative real-time PCR (QPCR)

QPCR titration was carried out using *baculo*QUANT ALL-IN-ONE™ (Oxford Expression Technologies Ltd) following the manufacturer's instructions. The purified DNA was loaded into a 96-well plate and amplified using an Applied Biosystems ABI 7500 instrumentusing; the cycling conditions listed in Table 2.12

Table2.12. QPCR cycling conditions

	Temperature	Time	Number of cycles
Enzyme activation	95°C	10 min	1
Denaturation	95°C	15 sec	
Annealing/ Extension	60°C	60 sec	40

On completion of the QPCR cycle programme, the unknown virus titre was calculated using C_t values which were calculated by the SDS software. Titres were expressed as Qpfu/ml.

2.2.3.IV BacMam concentration methods

a. High-speed centrifugation

Viral particles harvested with supernatant of infected Sf-9 cell medium were first clarified by centrifugation (4550 *xg* for 20 min at 4°C), then the viral particles were concentrated by high-speed centrifugation (Beckman Coulter Inc, J25-I rotor) at 75 600 *xg* for 1 h. Pelleted virus was re-suspended in 1 ml of 1X PBS and left to rest for 16 h at 4°C before were collected.

b. Low-speed centrifugation

A large volume of viral particles (1.2 litres) were concentrated by low-speed centrifugation. This methodology is similar to the high-speed centrifugation described above. BacMam viruses were initially harvested from Sf-9 cell by centrifugation (4550 *xg* for 20 min at 4°C) before be concentrated by low-speed centrifugation (Beckman Coulter Inc, JA-14 rotor) at 25 800 *xg* for 16 h. Virus pellet was re-suspended in 10 ml of 1X PBS . The concentrated virus was left to rest a 4°C for approximately 20 h before were collected.

2.2.3.V *In vitro* transduction of mammalian cells

Mammalian cells (Table 2.10) were seeded at the appropriate concentration and incubated overnight at 37°C in a 5% CO_2 incubator. The following day, cells were transduced with BacMam viruses (Table 2.6) at an MOI of 50-150 pfu/cell and incubated at 37°C for 1 h in 5% CO_2 incubator. The virus inoculum was then replaced with suitable medium (Table 2.10) and cells were returned to 37°C in 5% CO_2 incubator for the required time. In an experiment to improve transduction efficiency, cells were transduced in the presence and absence of different chemicals and transfection reagents (Tables 2.1 and 2.5, respectively) following the manufacturer's guidelines.

2.2.3.VI *Ex vivo* transduction of porcine kidneys

Flushed kidney organs (Section 2.1.8) were cannulated and perfused through the renal artery with 200 ml of cold Belzer University of Wisconsin (UW) solution (Bridge to Life Ltd) with BacMam virus (Group 1) or without virus (Group 2). During transduction, the solution was collected and recirculated using a low-speed (10 rpm) peristaltic pump (Watson Marlow 505 S, Gemini BV). Both groups of kidney were transduced for 24 h at 4°C. Tissue samples were collected using a 10 ml syringe at 0, 4 and 24 h post-transduction (hpt) and cells were immediately dissociated enzymatically using collagenase (Sigma-Aldrich Co. Ltd).

Tissue fragments were minced thoroughly using scalpel blades (Thermo Fisher Scientific Inc) and incubated in 1 mg/ml of collagenase enzyme (Sigma-Aldrich Co. Ltd) at 37°C for 20 min. Cells were sieved sequentially through a 100-µm and 40-µm cell strainer (BD Bioscience Ltd) to remove the undigested tissue. The filtered single cell suspension was then pelleted (500 *xg*, 5 min), washed in 1X PBS three times and re-suspended in culture medium for further analysis.

2.2.4 PROTEIN ANALYSIS TECHNIQUES

2.2.4.I Protein sample preparation

Protein samples from BacMam transduced mammalian cells (Sections 2.2.3.V and VI) were harvested, at different time points and analysed by sodium dodecyl sulfate polyacrylamide gel electrophoresis (SDS-PAGE). Samples were centrifuged at 2000 *xg* for 5 min. Supernatant was discarded and cell pellet re-suspended in 80 µl of 1X PBS and 20 µl of 5X loading buffer (250 mM Tris-HCl (pH 6.8), 25% (v/v) β-metacaptoethanol, 10% (v/v) SDS, 50% (v/v) glycerol and 0.5% bromophenol blue). Prepared samples were incubated for 10 min in a boiling water bath (100°C) before being loaded on a 12% SDS-PAGE gel and electrophoresed using the mini-PROTEAN vertical gel electrophoresis system (Bio-Rad).

2.2.4.II SDS-PAGE gel

12% SDS-PAGE gels were prepared as described in Sambrook and Russell (2001). Samples (section 2.2.4.I) were then loaded and electrophoresed at 100 V during passage through the stacking gel and the voltage was then increased to 200 V during passage through the resolving gel.

2.2.4.III Staining SDS-PAGE

a. Coomassie brilliant blue staining

Separated proteins (section 2.2.4.II) were visualized using the Coomassie blue staining method described in Meyer & Lambert, (1965). For long term storage, stained gels were, initially, equilibrated in a gel drying buffer (40% (v/v) methanol, 10% (v/v) glycerol and 7.5% glacial acetic acid) for 30 min. The equilibrated gels were then placed between two cellophane sheets, previously soaked in dH_2O. The cellophane sandwich was secured within a plastic drying frame (Bio-Rad Inc.) and left to air-dry at room temperature.

b. Silver staining

Proteins fractioned by PAGE gels (Section 2.2.4.II) were visualized using FASTSilver™ following the manufacturer's guidelines (G-Biosciences). All reagents and solutions except ethanol, glacial acetic acid and dH_2O were supplied with the kit. Images were recorded using an EPSON stylus SX105 visible light scanner.

2.2.4.IV Western blot

Proteins separated on SDS-PAGE gels (section 2.2.4.II) were transferred onto a nitrocellulose membrane (GE healthcare, UK) and analysed by Western blot. Initially, the protein gels were incubated in transfer buffer (48 mM Tris, 39 mM glycine, 20% methanol and 1.3 mM SDS) for 5 minutes together with the nitrocellulose membrane and filter papers as described in Sambrook and Russel (2001). Following the transfer, membranes were incubated in 5% milk dissolved in PBST (1X PBS containing 0.1% (v/v) of Tween20) and agitated at room temperature for 1 h to prevent non-specific binding. Blocked membranes were then treated with the appropriate primary antibodies using the optimized dilution for either 30 or 60 min depending on the antibody used (Table 2.7). Subsequently, membranes were washed 3X with PBST and incubated with a secondary antibody conjugated with alkaline phosphatase for 60 min (Table 2.8). To remove any background, membranes were washed 3X with PBST. Bound proteins were visualized using alkaline phosphatase buffer (100 mM Tris-HCl (pH=9.5), 100 mM NaCl and 5 mM MgCl) containing 66 µl of NBT and 33 µl of BCIP (Table 2.2). The membrane was washed with dH_2O and any excess liquid was removed using filter paper. Band densitometry was carried out using GelQuantNET softwar (BiochemLabSolutions). Statistical analysis was performed as described in Section 2.2.43.

2.2.5 MICROSCOPY, IMMUNOFLUORESCENCE/IMMUNOHISTOCHEMISTRY TECHNIQUES

2.2.5.I Fluorescence microscope

EGFP-positive cells were imaged using an inverted fluorescence microscope (Axiovert 135, ZEISS) 10X objective. Data were captured using a ProgRes® microscope camera (JENOPTIK Optical Systems).

a. Quantitative image analysis

The EGFP fluorescence cells were measured by ImageJ software. Region with the same area was drawn around each cell to be measured. For each images, the fluorescence of 13 EGFP positive cells was calculated. An identical region was also placed in an area without fluorescence to be used for background subtraction. The average fluorescence intensity in the area of interest was calculated for each measured cells. The following formula was used to calculate the corrected total cell fluorescence (CTCF).

CTCF= Integrated Density– (Area of selected cell x Mean fluorescence of background)

Fold change in *egfp* expression, related to the untreated transduced HEK cells, were calculated and plotted on a graph using GraphPad Prism version 5 for Windows (GraphPad Software Inc., USA). All parameters during image acquisition and quantification were the same.

2.2.5.II Confocal microscopy

Transduced BacMam cells (Sections 2.2.3.V and VI) were fixed, at different time points, in 4% paraformaldehyde solution (Thermo Fisher Scientific Inc.). Adherent cells were grown on glass coverslips in 35mm tissue culture dishes supplied by PAA Laboratories Ltd and at the required time, cells were washed twice with PBS before being treated for 1 h with 0.5 ml of 4% (v/v) paraformaldehyde. Suspension cells were harvested by centrifugation at 500 *xg* for 5 min; subsequently, the supernatant was discarded and the cell pellet was washed twice in 1X PBS before being fixed with 0.5 ml 4% (v/v) paraformaldehyde. Fixed cells where then washed once 1X PBS and re-suspended in 1 ml of fresh PBS. Samples were stored at 4°C or processed immediately as follows.

Fixed adherent samples were washed with 1X PBS containing 1% BSA (Sigma-Aldrich Co. Ltd) and 0.1% (v/v) Triton X-100 (Sigma-Aldrich Co. Ltd) which permeabilizes the cell membrane. Fixed suspension cells were deposited onto a clear defined area of a glass slide (Shandon cyto-spin 3 slides) using CytoSpin centrifuge (Shandon Cytospin 3, Thermo Scientific) before being treated with 1X PBS-BSA-Triton X-100. Samples were washed twice using 1X PBS and twice with 1X PBS-BSA blocking solution before being incubated for 1 h with the appropriate primary antibody (Table 2.7).

Cells were then washed three times with PBS-BSA and treated with secondary antibodies at the relevant dilution for 60 min (Table 2.8). Any unbound antibody was washed out and coverslips were mounted onto microscopy slides using Vectashield (Vector Laboratories), a mounting media containing the nuclear label 4',6-diamidino-2-phenylindole (DAPI). A clear nail-varnish was used to seal the mounted samples before being stored in the dark at 4°C.

Confocal microscopy was performed on fixed cells and tissue sections using a Zeiss LSM 510 Meta confocal system using either X40 or X63 oil immersion lens. Multitrack analysis was carried out in order to analyse green fluorescence (488nm excitation, band pass filter 505-530nm), red and blue (DAPI) fluorescence (543nm excitation, long pass filter 560nm for red, and 405 excitation, band pass filter 420-480nm for blue). Image data were analysed using LSM Image browser software.

2.2.5.III Histological analysis of kidney tissue

Transduced and non-transduced porcine kidneys (Sections 2.2.3. VI) were sectioned (5 mm horizontal and 1 cm vertical) for histological analysis. Paraffin-embedded tissue sections are the mostly used technique for immunochemistry and were utilized in this project. To preserve morphology, kidney sections were immediately fixed in 4% (v/v) formaldehyde and incubated for 3 h at room temperature. Fixed kidney tissues were dehydrated by incubating the samples in an increasing concentration of alcohol solutions, 70%, 90% and two changes of absolute ethanol (100%) of 1 hour each. This ensured that all the water was removed. When dehydration was completed, tissues were treated with an intermediate fluid that was miscible with ethanol and paraffin, xylene. Xylene was then drained off and specimens were placed in a disposable embedding mould to be infiltrated with two-three 30 min. changes of paraffin wax-embedding the kidney tissues in paraffin wax. Tissue paraffin blocks were sectioned to a thickness of 5 µm using a Spencer 820 microtome. Sections were collected with forceps and transferred to a 37°C water bath to ensure straight edges and the removal of excess wax. Tissues specimens were then mounted on positively charged microscope slides (Superfrost® Plus Micro Slide, VWR International) and dried in an incubator at 37°C.

2.2.5.IV Preparation of tissue sections

To perform histological analysis, paraffin was removed from the surface of the kidney sections; tissue sections were incubated twice in xylene for 5 min at room temperature. Sections were then rehydrated in 100%, 70% and 30% ethanol solutions for 1 min each.

The slides were then washed with dH_2O for 5 min before being used in further applications.

2.2.5.V Hematoxylin and eosin (H&E) staining

Histological specimens of kidney tissue were stained with H&E (Mayer, 1896) following manufacturer guidelines (Sigma-Aldrich Co. Ltd). Haematoxylin dye stains basophilic structures such as nuclei, ribosomes and rough endoplasmic reticulum a purple/blue colour. In contrast, the acidic dye eosin stains eosinophilic structures like cytoplasmic proteins a pink/red colour. Stained sections were mounted using Vectashield (Vector Laboratories) and examined using an Axioplan microscope (Carl Zeiss microscopy Ltd) and images captured using a ProgRes® C3 microscope camera (JENOPTIK Optical Systems).

2.2.5.VI Periodic acid-schiff (PAS) staining

PAS is a staining method used to detect polysaccharide, glycoproteins, glycolipids and tissue basement membranes; the periodic acid oxidises the tissue carbohydrates producing a pair of aldehyde groups in each broken monosaccharide ring. Subsequently, in the second reaction, the aldehyde groups react with the Schiff reagent staining the tissue component to which the carbohydrates are attached (purple-magenta colour). The intensity of the colour is related to the concentration of hydroxyl groups present in each monosaccharide unit. A basic stain (*e.g.* haematoxylin) is often used as a counterstain to visualize other tissue elements. PAS staining was used to characterise tubular and glomerular basement membranes following the manufacturer guidelines. Dehydrated tissue sections were mounted using Vectashield (Vector Laboratories). Stained sections were examined and imaged as described in H&E stain (Section 2.2.5.V).

2.2.5.VII Immunohistochemistry of sections

To detect intracellular proteins, deparaffinised and hydrated kidney sections were permeabilised with 1X PBS containing 0.1% (v/v) Triton X-100. Tissue sections were blocked in 1X PBS-BSA prior to being incubated in the appropriate primary antibodies for 60 min at room temeperature (Table 2.7). Slides were washed three times in 1X PBS and incubated with the indicated secondary antibodies for 60 min (Table 2.8) at room temperature. Finally, any unbound antibody was removed using PBS and sections were mounted with Vectashield (Vector Laboratories). Confocal analysis was carried out as described in Section 2.2.II

2.2.6 ENZYMATIC ASSAYS

Enzymatic assays were used following the manufacturers guidelines and summarised in the Table 2.13.

2.2.7 METHODS TO ANALYSE REPORTER GENES

2.2.7.I Flow cytometry

Mammalian cells containing a *egfp* and their controls were harvested and re-suspended in 1 ml of 1X PBS. The percentages of EGFP-positive cells was analysed by flow cytometer on a Gallios® flow cytometer (Beckman Coulter Inc). Samples were prepared in a polypropylene tube (Greiner bio-one) by diluting 0.5 ml of cells in 0.5 ml of IsoFlow sheath fluid. Calibration beads (10 µl) were also added to each sample to determine the number of cells. A quantitative analysis was carried out using the flow cytometer data; transduction efficiency was acquired by comparing the number of fluorescent cells with the fluorescence intensity obtained for non-treated control cells

2.2.7.II Fluorescence plate reader

Fluorescence cells were harvested and counted before being seeded at a density of $2x10^5$ cells/ well in a 96-well plate (flat clear bottom with black walls; Corning®). Fluorescence was recorded at an excitation wavelength of 485 nm and an emission wavelength of 535 nm using an Infinite® 200pro microplate reader (Tecan Group Ltd). Data were automatically inserted into an Excel Microsoft® file and the mean value of 16 readings per well calculated. Data were normalised against control cells.

Table 2.13. Enzymatic assays used in this study

Assay type	Used for the detection of	Supplied by
Cell viability	Trypan blue exclusion assay	Life Technologies Ltd
	Adenosine triphosphate (ATP) quantification	Promega
	Lactate Dehydrogenase (LDH) activity assay	Promega
SOD Kit-WST assay	SOD-2 activity	Sigma-Aldrich Co. Ltd
ApoTarget™	Caspase-3 protease Assay	Novex®, Life Technologies Ltd
JC-1	Mitochondrial membrane potential	Molecular Probes®, Life Technologies Ltd
X-Gal	β-galactosidase activity	Sigma-Aldrich Co. Ltd

2.1 Statistical analysis

All data were analysed using GraphPad Prism version 5 for Windows (GraphPad Software Inc., USA) with results displayed as mean ± SEM. Each experiment was performed in triplicate. Statistical analysis was performed using both one- and two-way ANOVA with a Bonferroni post-test that compare replicative mean values, unless otherwise stated. A p-value of <0.05 was considered statistically significant.

Chapter 3

BacMam concentration methods

3.1 INTRODUCTION

The ability of BacMam viruses to delivery recombinant genes into mammalian cells is well documented (reviewed by Kost *et al.,* 2010; Chatterjee *et al.,* 2013). To date BacMam has been widely used for the production of therapeutic proteins and for *in vivo* / *ex vivo* gene delivery applications (reviewed by Kost *et al.,* 2010; Wang *et al.,* 2010). The production of BacMam particles is relatively easy when compared to mammalian viruses; for example, BacMam are produced ($1x10^8$ to $2x10^8$ pfu/ml) and released into the insect cell culture media, unlike adenovirus that requires cell lysis during production (reviewed by Kost *et al.,* 2010). However, obtaining high purity and high titres ($1x10^{10}$ pfu/ml) of BacMam are critical for its application in gene therapy. The presence of impurities could initiate host immune response, leading to unwanted reactions, as well as enhancing or inhibiting transduction efficiencies (Tenenbaum *et al.,* 1999; reviewed by Rodrigues *et. al.,* 2007). Therefore, the development of an efficient scalable concentration method that allows the production of a pure and highly concentrated BacMam virus is of primary importance.

In the last decade, several methods have been described for purifying and concentrating baculovirus (Barsoum, 1999; Wu *et al.,* 2007; Gerster *et al.,* 2013). Ultracentrifugation, with or without a sucrose cushion, has been widely used (O'Reilly *et al.,* 1994; reviewed by Aucoin *et al.,* 2010). However, this is a time-consuming method and typically, less than 50% of the infectious material is recovered after the concentration step (O'Reilly *et al.,* 1994). Furthermore, there are several disadvantages with this method such as small volume capacity of high-speed rotors; difficulty in re-suspension of the virus pellet due to the presence of impurities (*e.g.* insect cell debris, cell proteins and host cell DNA); the formation of virus aggregates and loss of infectivity due to hydrodynamic shear stress. In the last two decades, these limitations have prompted researchers to seek to improve baculovirus concentration methods.

Barsoum (1999) was the first to report the use of a chromatography method, based on a cation-exchange resin, to concentrate baculovirus between 25- and 60-fold without causing any major virus aggregation (Patent number US 6326183 B1). Duisit *et al.* (1999) showed that baculovirus was able to strongly bind, through electrostatic interactions, to a heparin type I-sepharose column; however, because baculovirus fractions were partially eluted in 0.5 M NaCl solution and mostly eluted in 1M NaCl they were not infectious in insect cells. Two different hypotheses were assumed: 1M NaCl irreversibly inactivated the virus or alternatively, high salt fractions could correspond with a heterogeneous population of infectious or non-infectious baculovirus (Duisit *et al.,* 1999).

Subsequently, other researchers investigated different chromatographic approaches to concentrate baculovirus particles, including ion-exchange (Wu *et al.,* 2007; Transfiguracion *et al.,* 2011; Grein *et al.,* 2012), affinity (Chen *et al.,* 2009), size exclusion and resin-based chromatography (Hu *et al.,* 2003; Transfiguracion *et al.,* 2007) as well as using tangential flow ultrafiltration membranes (Michalsky *et al.,* 2009). All of these methods varied in a number of aspects such as the mechanism used to concentrate viral particles, the initial virus volume used, time required, cost and yield of active baculovirus recovered. Therefore, finding the conditions best suited for baculovirus concentration still remains a critical step.

The goal of this study was to identify a reproducible and efficient method to concentrate BacMam viruses. To this end a number of small-scale analytical methods were tested, including high-speed centrifugation without a sucrose cushion (Beckman Coulter Avanti®, J-25I, rotor J-25.5) and polyethylene glycol (PEG, Sigma-Aldrich) with a molecular weight (MW) of 4000 Dalton (Da). Additionally, Fast-Trap (Merck) and short monolithic chromatographic columns (CIM; BIA Separations) were also evaluated as alternative concentration methods. The second objective of this research was to concentrate large volumes (1.2 to 2.4 litres) of virus that could produce enough BacMam for *ex vivo* kidney transduction by low-speed centrifugation (Beckman Coulter Avanti® J-25I, rotor JA-14). Concentration methods were analysed on the basis of (1) virus recovery yield, (2) purity and (3) infectivity in insect cells.

In this Chapter only high- and low-speed centrifugation methods are presented; whereas, PEG, Fast-Trap and CIM concentration methods are included as supplementary data in the CD attached to this thesis (Chapter 3-S1, 3-S2 and 3-S3, respectively).

3.2 BACMAM CONCENTRATION BY HIGH-SPEED CENTRIFUGATION

BacMam viruses were generated (see supplementary data CD attached to this thesis) expressing either the *egfp* or *sod-2* gene under the control of the cytomegalovirus-immediate early (CMV-IE) promoter. Viruses were amplified in Sf-9 cells (Section 2.2.3.II) and then titrated by plaque assay (Section 2.2.3.III.a) before being used to assess the different concentration methods. QPCR (Section 2.2.3.III.b) was used to measure the viral DNA present within the samples; while, plaque assays were carried out to determine the yield of active virus after concentration.

Recovery and activity yields were calculated by dividing the total number of viral particles in the concentrated virus (CV) by that in the original virus (OV) stock used; this value was then multiplied by 100 to obtain a percentage (%).

$$\text{Recovery/ activity yield (\%)} = \frac{\text{№ CV particles}}{\text{№ OV particles}} \text{ X 100}$$

High-speed centrifugation is a quick and easy method for concentration of BacMam viruses. In this thesis a centrifugation step, without the need for a sucrose density gradient, was developed and optimized (Section 2.2.3.IV.a).

3.2.I Experimental optimization

To analyse whether long centrifugation periods had a detrimental effect on virus recovery yields, BacMam viruses were subjected to different times of centrifugation. Briefly, three AcCMV_EGFP samples of 21 ml each were centrifuged at 75600 *xg* (25 000 rpm) for 1, 4 and 24 hours (h), respectively (Beckman Coulter Avanti J25-I with J-25.5 rotor). After centrifugation the supernatant, devoid of BacMam virus, was discarded into an appropriate biohazard waste and a small amount was collected for further analysis. The virus pellet (concentrated-pool) was resuspended in 1X PBS, to a final volume of 1 ml, at 4°C for 16 h before being collected and analysed. A schematic representation of the concentration method is shown in Figure 3.1; BacMam virus was harvested and clarified from insect cell debris by centrifugation at 4 550 *xg* for 20 minutes (min) at 4°C (steps 1 and 2). Subsequently, the clarified BacMam was transferred into a polycarbonate tube and concentrated by centrifugation at 75 600 *xg* (step 3 and 4). The concentrated-pool was re-suspended and virus titre analysided by QPCR and plaque assay (step 5).

Figure 3.2 shows the results of the recovery yields and virus infectivity over-time for the concentrated AcCMV_EGFP. Results obtained by QPCR analysis (Figure 3.2 A) indicated that 1 h of high-speed centrifugation efficiently pelleted BacMam, 98% of virus was recovered (Figure 3.2 A, 1 h), compared to the virus stock prior centrifugation (100%). A total titre of 2.22×10^6 Qpfu/ml (QPCR plaque forming unit per millilitre), less than 1%of the AcCMV_EGFP virus, from the original stock, was found to remain in the supernatant after the centrifugation (data not shown).

However, QPCR titration of the concentrated pool, after either 4 h or 24 h high-speed centrifugation, resulted in a significantly decreased recovery yield, 49% and 50% respectively (Figure 3.2 A, 4 and 24 h), when compared to pre-concentrated AcCMV_EGFP and AcCMV_EGFP centrifuged for only 1 h (F (3, 18)= 11.94; p= 0.0002). Harvested supernatants were also analysed for the presence of AcCMV_EGFP virus where 1 and 12%, respectively, were found to still be present following centrifugation (data not shown).

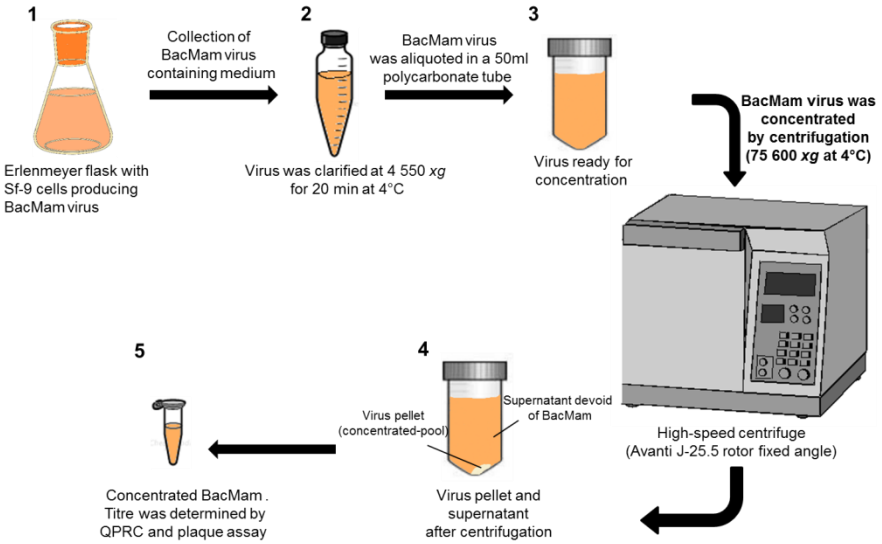

Figure 3.1. Schematic representation of BacMam concentration using high-speed centrifugation. (**1**) Sf-9 cells were infected with BacMam virus at multiplicity of infection (MOI) 0.1 in order to elicit the release of viral particles into the cell medium. (**2**) Five days post-infection, the virus-containing medium was collected and clarified by centrifugation (4 550 *xg*, 20 min at 4°C). (**3**) The virus-containing supernatant was aliquoted into a 50 ml polycarbonate centrifuge tubes; the virus was then concentrated by centrifugation (75 600 *xg* at 4°C). (**4**) After high-speed centrifugation, the virus pellet (concentrated-pool) was resuspended in 1X PBS whilst the supernatant was discarded. (**5**) The concentrated BacMam virus was titrated by QPCR and plaque assay.

Plaque assay analysis was performed to determine the amount of active virus after concentration. Figure 3.2 B, shows that AcCMV_EGFP infectivity decreased to approximately 70% after 1 h of high-speed centrifugation compared to the pre-concentrated virus stock (100%) and that extending the centrifugation time to 4 and 24 h, did not further decrease infectivity (71 and 65%, respectively). These recovery yields were not statistically significant (F (3, 8)= 2.141; p=0.17). Furthermore, plaque assay analysis of the supernatants, harvested from 1 h, 4 h and 24 h centrifugation runs, detected almost no virus presence; 1% or less (data not shown).

Overall, these results suggested that centrifugation at 75 600 *xg* for 1 h results in a 30% loss of the virus and increasing centrifugation time did not result in more losses. Importantly, no statistical difference was found between QPCR and plaque assay results when compared to each other (F (5, 22)= 4.588; p >0.05). From this preliminary study, 1 h of high-speed centrifugation was selected as the optimal time of concentration for use in subsequent studies.

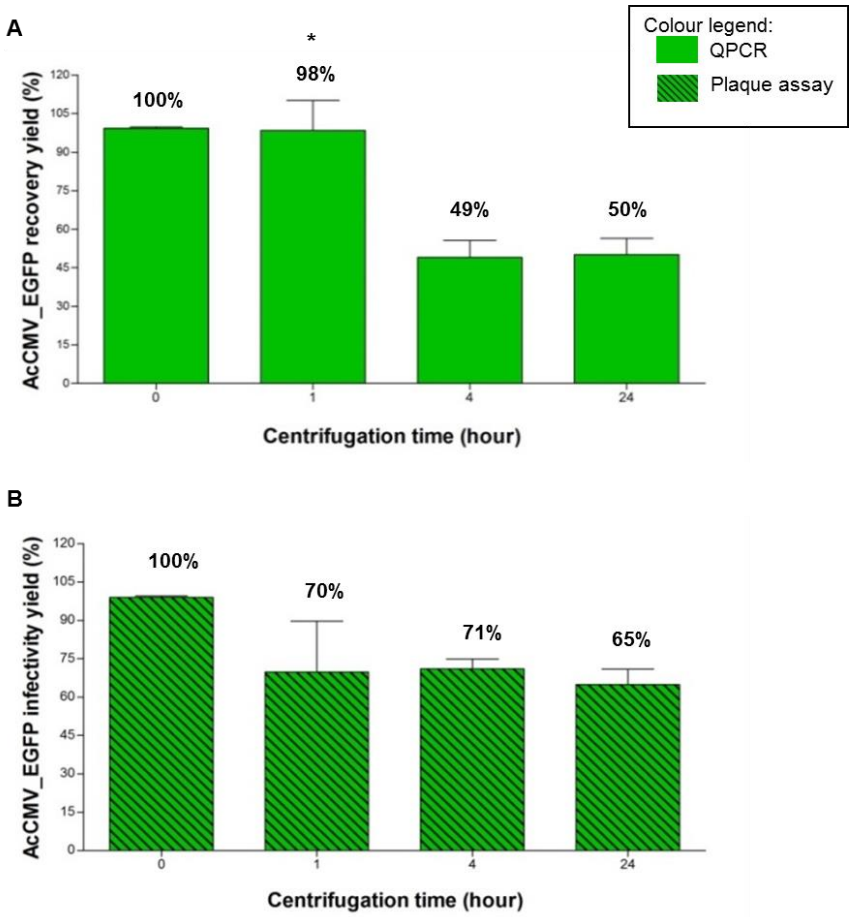

Figure 3.2. Time course concentration of AcCMV_EGFP using high-speed centrifugation. The AcCMV_EGFP recovery and infectivity yield were evaluated pre- and post-concentration using (**A**) QPCR and (**B**) plaque assay. Bars represent mean ± standard error (SEM; n=5) of results from a single experiment; *p= 0.0002 indicates a significant difference between 1 h high-speed centrifugation and 4 and 24 h centrifugation (one-way ANOVA).

3.2.II Validation of optimized concentration conditions

AcCMV_EGFP and AcCMV_SOD-2 were used to validate the optimized concentration method described above Three aliquots of 19 ml for each virus were used in three independent experiments as describe on Section 3.2.I. The collected virus pellets were then resuspended in 1X PBS and then analysed by QPCR and plaque assay. The virus titres, recovery and infectivity yields are shown in Table 3.1.

The average titres obtained by QPCR analysis for AcCMV_EGFP and AcCMV_SOD-2 after concentration were $4.1x10^9$ Qpfu/ml and $3.7x10^9$ Qpfu/ml with recoveries of 84% and 81%, respectively (Table 3.1 A). Moreover, QPCR analysis detected less than 1% of viral particles, in the supernatant harvested after centrifugation (Table 3.1 A). These results were not statistically different (F (2, 11)=1.143; p=0.3540) from those observed in the optimization study (Section 3.2.I). Subsequently, virus activity was confirmed by plaque assay analysis. The total yields after concentration were $2.33x10^9$ pfu/ml for AcCMV_EGFP and $2x10^9$ pfu/ml for AcCMV_SOD-2, this corresponded to an infectivity yield of 61.4% and 52.6%, respectively (Table 3.1 B). However, no active viral particles were observed when Sf-9 cells were infected with the supernatant harvested after centrifugation (Table 3.1 B).

In conclusion, statistical analysis demonstrated that recovery and infectivity yields were significantly different when compared to each other by one-way ANOVA (F (3,12)= 8090; p<0.0001).

Table 3.1. BacMam virus concentration by high-speed centrifugation.

	(A) QPCR analysis			(B) Plaque assay analysis	
BacMam virus	**Volume harvested (ml)**	**BacMam virus titre (Qpfu/ml)***	**Recovery yield (%)**	**BacMam virus titre (pfu/ml)***	**Infectivity yield (%)**
AcCMV_EGFP Pre-concentration	19	$2.6X10^8$	100	$2X10^8$	100
AcCMV_EGFP post-concentration	1	$4.1x10^9$	84	$2.33X10^9$	61.4
Supernatant from centrifugation	19	$3.6X10^5$	0.007	-	-
AcCMV_SOD-2 Pre-concentration	19	$2.4X10^8$	100	$2X10^8$	100
AcCMV_SOD-2 post-concentration	1	$3.7X10^9$	81	$2X10^9$	52.6
Supernatant from centrifugation	19	$1.6X10^6$	0.03	-	-

* Each value represents the average of three replicative samples of a single experiment.

3.2.III One-step virus growth analysis

Once the concentrated BacMam viruses, AcCMV_EGFP and AcCMV_SOD-2 (Section 3.2.II), were accurately titered (Sections 2.2.3.III.a and b), it was necessary to carry out a growth curve analysis.

The purpose of this single experimental study was to determine whether or not BacMam concentration by high-speed centrifugation had a detrimental effect on virus infectivity and replication. To avoid any confusion, pre-concentrated BacMam were called AcCMV_EGFP and AcCMV_SOD-2 and were included as controls; whereas, concentrated BacMam were designated AcCMV_EGFP/C and AcCMV_SOD-2/C. One-step growth analysis was carried out by the addition of each BacMam virus to triplicate cultures of Sf-9 cells (20 ml) using an multiplicity of infection (MOI) of 5. Triplicate samples for each culture were collected at 0, 6, 12, 24 and 48 hours post-infection (hpi). Virus production at each time point was then analysed by QPCR (Section 2.2.3.III.b).

The growth curve for AcCMV_EGFP *vs.* AcCMV_EGFP/C (Figure 3.3 A) indicated that budded virus (BV) production increased exponentially between harvest times. The growth profile of AcCMV_EGFP/C mimicked that of AcCMV_EGFP at 12 hpi. However, a slight increase in BV production was detected between 24 and 48 hpi in the control virus AcCMV_EGFP ($1.39x10^8$ Qpfu/ml and $2.4x10^8$ Qpfu/ml, respectively) compared to AcCMV_EGFP/C ($7x10^7$ Qpfu/ml and $1.5x10^8$ Qpfu/ml, respectively). Overall, there was approximately a two-fold increase in the titre of the non-concentrated virus; the difference in BV production was significantly different at 24 and 48 hpi (F (4, 59)= 256.43; p<0.0001).

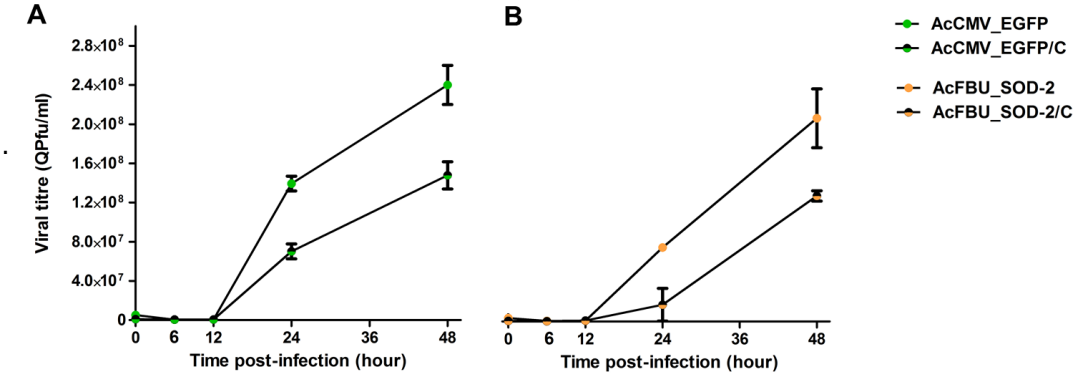

Figure 3.3. Virus growth curve analysis of AcCMV_EGFP and AcCMV_SOD-2 after concentration by high-speed centrifugation. Sf-9 cells seeded at 2 x 10^6 cells/ml were infected with either AcCMV_EGFP and AcCMV_EGFP/C (**A**) or AcCMV_SOD-2 and AcCMV_SOD-2/C (**B**) at an MOI of 5 and budded virus (BV) samples were harvested at 0, 6, 12, 24 and 48 hpi. BV titres were estimated using QPCR (n=3) and error bars are indicated (mean ± SEM).

Similarly, the growth profiles of AcCMV_SOD-2 and AcCMV_SOD-2/C demonstrated an exponential increase between 0 and 48 hpi (Figure 3.3 B). Both growth curves showed the same pattern of BV production between 0 and 12 hpi although following this time point virus production increased for AcCMV_SOD-2.

The growth curves showed that at 24 and 48 hpi AcCMV_SOD-2 was generated at titers of $7.7x10^7$ Qpfu/ml and $1.8x10^8$ Qpfu/ml; while, titers of $1.7x10^7$ Qpfu/ml and $1.3x10^8$ Qpfu/ml were obtained for AcCMV_SOD-2/C. Two-way ANOVA analysis of raw data showed no significant difference in virus production between the two viruses at 0, 6 and 12 hpi (p>0.05); however, they were statistical different at 24 and 48 hpi (F (4, 59)= 256.43; p<0.0001).

3.3 LOW-SPEED CENTRIFUGATION FOR CONCENTRATION OF LARGE VOLUMES OF BACMAM VIRUS

The increased interest in BacMam for *ex vivo* / *in vivo* gene delivery applications requires an efficient method to produce large volumes of purified and concentrated virus. Indeed, long-term viral stability, high purity and high titres are required for *in vivo* applications. The goal of this study was to evaluate a BacMam concentration protocol on a scale suitable to obtain high viral titres for porcine kidney transduction whilst minimizing virus loss (Section 2.2.3.IV.b).

Different volumes of AcCMV_EGFP were used in this study and the utility of a low-speed centrifugation procedure to concentrate BacMam virus was investigated. AcCMV_EGFP viral particles, harvested from infected Sf-9 cells, were clarified by centrifugation (4 550 *xg* for 20 min at 4°C) before being pelleted by low-speed centrifugation at 23 000 *xg* (12 000 rpm) for 16 h (Avanti® J-25 I, JA-14 rotor; Beckman culture). Following centrifugation, the supernatant (devoid of BacMam virus) was harvested for further analysis whilst the virus pellet was re-suspended in 1X PBS (1-15 ml). The concentrated virus pellet was resuspended at 4°C for approximately 20 h. Plaque assays were then carried out to determine virus titre; yields were calculated using the formula illustrated in Section 3.2. Table 3.2 shows AcCMV_EGFP recovery results from four independent experiments.

Less than 1% of active virus was detected in the supernatant fractions in all four tested volumes (Table 3.2, A, B, C, D) suggesting that BacMam particles were efficiently concentrated. However, recovery yields were variable, ranging from 38% to 63.5% after concentration. As shown in Table 3.2 A, when 250 ml of virus suspension was used to concentrate AcCMV_EGFP ($1.3x10^8$ pfu/ml), 38.5% of the viral particles were recovered with a titre of $1.25x10^{10}$ pfu/ml and only a small amount of active viral particles were detected in the supernatant sample (0.08%).

The average starting titre of 400 ml of AcCMV_EGFP, in the second experiment, was $2x10^8$ pfu/ml (Table 3.2 B). Following concentration, viral titre was an average of $2.18x10^{10}$ pfu/ml in a volume of 2 ml, resulting in a recovery of 54.4% (Table 3.2 B). Further analysis of supernatant, harvested after centrifugation, indicated that 0.3% of particles were retained.

Table 3.2. AcCMV_EGFP concentration by low-speed centrifugation.

A

		Volume (ml)	Virus Titre (pfu/ml)	Recovery yield (%)
AcCMV_EGFP	Pre-centrifugation	250	$1.3x10^8$	100
-	Post-centrifugation (concentrated pool)	1	$1.25x10^{10}$	38.5
-	Supernatant	250	$1.1x10^6$	0.08

B

		Volume (ml)	Virus Titre (pfu/ml)	Recovery yield (%)
AcCMV_EGFP	Pre-centrifugation	400	$2x10^8$	100
-	Post-centrifugation (concentrated pool)	2	$2.18x10^{10}$	54.4
-	Supernatant	400	$5.85x10^5$	0.3

C

		Volume (ml)	Virus Titre (pfu/ml)	Recovery yield (%)
AcCMV_EGFP	Pre-centrifugation	1200	$1.8x10^8$	100
-	Post-centrifugation (concentrated pool)	10	$1.09x10^{10}$	50
-	Supernatant	1200	$2.4x10^5$	0.1

D

		Volume (ml)	Virus Titre (pfu/ml)	Recovery yield (%)
AcCMV_EGFP	Pre-centrifugation	2400	$1.1x10^8$	100
-	Post-centrifugation (concentrated pool)	15	$1.05x10^{10}$	60.6
-	Supernatant	2400	$6.81x10^5$	0.6

A BacMam volume of 1200 ml showed a recovery of 50% following centrifugation and approximately 61-fold increase in virus titre, from $1.8x10^8$ pfu/ml to $1.09x10^{10}$ pfu/ml (Table 3.2 C). Almost no BacMam activity (0.1%) was detected in supernatants (Table 3.2 B).

Subsequently, for the final experiment AcCMV_EGFP volume was increased to 2400 ml. As shown in Table 3.2 D, more than half of the starting virus particles were recovered (60.6%) in a volume of 15 ml, with an average tire of $1.05x10^{10}$ pfu/ml; this corresponded to 95-fold increase above the starting AcCMV_EGFP titre ($1.1x10^{8}$ pfu/ml). One-way ANOVA analysis of AcCMV_EGFP recovery yields revealed no statistical difference in virus recovery amongst the four experiments (F (3, 5) = 4.981; p=0.0581).

3.4 PURITY ANALYSIS OF CONCENTRATED BACMAM SAMPLES

The purity of the concentrated AcCMV_EGFP obtained from both high-speed and low-speed (1200 ml) centrifugation (Sections 3.2 and 3.3) was determined by SDS-PAGE analysis (Section 2.2.4.II) and silver staining (Section 2.2.4.III.b). Virus identification was performed by western blot analysis (Section 2.2.4.IV) using antibodies against either the virus envelope protein (anti-GP64) or the capsid protein (anti-VP39) (Section 2.1.5, Table 2.6). A non-concentrated AcCMV_EGFP virus was included as a control to compare the purity of the concentrated virus and to confirm the presence of specific-baculovirus proteins (GP64 and VP39). Briefly, concentrated and non-concentrated AcCMV_EGFP viruses were denatured by boiling in 1% loading buffer (Section 2.2.4.I) and $1x10^{6}$ pfu/ml of viral particles were separated on a 12% SDS-PAGE gel. Subsequently total proteins were visualized by silver staining according to the manufacturer guidelines. The SDS-PAGE profile is shown in Figure 3.4.

As expected, numerous bands were detected in the non-concentrated sample (Figure 3.4 A, lane 2); one major band with molecular weight between 55 kDa and 75 kDa was visualized corresponding to GP64. In contrast, the host cell proteins were absent in AcCMV_EGFP concentrated by high-speed centrifugation (Figure 3.4 A, lane 3). As shown in Figure 3.4 A: lane 4, a number of bands are also visible in the sample concentrated by low-speed centrifugation; these are comparable to the non-concentrated AcCMV_EGFP virus (Figure 3.4 A, lane 2). Based on the SDS-PAGE profile of concentrated BacMam, two main proteins were detected with molecular weights of 64 kDa and 39 kDa (illustrated in Figure 3.4 by the arrows).

Supernatants harvested after centrifugation were also analysed by SDS-PAGE (Figure 3.4 B). One major band, with a molecular weight between 55-75 kDa, was detected in the supernatant obtained after high-speed AcCMV_EGFP centrifugation (Figure 3.4 B, lane 2).

Whereas more protein bands were detected in the supernatant harvested after virus concentration by low-speed centrifugation (Figure 3.4 B, lane 3). These proteins may be related to the host cells, to the medium (*e.g.* fetal bovine serum; FBS) or to the virus itself.

A western blot analysis was performed to confirm the identity of the 64 kDa and 39 kDa protein bands observed in the silver-stained SDS-PAGE gel. Samples were loaded on a 12% SDS-PAGE gel and then transferred onto a nitrocellulose membrane. Proteins were detected with BacMam specific antibodies, anti-GP64 and anti-VP39, labelled with alkaline phosphatase (Section 2.1.5, Table 2.6). Figure 3.5 shows the western blot analysis profile of non-concentrated and concentrated AcCMV_EGFP samples.

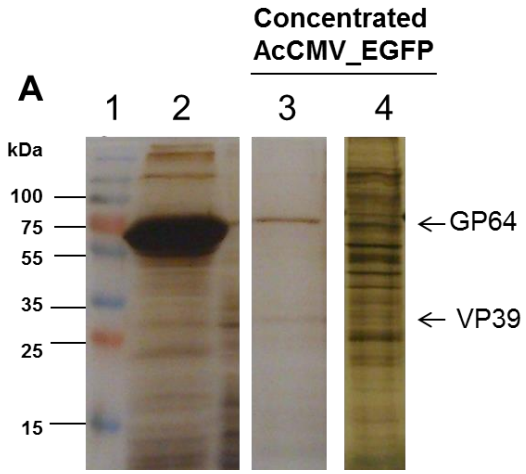

1	PageRuler plus prestained protein ladder
2	AcCMV_EGFP (non-concentrated)
3	AcCMV_EGFP high-speed centrifuged
4	AcCMV_EGFP low-speed centrifuged

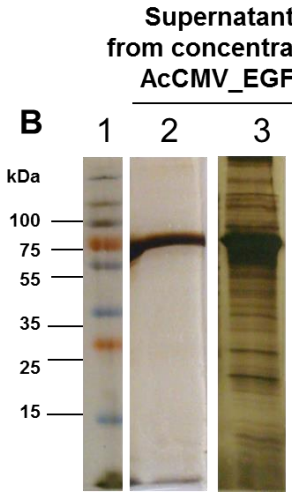

1	PageRuler plus prestained protein ladder
2	Supernatant from AcCMV_EGFP centrifuged high-speed
3	Supernatant from AcCMV_EGFP centrifuged low-speed

Figure 3.4. Silver-stained SDS–PAGE analysis of concentrated AcCMV_EGFP. (**A**) SDS-PAGE profile of concentrated AcCMV_EGFP; lane 1, PageRuler Plus Prestained Protein Ladder; lane 2, non-concentrated AcCMV_EGFP control; lane 3, high-speed and lane 4 low-speed centrifuged AcCMV_EGFP. Arrows indicate the size of GP64 and VP39. (**B**) SDS-PAGE profile of supernatant harvested after AcCMV_EGFP concentration. Lane 1, PageRuler Plus Prestained Protein Ladder; lane 2, supernatant after high-speed centrifugation and lane 3, supernatant after low-speed centrifugation.

Western blot analysis confirmed the presence of BacMam proteins with their correct molecular weights (Figure 3.5). Immunoblotting with anti-GP64 identified a ~64 kDa band representing the GP64 envelope protein (Blissard, & Rohrmann, 1989) in both concentrated AcCMV_EGFP samples (Figure 3.5 A, lanes 3 and 4); however, only the lower edge of the band was visualized in the non-concentrated virus (Figure 3.5 A, lane 2). As illustrated in Figure 3.5 B by the arrow, the anti-VP39 antibody also recognized a ~39 kDa band corresponding to VP39 protein in the non-concentrated and concentrated BacMam (Figure 3.5 B; lanes 2, 3 and 4). The relative intensity of GP64 and VP39 were quantified by densitometry and data are shown in Figure 3.5 (above the western blot). As shown in Figure 3.5 A, the expression levels of the envelope protein were 63% and 22% for the AcCMV_EGFP concentrated by high-speed centrifugation (lane 3) and low-speed centrifugation (lane 4) respectively. While, the relative intensity of GP64 in the non-concentrated virus sample was also quantified (the lower edge) and was found to be 6% (Figure 3.5 A; lane 2). Densitometry analysis indicated comparable VP39 expression levels between the non-concentrated virus and the high-speed viral preparation (Figure 3.5 B lane 2 *vs.* lane 3) with band intensities of 36.9% and 39%, respectively.

3.5 DISCUSSION

During the last decade, the increased use of BacMam as a gene delivery vehicle has required the development of more efficient methods for virus purification and concentration. Indeed, the use of BacMam for gene therapy applications is dependent on its purity and usually requires high doses of virus in order to achieve a therapeutic effect (Vicente *et al.,* 2009). The vast majority of studies to date have utilized purification and concentration protocols based on ultracentrifugation and chromatography (reviewed by Aucoin *et al.,* 2010). Therefore, the initial part of this research study evaluated the ability of a number of techniques to generate a high titre BacMam stocks in small analytical volumes such as high-speed centrifugation for use in *in vitro* transduction studies. *In vivo* applications may require larger amounts of BacMam virus *e.g.* for repeated applications of virus or require higher concentrations of virus to ensure efficient gene delivery and expression. Therefore, low-speed centrifugation was also evaluated as a large capacity method of concentration. The two different methods are discussed below.

3.5.I BacMam concentration by high-speed centrifugation

Centrifugation steps have been routinely used to concentrate viral particles from different sources (O'Reilly et al., 1994). In particular, high-speed centrifugation has been reported for the concentration of BacMam (Condreay et al., 1999).

Condreay et al. (1999) generated a BacMam virus containing gfp under the control of the CMV-immediate early (IE) promoter which was concentrated by centrifugation at 35,000 xg for 60 min. The pelleted virus was re-suspended in PBS supplemented with 1% (vol/vol) FBS. Similarly, they used the concentrated virus in transduction experiments and demonstrated high levels of GFP in a number of cell lines. However, Condreay and colleagues (1999) did not quantifiedquantify the recovery yield of active virus following concentration.

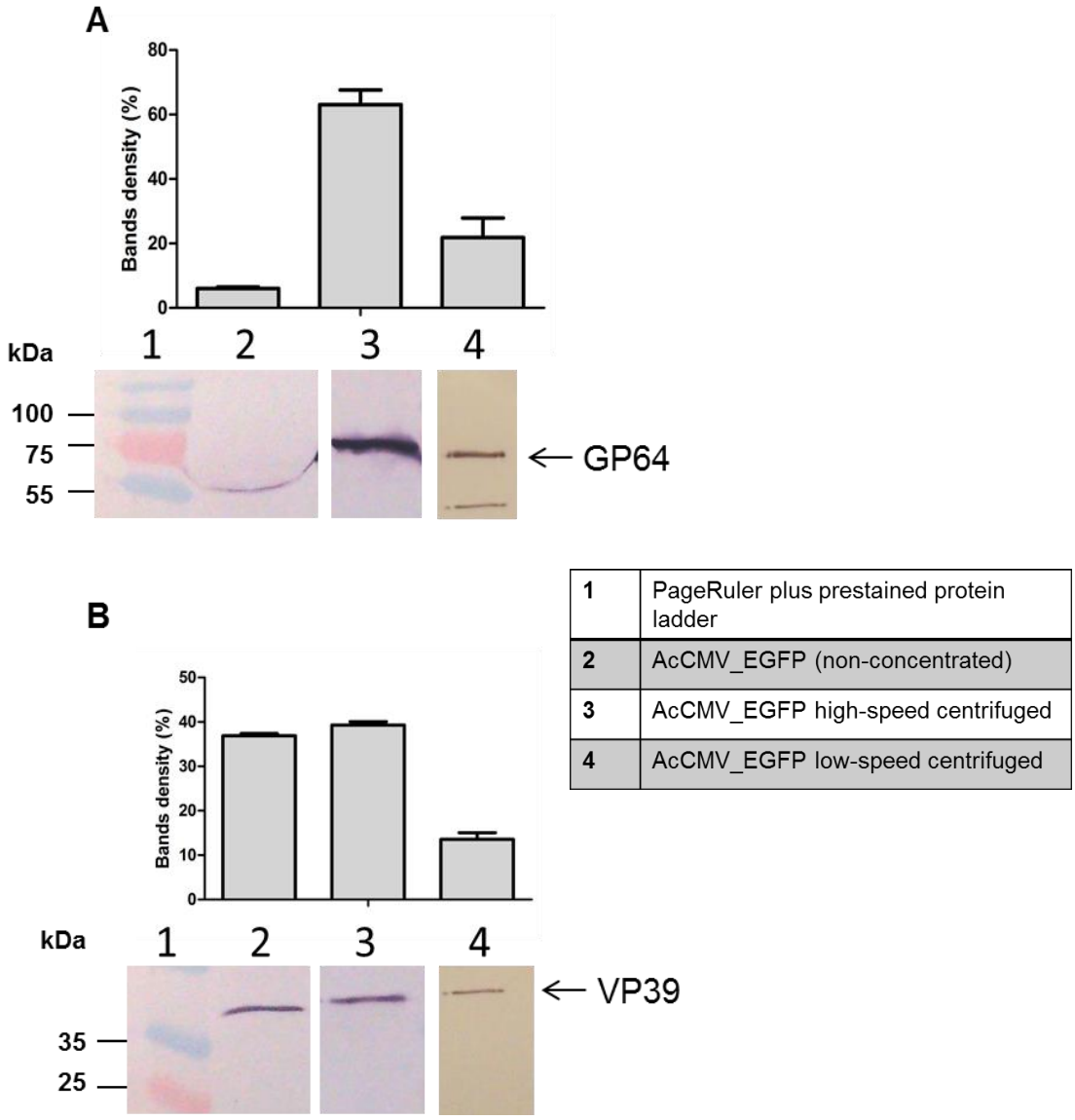

1	PageRuler plus prestained protein ladder
2	AcCMV_EGFP (non-concentrated)
3	AcCMV_EGFP high-speed centrifuged
4	AcCMV_EGFP low-speed centrifuged

Figure 3.5. Western blot analysis of concentrated AcCMV_EGFP using three different concentration methods. Expression levels of GP64 (**A)** and VP39 (**B**). Lane 1, PageRuler Plus Prestained Protein Ladder. Lane 2, non-concentrated AcCMV_EGFP included as a control. AcCMV_EGFP concentrated by: lane 3, high-speed centrifugation; lane 4, low-speed centrifugation. Densitometry analysis of western blot results (n=3) was performed and data are shown as means ±SE (above western blot). Western blots were stained with anti-GP64 and anti-VP39 primary antibodies and alkaline phosphatase conjugated anti-mouse IgG secondary antibody. Arrows indicate GP64 and VP39.

Philipps *et al.* (2005) described the centrifugation of a recombinant baculovirus, carrying *gfp* under the control of the AcMNPV basic protein promoter (*p6.9*), for 1 h at 45,000 *xg* (~22000 rpm). The resulting virus pellet was re-suspended in 1 ml of PBS and recovery yield calculated by end-point dilution method. They showed that the concentrated retained similar levels of infectivity compared to the starting material (64.5%) with a 28-fold increase in viral titre. Based on these reports, three different times of centrifugation were evaluated and compared in this study. Based on both QPCR and plaque assay data, an average of 70-98% of AcCMV_EGFP was recovered after 1 h of centrifugation, while 49-71% of virus was recovered after 4 h of centrifugation (Figure 3.2). Increasing the time of centrifugation, from 4 to 24 h, showed 50-65% recovery of AcCMV_EGFP virus (Figure 3.2). However, the recovery yields obtained with the three different centrifugation times were not significantly different from each other which was consistent with previous reports (*e.g.* Philipps *et al.*,2005). Moreover, the recovery yields obtained in this study were similar to the 64-71% recovery reported by Transfiguracion *et al.* (2007) following ultracentrifugation (37,000 ×*g* for 3.5 h) on a 25% sucrose cushion.

Active virus was present in the supernatant samples harvested from all three centrifugation times tested, with an average titre of $2.5x10^5$ pfu/ml, corresponding to <1% of virus from the starting material (data not shown). These observations were in accordance with previous reports. Philipps *et al.* (2005) showed that approximately 1% of the BacMam particles were found to remain in the supernatant fraction after centrifugation.

Following ultracentrifugation, approximately 30% of virus was lost which could be explained by the irreversible formation of virus aggregates. Aggregation of viral particles remains one of the major problems in the purification and concentration of viruses (Barsoum, 1999; Transfiguracion *et al.,* 2007; Vicente *et al.,* 2009). To circumvent this disadvantage a number of strategies have been developed in the last decade; these have included the use of a 25% sucrose cushion and non-ionic detergent during the ultracentrifugation step (O'Reilly *et al.,* 1992; Transfiguracion *et al.,* 2003; Kato *et al.,* 2011).

Based on the preliminary experiments shown in Figure 3.2 and in accordance with previous studies, it was speculated that 1 h high-speed centrifugation should be sufficient to obtain high-titre BacMam stocks. Recovery yields after concentration ranged between 61-84% for AcCMV_EGFP, and between 52-81% for AcCMV_SOD-2 (Table 3.1).

Both viruses showed a similar recovery yield, although yields obtained by QPCR (84% and 81%, respectively) were higher than those obtained by plaque assay (61.4% and 52.6%, respectively). This likely reflects the tendency of QPCR to overestimate virus titres by including non-infectious virus DNA and the tendency of plaque assays to under estimate titres, due to inherent virus particle loss *e.g.* by adhering to plastic ware. Statistical analysis between QPCR and plaque assay results showed them to be significantly different. However, the recovery yields obtained in this study were not dissimilar to recovery yields reported in the literature when high-speed centrifugation, ion-exchange chromatography, ultracentrifugation with sucrose cushion and cross-flow ultrafiltration were used to concentrate BacMam viruses (Barsoum, 1999; Philipps *et al.* 2005; Transfiguracion *et al.,* 2007; Vicente *et al.,* 2009).

A growth curve analysis was performed to determine whether high-speed centrifugation had any detrimental effect on virus infectivity. BV production of AcCMV_EGFP/C (concentrated virus) and AcCMV_EGFP (non-concentrated virus) increased exponentially between 0 and 48 hpi (Figure 3.3 A). Statistical analysis showed a significant difference in BV production of AcCMV_EGFP with an increase of approximately 2-fold when compared to AcCMV_EGFP/C at 24 and 48 hpi. As shown in Figure 3.3 B, BV production of AcCMV_SOD-2/C showed a similar pattern to that seen in the growth analysis of AcCMV_EGFP/C (Figure 3.3 A). Production of BV of AcCMV_SOD-2/C mimicked that of AcCMV_SOD-2, with an exponential increase between 0 hpi and 48 hpi. However, ANOVA analysis revealed a statistical difference between the two viruses at 24 and 48 hpi. Therefore, the concentrated BacMam, described in this study had slightly reduced infectivity compared to non-concentrated virus. This decreased production may be due to shear stress during centrifugation reducing BV stability. However, little is known about the effect of shear force on viruses (Summers & Volkman, 1976; Michalsky *et al.,* 2008).

The data obtained in this study demonstrated that ultracentrifugation is a reproducible process; recovery yields obtained were within the same order of magnitude as those of published reports further confirming process robustness. Furthermore, these results supported the previous assumption that high-titre BacMam stocks can be easily generated with this procedure. However, the amount of virus that can be processed by this method is limited by the low volume capacity of high-speed centrifuge rotors.

3.5.II Low-speed centrifugation for concentration of BacMam virus

Successful concentrations of animal viruses have been achieved using large culture volumes; for example, volumes in excess of 1000 ml of lentivirus have been concentrated with recovery up to 70% by overnight (16 h) low-speed centrifugation (reviewed by VandenDriessche *et al.,* 2002).

In this study, a modified method based on low-speed centrifugation (developed by Prof. Robert Possee, NERC Centre for Ecology and Hydrology, Oxford, UK) was evaluated for the production of high-titre BacMam stocks. This method allowed volumes of virus higher than 1 litre (L) to be concentrated using a standard low speed centrifuge. Plaque assays were performed on the supernatant fractions from the centrifuged samples confirming that almost all of the active BacMam virus was pelleted; containing less than 1% virus. Results demonstrated that 39-61% of active AcCMV_EGFP was recovered amongst the tested volumes (Table 3.2). Although 40% to 60% of virus was lost, this viral concentration protocol consistently increased the titre of AcCMV_EGFP by ~100-fold ($1x10^{10}$ pfu/ml).

These data are comparable to the recovery yields obtained with enveloped retroviruses and lentiviruses. Prachař *et al.* (1988) were the first to report a successful concentration of retroviruses, from volumes of up to 6 L, by low-speed centrifugation. An average titre between $1.3x10^{10}$ and $1.2x10^{12}$ cfu/ml (colony-forming units per millilitre) was obtained following retrovirus concentration by low-speed centrifugation (6000 *xg* for 16 h), with recovery ranging from 87% to 92% (Nanmoku *et al.,* 2003).

This method is particularly relevant for *ex vivo* gene delivery studies where transduction of large solid organ requires high-titre BacMam in low volumes in order to reach maximum transduction efficiencies.

3.1 Assessment of BacMam purity

Viral purity was assessed after AcCMV_EGFP concentration with methods discussed in Sections 3.2 and 3.3. For this purpose, silver stained SDS–PAGE, western blot and densitometry analysis were used. The protein profile illustrated in Figure 3.4 A, revealed the presence of a 64 kDa and a 39 kDa band which represented the envelope and capsid proteins of baculovirus, respectively. The molecular weights of these proteins corresponded to the proteins described in previously published studies (Transfiguration *et al.,* 2007; Wu *et al.,* 2007; Gerster *et al.,* 2013).

In these studies, purified wild-type and recombinant baculovirus were analysed by SDS-PAGE and proteins with apparent molecular weights of 64 and 39 kDa were identified, correlating to GP64 and VP39 proteins. Additional proteins band were visible in AcCMV_EGFP preparations after low-speed centrifugation (Figure 3.4 A, lane 4) in comparison to the concentrated virus obtained after high-speed centrifugation (Figure 3.4 A, lane 3). The reduced number of proteins band demonstrated the high purity of the viral preparation (Figure 3.4 A, lane 3).

A major band was visible in the non-concentrated AcCMV_EGFP, migrating between 55 and 75 kDa (Figure 3.4 A, lane 2). The bovine serum albumin (BSA) protein represents the major component of FBS, which is routinely added to a concentration of 5% (v/v) to virus stocks. From this observation, it was assumed that this strong protein band represented GP64 that co-migrates with the BSA protein (~69 kDa) present in the viral solution. Furthermore, the non-concentrated AcCMV_EGFP virus (control virus) served as a positive control for the detection of both GP64 and VP39 viral proteins; the presence of these proteins was used to characterize the BacMam samples obtained from high- and low-speed concentration. Only the lower edge of GP64 was detected in the control virus (Figure 3.5 A, lane 2) and based on the previous stated observation, it was suggested that the GP64 antigenic epitope, necessary for antibody recognition, was physically obscured by the overlapping BSA protein. Western blot analysis, using anti-GP64 antibody, of supernatant harvested following AcCMV_EGFP concentration also confirmed that the intensive band of 55-75 kDa observed in the SDS-PAGE gel (Figure 3.4 B) was not the virus envelope protein and therefore, it was assumed to be the BSA protein. This was supported by the observation made by Gerster *et al.* (2013). They detected a strong band which migrated to the same distance of GP64 in fractions from starting material and flow-through after CIM® QA baculovirus purification. They identified this band as BSA protein using mass spectrometry.

The purified and concentrated BacMam viruses were identified by confirming the presence of the two viral proteins in all sample preparations; this was achieved by the use of antibodies against GP64 (Figure 3.5, A) and VP39 (Figure 3.5, B). These results are in accordance with those obtained from previous baculovirus concentration and purification studies (Transfiguration *et al.,* 2007). Transfiguration *et al.* (2007) performed western blot analysis following BacMam concentration and size-exclusion chromatography (SEC) purification; a 64 kDa band was confirmed to be the GP64 envelope protein.

In conclusion, concentration methods were assessed for their ability to produce high-titre BacMam stocks. Both methods were successful to varying degrees and concentrated BacMam viruses maintained their infectivity. The concentrated virus fractions were easily re-suspended in a serum-free medium and relatively pure viral stocks were obtained. Therefore, it was decided to utilize high-speed centrifugation method for the *in vitro* experiments described in Chapter 5. Low-speed centrifugation was the method of choice for obtaining the high-titre virus stocks that were needed for the *ex vivo* study described in Chapter 6 of this thesis.

Chapter 4
In vitro transduction and expression optimization

4.1 GENERAL OVERVIEW

Transient gene expression is a widely used method for the rapid production of recombinant proteins for *in vitro* study and *ex vivo*/ *in vivo* therapeutic applications. To date, recombinant protein production still remains an important cornerstone for research in biopharmaceutical companies and academia. During the last two decades, significant improvements have been made in delivering therapeutic exogenous genes to different target cells (reviewed by Bouard *et al.,* 2009). However, interest has progressively increased over recent years in developing new approaches for enhancing therapeutic gene expression levels and efficacy (reviewed by Assenberg *et al.,* 2013).

The mammalian expression system is an attractive option compared to other systems (Majors *et al.,* 2008) and the most commonly used mammalian cell lines for transient gene expression comprise COS (fibroblast-like cell line derived from monkey kidney tissue), BHK (baby hamster kidney), CAP-T (human amniocyte-derived cells) and avian EB66 (duck embryonic stem cell-derived), as well as HEK (human embryonic kidney) and CHO (Chinese hamster ovary) cells (Brown & Mehtali, 2010; Geisse & Voedisch, 2012; reviewed by Assenberg *et al.,* 2013). In particular, viral vectors have been extensively used for transient gene expression, these include vectors derived from retrovirus, adenovirus, adeno-associate virus (AAV) but also from baculovirus (BacMam) (Condreay *et al.,* 1999; Sarkis *et al.,* 2000; reviewed by Jin *et al.,* 2014). However, the efficacy of the virus-mediated transgene expression is limited by a number of factors including the initial contact of the virus with the target cells, transport of the viral DNA to the host nucleus and subsequent recombinant gene expression (reviewed by Bouard *et al.,* 2009).

Previously, a number of studies investigated whether chemical compounds such as histone deacetylases inhibitors (HDACis), DNA synthesis and topoisomerase inhibitors could enhance *in vitro* virus gene transfer and expression in mammalian cells (Russell *et al.,* 1995; Mizuno & Yoshida, 1998; Zhang *et al.,* 2012; Gosnell *et al.,* 2014). Therefore, based on published studies, four chemical compounds (hydroxyurea, etoposide, protamine and cycloheximide) were chosen and evaluated, as novel agents to augment exogenous gene expression in BacMam transduced HEK293 cells. Furthermore, sodium butyrate has been previously demonstrated to markedly enhance BacMam-mediated *gfp* expression in CHO cells (Condreay *et al.,* 1999); thus, its effect on transgene expression was also evaluated in this study and used as a positive control for increased fluorescence. Chemical compounds effects were also evaluated on BacMam-mediated transgene expression in CHO cells and results are included as supplementary data in the CD attached to this thesis (Chapter 4-S3).

4.2 HEK293 CELL TRANSIENT GENE EXPRESSION: PARAMETER OPTIMIZATION

The effect of different chemical treatments (Chapter 2, Table 2.1) on BacMam-mediated transgene expression was evaluated in HEK293 cells. Preliminary experiments aimed to identify the optimal chemical concentration; therefore, cells were either pre-incubated overnight with different concentrations of hydroxyurea (5, 20, 40, 75 and 100 mM), etoposide (0.5, 1.5, 3, 4.5 and 10 µM) or 3 h prior-transduction with cycloheximide (1, 5, 3 and 5 µg/ml). Treated cells were then transduced with AcCMV_EGFP at a MOI 50 and incubated for 24 hpt. HEK293 cells were also transduced with AcCMV_EGFP virus in the presence of different concentrations of protamine (0.5, 5, 10, 50 and 100 µg/ml).

Controls included cells with medium supplemented with 10 mM of sodium butyrate followed by transduction with AcCMV_EGFP (MOI 50). Furthermore, mock-transduced (no virus) and untreated (no chemical) AcCMV_EGFP transduced cells were included as controls. At 24 hpt, treated and untreated transduced cells were analysed for *egfp* (enhanced green fluorescence protein) expression using a fluorescence microscope. Quantitative image analysis, based on the quantification of pixel intensities, was then performed to calculate the total fluorescence for 13 individual cells using ImageJ software (Section 2.2.5.I.a). The numbers of cells were chosen based on the maximum number of EGFP positive cells in the transduced untreated control cells. The fold change in fluorescence was calculated and plotted as graph bar next to the photomicrographs.

As expected, fluorescence microscopy analysis revealed that the addition of sodium butyrate to the cell culture medium after transduction resulted in a three-fold increase in the number of EGFP positive cells and exhibited an intensely green fluorescence (Figures 4.1 to 4.4, panel C) compared to the untreated control (Figures 4.1 to 4.4, panel B). The fluorescence photomicrographs, shown in Figure 4.1, panel D also demonstrated the enhancing effect of hydroxyurea on *egfp* expression. As compared with the untreated transduced control cells (Figure 4.1, panel B), pre-transduction treatment of cells with hydroxyurea at concentrations of 5, 20, 75 and 100 mM induced a two- to three-fold increase in fluorescence (Figure 4.1, panel D). The maximum fluorescence was achieved by pre-treating the cells with 40 mM of hydroxyurea; this concentration increased the fluorescence intensity three-fold compared to the transduced control cells (Figure 4.1, panel B). Statistical analysis showed that the expression levels of hydroxyurea treated transduced cells were significantly higher than the untreated transduced cells (F (6, 82)= 11.12; p<0.0001). Therefore, 40 mM was the concentration used for subsequent experiments.

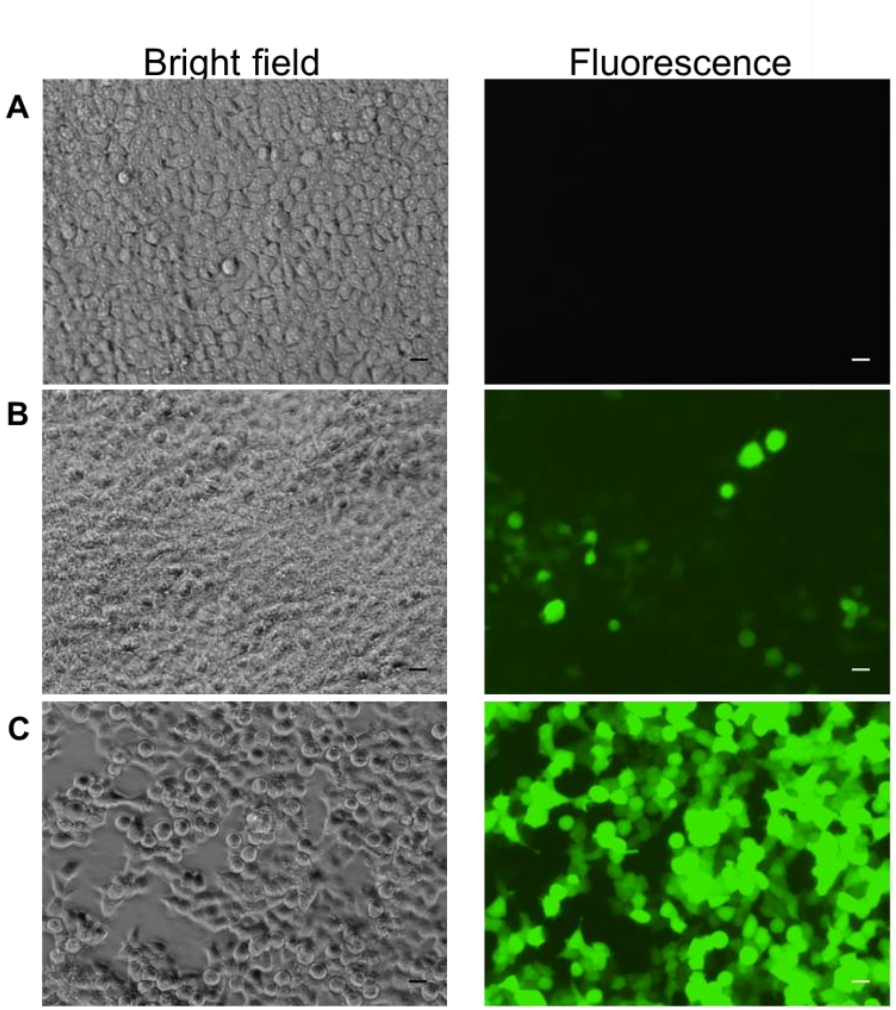
Bright field
Fluorescence
A
B
C

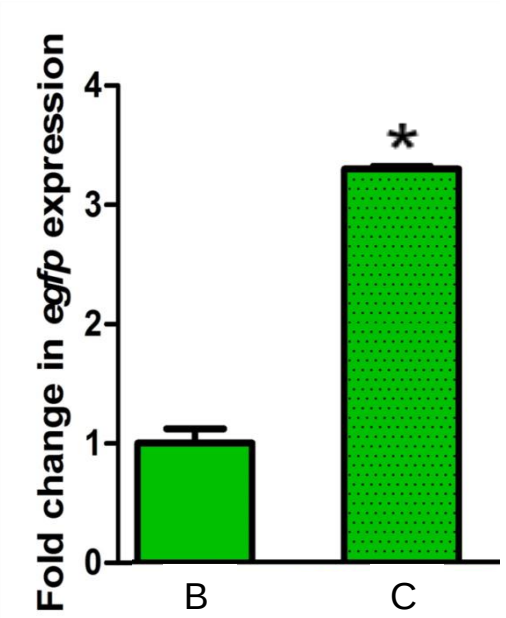
Fold change in egfp expression
0
1
2
3
4
*
B
C

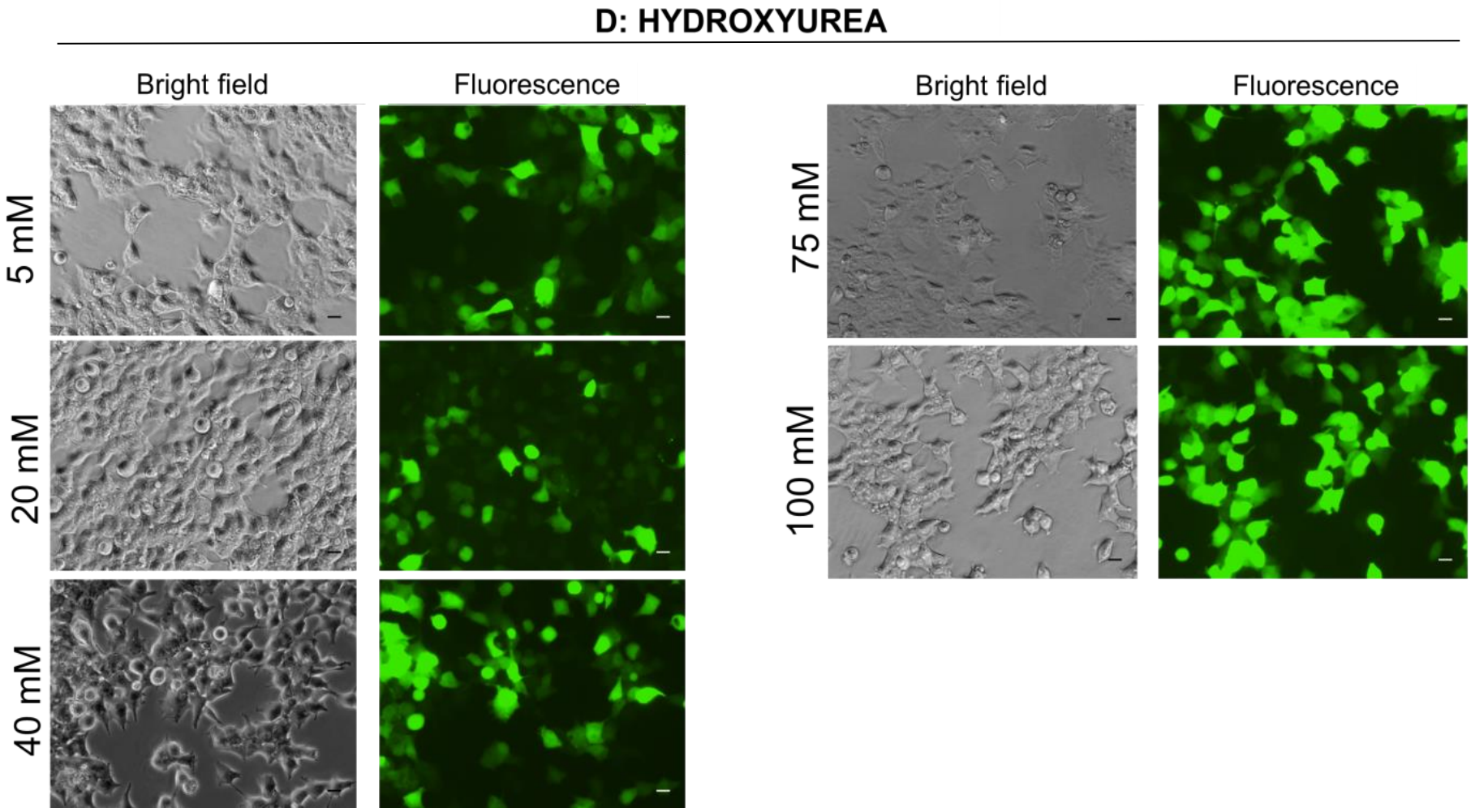
D: HYDROXYUREA
Bright field
Fluorescence
Bright field
Fluorescence
5 mM
20 mM
40 mM
75 mM
100 mM

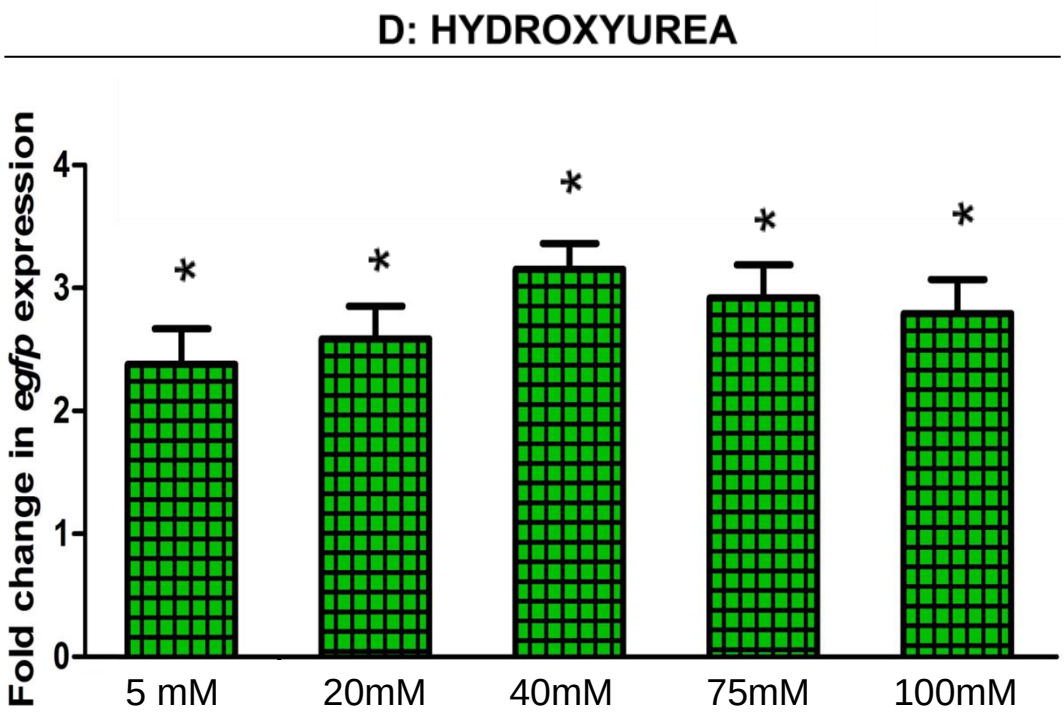

Figure 4.1. Effect of different hydroxyurea concentrations on transgene expression in AcCMV_EGFP transduced HEK293 cells. Representative photomicrographs of bright field (left images) and fluorescence (right images) taken at 24 hpt using a 10X objective and graph bar illustrating fluorescence fold change of results from a single experiment. HEK293 cells, treated and untreated with different concentrations of hydroxyurea, were transduced at MOI 50 with AcCMV_EGFP. Fold change was calculated by dividing the average fluorescence level of EGFP cells in the presence of sodium butyrate or hydroxyurea with the EGFP signal intensity of AcCMV_EGFP (virus alone) transduced HEK cells. (**A**) Untreated mock-transduced cells (negative control). (**B**) Untreated HEK293 cells transduced with AcCMV_EGFP. (**C**) AcCMV_EGFP transduced cells were incubated in the presence of 10 mM of sodium butyrate. (**D**) HEK293 cells were treated with the indicated concentration of hydroxyurea before AcCMV_EGFP transduction. Scale bar = 10 µm. *p<0.0001 indicated a significant difference between treated transduced cells and AcCMV_EGFP untreated transduced cells (One-way ANOVA).

Similar results were observed for etoposide; etoposide treatment with concentrations of 1.5, 3 and 4.5 µM significantly enhanced (F (4, 47)=81.65; p<0.0001) fluorescence intensity by approximately two-fold respectively (Figure 4.2, panel E) compared to the untreated AcCMV_EGFP transduced cells (Figure 4.2, panel B). Cells treated with 0.5 and 10 µM of etoposide (Figure 4.2, panel E) were not statistically different from transduced control cells (F (2, 35)=0.3601; p=0.7001) and only showed one-fold increase in *egfp* expression, respectively. Because the maximum value of fold change in fluorescence was obtained with 1.5 µM etoposide, this was the concentration chosen for use in future experiments.

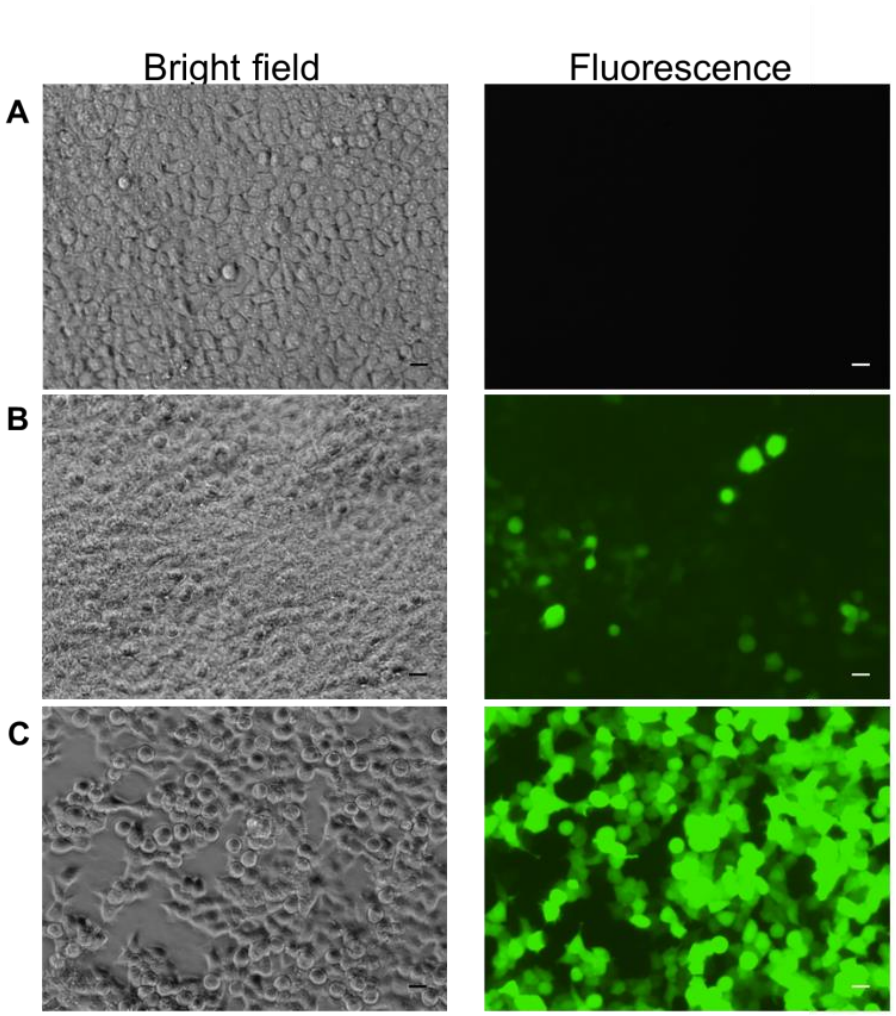
Bright field
Fluorescence
A
B
C

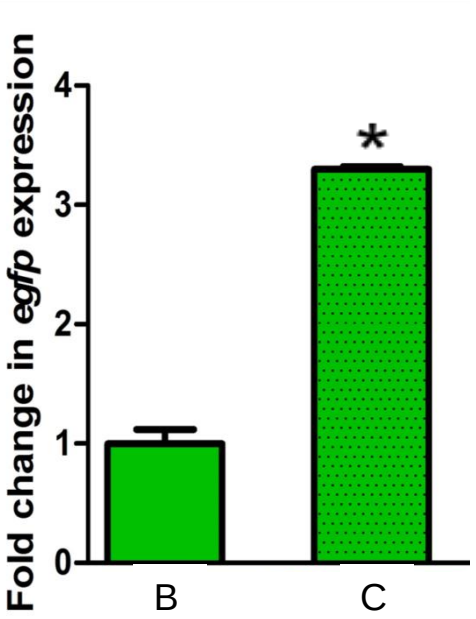
Fold change in egfp expression
0
1
2
3
4
*
B
C

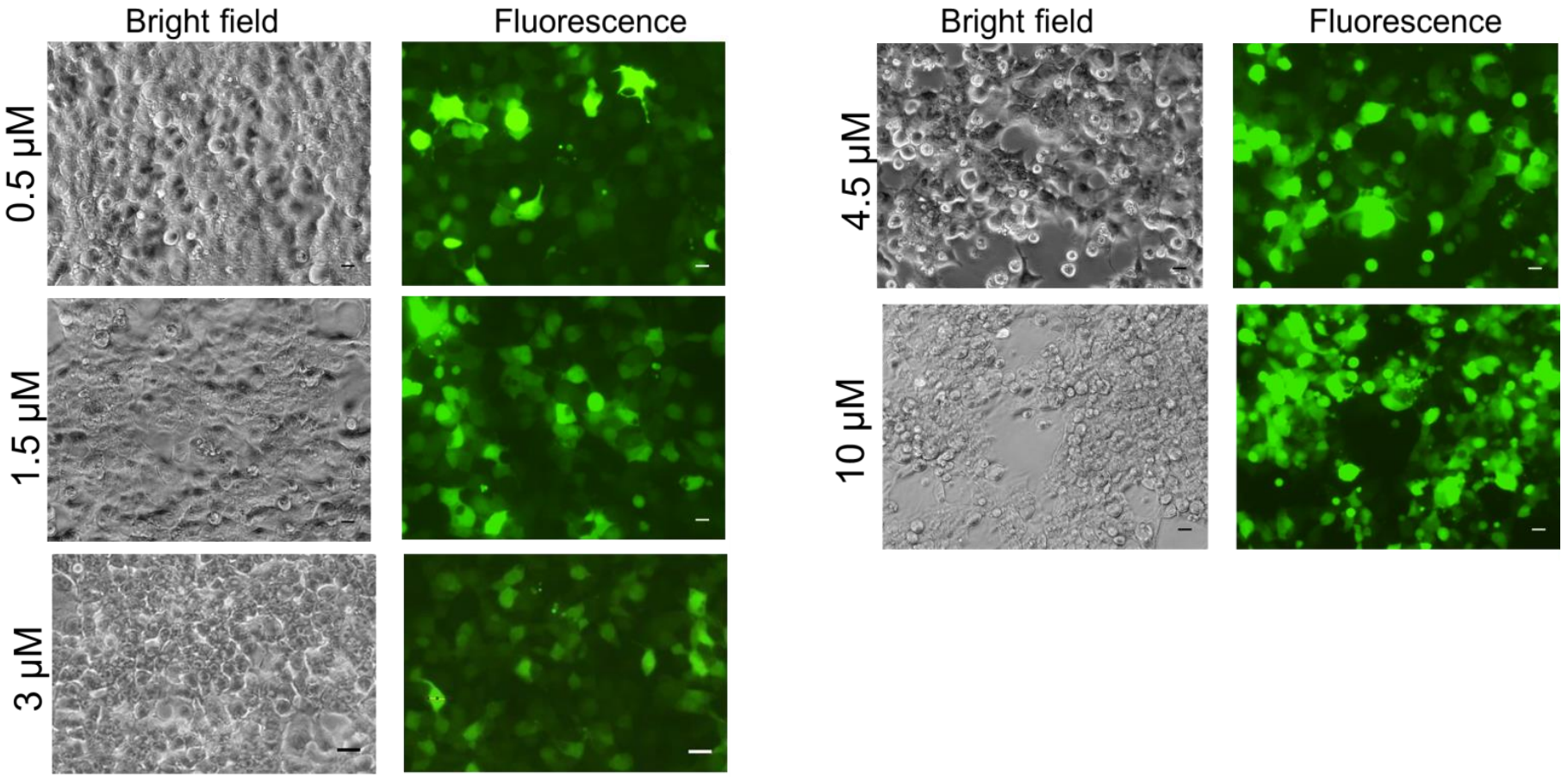
E: ETOPOSIDE
Bright field
Fluorescence
Bright field
Fluorescence
0.5 µM
1.5 µM
3 µM
4.5 µM
10 µM

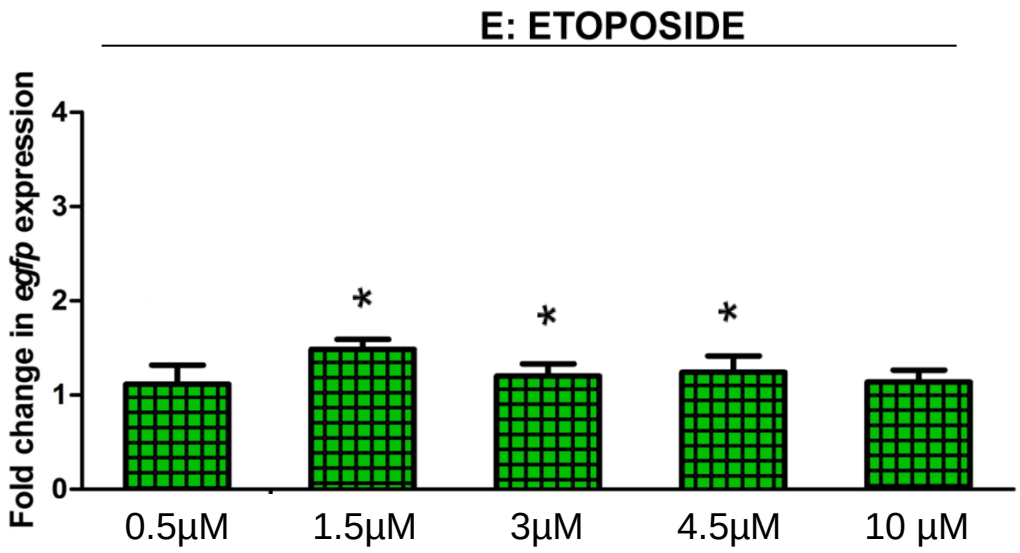

Figure 4.2. Effect of different etoposide concentrations on transgene expression in AcCMV_EGFP transduced HEK293 cells. Representative photomicrographs of bright field (left images) and fluorescence (right images) taken at 24 hpt using a 10X objective and graph bar illustrating fluorescence fold change of results from a single experiment. Culture of HEK293 cells, treated and untreated with different concentrations of etoposide, were transduced at MOI 50 with AcCMV_EGFP. Fold change was calculated by dividing the average fluorescence level of EGFP cells in the presence of sodium butyrate or etoposide compounds with the EGFP signal intensity of AcCMV_EGFP (virus alone) transduced HEK293 cells. (**A**) Untreated mock-transduced cells (negative control). (**B**) Untreated HEK293 cells transduced with AcCMV_EGFP. (**C**) Transduced cells were incubated in the presence of 10 mM sodium butyrate. AcCMV_EGFP. (**E**) HEK293 cells were treated with the indicated concentration of etoposide before transduction. Scale bar = 2 mm. *p<0.0001 indicated a significant difference between treated transduced cells and AcCMV_EGFP untreated transduced cells (One-way ANOVA).

As shown in Figure 4.3; panel F, protamine treatment did not have any significant effect (F (5, 67)= 1.787; p=0.1273) when tested at concentrations of 0.5, 5, 10 and 50 µg/ml (less than one-fold, respectively); and at 100 µg/ml *egfp* fluorescence was significantly reduced (F (5, 67)= 1.787; p<0.05).

Similar results to protamine were observed after treatment with cycloheximide (Figure 4.4, panel G) and statistical analysis revealed no difference (F (3, 48)= 0.6662; p=0.5770) in fluorescence intensity between the concentrations tested and the untreated transduced control cells (Figure 4.4, panel B). No toxicity was observed in cells treated with protamine and cycloheximide; whilst some cytotoxic effects were observed in transduced HEK293 cells pre-treated with hydroxyurea (75 and 100 mM) and etoposide (4.5 and 10 µM).

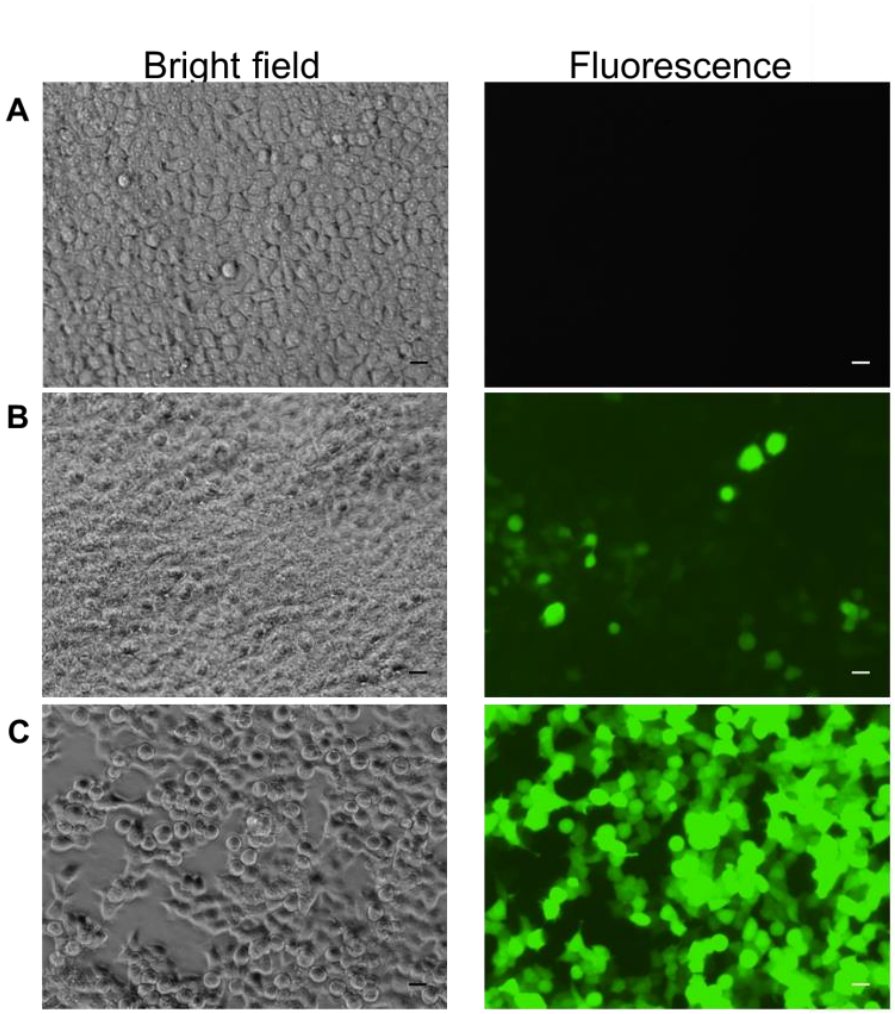
Bright field
Fluorescence
A
B
C

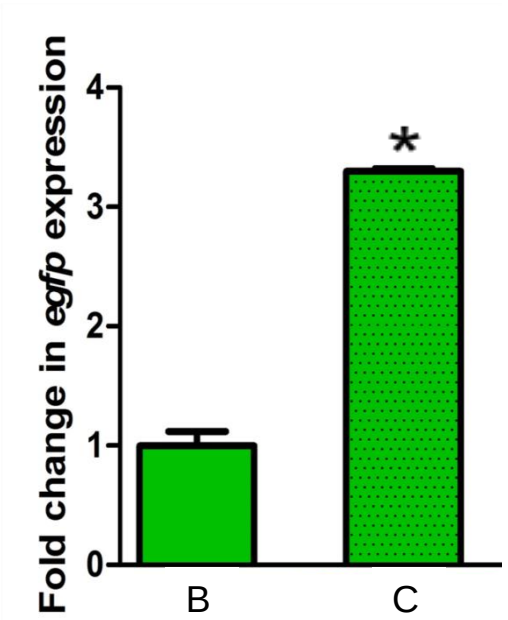
Fold change in egfp expression
0
1
2
3
4
*
B
C

F: PROTAMINE

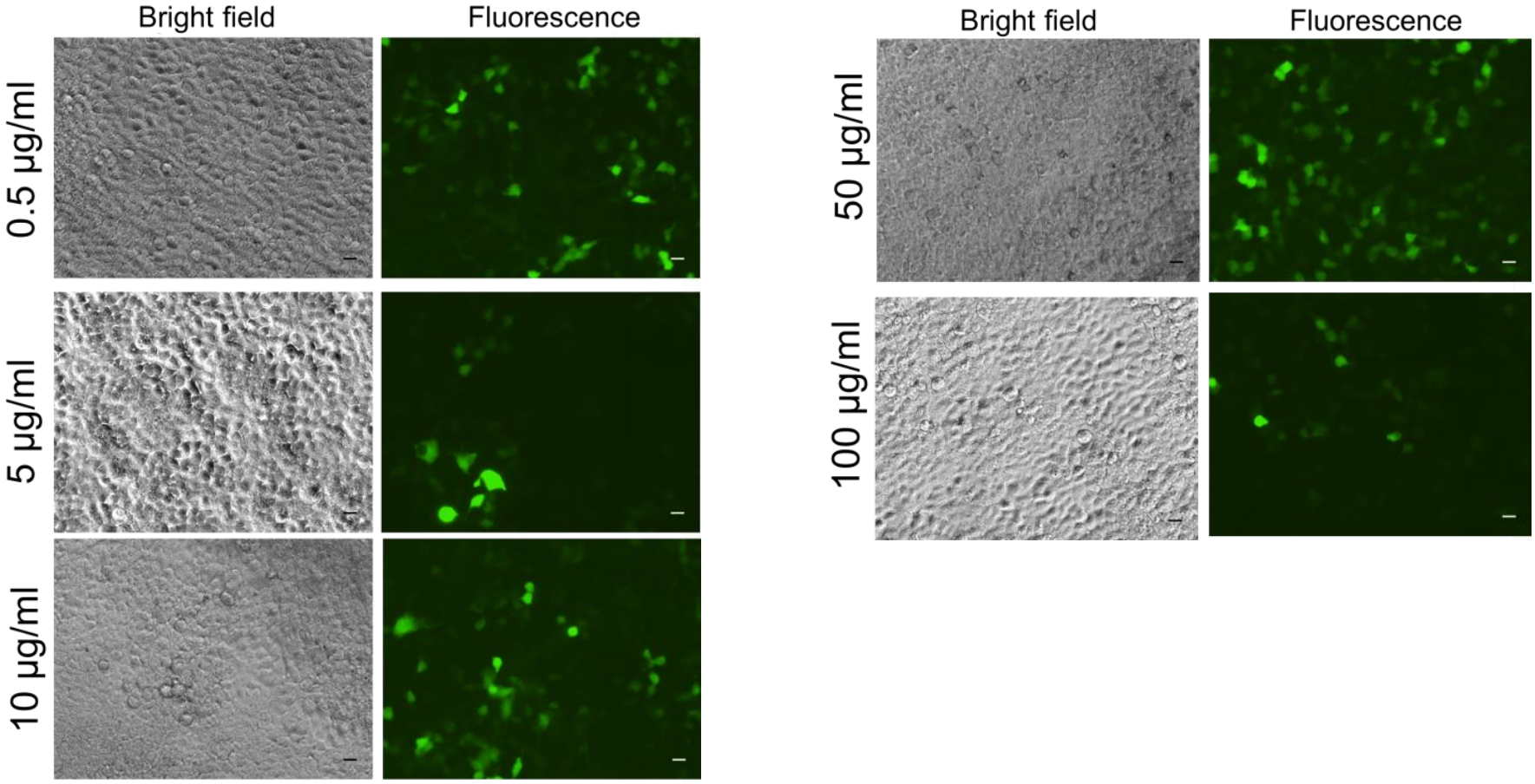
Bright field
Fluorescence
0.5 µg/ml
5 µg/ml
10 µg/ml
Bright field
Fluorescence
50 µg/ml
100 µg/ml

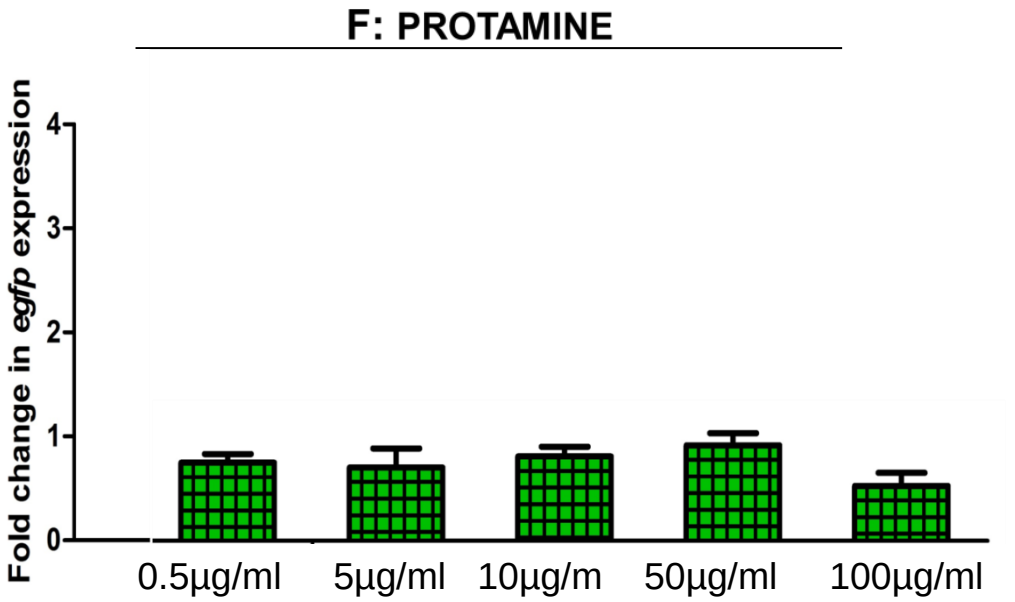

Figure 4.3. Effect of different protamine concentrations on transgene expression in AcCMV_EGFP transduced HEK293 cells. Representative photomicrographs of bright field (left images) and fluorescence (right images) taken at 24 hpt using a 10X objective and graph bar illustrating fluorescence fold change of results from a single experiment. HEK293 cells, treated and untreated with different protamine concentrations, were transduced at MOI 50 with AcCMV_EGFP. Fold change was calculated by dividing the average fluorescence level of EGFP cells in the presence of sodium butyrate or protamine compounds with the EGFP signal intensity of AcCMV_EGFP (virus alone) transduced HEK293 cells. (**A**) Untreated mock-transduced cells (negative control). (**B**) Untreated HEK293 cells transduced with AcCMV_EGFP. (**C**) Transduced cells were incubated in the presence of 10 mM sodium butyrate. AcCMV_EGFP. (**F**) HEK293 cells were co-incubated with the indicated concentrations of protamine during AcCMV_EGFP transduction. Scale bar =10 µm. *p<0.0001 indicated a significant difference between treated transduced cells and AcCMV_EGFP untreated transduced cells (One-way ANOVA).

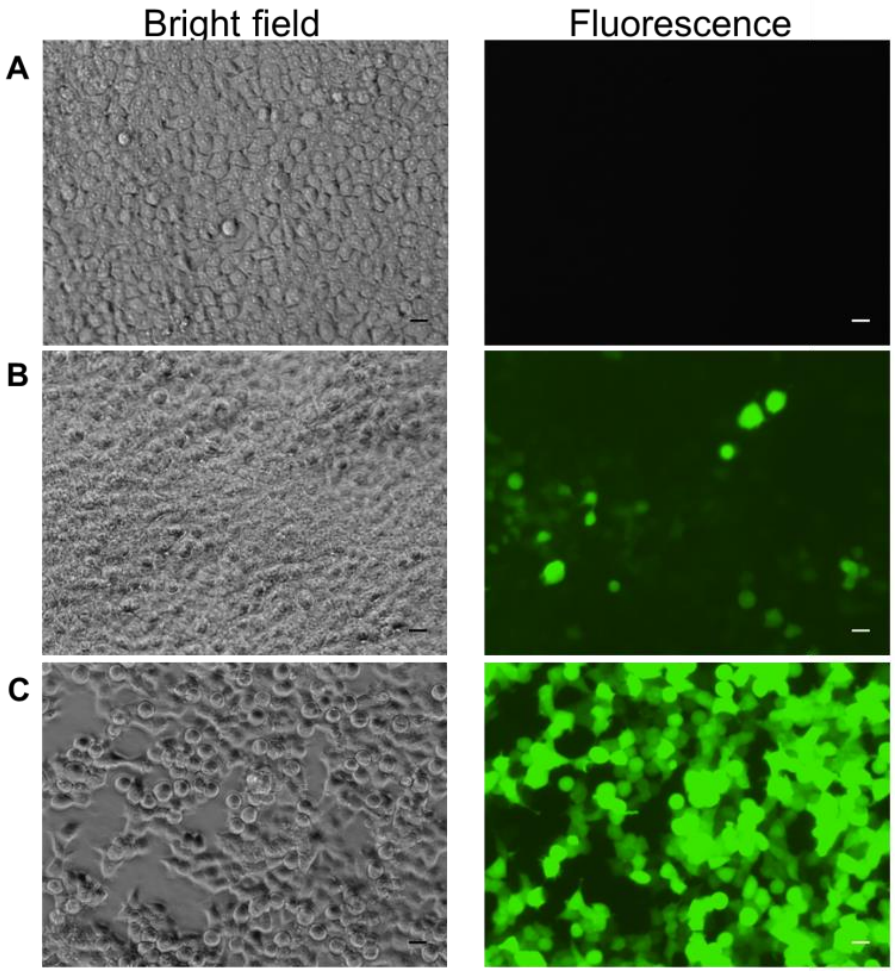
Bright field
Fluorescence
A
B
C

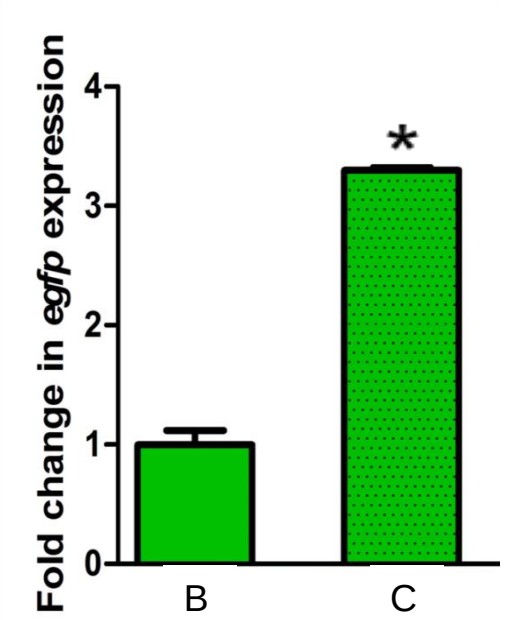
Fold change in egfp expression
4
3
2
1
0
*
B
C

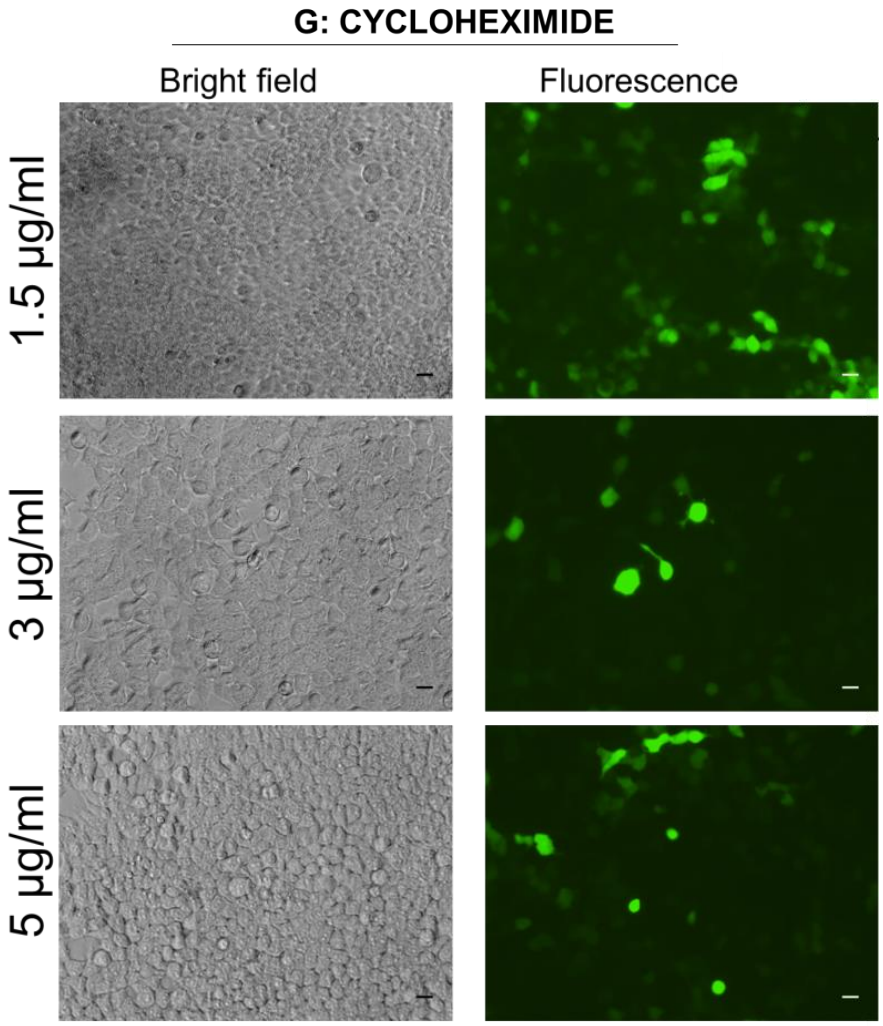
G: CYCLOHEXIMIDE
Bright field
Fluorescence
1.5 µg/ml
3 µg/ml
5 µg/ml

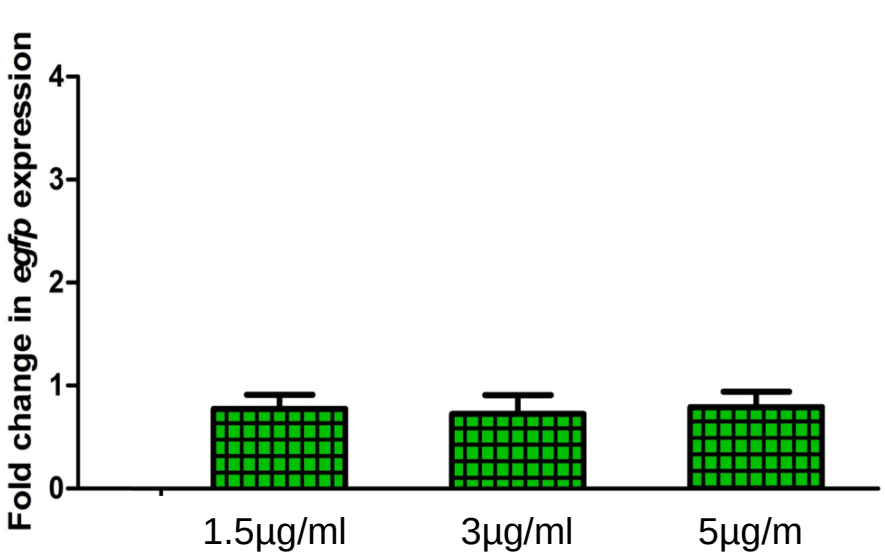
Fold change in egfp expression
0
1
2
3
4
1.5µg/ml
3µg/ml
5µg/m

Figure 4.4. Effect of different cycloheximide concentrations on transgene expression in AcCMV_EGFP transduced HEK293 cells. Representative photomicrographs of bright field (left images) and fluorescence (right images) taken at 24 hpt using a 10X objective and graph bar illustrating fluorescence fold change of results from a single experiment. HEK293 cells, treated and untreated with different concentration of cycloheximide, were transduced at MOI 50 with AcCMV_EGFP. Fold change was calculated by dividing the average fluorescence level of EGFP cells in the presence of sodium butyrate or cycloheximide compounds with the EGFP signal intensity of AcCMV_EGFP (virus alone) transduced HEK293 cells. (**A**) Untreated mock-transduced cells (negative control). (**B**) Untreated HEK293 cells transduced with AcCMV_EGFP. (**C**) Transduced cells were incubated in the presence of 10 mM sodium butyrate. AcCMV_EGFP. (**G**) HEK293 cells were pre-treated with the indicated concentration of cyclohexamide before transduction. Scale bar = 10 µm. *p<0.0001 indicated a significant difference between treated transduced cells and AcCMV_EGFP untreated transduced cells (One-way ANOVA).

4.3 EFFECT OF CHEMICAL COMPOUNDS ON BACMAM TRANSGENE EXPRESSION IN HEK293 CELLS

Optimization studies, in Section 4.2, shown that BacMam-mediated transgene expression was considerably improved by addition of sodium butyrate, hydroxyurea and etoposide. The optimal concentrations identified in Section 4.2 for hydroxyurea (40 mM) and etoposide (1.5 µM) were used in the following studies. Protamine (50 µg/ml) and cyclohexamide (1.5 µg/ml) were also further tested.

To compare the effects of these chemical compounds on transgene expression, triplicate dishes of HEK293 cells ($0.8x10^5$ cells/well), in four independent experiments, were pre-exposed to hydroxyurea (40 mM), etoposide (1.5 µM), cyclohexamide (1.5 µg/ml) or sodium butyrate (10 mM) or co-incubated with protamine (50 µg/ml) and transduced with AcCMV_EGFP virus (MOI 50). Cultures were examined 24 later by fluorescence microscopy and fluorescence intensity quantified as previously described. Representative data from a single experiment are shown in this thesis Section.

As expected, sodium butyrate significantly increased (F (5, 62)= 7.499; p<0.0001) fluorescence intensity by three-fold (Figure 4.5, panel C) compared to the untreated control cells (Figure 4.5, panel B). Hydroxyurea showed a two-fold increase (Figure 4.5, panel D) which was also significantly higher than control cells (F (5, 62)= 7.499; p<0.0001). Transduced cells treated with etoposide (Figure 4.5, panel E) were approximately two-fold higher than AcCMV_EGFP untreated cells but were not significantly different (F (3, 46) = 2.017; p=0.1247). Only a slight increase in expression was observed in HEK293 cells transduced with AcCMV_EGFP co-incubated with protamine (Figure 4.5, panel F). Whereas, no increase in fluorescence was observed in cells pre-treated with cycloheximide (Figure 4.5, panel G); this may have been due to its cytotoxic effect.

To evaluate the influence of chemical compounds and cationic lipids on cell viability, a Trypan blue dye exclusion assay was carried out (Section 2.2.6). As shown in Figure 4.6; Bars 3 to 6, chemical treatment with sodium butyrate (86%), hydroxyurea (85%), etoposide (88%) and protamine (87%) did not significantly reduce cell viability (F (5, 15)= 2.826; p=0.0542) compared to control cells, mock (91%) or AcCMV_EGFP (90%) transduced cells (Figure 4.6; Bars 1 and 2, respectively). The viability of transduced HEK cells treated with cycloheximide (Figure 5.12, Bar 7) decreased significantly from 91% to 73% (F (11, 27)= 7.140; p< 0.0001).

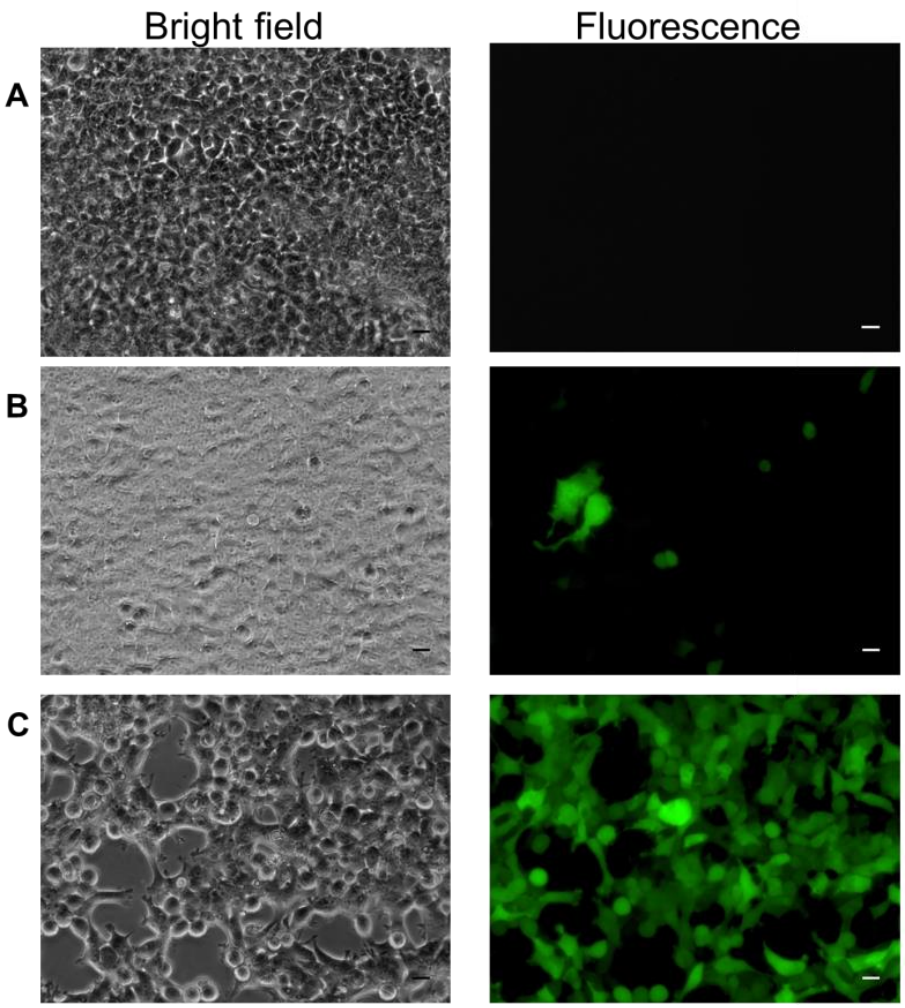
Bright field
Fluorescence
A
B
C

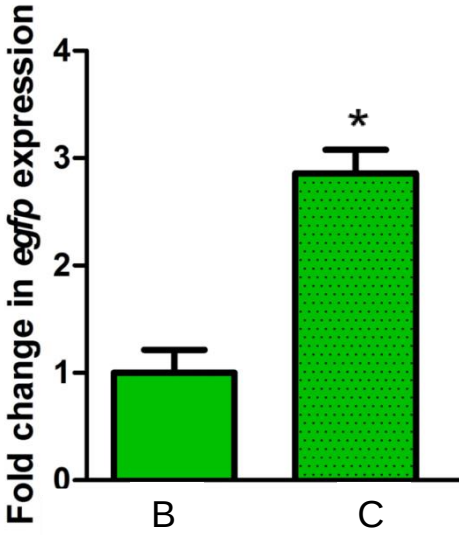
Fold change in egfp expression
4
3
2
1
0
*
B
C

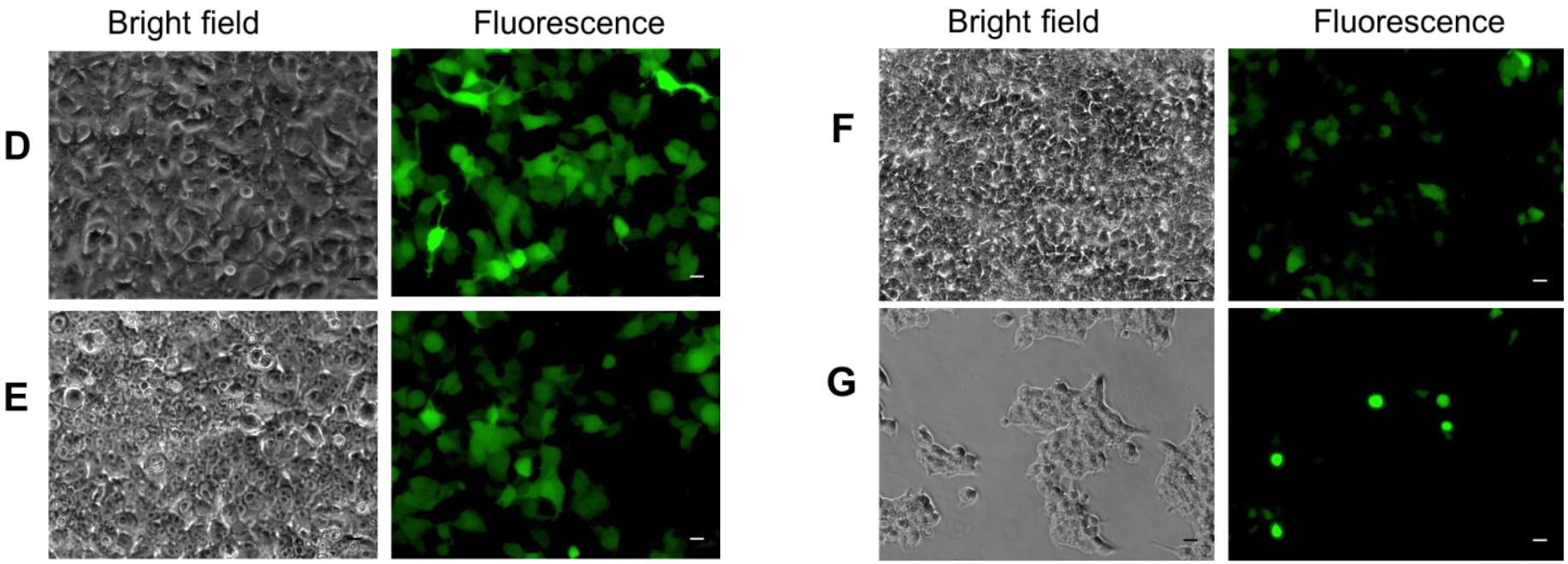
Bright field
Fluorescence
D
E
Bright field
Fluorescence
F
G

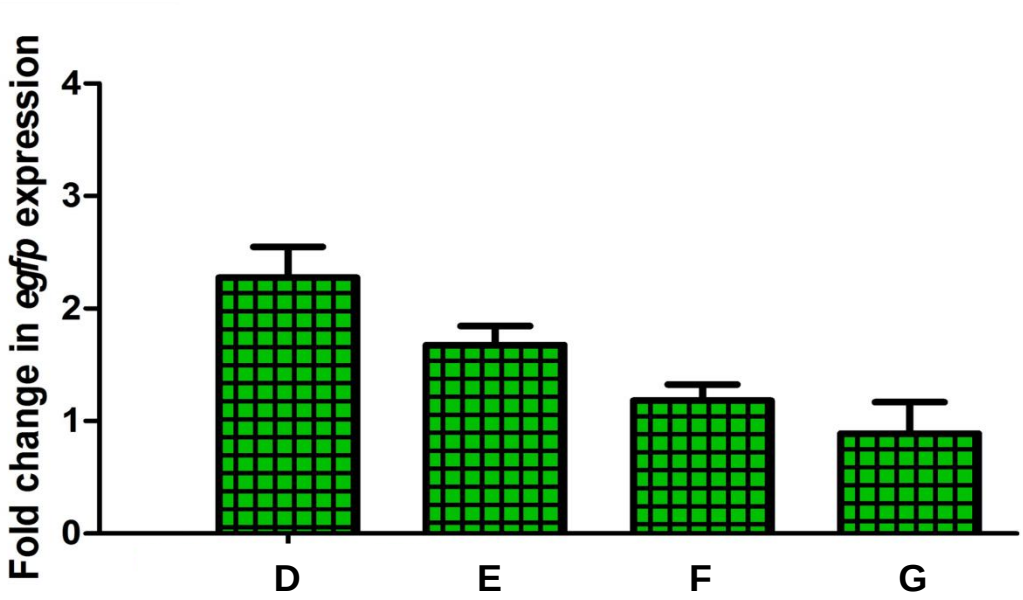

Figure 4.5. *Egfp* expression in HEK293 cells transduced with AcCMV_EGFP in the presence or absence of chemical compounds. Representative photomicrographs of bright field (left), and fluorescence (right), images taken at 24 hpt using a 10X objective and graph bar illustrating fluorescence fold change of a representative single experiment. Fold change was calculated by dividing the average fluorescence level of treated AcCMV_EGFP cells with the EGFP signal intensity of AcCMV_EGFP (virus alone) transduced HEK293 cells. (**A**) Mock-transduced HEK293 cells (negative control). (**B**) Untreated HEK cell transduced with AcCMV_EGFP (virus alone). (**C-G**) Transduced HEK293 cells pre- or post-treated with different chemical compounds: (C) sodium butyrate, (D) hydroxyurea, (E) etoposide, (F) protamine and (G) cyclohexamide. Scale bar = 10 µm. *p<0.0001 indicated a significant difference between treated transduced cells and AcCMV_EGFP untreated transduced cells (One-way ANOVA).

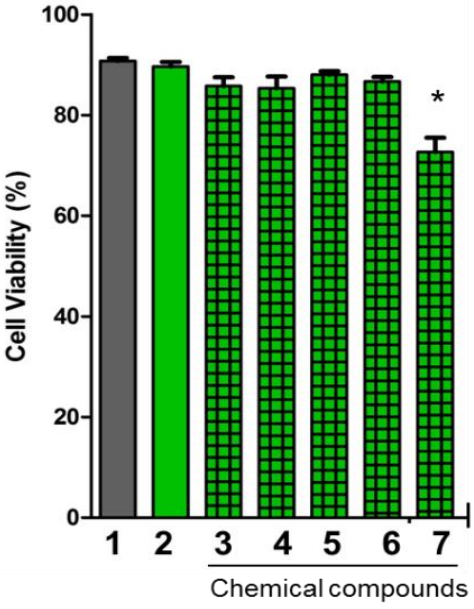

Bars	Virus ± Chemical compound or Cationic lipids transduced HEK cell	Cell viability (%)
1	Mock-transduced cells	91
2	AcCMV_EGFP	90
3	AcCMV_EGFP +Sodium butyrate	86
4	AcCMV_EGFP + Hydroxyurea	85
5	AcCMV_EGFP + Etoposide	88
6	AcCMV_EGFP + Protamine	87
7	AcCMV_EGFP +Cycloheximide	73*

Figure 4.6. Cytotoxic effect of chemical on HEK293 cells. HEK cells ($0.8x10^5$ cells/ml) were chemically treated before or after transduction. 24 hpt cell viabilities were determined using Trypan blue exclusion assay. The data presented are the mean ± standard deviations from triplicate samples of a representative single experiment. *p<0.0001 indicated a significant difference compared to controls cells.

The results obtained by fluorescence microscopy were further confirmed by flow cytometry (Section 2.2.7.I). Representative flow cytometry dot plot images are shown in Figures 4.7. The plots were divided into two sections to distinguish populations of cells that were considered EGFP negative (green dots in the lower region) and EGFP positive (red dots in the upper region). Fluorescence intensity (FL1, y-axis) was plotted on a log scale against the forward scatter signal (FS, x-axis), which is directly related to cell size. As illustrated in Figures 4.7 A, low fluorescence (5%) was detected in populations of mock-transduced cells representing background fluorescence from cells and was subtracted from the values obtained from transduced samples. Following AcCMV_EGFP transduction of untreated cells, 32% of HEK293 cells emitted fluorescence, compared to the mock-transduced cells (Figures 4.7 panels B *vs.* A).

As shown in Figure 4.7, flow cytometer dot plots indicated that 24 hpt, treatment with sodium butyrate (panel C), hydroxyurea (panel D) and etoposide (panel E) greatly enhanced the number of EGFP-expressing cells (70%, 70% and 63%, respectively); however, expression levels similar to the untreated control (panel B) were observed for AcCMV_EGFP transduced cells in the presence of protamine (panel F) or treated with cycloheximide (panel G). These results were consistent with earlier observations (see Figures 4.1-4.4).

The fold change in fluorescence after transduction with AcCMV_EGFP alone (positive control) was calculated (Figure 4.8, A) and plotted as a bar diagram (Figure 4.8, B). Statistical analysis of the data revealed a significant difference (F (5, 11)= 245.1; p<0.0001) between *egfp* expression levels of cells treated with sodium butyrate, hydroxyurea or etoposide and untreated transduced cells (Figure 4.8); these chemical treatments showed an approximately two-fold increase in transgene expression.

Controls

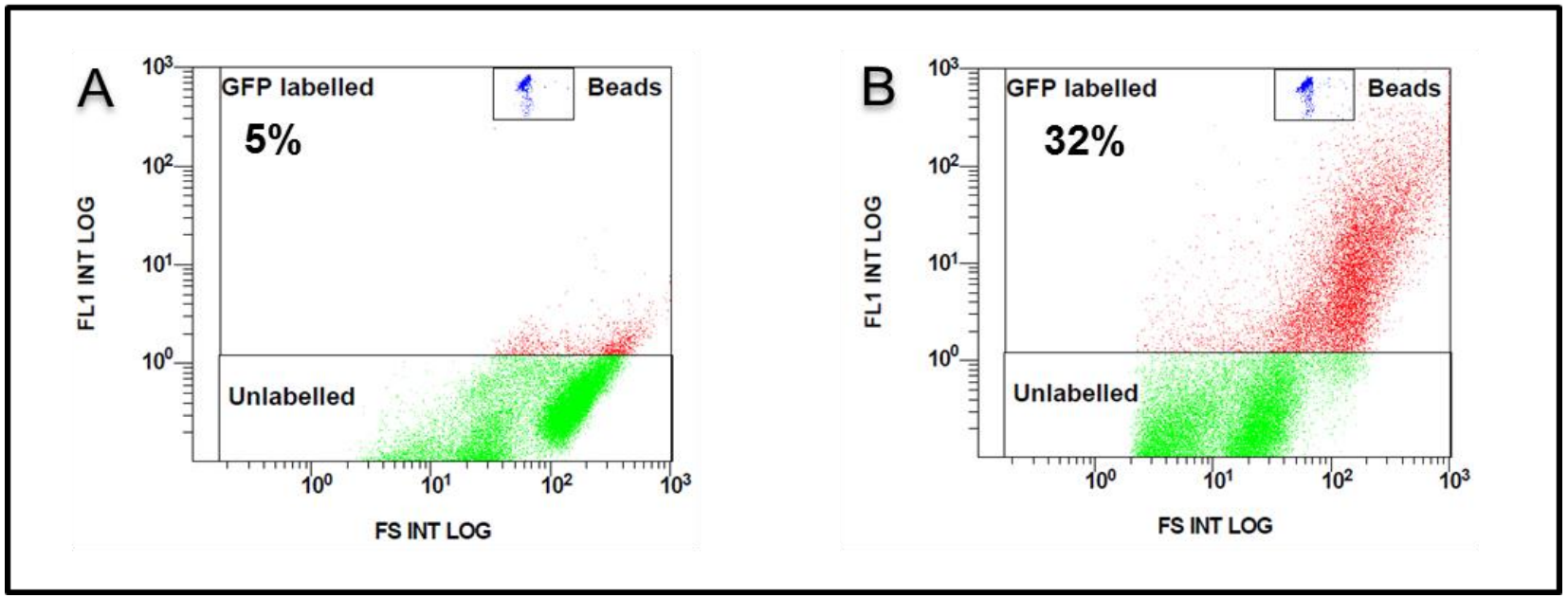
A
GFP labelled
5%
Beads
Unlabelled
FL1 INT LOG
FS INT LOG
B
GFP labelled
32%
Beads
Unlabelled
FL1 INT LOG
FS INT LOG

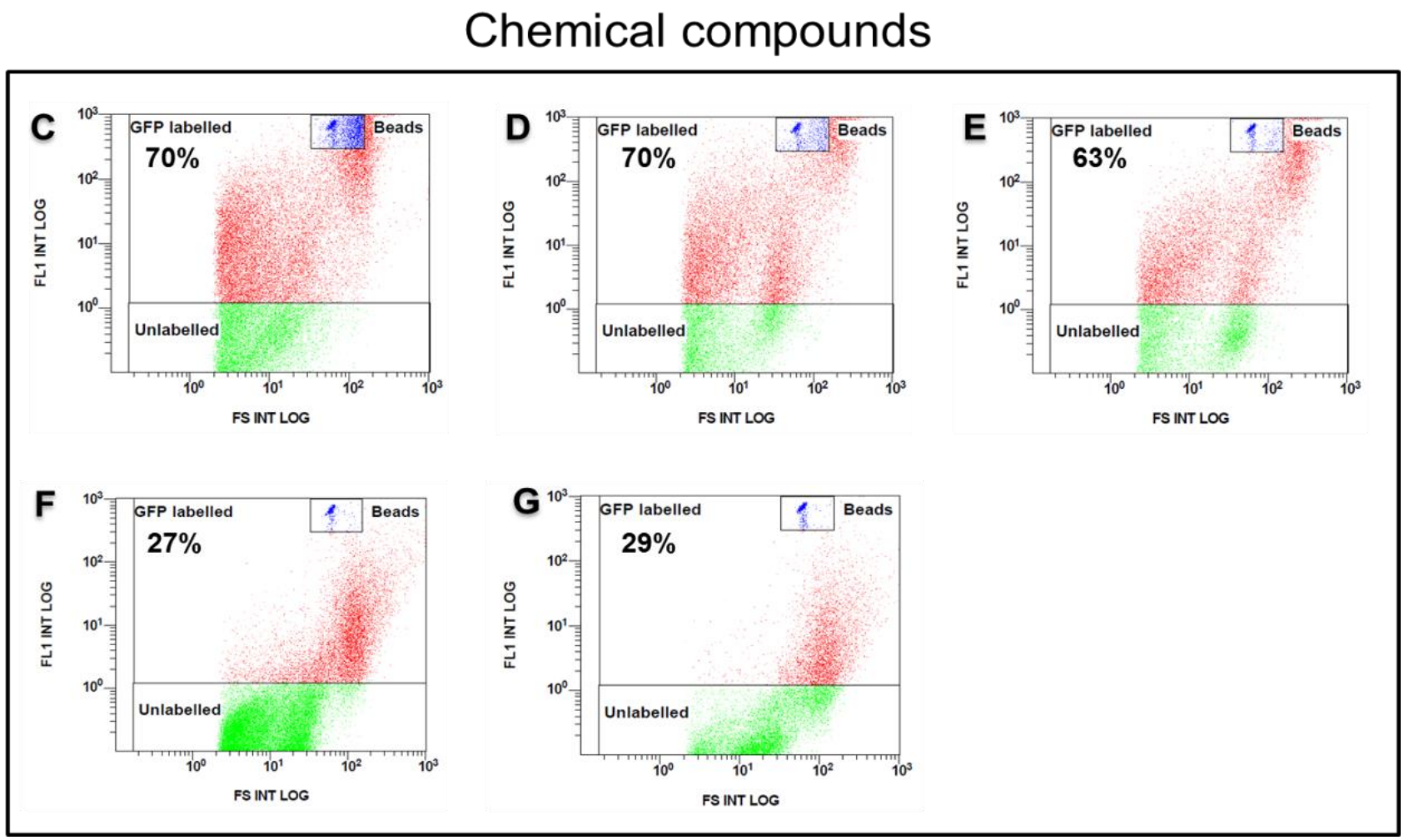
Chemical compounds
C
GFP labelled
70%
Beads
Unlabelled
FL1 INT LOG
FS INT LOG
D
GFP labelled
70%
Beads
Unlabelled
FL1 INT LOG
FS INT LOG
E
GFP labelled
63%
Beads
Unlabelled
FL1 INT LOG
FS INT LOG
F
GFP labelled
27%
Beads
Unlabelled
FL1 INT LOG
FS INT LOG
G
GFP labelled
29%
Beads
Unlabelled
FL1 INT LOG
FS INT LOG

Figure 4.7. Representative dot plot images of a single experiment from flow cytometry analysis of AcCMV_EGFP transduced HEK293 cells treated with chemical compounds. EGFP fluorescence intensity (FL1, y-axis) was plotted against the forward scattered light (FS, x-axis). Both axes are log- scale and each dot represents a single cell; approximately 80,000 cells are represented in each plot. The line in the plots depicts the boundary between the two populations of EGFP-positive (red) and EGFP-negative (green) cells. The counting beads are indicated in dark blue. The top two panels represent control cells: (**A**) dot plot of mock-transduced cells (negative control) and (**B**) AcCMV_EGFP transduced cells (untreated cells; positive control). Flow cytometry plots of transduced HEK293 cellstreated with 10 mM sodium butyrate (**C**), 40 mM hydroxyurea (**D**), 1.5 µM etoposide (**E**), 50 µg/ml protamine (**F**) and 1.5 µg/ml cycloheximide (**G**).

A

Virus ± Chemical compound or Cationic lipids	EGFP-positive cells (%)	Fluorescence fold change
AcCMV_EGFP	32	1
AcCMV_EGFP +**Sodium butyrate**	70	2.2
AcCMV_EGFP + **Hydroxyurea**	70	2.2
AcCMV_EGFP + **Etoposide**	63	2
AcCMV_EGFP + Protamine	27	0.8
AcCMV_EGFP +Cycloheximide	29	0.9

B

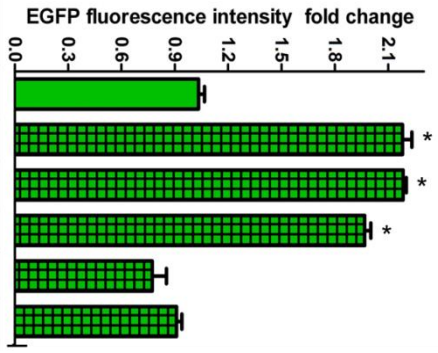

Figure 4.8. Fold change in EGFP fluorescence intensity in transduced HEK293 cells after addition of chemical compounds. Fold change was calculated by dividing the average fluorescence intensity level of EGFP cells in the presence of chemical compound with the EGFP signal intensity of AcCMV_EGFP (virus alone) transduced HEK293 cells. (**A**) Table showing the number of EGFP positive cells and the fluorescence fold change. (**B**) Graph bar illustrating the fold change in *egfp* expression normalized to the AcCMV_EGFP (virus alone) transduced HEK293 cells. The data presented are the mean ± standard deviations from triplicate samples. **p*<0.0001 indicated a significant difference with the control sample.

In conclusion, fluorescence microscopy and flow cytometry analysis confirmed that *egfp* expression in transduced cells was enhanced by the presence of chemical compounds hydroxyurea and etoposide. On the basis of these findings, the effects of 40 mM hydroxyurea and 1.5 µM etoposide compounds were further investigated in BacMam transduced cells.

In order to determine the broader utility of these chemical compounds they were tested with viruses expressing *bcl-2*. HEK293 cells treated with chemical compounds, individually or in combination (Table 4.1) and were transduced with AcCMV_BCL-2 viruses (MOI 50). *LacZ* expression was tested in this study and results are included in the supplementary data CD attached to this thesis (Chapter 4-S1).

The effect of these chemicals on *bcl-2* expression was evaluated in two independent experiments by western blot analysis (Section 2.2.4.IV). AcCMV_BCL-2 transduced treated and untreated cells were harvested at 24 hpt and cell pellets were processed for SDS-PAGE (Sections 2.2.4.I and II). Proteins were then transferred from the gel onto a nitrocellulose membrane (Section 2.2.4.IV) and immunoblotted using an antibody against BCL-2 (Chapter 2; Tables 2.7 and 2.8).

Table 4.1. Different chemical treatments used in HEK293 cells.

Chemical treatment	Time of treatment	
Sodium butyrate (10 mM)	Post-transduction	Individually
Hydroxyurea (40 mM)	Pre-transduction	
Etoposide (1.5 µM)	Pre-transduction	
Hydroxyurea (40 mM) + Etoposide (1.5 µM)	Pre-transduction	In pairwise combination
Hydroxyurea (40 mM) + Sodium butyrate (10 mM)	Pre-transduction / Post-transduction	
Etoposide (1.5 µM) + Sodium butyrate (10 mM)	Pre-transduction / Post-transduction	

Expression levels of *bcl-2* for a single representative experiment are shown in Figure 4.9 for all the culture conditions. β-tubulin expression was also included as it was used as a loading control (lower membrane). The anti-BCL-2 antibody identified a ~25 kDa band corresponding to the expected size of recombinant BCL-2 protein in all transduced cells (Figure 4.9, lanes 2 to 8, highlighted by the arrow); however the intensity of the band differed between all the cell culture conditions.

As shown in Figure 4.9, densitometry analysis confirmed that *bcl-2* expression was significantly higher (F (6, 14)= 193.3; p<0.0001) in transduced cells treated with sodium butyrate (21%; lane 3), hydroxyurea (13%; lane 4) and etoposide (13%; lane 5) compared to transduced untreated control cells (3.2%; lane 2).

Furthermore, the intensity of BCL-2 bands, shown in Figure 4.9, were significantly greater (F (6, 14)= 193.3; p<0.0001) in transduced cells treated with hydroxyurea + sodium butyrate (19%; lane 6), sodium butyrate + etoposide (20%; lane 7) and hydroxyurea + etoposide (12%; lane 8) than that of the control cells (3.2%; lane 2). Although *bcl-2* expression in transduced cells, treated with different chemical combinations, was higher than that observed in transduced untreated cells, their effect was not greater than that induced by sodium butyrate alone (21%). These results were similar to those observed with the reporter gene *lacZ* (included in the supplementary data CD, Chapter 4-S1).

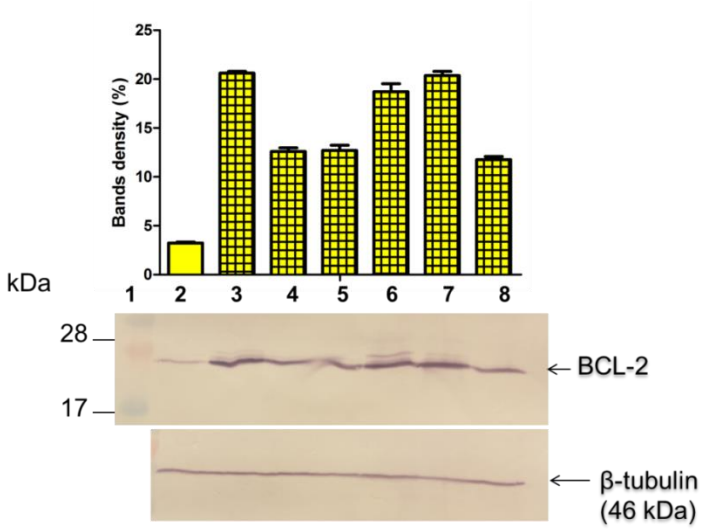

Figure 4.9. Transgene expression in chemically treated and untreated HEK293 cells transduced with AcCMV_BCL-2. Expression levels of BCL-2 in BacMam transduced HEK cells 24 hpt. Lane 1, PageRuler Plus Prestained Protein Ladder; lane 2, transduced untreated cells (positive control); transduced HEK293 cells treated with sodium butyrate (lane 3), hydroxyurea (lane 4), etoposide (lane 5), hydroxyurea + sodium butyrate (lane 6), sodium butyrate + etoposide (lane 7) and hydroxyurea + etoposid (lane 8). Densitometry analysis of western blot was performed and data are shown as means ± SE (n=3; above western blot); *p<0.0001 indicated a significant difference compared to transduced untreated cells. Western blots were stained with anti-BCL-2 primary antibody and alkaline phosphatase conjugated anti-mouse IgG secondary antibody. β-Tubulin was included as a loading control.

4.4 COMPARISON OF TRANSGENE EXPRESSION LEVELS IN HEK293 CELL, DELIVERED VIA PLASMID TRANSFECTION OR VIRAL TRANSDUCTION, WITH CHEMICALS

In order to determine whether chemical compounds could enhance transgene expression levels by a similar order of magnitude when delivered by transfection or transduction, HEK293 cells were transfected with a transfer vector using baculoFectin (Section 2.2.3.I.a) or transduced with BacMam (Section 2.2.3.V). For the purpose of this single experimental study, the transfer vector pAcEGFP and BacMam AcCMV_EGFP, both encoding for *egfp,* were employed. HEK293 cells were treated with sodium butyrate, hydroxyurea, etoposide or their pairwise combination before or after delivery of the recombinant gene. Based on preliminary studies described in this chapter, the optimal working concentration for each chemical was chosen. Treated cells were then incubated for 5 h, at room-temperature, with pre-prepared complexes of baculoFectin-pAcEGFP in serum-free medium, or transduced by AcCMV_EGFP for 1 h, at room-temperature. Following 24 h of incubation, transfected, transduced and controls cells were analysed by fluorescence microscopy and fluorescence intensity measured using a fluorescence plate reader (Figures 4.10 and 4.11).

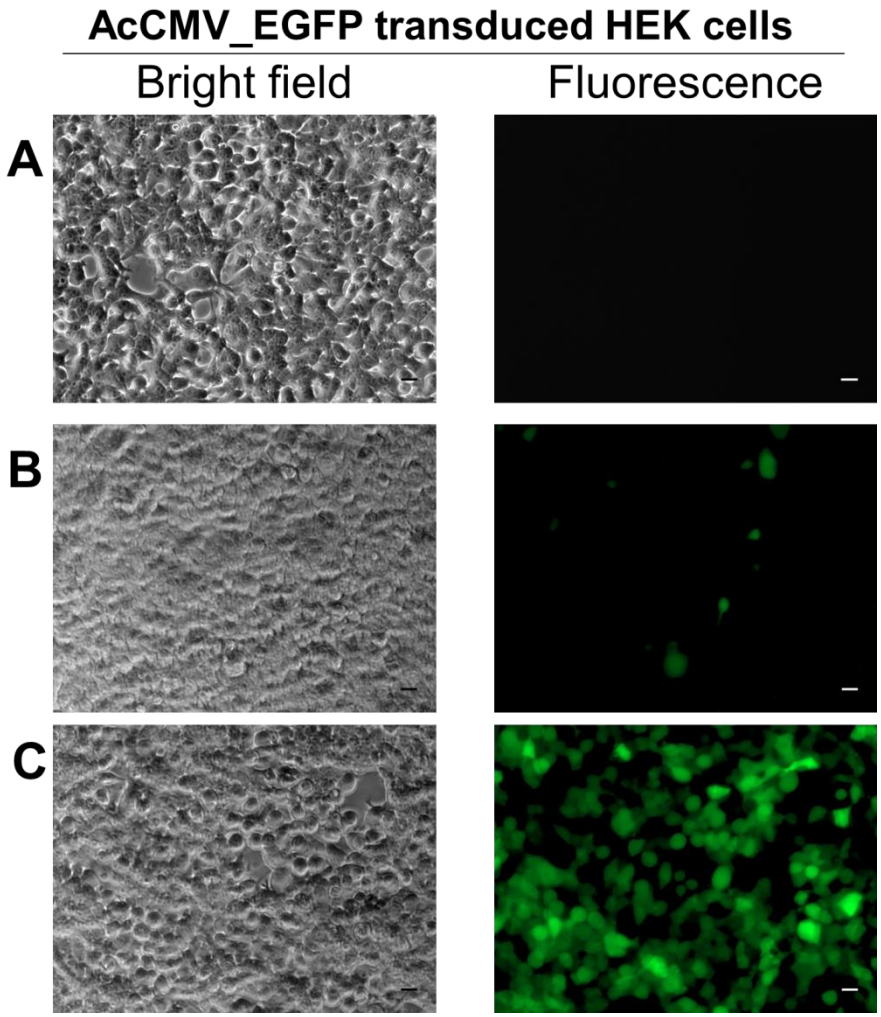
AcCMV_EGFP transduced HEK cells
Bright field
Fluorescence
A
B
C

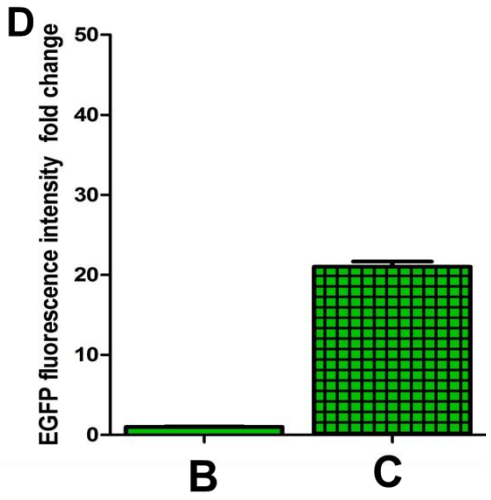
D
EGFP fluorescence intensity fold change
50
40
30
20
10
0
B
C

AcCMV_EGFP transduced HEK cells

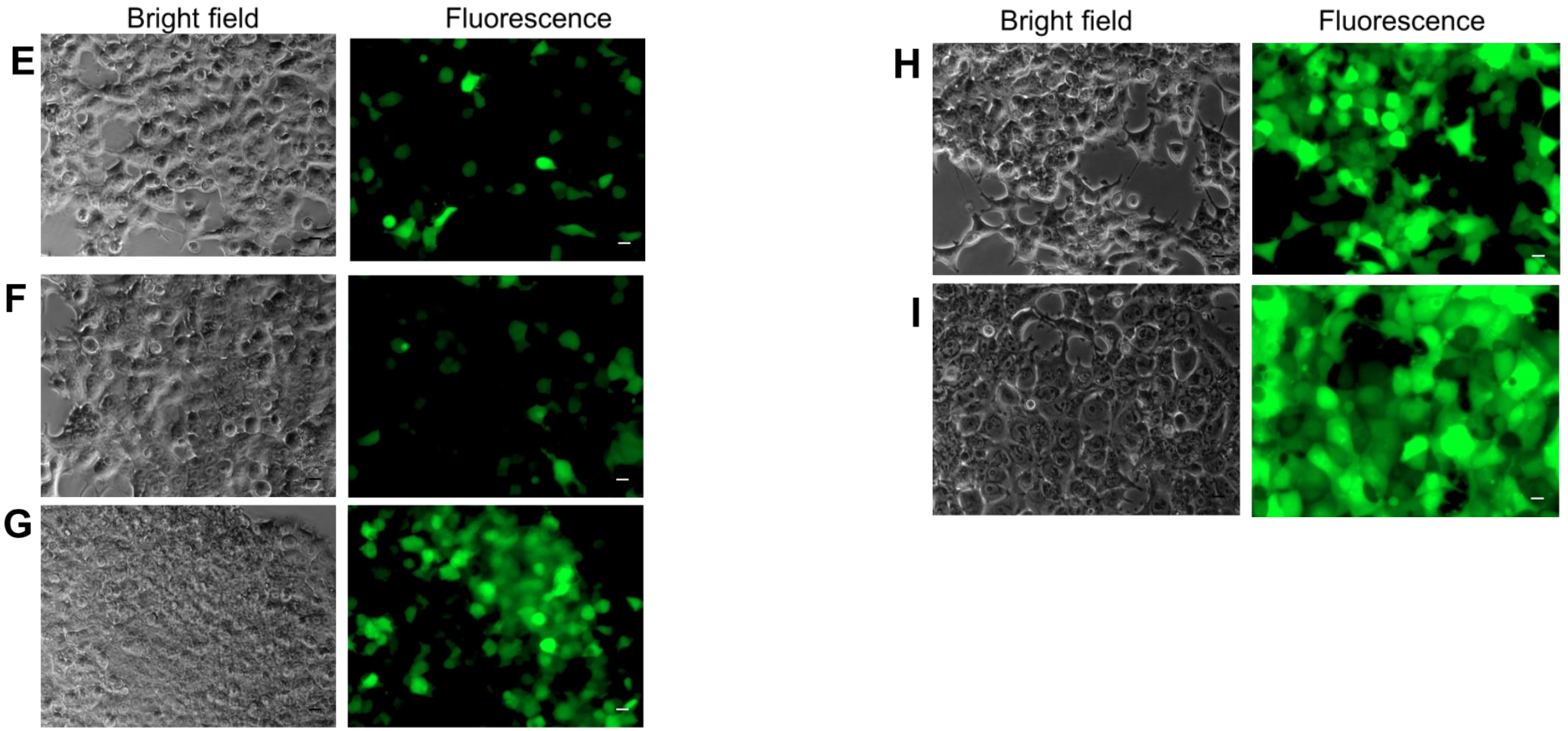

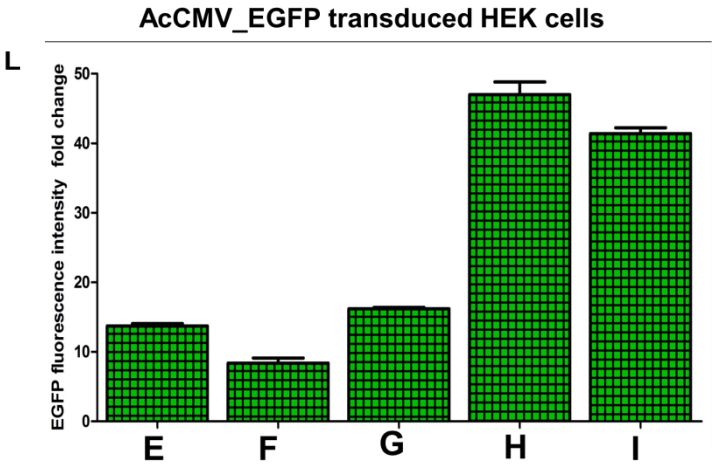

Figure 4.10. Effect of chemical compounds, individually or in pairwise combination, on *egfp* expression in transduced HEK293 cells. Representative photomicrographs of bright field (bottom images), and fluorescence (top images) taken at 24 h following incubation using the 10X objective and graph bar illustrating fluorescence fold change. (**A**) Mock-transduced HEK293 cells (negative control). (**B**) Untreated HEK cell transduced with AcCMV_EGFP (virus alone). Transduced HEK293 cells pre- or post-treated with (**C**) sodium butyrate, (**E**) hydroxyurea, (**F**) etoposide, (**G**) hydroxyurea + etoposide, (**H**) hydroxyurea + sodium butyrate and (**I**) sodium butyrate + etoposide. (**D** and **L**) Fluorescence intensity fold change was calculated by dividing the average fluorescence level of EGFP cells in the presence of chemical compounds with the EGFP signal intensity of AcCMV_EGFP untreated HEK293 cells. Scale bar =10 µm. **p*<0.0001 indicated a significant difference between treated cells and untreated cells (One-way ANOVA; n=3).

As shown in Figure 4.10, no fluorescence was observed in either mock-transduced or non-transfected HEK293 cells (Figure 4.10 A). The maximal *egfp* expression level in transduced HEK293 cells, treated with individual chemicals, was observed with sodium butyrate (Figure 4.10 C). Moreover, as shown in Figure 4.10, the transgene expression was also increased by addition of hydroxyurea (E) or etoposide (F) compared to untreated transduced cells (B), but lower than those observed in the presence of sodium butyrate (C).

Quantification of fluorescence intensity, further confirmed that transgene expression was significantly enhanced more than 20-fold when using sodium butyrate and approximately 14- and eight-fold with hydroxyurea and etoposide respectively (F (6, 51)= 342.1; p<0.001). Although the increase in *egfp* fluorescence intensity in transduced cells was considerably higher in all three tested pairwise chemical combinations, it was significantly greater in cells treated with the chemical combination hydroxyurea + sodium butyrate (Figure 4.10 H) and etoposide + sodium butyrate (Figure 4.10 I). Indeed, fluorescence measurements revealed that *egfp* expression levels were significantly enhanced (F (6, 51)= 342.1; p<0.001) by 16-, 47- and 41-fold in the presence of hydroxyurea + etoposide, hydroxyurea + sodium butyrate and etoposide + sodium butyrate, respectively (Figure 4.10 G, H and I, respectively).

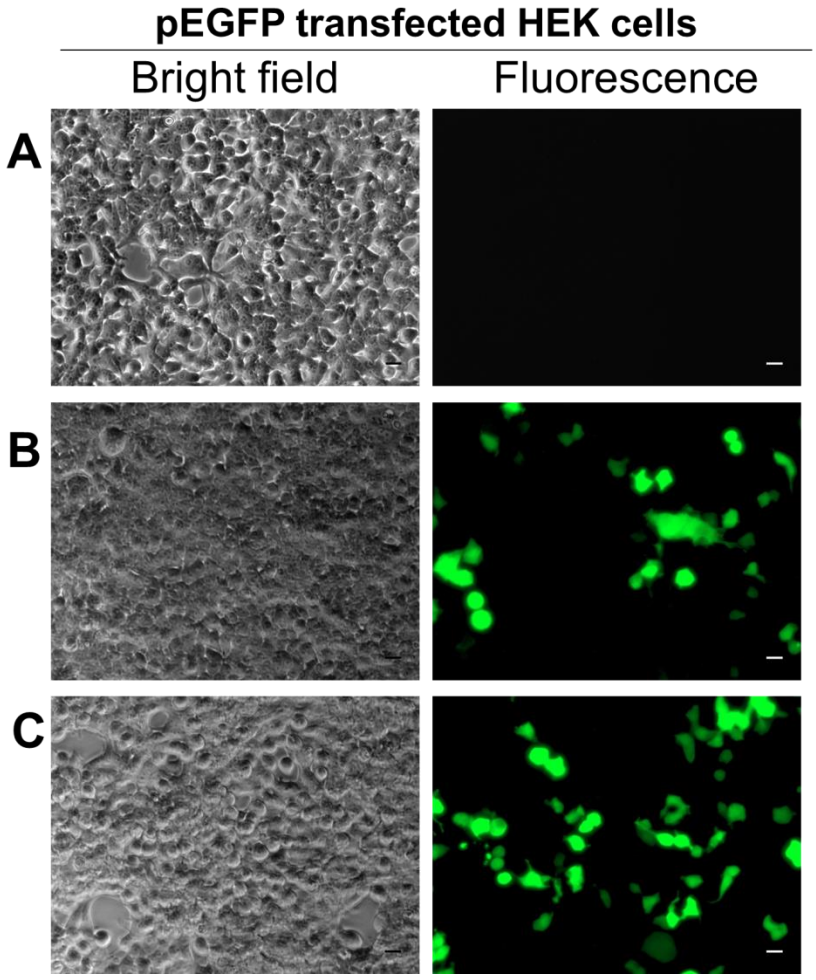
pEGFP transfected HEK cells
Bright field
Fluorescence
A
B
C

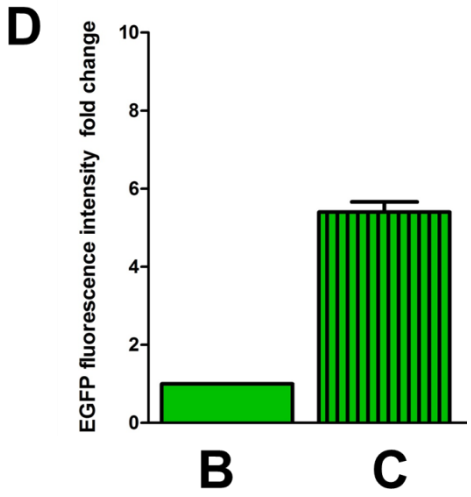
D
EGFP fluorescence intensity fold change
10
8
6
4
2
0
B
C

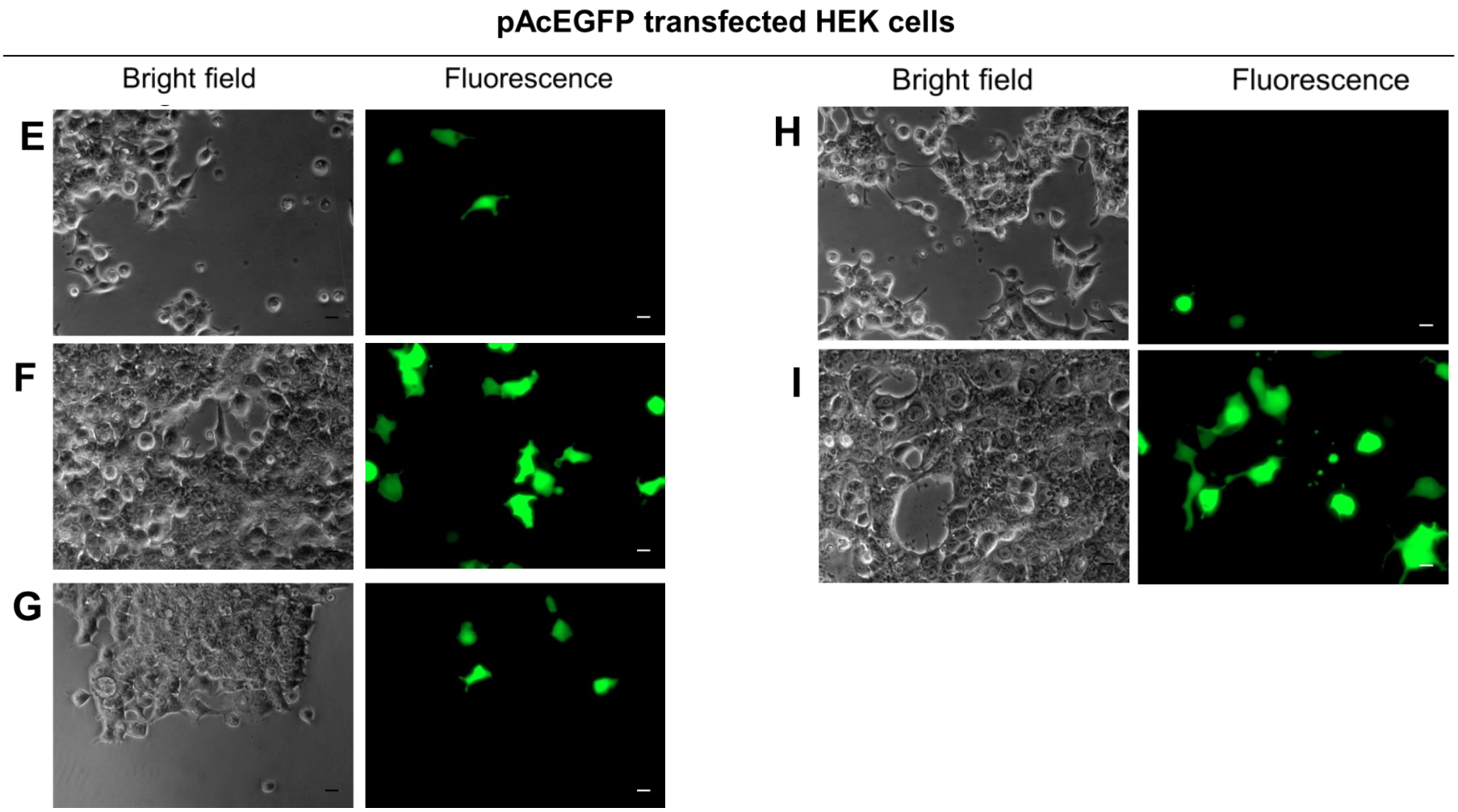
pAcEGFP transfected HEK cells
Bright field
Fluorescence
Bright field
Fluorescence
E
F
G
H
I

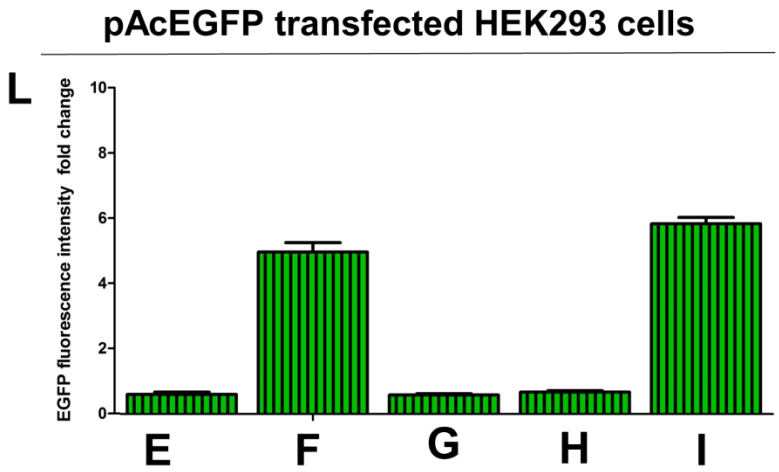

Figure 4.11. Effect of chemical compounds, individually or in pairwise combination, on *egfp* expression in transfected HEK293 cells. Representative photomicrographs of bright field (bottom images), and fluorescence (top images) taken at 24 h following incubation using the 10X objective and graph bar illustrating fluorescence fold change. (**A**) Mock-transfected HEK293 cells (negative control). (**B**) Untreated HEK cell transfected with pAcEGFP (virus alone) DNA using baculoFectin reagent. Transfected HEK293 cells pre- or post-treated with (**C**) sodium butyrate, (**E**) hydroxyurea, (**F**) etoposide, (**G**) hydroxyurea + etoposide, (**H**) hydroxyurea + sodium butyrate and (**I**) sodium butyrate + etoposide. (**D** and **L**) Fluorescence intensity fold change was calculated by dividing the average fluorescence level of EGFP cells in the presence of chemical compounds with the EGFP signal intensity of AcCMV_EGFP or pAcEGFP untreated HEK293 cells. Scale bar =10 µm. **p*<0.0001 indicated a significant difference between treated cells and untreated cells (One-way ANOVA; n=3).

Under the same cell culture treatments as the transduction experiments, pAcEGFP transfected cells showed a much lower level of *egfp* expression (Figure 4.11). As shown in Figure 4.11, by comparison with transfected untreated cells (B), addition of hydroxyurea resulted in low *egfp* expression (E); whilst, sodium butyrate (C) and etoposide (F) significantly increased (F (6, 56)= 223.4; p<0.001) transgene expression more than five-fold. Similar observations were made when pAcEGFP transfected HEK293 cells were exposed to chemical combinations; treatment with hydroxyurea + etoposide or hydroxyurea + sodium butyrate had a negative effect on transgene expression (Figure 4.11 G and H, respectively). Maximal *egfp* expression in pAcEGFP transfected HEK293 cells was detected in the presence of etoposide + sodium butyrate (Figure 4.11 I); these transgene levels were significantly different (F (6, 56)= 223.4; p<0.001) than control cells (Figure 4.11 B).

In order to assess consistency of results across the delivery methods, transfer vectors and BacMam viruses encoding *lacZ*, *sod-2* and *bcl-2* were also assessed and a summary of these experimental results are included into the supplementary data CD attached to this thesis (Chapter 4-S2).

Taking together these findings indicated that the chemical compounds sodium butyrate, hydroxyurea and etoposide modulate with different orders of magnitude the transgene expression in HEK293 cells. In particular, etoposide and hydroxyurea compounds and the pairwise combinations of sodium butyrate + hydroxyurea and sodium butyrate + etoposide treatments consistently increased BacMam-delivered transgene expression. Whilst, individual etoposide treatment as well as in combination with sodium butyrate (sodium butyrate + etoposide) enhanced the transgene expression in pAcEGFP transfected HEK293 cells.

4.5 TIME COURSE OF *EGFP* EXPRESSION IN HEK293 CELLS AFTER ADDITION OF SODIUM BUTYRATE + ETOPOSIDE

Based on previous results (Section 4.4), the compound combination sodium butyrate + etoposide was chosen to assess their time-dependence effect on BacMam-mediated transgene expression. A single experiment was carried out using triplicate samples of HEK293 cells, with or without 10 mM sodium butyrate + 1.5 µM etoposide; cells were transduced with AcCMV_EGFP or transfected with pAcEGFP. HEK293 cells were then harvested over-time and analysed by fluorescence microscopy (Section 2.2.5.I); fluorescence intensity was also measured using a fluorescence plate reader (Section 2.2.7.II). Figures 4.12 illustrate the *egfp* fluorescence intensity fold change in response to chemical treatment before or after cells were transduced with AcCMV_EGFP or pAcEGFP transfected.

As shown in Figure 4.12 A, after 24 h of incubation, *egfp* expression increased approximately nine-fold in sodium butyrate + etoposide treated and AcCMV_EGFP transduced HEK cells compared to untreated transduced control cells. This increase in expression levels, remained unchanged between 24 and 288 h post-transduction with an approximately 9-fold increase in *egfp* expression in all sodium butyrate + etoposide treated cells; and expression was significantly higher than untreated transduced control cells (F (1, 52)= 1438; p<0.0001). Under the same cell culture conditions, at 24 h post-transfection the *egfp* expression in treated cells was enhanced two-fold above the pAcEGFP transfected control cells (Figure 4.12 B). This time course study also showed that the effect of sodium butyrate + etoposide on *egfp* expression remained unchanged (p>0.05) amongst the treated transfected cells, with an increase in expression approximately two- to three-fold above transfected control cells, between 48 and 288 h post-transfection (Figure 4.12 B).

Statistical analysis demonstrated a significant increase in *egfp* expression in treated cells compared to untreated transfected cells (F (1, 49)= 530.3; p<0.0001).

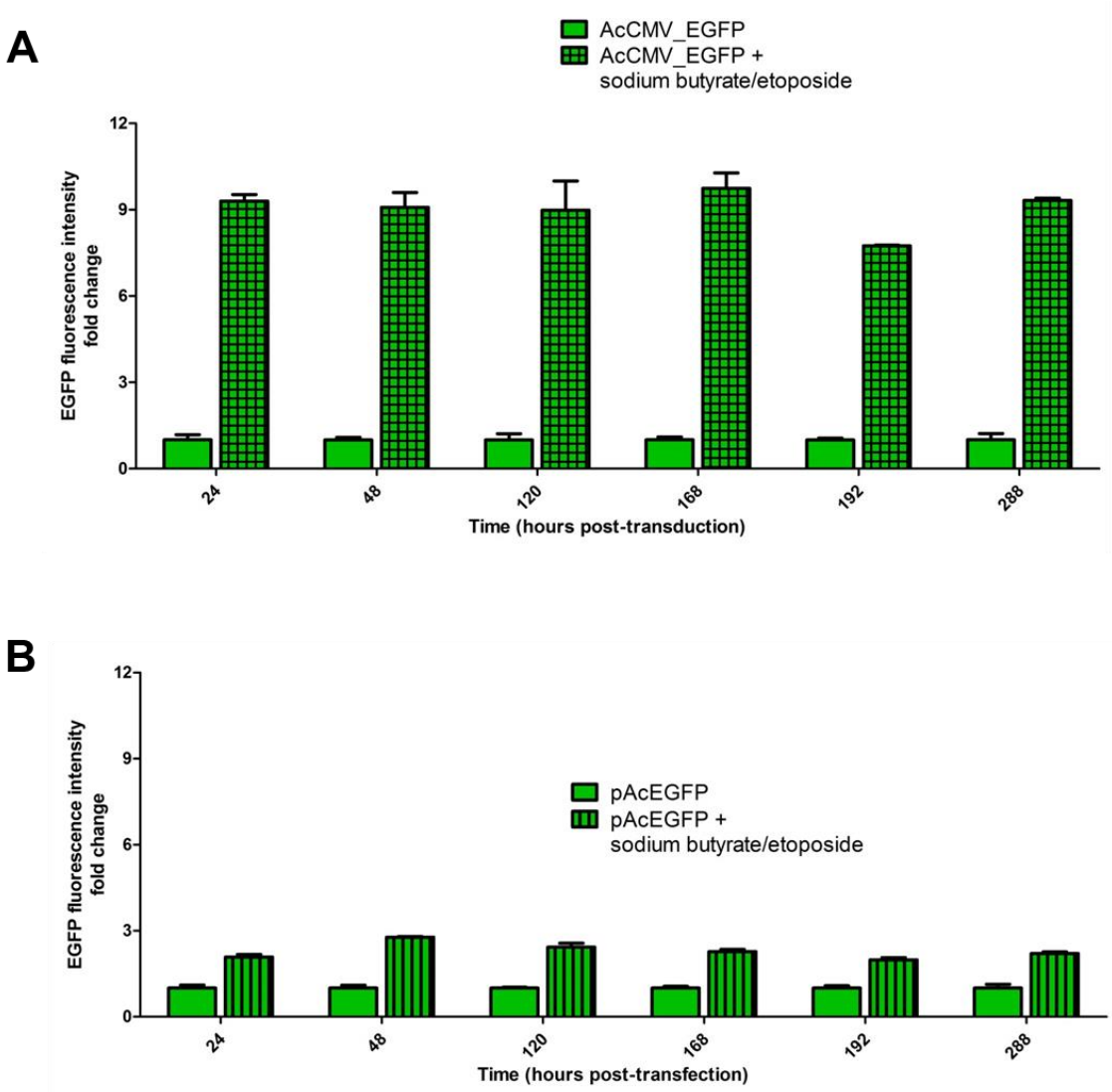

Figure 4.12. Time course of the effect of sodium butyrate/etoposide on BacMam-mediated *egfp* expression in HEK293 cells. Cells were treated with 10 mM of sodium butyrate and 1.5 µM of etoposide before or after be transduced with AcCMV_EGFP (MOI 50) or transfected with pAcEGFP using baculofectin. At the indicated time, samples of cells were harvested and egfp fluorescence intensity was quantified as described in Chapter 2, Section 2.2.7.II. The *egfp* fluorescence intensity fold change was calculated by dividing the mean intensity of transduced or transfected HEK293 cells treated with sodium butyrate/etoposide, with the *egfp* signal intensity of transduced or transfected untreated control cells. Data from a single experiment are presented as mean ± S.E.M. (n=3); * p<0.0001 indicated a significant difference in expression of treated cells *vs.* untreated control cells.

Overall, *egfp* expression was enhanced in both transfected and transduced cells by sodium butyrate + etoposide treatment; however, a significant increase (F (3, 20)= 92.93; p<0.0001) in expression was observed in treated AcCMV_EGFP transduced cells (Figure 4.12 A) compared to treated pAcEGFP transfected cells (Figure 4.12 B). It can be concluded from preliminary studies that the addition of chemicals to AcCMV_EGFP transduced cells increased expression 4.5 times higher than cells directly transfected with plasmid pAcEGFP.

4.6 DISCUSSION

BacMam technology has undergone great improvements over the last few years and recent studies have suggested their potential use as a gene delivery tool in numerous applications (reviewed by Airenne *et al.,* 2012; and by Paul *et al.,* 2014). However, one of the major limitations of BacMam gene delivery is the limited expression levels of transgene that it mediates (Shen *et al.,* 2008; Lo *et al.,* 2009).

A number of strategies have been developed in order to improve BacMam performance as a gene delivery tool for *in vitro* and *in vivo* applications. These have included genetic modification of the envelope protein GP64, modification of cell culture media composition and pH (potential of hydrogen) as well as conjugation of BacMam surface proteins with chemicals such as cationic polyethylenimine and polyethylene glycol (reviewed by Grabherr *et al.,* 2001; reviewed by Paut *et al.,* 2014). Transgene modification by epigenetic factors has been reported to play an important role in modulating BacMam mediated expression (Hu *et al.,* 2003; Guo *et al.,* 2010; Paul *et al.,* 2010; Tang *et al.,* 2011). Therefore, regulating transgene expression in mammalian cells represents an important step towards the full scale-utilization of BacMam viruses in a variety of clinical applications (Hu *et al.,* 2003; Lo *et al.,* 2009; Guo *et al.,* 2010; Yin *et al.,* 2010; Tang *et al.,* 2011).

The main goals of the work described in this thesis chapter was to investigate the influence of epigenetic regulation (such as acetylation, methylation and compaction of chromatin), brought about by exposure of cells to chemical compounds on transgene expression in BacMam transduced HEK293 cells. The experimental approach of this chapter has been mainly based on the use of the BacMam virus carrying the egfp gene under the control of the CMV-IE promoter. Numerous studies have suggested egfp as a useful reporter to quantify gene expression (Hack *et al.,* 2000; Lissemore *et al.,* 2000; Soboleski *et al.,* 2005).

In particular, EGFP fluorescence intensity can be measured using either fluorescence microscopy or by flow cytometry analysis; these are the techniques used in this thesis chapter. Fluorescence microscopy offers a unique approach to the study of living cells due to its sensitivity, specificity and importantly, its direct visualization of fluorescence-positive cells (Soboleski *et al.,* 2005; Yuste, 2005). While, flow cytometry provides greater accuracy of fluorescence intensity at various wavelengths and light-scattering properties. It can determine the number of fluorescence-positive cells within a cell population (% positive cells), as they flow in single file through an illumination zone with detectors. Flow cytometry can also measure the magnitude of a pulse representing the intensity of the fluorescence emitted. Furthermore, flow cytometry allows the analysis of cell-specific characteristics such as cell size, separation of distinct populations of cells, protein and DNA content (reviewed by Rieseberg *et al.,* 2001).

4.6.I Preliminary studies using chemical compounds in HEK293 cells

Early reports have shown that certain chemicals can increase virus-mediated gene expression in mammalian cells. Sodium butyrate was the first HDACis to be identified in 1978 by Boffa and is produced by bacterial fermentation of dietary fibres as a four-carbon short-chain fatty acid. Sodium butyrate has been successful used in experimental cancer therapy (Nudelman *et al.,* 1992; Warrell *et al.,* 1998). It relaxes chromatin by inducing the hyperacetylation of chromosomes which enhance the accessibility of genes to the transcriptional machinery and thereby facilitates gene expression in mammalian cells (Chen *et al.,* 1997; Condreay *et al.,* 1999; Sarkis *et al.,* 2000; Guo *et al.,* 2010; Tang *et al.,* 2011). It also affects metabolism and other enzyme system by enhancing such as those involved in phosphorylation and methylation of proteins (Archer & Hodin, 1999). Studies focusing on improving BacMam expression in mammalian cells have demonstrated that the addition of sodium butyrate to BacMam transduced mammalian cell lines, dramatically increased the levels of transgene expression (Condreay *et al.,* 1999; Sarkis *et al.,* 2000; Guo *et al.,* 2010). Condreay *et al* (1999) demonstrated that in four cell lines derived from kidney tissue (BHK, CV-1, Cos-7 and HEK cells), 10 mM of sodium butyrate enhanced BacMam-mediated *gfp* expression between five- and 20-fold compared to the mean fluorescence of transduced untreated cells. Therefore, in this preliminary study, sodium butyrate was included as a known enhancer of expression and used to treat HEK293 cells at concentration of 10 mM as a positive control.

The purpose of this preliminary study was to identify chemical compounds capable of enhancing BacMam transgene expression in mammalian cells, based on literature reviews. Studies aimed at improving AAV transduction efficiency and transgene delivery showed that hydroxyurea (a DNA synthesis inhibitor) and etoposide (a type II topoisomerase inhibitor) increased transgene expression in human fibroblast cultures and in human marrow mesenchymal cells (Russell *et al.,* 1995; Ju *et al.,* 2004); hydroxyurea further enhanced the level of adenovirus-mediated transgene in human colon and hepatocellular carcinoma cells (Huang *et al.,* 2005), whilst co-treatment of UMR106 osteosarcoma cells with adenovirus + etoposide effectively increased transgene expression with minimal effects on normal cell physiology (Triplett *et al.,* 2005). The precise mechanism of action of hydroxyurea and etoposide on virus mediated transgene expression is not yet clear, but it appears that they alter chromosome structure by various mechanisms all of which activate DNA repair mechanisms. Therefore, this suggests that repair synthesis activities associated with DNA repair may be involved in virus transduction rather than replicative DNA synthesis (Russell *et al.,* 1995).

Other studies on adenovirus and AAV gene delivery demonstrated that gene transfer efficiency can be improved by the addition of polycations such as protamine (Lanuti *et al.,* 1999). In these reports it was hypothesized that protamine enhances transgene expression by either neutralizing electrostatic repulsion between the virus and the cell membrane or by linking virus particles with cell surfaces. To date, there are no reports in the literature describing the use of any of these compounds for enhancing the efficiency of BacMam-mediated gene delivery. Therefore, the effect of hydroxyurea, etoposide and protamine on transgene expression in BacMam transduced HEK293 cells was investigated.

The effect of cycloheximide, an inhibitor of protein biosynthesis, on AAV transduction has also been evaluated in stationary human fibroblast cells (Russell *et al.,* 1995). Clycloheximide has been proved to significantly increase the nuclear import channel pore size after 3 h of treatment (Feldherr *et al.,* 2001). It acts mainly by interrupting both initiation and elongation steps of translation by interacting with the P site on the ribosomal subunit 60S (Obrig *et al.,* 1971). Mizutani *et al.* (2000) demonstrated that 5 h of treatment with cycloheximide increased Borna disease virus (BDV) transcription in Madin-Darby canine kidney (MDCK) cells persistently infected by BDV. Feldherr *et al.* (2001) showed no effect of cycloheximide on either the transport rate or passive diffusion of FITC (fluorescein isothiocyanate)-labeled ovalbumin or BSA proteins through the nuclear pore. Interestingly, the mechanism by which BacMam delivers genes into the nucleus of the host cell is still poorly characterized (reviewed by Au *et al.,* 2013).

Therefore it was decided to also investigate the effect of cycloheximide on BacMam gene delivery in HEK293 cells.

Initially, the optimal chemical dosage to ensure high levels of transgene expression and low cytotoxicity was assessed by treating HEK293 cells with various concentrations of hydroxyurea, etoposide, protamine and cycloheximide compounds. Treatment of AcCMV_EGFP transduced cells with 10 mM sodium butyrate resulted in a three-fold increase in *egfp* fluorescence compared to untreated transduced cells (Figures 4.1 to 4.4, panel C *vs* panel B); this was consistent with previous studies in other cell lines (Condreay *et al.,* 1999; Sarkis *et al.,* 2000). Condreay and colleagues showed an approximately three-fold increase in *gfp* expression levels following the addition of 10 mM of sodium butyrate to BacMam transduced cervical epithelial (W12) cells. Similarly, addition of sodium butyrate to cell media after BacMam transduction resulted in three-fold increase in the number of GFP-positive cells and in the intensity of mean fluorescence in HeLa cells and in a neuroblastomal cell line, CHP212 (Sarkis *et al.,* 2000).

Fluorescence microscopy and quantitative image analysis demonstrated that pre-transduction treatment of HEK293 cells with different concentrations of hydroxyurea, ranging from 5 to 100 mM, significantly increased *egfp* fluorescence intensity by approximately two- to three-fold (Figure 4.1, panel D). In particular, 40 mM hydroxyurea increased *egfp* expression more than three-fold. This result was consistent with published studies. Russell *et al.* (1995) identified 40 mM hydroxyurea as the optimal concentration producing a three- to four-fold increase in AAV transduction efficiency in dividing human fibroblast cultures compared to the transduced stationary culture and 30-fold increase when compared to dividing untreated transduced fibroblast cells.

Increased *egfp* fluorescence intensity was also observed in transduced cells pre-treated with etoposide. The maximum increase in the reporter gene expression in the presence of 1.5 µM etoposide was approximately two-fold higher than untreated transduced cells (Figure 4.2, panel E *vs* panel B). The fluorescence intensity in transduced HEK cells treated with etoposide concentrations above or below 1.5 µM was similar to control cells; these observations were consistent to those made by other studies. Incubation of osteosarcoma cells with a lower dose of etoposide (100 nM) during the first 24 h of adenoviral infection resulted in a significant increase in transgene expression, approximately two-fold, with no increased cytotoxicity compared with vehicle-treated controls (Triplett *et al.,* 2005). In contrast, etoposide (3 µM) increased AAV transduction efficiency in dividing human fibroblast cultures three-fold higher than untreated dividing cultures (Russell *et al.,* 1995).

Quantitative image analysis indicated that co-transduction cells with AcCMV_EGFP + protamine at various concentrations (0.5 to 100 µg/ml) did not augment transgene expression in these cells. (Figure 4.3; panel F *vs* panel B). These results were different from published observations. Swaney *et al.* (1997) observed a five-fold increase in *lacZ*-positive cells when retrovirus pre-treated with protamine (4 µg/ml) was used to transduced CHO cells. Similarly, flow cytometry analysis indicated that AAV transduction efficiency in HepG2 (human hepatoma) cells and number of GFP expressing cells were significantly increased in the presence of 5 µg/ml of protamine (Yang & Hsieh, 2001).

In the work described in this thesis chapter it was also demonstrated that there was no increase in transgene expression between HEK293 cells incubated with different concentrations of cycloheximide and untreated transduced cells (Figure 4.4, panel G *vs* panel B). Although low concentrations of cycloheximide were tested in this study, results confirmed observations made by Russell *et al.,* (1995); cycloheximide (50 mg/ml) failed to increase AVV transduction efficiency in both dividing and stationary human fibroblast cells.

4.6.II Chemical compounds effect on *egfp* and *bcl-2* expression

Since it was observed that chemical compounds administered prior or post BacMam transduction had a positive effect on transgene expression, further study was carried out to assess the reproducibility of the method. It was also decided to test the chemical compounds protamine (50 µg/ml) and cyclohexamide (1.5 µg/ml) to further confirm their effect on the transgene expression.

Results illustrated in Figure 4.5 showed that *egfp* fluorescence intensity was significantly increased (two- to three-fold) in transduced cells treated with the chemical compounds sodium butyrate (panel C), hydroxyurea (panel D) and etoposide (panel E). These results were consistent with those of other studies who reported that sodium butyrate significantly improved transduction efficiency of BacMam and the expression level of exogenous genes (Condreay *et al.,* 1999; Sarkis *et al.,* 2000; Guo *et al.,* 2010; Yin *et al.,* 2010). Hydroxyurea and etoposide have been shown previously to enhance transgene expression mediated by adenoviral vectors in various cell types (Russell *et al.,* 1995; Triplett *et al.,* 2005). Shieh *et al.* (2006) demonstrated that low-dose etoposide 0.1 µg/ml (1.6 µM) increased approximately two-fold the transduction efficacy of adenovirus encoding cytosine deaminase (*cd*) through up-regulation of the hTERT promoter activity in telomerase-positive bladder cancer cells.

Subsequently, cell viability analysis revealed no obvious cytotoxicity in transduced HEK293 cells treated with chemicals, 85-87% (with the exception of cycloheximide) compared to control cultures (90-91%) (Figure 4.6; Bars 3-6 *vs* 1-2, respectively). These data were in agreement with previous reports (Triplett *et al.,* 2005; Yin *et al.,* 2010).

To further confirm fluorescence microscopy observations, the number of EGFP-positive cells was quantified by flow cytometry. As cells intersect the laser beam, intrinsic cellular characteristics can be reflected, analysed, and shown in a scatter plot. In the cytograms of this study, EGFP fluorescence intensity (FL1) is shown in the y axis and forward scatter (FS) is plotted on the x axis, which represents the relative cell size. From the dot plot images, it appears evident that changes in cell size depend on the culture treatment rather than BacMam transduction; indeed, the FS of mock-transduced cells appeared similar to the FS of the AcCMV_EGFP transduced cells (untreated cells), ranging from 100 to 1000 of the logarithmic (Log) scale (Figure 4.7 A vs. B). In contrast, as shown in Figure 4.7, upon BacMam transduction and sodium butyrate (panel C), hydroxyurea (panel D) or etoposide (panel E) treatment, it is possible distinguish a decrease in the cell size population (10 to 100 of the Log scale), compared to the control dot plot images (panels A & B). The relative cell size for AcCMV_EGFP transduced cells treated with protamine and cycloheximide varied between 10 to approximately 1000 of the FS Log scale (Figure 4.7 panels F and G, respectively). Chico & Jäger (2002) and Janakiraman *et al.* (2006) demonstrated, using flow cytometry, that baculovirus increased viable insect cell size/diameter following infection. However, to date, there is no evidence that BacMam induce change in mammalian cell size; BacMam virus do not replicate in mammalian cells. Furthermore, the dot plot analysis showed that the percentage of EGFP-positive cells had markedly increased from 32% in cells transduced with virus alone (untreated cells) to 63-70% in transduced cells treated with sodium butyrate, hydroxyurea or etoposide (Figure 4.7, panels C, D and E *vs* B) but not with protamine or cycloheximide (Figure 4.7, panels F and G *vs* B).

Quantitatively, the fluorescence fold change demonstrated that a significant increase of approximately two-fold in the presence of chemical compounds compared to transduced untreated cells (Figure 4.8). These data were consistent with Yin *et al.* (2010) who demonstrated by flow cytometry that sodium butyrate (5 mM/L) consistently improved approximately two-fold the transduction efficiency and GFP fluorescence intensity of SW1116 tumour cells transduced with BacMam at different MOI.

In conclusion, results from this study provided further support to the preliminary data described above in Section 4.6.I and confirmed that *egfp* expression in transduced cells was significantly improved by sodium butyrate, hydroxyurea and etoposide compounds : Although, It was decided to omit the chemical protamine from future experiments it should be noted that protamine is a well-established and safe drug used in human clinical settings (Sorgi *et al.,* 1997); it improves uptake of a number of viruses by reducing the repulsive-charge interactions between the viral envelope and the host cell membrane (Cornetta & Anderson, 1989; Lanuti *et al.,* 1999; Lin *et al.,* 2012). Therefore, further studies will be necessary to better understand the mechanisms of action of protamine in increasing BacMam entry into mammalian cells. Similarly, based on the results from this study, cycloheximide was excluded from subsequent experiments; however, more studies are needed to further elucidate whether this compound could have either a detrimental or beneficial effect on viral processing rather than on transgene expression. Indeed, in the early 1970s, Craig & Raskas demonstrated that the presence of cycloheximide, during the early phase of adenovirus replication in cultured human KB cells, caused an increase in the virus-specific content of newly synthesized mRNA (Craig & Raskas, 1970). In contrast, other studies suggested that presence of cycloheximide during virus infection inhibited the synthesis of viral proteins and the replication of viral RNA (Hay *et al.,* 1997; Sanfilippo *et al.,* 2004; Landeras-Bueno *et al.,* 2011).Subsequently, the effect of sodium butyrate, hydroxyurea and etoposide chemicals was further evaluated individually or in combination, in HEK293 cells. In particular, their effect on *bcl-2* gene expression was examined in BacMam transduced cells.

A four- to six-fold enhancement in *bcl-2* expression was found in cells treated with individual compounds (Figure 4.9, lanes 3-5 *vs* lane 2). This study also demonstrated that transduced cells expressing *bcl-2* responded to the chemical combination treatments positively, increasing four to six-fold the transgene levels (Figure 4.9, lanes 6-8). Although *bcl-2* expression in these cells was higher than that observed in transduced untreated cells, their effect was not greater than that of individual chemical treatments. These results were similar to those reported in the literature (Russell *et al.,* 1995; Triplett *et al.,* 2005; Lo *et al.,* 2009; Yin *et al.,* 2010). The use of etoposide (100 nM) increased *gfp* expression approximately three-fold in UMR106 cells and two-fold in rat embryo fibroblast (RF52) cells compared to vehicle-untreated controls (Triplett *et al.,* 2005). Guo *et al.* (2010) showed an approximately two-fold increase in BacMam-mediated human sodium/iodide symporter (hNIS) expression in sodium butyrate (1 mM/L) treated A549 cells.

4.6.III Comparison of BacMam *vs* plasmid DNA transgene delivery in the presence of chemical compounds.

One of the advantages of using plasmid DNA for gene delivery applications is a reduced immunogenic effect when compared with mammalian viral vectors; however, several factors may contribute to low transfection efficiency such as degradation by nucleases and cationic liposome toxicity (Wolff & Budker, 2005). In the last two decades, researchers have directed attention toward increasing plasmid DNA transfection efficiency; amongst these studies, Gorman *et al.* (1983) were the first to show that sodium butyrate (2 mM to 10 mM) treatment, immediately following transfection, increased by three- to four-fold the number of cells able to transiently express foreign DNA. It has also been reported that plasmid DNA harbouring the human IgG-heavy and light chain (chCE7 F(ab′)2) fragments transfected into HEK293 cells in combination with sodium butyrate increased expression of recombinant antibody fragments (Nahreini *et al.,* 2003).

Despite different approaches being used, the efficiency of transfection, level of transgene expression and limitation to scale-up after non-viral DNA delivery still remain low when compared to virus-mediated delivery (Tang *et al.,* 2011; Hohsfield *et al.,* 2013). A recent study evaluated different gene delivery methods for commercially available fluorescence genes in amphibian (A6) and CHO cells (Ramirez-Gordillo *et al.,* 2011). In every instance, they demonstrated that efficiency of gene delivery using the BacMam system was greater than that found using electroporation or transfection with lipid-mediated reagents (Lipofectamine™2000, Metafectene® and Pro). The present study compared the effect of chemical compounds on efficiency and expression of plasmid DNA transfection and BacMam transduction in HEK293 cells.

Although, BacMam transduction of chemically untreated HEK293 cells was slightly less efficient than DNA transfection, significantly higher level of *egfp* expression were observed in transduced cells treated with individual chemicals (eight – to 20-fold) as compared with pAcEGFP transfected chemically treated cells (five-fold). Treatment with three chemical combinations further increased *egfp* fluorescence in the transduced cells (16-47-fold) compared to approximately six-fold in individually treated transfected cells (Figure 4.10 A *vs.* B). Consistent with previous results in this study, hydroxyurea in combination with either + etoposide or + sodium butyrate greatly increased transgene expression over five-fold compared to transduced untreated cells (Figure 4.9). These findings were also consistent with published reports (Russell *et al.,* 1995; Hendrick *et al.,* 2001; Sugano *et al.,* 2005; Mohan *et al.,* 2007; Lo *et al.,* 2009).

Vadolas *et al.,* (2004) demonstrated a significant dose-dependent increase in the relative levels of *egfp* expression (three- to seven-fold) following treatment of sodium butyrate and hydroxyurea in stably transfected K562 (human immortalised myelogenous leukemia) cells. They observed maximal transgene expression with 100 µM hydroxyurea (75±10%) and 1000 µM sodium butyrate (82±29%); however, they showed that combinations of both chemicals resulted with an additive effect on *egfp* expression after 5 days (159±72%). In addition, the differences in delivery efficiency between transduction and transfection observed in the present study were consistent with those made by Lo *et al.* (2009); who observed that the number of GFP-positive cells was significantly higher in BacMam transduced cells than in transfected cells across three different cell lines. Lo and colleagues also demonstrated by flow cytometry that sodium butyrate (10 mM/L) treatment tremendously increased (seven-fold) *gfp* fluorescence intensity in transduced HEK293 cells, 48 hpt; however, 20-fold increase in *egfp* expression was achieved in the present study (Figure 4.10).

Overall, this study demonstrated that etoposide treatment was able to increase transgene expression but to a less extended compared to sodium butyrate and hydroxyurea compounds used undividually. However, etoposide in combination with sodium butyrate consistently improved with different orders of magnitude plasmid-mediated *egfp* expression in HEK293 cells. While, combined treatment of sodium butyrate + etoposide and sodium butyrate + hydroxyurea increased BacMam-mediated transgene expression in HEK293 cells.

4.1 Temporal effect of chemical compounds.

Based on the observations discussed in Section 4.6.III, the time-dependence effect of sodium butyrate + etoposide on plasmid- and BacMam-mediated *egfp* expression was assessed in HEK293 cells. Results showed that *egfp* fluorescence intensity was approximately nine-fold higher in treated transduced cells compared to untreated transduced cultures. Relatively constant *egfp* expression levels were observed over-time (Figure 4.12, A). Similarly, a two-fold increase in *egfp* expression was detected in treated transfected cells when compared to control cells (untreated transfected cultures). The time course study also demonstrated that *egfp* expression levels remained unchanged between 48 and 288 hpt (Figure 4.12 B).

Although the combined effect of sodium butyrate + etoposide enhanced *egfp* expression in both transfected and transduced HEK293 cells, levels of *egfp* were significantly increased in the transduced cells by five orders of magnitude above the transfected cells.

These preliminary results were consistent with previous studies to investigate the transduction efficiency of BacMam compared to other systems (Lo *et al.,* 2009; Ramirez-Gordillo *et al.,* 2011; Tang *et al.,* 2011). In contrast, Sarkis *et al.* (2000) demonstrated that 5 mM of sodium butyrate alone increased mean fluorescence intensity four-fold in BacMam transduced telencephalic cells at 48 hpt. Subsequently they observed a decreased level of expression at 96 hpt (two-fold). Consistent with the observations made by Sarkis and colleagues, sodium butyrate enhanced antibody yield 10-fold in transiently transfected HEK293E cells between 120 h and 216 h post-transfection (Backliwal *et al.,* 2008).

The present study showed that individual or combined chemical treatments with sodium butyrate, hydroxyurea and etoposide enhanced the level of transgene expression in BacMam transduced HEK293 cells with different orders of magnitude; the enhancement was variable but similar between reporter and target gene. The observed differences in expression may be partly attributable to the different methods used to analyse transgene expression (*e.g.* plate reader, flow cytometry, image quantification and western blot). It can also be hypotesized that gene response to different chemicals may vary. However, the data from these experiments clearly support previous findings regarding the direct effect of sodium butyrate on transduced cultures but also indicated for the first time that BacMam-mediated transgene expression can be modulated and enhanced by addition of 40 mM hydroxyurea. Both sodium butyrate and hydroxyurea have been used individually in a number of clinical trials such as sickle cell disease to induce reactivation of fetal hemoglobin (Fathallah & Atweh, 2006; reviewed by Canani *et al.,* 2011; and Green & Barral, 2014). Therefore, it was decided to assess whether sodium butyrate alone could ameliorate the severity of injury in a simulated *in vitro* model of I/R injury in human kidney 2 (HK-2) cells (Chapter 5) as well as in combination with hydroxyurea in an *ex vivo* porcine kidney model (Chapter 6).

Chapter 5

Development of an *in vitro* I/R injury model

5.1 INTRODUCTION

Ischaemia (transient disruption of blood supply) followed by reperfusion (restoration of the blood flow) is a pivotal mechanism of organ injury in various medical conditions; I/R injury is a common cause of injury in myocardial infarction, circulatory shock, various toxic insults, and surgical interventions (reviewed by Lorenzen *et al.,* 2013). Importantly I/R injury still remains a major cause of acute kidney injury (AKI) with high morbidity and mortality (Versteilen *et al.,* 2004) and is a major determinant of graft survival in kidney transplantation (Cassis *et al.,* 2014). The National Institute for Health and Care Excellence (NICE) reported in 2013 that AKI was present in 13–18% of all people admitted to UK hospitals, predominantly in older adults.

The etiology of renal I/R injury is complex. Induced renal epithelial cell injury has been shown to be related to a number of biochemical, physiological and morphological alterations such as ROS, decreased intracellular ATP levels as well as activation of apoptotic pathways (Lee *et al.,* 2004; Yang *et al.,* 2005). Many studies have demonstrated that cell death via the apoptosis pathway significantly contributed to the pathophysiology of renal I/R injury (Gobe *et al.,* 2000; Bonegio & Lieberthal, 2002; Linkermann *et al.,* 2012; Stiegler *et al.,* 2013). A large number of experimental studies have shown that overexpression of antioxidant (*sod, gss*, *gpx3*) and anti-apoptotic (*bcl*, *bcl-2l1, bcl-xl*) genes protected against cellular injury in various *in vitro* injury models (Chen *et al.,* 1998; Yin *et al.,* 2001; Cruthirds *et al.,* 2005; Xie & Guo, 2006 and 2007; Chen *et al.,* 2009; Stiegler *et al.,* 2013; Bagcik *et al.,* 2014).

Gene delivery studies in mammalian cells have demonstrated the protective effect of *bcl-2* efficiently deliverered by defective herpes-simple virus (Lawrence *et al.,* 1996) and adenovirus-mediated gene transfer (Bilbao *et al.,* 1999). Ni *et al.* (2013) also showed that adenoviral mediated *bcl-xl* overexpression significantly protected human umbilical vein endothelial cells from H_2O_2-induced cell damage and apoptosis. Amongst all of the antioxidant enzymes, the three SOD isoforms (SOD-1, SOD-2 and SOD-3) have been the most widely studied for their protective properties against I/R injury (Chapter 1, Section 1.3.4.II). Over two decades ago, Johnson & Weinberg (1993) demonstrated a small protective effect by administering SOD-3 into injured tissues; it was hypothesized by Bayati *et al.* (1988) that this marginal effect was due to plasma elimination of SOD within several minutes of its administration. Since this time, various attempts have been made to increase intracellular SOD levels and extend their circulating life (Yin *et al.,* 2000; reviewed by Levonen *et al.,* 2008; Liang *et al.,* 2009).

Stable transfection of *sod-2* provided protection to alveolar epithelial cells from both hyperoxia and superoxide-induced injuries (Ilizarov *et al.,* 2000). Adenovirus-mediated *sod-2* delivery increased *sod-2* expression and activity three-fold as well as effectively reducing hepatic oxidative stress (Wheeler *et al.,* 2001).

The aim of this study was to examine the effect of BacMam delivered *sod-2* and *bcl-2* genes in ameliorating I/R injury in an *in vitro* model that closely mimicked renal I/R injury. After reviewing the literature, no other studies were found describing an experimental renal I/R injury model in which the effects of protective genes delivered by BacMam viruses was investigated. Therefore, a novel BacMam transduction model was developed and optimized based on previously established ATP depletion-recovery protocols (Liang *et al.,* 2009). The ATP depletion-recovery protocols was first optimized and evaluated in HEK293 cells and results are included in the supplementary data CD attached to this thesis (Chapter 5-S1). Subsequently, the *in vitro* model was assessed using HK-2 cells and results are described in this thesis Chapter.

Overexpression of *sod-2* for protective function was supported by evidence that the mitochondria are the main cellular sites of oxygen radical production; consequently they represent an early target of oxygen injury via enhanced production of ROS which is followed by mitochondrial dysfunction (Quinlan *et al.,* 2013). Mitochondria also play a key role in activating cell death pathways during I/R injury (reviewed by Weiss *et al.,* 2003). Furthermore, *bcl-2* was chosen based on its well documented role in preventing cell death induced by various insults (reviewed by Czabotar *et al.,* 2014) but also because *bcl-2* regulates the mitochondrial transition pore which is important in the regulation of apoptosis (reviewed by Czabotar *et al.,* 2014).

5.2 *IN VITRO* ATP DEPLETION-RECOVERY MODEL OF HK-2 CELLS

Preliminary study in HEK293 cells demonstrated that BacMam-mediated *sod-2* overexpression was able to partially attenuate ATP depletion-reperfusion injury (see supplementary data CD attached to this thesis; Chapter 5-S1); therefore, the *in vitro* model of simulated ischaemia described for HEK293 cells was then adapted for use in proximal tubular cells. Several studies have demonstrated that tubular epithelial cells, in particular cells from the S3 segment, are very susceptible to ischemic injury resulting in loss of epithelial cell polarity, disruption of the actin cytoskeleton and dis-assembly of junctional complexes for cell-cell contacts (reviewed by Weinberg, 1991; Lee & Emala, 2002; Breggia & Himmelfarb, 2008; Luo *et al.,* 2010; reviewed by Bonventre & Yang,

2011). Protecting proximal tubular cells from I/R injury has long been considered a good strategy for improving the short- and long-term outcomes of renal transplant and expanding the use of “marginal donor organs” which are more vulnerable to ischaemic injury (Tanaka & Takahara, 2010). Therefore, in this study the human proximal tubular cell line (HK-2) was chosen to (1) further assess the ATP depletion-recovery method developed and optimized in HEK293 cells and (2) to further establish whether BacMam-mediated *sod-2* overexpression can confer renal protection after I/R injury. Furthermore, all viruses stock used in this study were concentrated by high-speed centrifugation (Chapter 3, Section 3.2) and dissolved in phosphate buffered saline (PBS) solution.

5.2.I Chemical depletion of intracellular ATP in HK-2 cells

The first objective of this study was to determine whether antimycin A and 2-deoxy-glucose treatment would result in a severe cellular injury which increased as a function of time. In a single experiment, ischaemic injury was induced by depleting intracellular ATP using antimycin A (10 µM) and 2-deoxy-glucose (10 mM) dissolved in PBS solution. Triplicate dishes of HK-2 cells were either incubated under normal culture conditions (in keratinocyte serum-free medium; KSFM) or exposed over-time (0 to 60 min) to ATP-depleting compounds. Furthermore, because chemicals were dissolved in PBS, it was also decided to assess whether incubation of HK-2 cells with PBS (no chemical) could induce cytotoxicity. Therefore, non-injured cells incubated with PBS were also included in this study as control. Subsequently, intracellular ATP levels were quantified and normalized to the number of cells used in the assay ($2x10^4$ cells) and expressed as Relative Luciferase Units (RLU) in Figure 5.1.

As shown in Figure 5.1, similar intracellular ATP levels were detected at 0 h for all the different conditions (1781-2020 RLU). Subsequently, treatment with chemicals produced a significant (F (2, 12)= 13.72; p<0.001) ATP depletion (691 RLU) within 30 min of their addition to the cells (Figure 5.1, red line) when compared with control cells (black & grey lines). The lowest levels of ATP were detected after 45 min of simulated ischaemia (368 RLU); whereas, slightly increased ATP levels (493 RLU) were observed at 60 min post injury (Figure 5.1, red line). These results confirmed that the *in vitro* model of simulated ischaemia, based on ATP-depletion, induced injury in HK-2 cells.

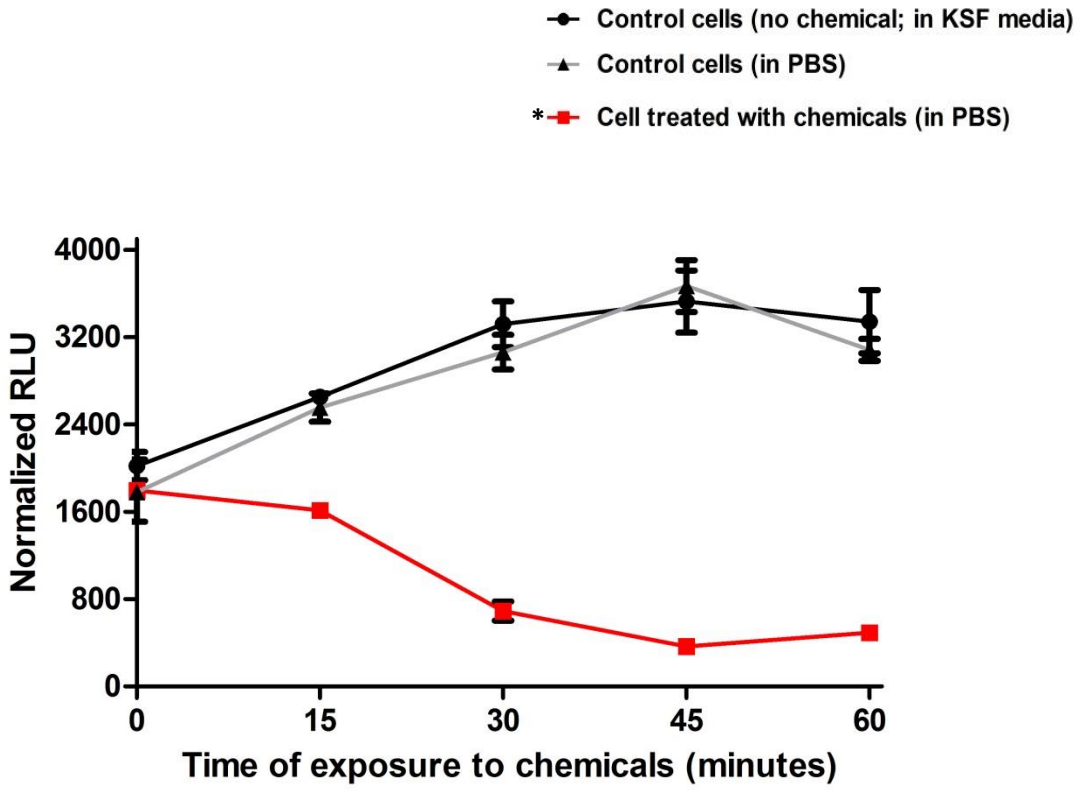

Figure 5.1. Time-course of ATP decay during simulated ischaemia in HK-2 cells. Control cells were either incubated in KSF medium or in PBS. HK-2 cells were exposed to antimycin A and 2-Deoxy-D-Glucose and ATP levels were then determined every 15 min. using a Cell TitreGlo assay (Promega). * p<0.001 indicated a significant difference between control and injured cells (two-way ANOVA; n=3;).

5.2.II Validating the effect of AcCMV_SOD-2 on an optimized *in vitro* I/R injury model

The next series of experiments were designed to determine the *in vitro* beneficial effect of *sod-2* in transduced injured HK-2 cells. Initially, in order to achieve the highest BacMam transduction efficiencies experimental conditions (MOI, cell viability and transgene expression levels) were optimized for the HK-2 cell line and are included in the supplementary data CD attached to this thesis (Chapter 5-S2). Furthermore, based on the results obtained in Section 5.2.I, it was decided to further optimize the injury exposure times; these experiments are included in the supplementary data CD attached to this thesis (Chapter 5-S3).

Based on the optimization studies, four independent experiments were carried out using the following BacMam transduction conditions and *in vitro* I/R injury protocol. HK-2 cells were transduced with AcCMV_NULL and AcCMV_SOD-2 using MOI 150; cells were incubated for 72 h at 37°C 5% CO_2. At 72 hpt HK-2 cells were subjected to 60 min of I/R

injury followed by 72 h of reperfusion. Non-injured HK-2 cells were also included as a control. During reperfusion cells were harvested at 0, 6, 24, 48, 72 hpr (hour post-reperfusion) and analysed for intracellular ATP levels and cell viability. Representative results of a single experiment are shown in Figure 5.2.

As expected, injured cells overexpressing *sod-2* showed a trend of increasing intracellular ATP levels between 0 and 72 hpr compared to AcCMV_NULL injured cells (Figure 5.2 A). Following 60 min of ATP depletion, 0 hpr, AcCMV_NULL and AcCMV_SOD-2 injured cells showed very similar ATP levels (20% 19%, respectively); these were significantly lower (F (4, 24)= 48.23; p<0.001) compared to non-injured control cells (Figure 5.2 A, solid and striped red bars *vs.* solid black bar). After 6 h of reperfusion, a substantial ATP recovery (54%) was detected in AcCMV_SOD-2 injured cells compared to AcCMV_NULL injured cells (39%); however, these levels were still significantly lower (F (4, 24)= 48.23; p<0.001) than control cells (Figure 5.2 A).

As shown in Figure 5.2 A, compared to 6 hpr a slight increase in ATP content was noted at 24 hpr in both AcCMV_NULL (42%) and AcCMV_SOD-2 (64%) injured HK-2 cells; despite this increase, these levels were significant lower (F (4, 24)= 48.23; p<0.001 and F (4, 24)= 48.23; p<0.05, respectively) compared to control cells. By 48 hpr, intracellular ATP levels in AcCMV_SOD-2 injured cells had already improved to levels similar to those of non-injured control cells, 91% compared to 100%, respectively. Whilst, relative to non-injured control cells and AcCMV_SOD-2 injured cells, ATP levels were still significantly lower (F (4, 24)= 48.23; p<0.001) in AcCMV_NULL injured cells (38%). As shown in Figure 5.2 A, at 72 hpr, injured HK-2 cells overexpressing *sod-2* completely recovered the cells intracellular ATP levels (146%); they were significantly higher (F (4, 24)= 48.23; p<0.001) to those of control non-injured cells. In contrast, ATP levels in AcCMV_NULL injured cells only partially recovered at 72 hpr (86%) and remained lower than control cells (Figure 5.2 B). Statistical analysis also revealed that ATP levels in AcCMV_NULL injured cells were significantly lower (F (4, 24)= 48.23; p<0.001) than those of AcCMV_SOD-2 injured HK-2 cells.

Cell viability was then measured in control and transduced injured HK-2 cells. As shown in Figure 5.2 B, compared to 96% viability observed for control cells (solid black bar), cell viability was significantly decreased after I/R injury in both AcCMV_NULL (F (4, 20)= 5.259; p<0.05) and AcCMV_SOD-2 (F (4, 20)= 5.259; p<0.001) injured cells, 90% and 83 %, respectively (Figure 5.2 B, solid and striped blue bars). Although, at 6 hpr, cell viability increased slightly to 91% in AcCMV_NULL injured cells, it was still significantly lower (F (4, 20)= 5.259; p<0.001) than non-injured control cells; whereas, at 6 hpr AcCMV_SOD-2

injured cells reached a similar cell viability of control cells (96% *vs.* 97%, respectively). In contrast, at 24 hpr, cell viability in AcCMV_NULL injured HK-2 cells (95%) was the same as control cells (95%), whilst cells transduced with AcCMV_SOD-2 decreased to 90%.

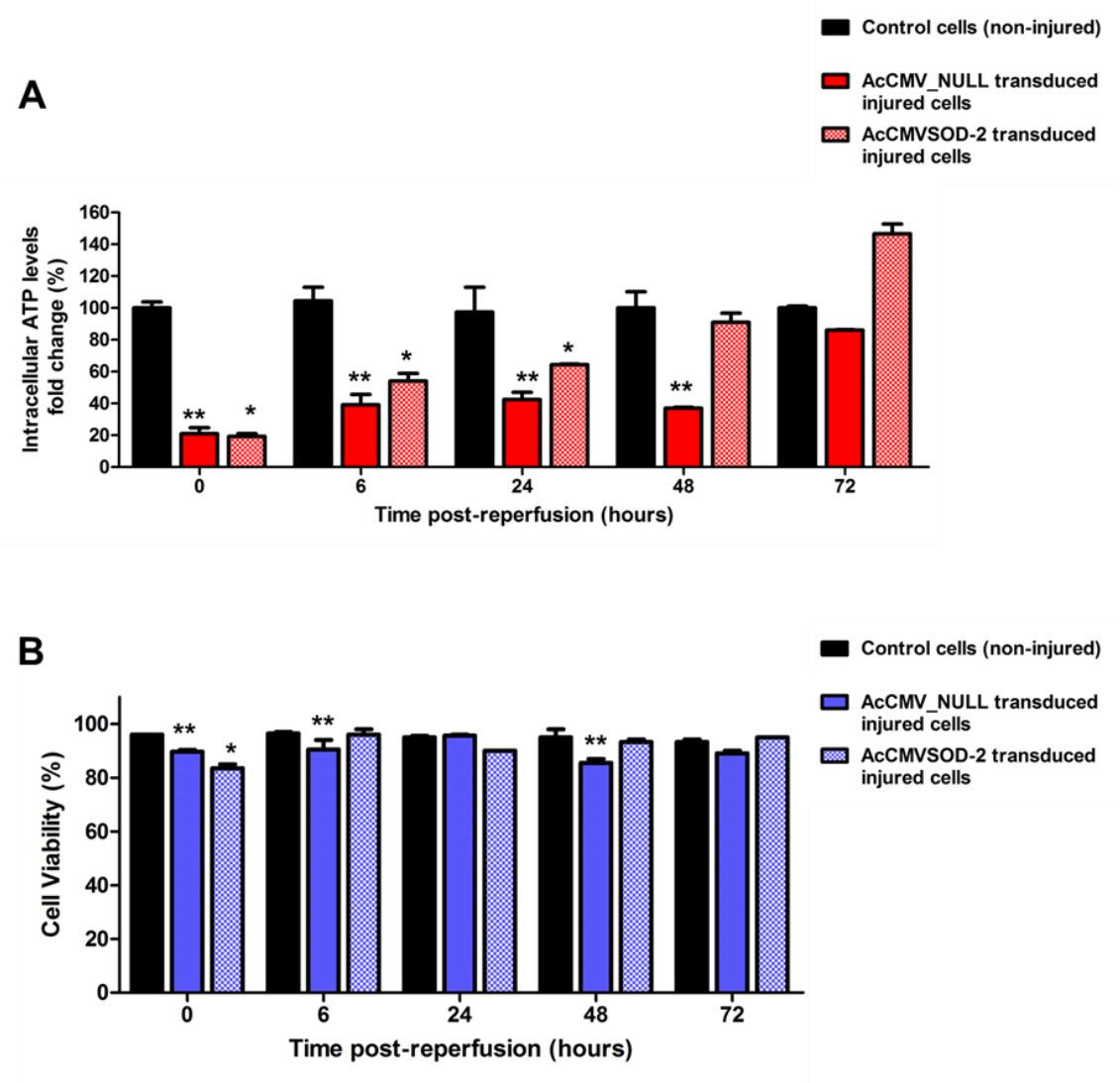

Figure 5.2. Cell viability and intracellular ATP levels in I/R injured HK-2 cells. HK-2 cells were transduced with either AcCMV_NULL or AcCMV_SOD-2 at MOI 150. At 72 hpt transduced HK-2 cells were subjected to 60 min of simulated ischaemia. Intracellular ATP levels (**A**) and cell viability (**B**) were quantified over-time. Bars represent mean ± SEM (n=3) of a single representative experiment; *p<0.001 (in A at 0 and 6 hpr and in B at 0 hpr) and p<0.05 (in A at 24 hpr) indicated a significant difference between control cells (non-injured) and AcCMV_SOD-2 transduced injured cells; while, **p<0.001 (in A at 0, 6, 24 and 48 hpr and in B at 48 hpr) an p<0.05 (in B at 0 and 6 hpr) indicated a significant difference between control cells and AcCMV_NULL transduced injured cells.

As expected, following 24 h of reperfusion AcCMV_SOD-2 injured cells showed a trend of increasing cell viability compared to injured AcCMV_NULL cells (Figure 5.2 B). In particular, cell viability was approximately 93% at 48 hpr and higher than control cells at 72 hpr (95% *vs.* 93%, respectively). When compared to AcCMV_SOD-2 injured cells, a

significantly decrease in viability was observed for AcCMV_NULL injured HK-2 cells at 48 and 72 hpr (F (4, 20)= 5.259; p<0.01 and p<0.05, respectively), 86% and 89%, respectively (Figure 5.2 B, striped *vs.* solid blue bars). Additionally, Two-way ANOVA analysis showed that at 48 hpr cell viability of AcCMV_NULL transduced cells was significantly lower (F (4, 20)= 5.259; p<0.001) than that of non-injured control cells (Figure 5.2 B, striped blue bar *vs.* solid black bar).

5.3 Effects of sodium butyrate IN HK-2 cells subjected to I/R injury

5.3.I Optimizing sodium butyrate concentration in HK-2 cells

As described in Chapter 4 of this thesis, sodium butyrate is a member of the histone deacetylase inhibitor (HDACis) family; it is known to modulate gene expression in mammalian cells and to induce apoptotic effects in a number of cancers (Sugano *et al.,* 2005; Guo *et al.,* 2010). In particular, it has been reported recently, that sodium butyrate ameliorated myocardial I/R injury (Hu *et al.,* 2010). However, the exact mechanism of action of sodium butyrate is not well understood. In light of the beneficial effects reported for sodium butyrate, together with the findings described in Chapter 4 of this thesis, a pilot study was carried out to investigate the effect of sodium butyrate in combination with BacMam transduction, using an *in vitro* I/R injury model.

Initially, sodium butyrate concentration was optimized in HK-2 cells using a BacMam virus encoding *egfp*. HK-2 cells at a density of $1x10^5$ cells/well, were transduced with AcCMV_EGFP (MOI 150); culture media containing different concentrations of sodium butyrate (1, 4, 7 and 10 mM) was added to cells following transduction. Cell viability and *egfp* expression results of a single experimental study are shown in Figure 5.3.

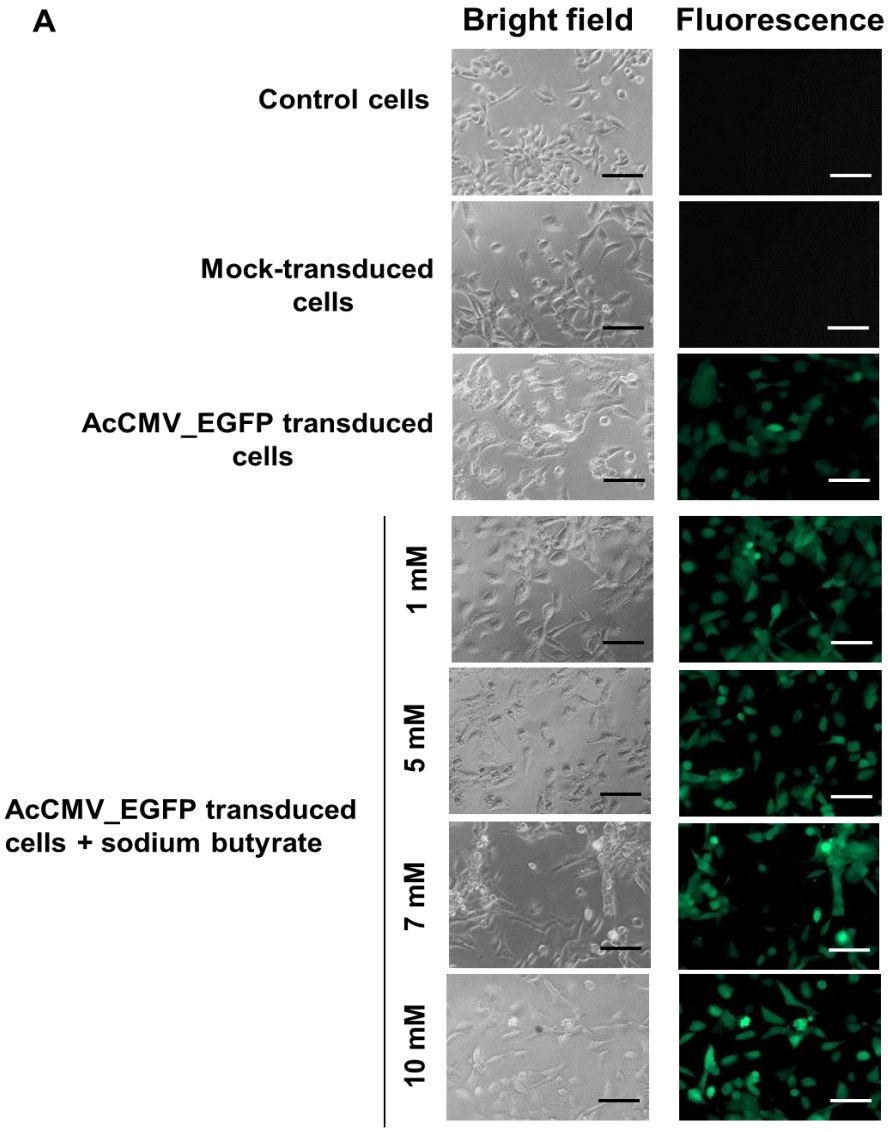

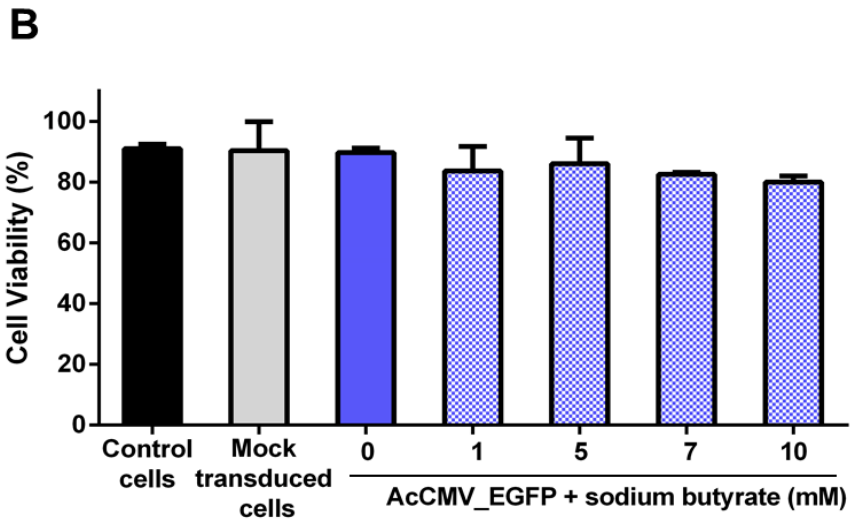

Figure 5.3. Concentration optimization of sodium butyrate and its effect on cell viability in HK-2 cells. HK-2 cells were not transduced (control cells) or mock- and AcCMV_EGFP transduced at MOI 150 (n=3). Post-transduction cells were treated with different concentrations of sodium butyrate (1, 5, 7 and 10 mM). At 24 hpt cells were analysed for *egfp* expression and cell viability. Bar scale 30 µm.

As shown in Figure 5.3 A, *EGFP* was only detected in AcCMV_EGFP transduced cells. As expected, control and mock-transduced cells appeared to be viable with no fluorescence observed by microscopy. Fluorescent cells were detected in AcCMV_EGFP transduced HK-2 cells (no sodium butyrate). However, increased fluorescence was observed in AcCMV_EGFP transduced HK-2 cells treated with increasing concentrations of sodium butyrate ranging from 1 mM to 10 mM (Figure 5.3 A). As shown in Figure 5.3 A, increasing sodium butyrate concentration, in particular at 7 and 10 mM, appeared to correspond to decreased cell viability. Therefore, the effect of different concentrations of sodium butyrate on cell viability was investigated by Trypan blue exclusion assay.

There was no significant difference (F (6, 11)= 1.332; p=0.3215) in cell viability between control cells, mock- and AcCMV_EGFP transduced HK-2 cells, (91%, 90% and 89%, respectively; Figure 5.3 B). Addition of 1 mM and 5 mM sodium butyrate induced a slight decrease in cell viability compared to AcCMV_EGFP transduced HK-2 cells (89% to 84% and 86% respectively; Figure 5.3 B solid blue bar *vs*. striped blue bars). Consistent with the microscopic observations, cell viability decreased further (82% and 80%) in transduced HK-2 cells post-treated with sodium butyrate at concentrations of 7 mM and 10 mM (Figure 5.3 B, striped blue bars). These results suggested that concentrations below 5 mM of sodium butyrate were optimal for HK-2 viability.

5.3.II Sodium butyrate effect against simulated I/R injury

In previous experiments, the use of sodium butyrate was associated with increased BacMam-mediated transgene expression (See Chapter 4); therefore, these pilot experiments were carried out to verify whether sodium butyrate treatment would protect against *in vitro* renal I/R injury by increasing BacMam-delivered *sod-2* expression.

Two experimental protocols were designed and are summarized in Figure 5.4. An intracellular ATP assay was performed in control and HK-2 injured cells in the presence or absence of sodium butyrate. In protocol-1 HK-2 cells were transduced with AcCMV_NULL and AcCMV_SOD-2 for 24 h before 60 min of ischaemic injury followed by 48 h of reperfusion; whereas, in protocol-2 cultures were transduced and treated with 5 mM of sodium butyrate for 24 h. AcCMV_NULL and AcCMV_SOD-2 transduced treated cells were then subjected to simulated ischaemia and reperfused for 48 h. Untreated, non-transduced and non-injured cells were also included as controls.

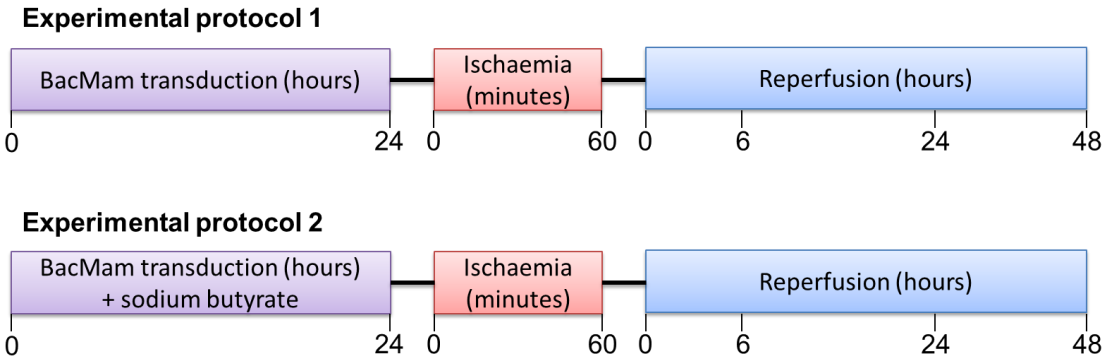

Figure 5.4. Schematic representation of the time-lines and respective conditions used for the two I/R injury experimental protocols.

Experimental protocol 1:

As shown in Figure 5.5 A, compared to the control cells (non-injured), significantly lower intracellular ATP levels (F (3, 24)= 81.31; p<0.001) were detected at 0 hpr in both AcCMV_NULL and AcCMV_SOD-2 transduced injured cells (31% and 14% respectively). However, ATP levels AcCMV_NULL and AcCMV_SOD-2 transduced injured cells were significantly different (F (3, 24)= 81.31; p<0.01) from each other (Figure 5.5 A). Following 6 h of reperfusion, intracellular ATP levels markedly increased (86%) in AcCMV_NULL and AcCMV_SOD-2 (87%) injured cells, but they were still significantly lower (F (3, 24)= 81.31; p<0.05) than control cells (Figure 5.5 A, solid and striped red bars vs. solid black bar).

ATP levels in transduced injured cells following 24 hpr were not significantly different (F (3, 24)= 81.31; p>0.05) compared to the control cells (Figure 5.5 A); however, they were significantly higher (F (3, 24)= 81.31; p<0.01) in AcCMV_NULL transduced cells (105%) compared to AcCMV_SOD-2 transduced cells (90%). As shown in Figure 5.5 A, intracellular ATP levels in AcCMV_SOD-2 injured cells did not improve further than control cells and AcCMV_NULL transduced injured cells but decreased to 80%, indeed they were significantly lower than control cells and AcCMV_NULL injured cells at 48 hpr (Figure 5.5 A).

Experimental protocol 2:

Similar to the results observed in experimental protocol 1, intracellular ATP declined significantly at 0 h of reperfusion (F (3, 24)= 81.31; p<0.001) to 22% in AcCMV_NULL + sodium butyrate injured cells (Figure 5.5 B, solid red bar) and 11% in AcCMV_SOD-2 + sodium butyrate injured cells (Figure 5.5 B, striped red bar) compared to control HK-2 cells (not treated and non-injured; Figure 5.25 B, solid black bar).

As shown in Figure 5.5 B, following 6 hpr intracellular ATP levels markedly improved in AcCMV_SOD-2 injured cells pre-treated with 5 mM of sodium butyrate (157%). These ATP levels were significantly higher (F (3, 24)= 81.31; p<0.001) compared to control cells (100%) and AcCMV_NULL (107%) pre-treated injured cells (Figure 5.5 B, striped red bar *vs.* solid black and red bars, respectively).

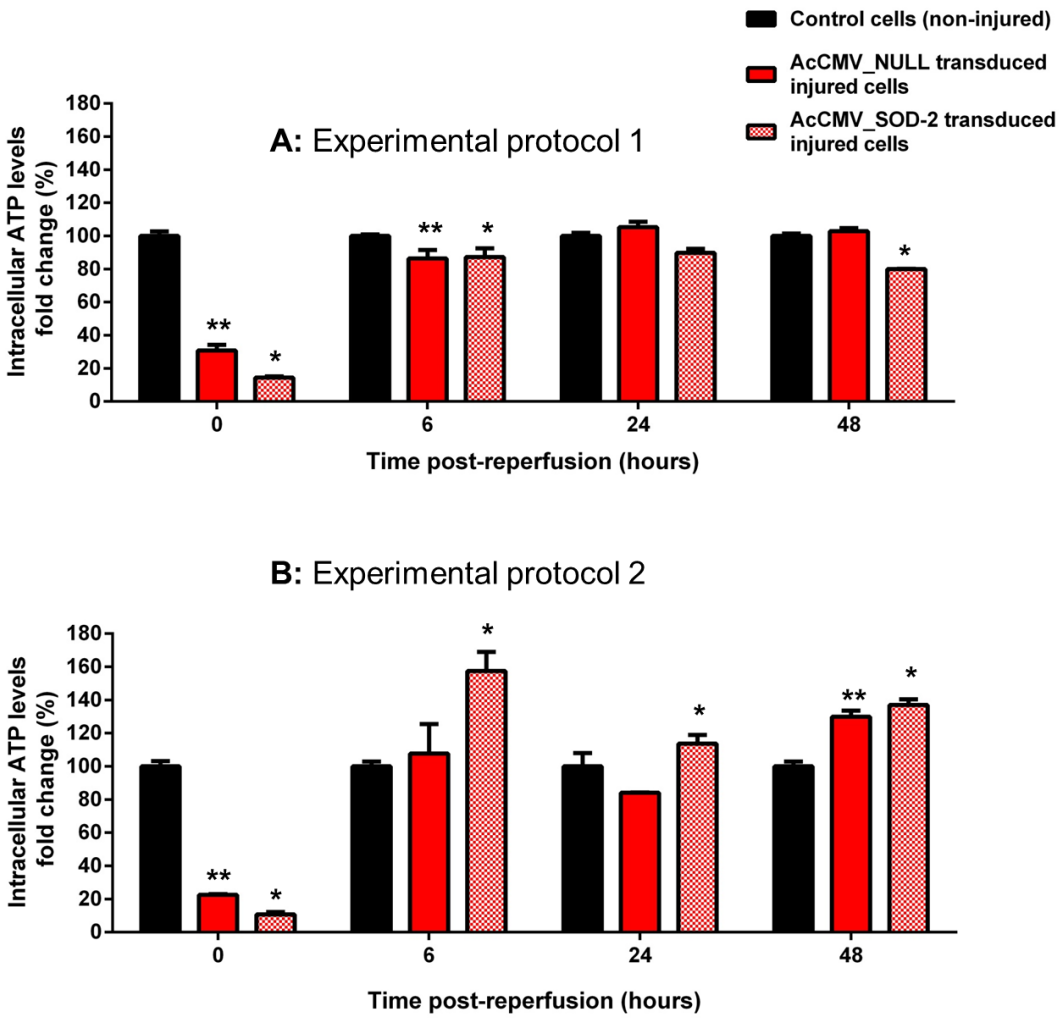

Figure 5.5. Effect of sodium butyrate in I/R injured HK-2 cells. (**A**) HK-2 cells were either AcCMV_NULL or AcCMV_SOD-2 transduced at MOI 150. At 24 hpt transduced cells were subjected to 60 min of simulated ischaemia. Intracellular ATP levels were then quantified over-time (0, 6, 24 and 48 hpr). (B) HK-2 cells were transduced with AcCMV_NULL and AcCMV_SOD-2 (MOI 150) and treated for 24 h with 5 mM of sodium butyrate. Subsequently, transduced treated cells were subjected to 60 min of ischaemia followed by reperfusion for 48 h. Intracellular ATP levels were quantified as in (B). Bars represent mean ± SEM (n=3) of results from a single experiment; *p<0.001 (A - 0 and 48 hpr, B - 0 and 6 hpr), p<0.05 (A - 6 hpr) and p<0.01 (B - 48 hpr) indicated a significant difference between control cells (non-injured) and AcCMV_SOD-2 transduced ± sodium butyrate injured cells; while, **p<0.001 (0 hpr in A and B) an p<0.05 (A - 6 hpr, B - 48 hpr) indicated a significant difference between control cells and AcCMV_NULL transduced ± sodium butyrate injured cells.

ATP levels decreased at 24 hpr in both AcCMV_NULL (80%) and AcCMV_SOD-2 (114%) + sodium butyrate injured cells (Figure 5.5 B, solid and striped red bars). However, statistical analysis indicated that the ATP content in AcCMV_NULL + sodium butyrate injured cells were significantly lower (F (3, 24)= 81.31; p<0.05) than AcCMV_SOD-2 + sodium butyrate injured cells (Figure 5.5 B, solid *vs.* striped red bar). There was no significant difference (F (3, 24)= 81.31; p>0.05) in ATP levels of transduced + sodium butyrate injured cells when compared to those of control cells (Figure 5.5 B). In contrast, relative to control cells, significantly (F (3, 24)= 81.31; p<0.05) higher ATP levels (130%) were detected at 48 hpr in AcCMV_NULL + sodium butyrate injured cells (Figure 5.5 B). As shown in Figure 5.5 B, intracellular ATP levels significantly increased (F (3, 24)= 81.31; p<0.01) to 137% in AcCMV_SOD-2 + sodium butyrate injured cells (striped red bar) compared to control cells (solid black bar). There was no statistical difference (F (3, 24)= 81.31; p>0.05) in ATP content at 48 hpr between AcCMV_NULL and AcCMV_SOD-2 + sodium butyrate injured cells.

In conclusion, this preliminary study suggested that overexpression of *sod-2* in HK-2 cells 24 h prior to simulated I/R injury did not fully protect and improve ATP levels to those of control cells (non-injured). However, pre-ischaemia treatment of BacMam transduced cells with 5 mM of sodium butyrate improved cell viability as indicated by increased ATP levels after reperfusion. Importantly, the combination of AcCMV_SOD-2 + sodium butyrate further increased intracellular ATP levels from early reperfusion times (6 hpr) compared to AcCMV_NULL + sodium butyrate in injured HK-2 cells.

5.4 EFFECT OF THERMAL PRECONDITIONING ON I/R INDUCED-INJURY IN BACMAM TRANSDUCED HK-2 CELLS

The purpose of this study was to examine the renoprotective effect of heat preconditioning (42°C for 20 min) in combination with BacMam-mediated *sod-2*/ *bcl-2* expression on a simulated I/R injury in HK-2 cells. The choice of 42°C was based on the data of Jo *et al.* (2006); they demonstrated that heat preconditioning at this temperature provided functional and histologic renal protection during ischaemic acute renal failure in rats. A schematic illustration of the experimental protocols is shown in Figure 5.6. Two independent experiments were carried out for each protocol showing same results. Firstly, the beneficial effect of BacMam transduction for 72 h + heat preconditioning prior to I/R injury of HK-2 cells (experimental protocol 1) was investigated and results are included in the supplementary data CD attached to this thesis (Chapter 5-S4).

Secondly, a more clinically relevant preconditioning model was developed (experimental protocol 2), using a shorter timeframe of BacMam transduction, 24 h (Figure 5.6 B).

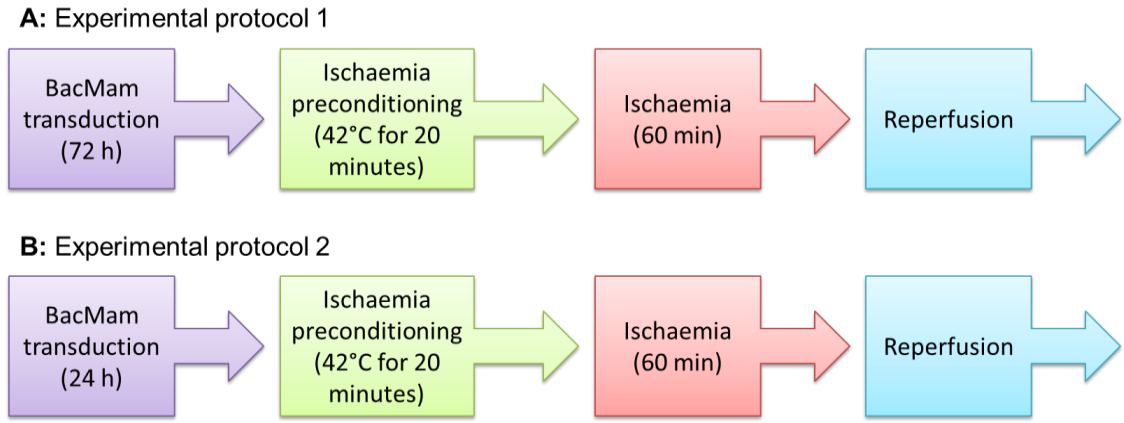

Figure 5.6. Schematic representation of the preconditioning experimental protocol used in this study.

5.4.I *Effect on ATP levels*

The duration of ischaemic injury and the timeframe of recovery represent one of the important factors that make an experimental model clinically applicable. In this study, it was evaluated whether reducing the time of BacMam transduction to 24 h could exert a protective effect when in combination with heat preconditioning strategy. Furthermore, the combined action of protective genes, *sod-2* and *bcl-2*, together with heat preconditioning was also investigated in this study; HK-2 cells were co-transduced with AcCMV_SOD-2 + AcCMV_BCL-2 with a ratio of 1:1.

Representative results of a single experimental study are shown in Figure 5.7; a trend of improved intracellular ATP levels, between 0 and 48 hpr, was observed in BacMam transduced + preconditioned injured HK-2 cells. As expected, following 60 min of ischaemia (0 hpr) the intracellular ATP levels were decreased significantly (F (4, 49) = 79.37; p<0.001) in preconditioned AcCMV_NULL (17%), AcCMV_SOD-2 (27%), AcCMV_BCL-2 (16%) and in AcCMV_SOD-2 + AcCMV_BCL-2 (31%) injured cells compared to the non-preconditioned control cells (Figure 5.7). After 4 h of reperfusion these intracellular ATP levels were still significantly lower (F (4, 49) = 79.37; p<0.001) than control cells; however they were increased in the preconditioned transduced injured cells by 42% in AcCMV_NULL, 58% in AcCMV_SOD-2, 36% in AcCMV_BCL-2 and 61% in AcCMV_SOD-2 + AcCMV_BCL-2 (Figure 5.7).

As shown in Figure 5.7, at 8 hpr a significant increase in ATP levels was observed in preconditioned AcCMV_NULL injured cells (F (4, 49) = 79.37; p<0.01), AcCMV_BCL-2

injured cells (F (4, 48) = 117.2; p<0.001) and AcCMV_SOD-2 + AcCMV_BCL-2 (F (4, 48) = 117.2; p<0.001) injured cells (89%, 96% and 86%, respectively) compared to the ATP levels detected in the preconditioned AcCMV_SOD-2 injured cells (41%). Statistical analysis revealed no significant difference (F (4, 48) = 117.2; p>0.05) in the ATP levels of preconditioned AcCMV_NULL, AcCMV_BCL-2 and AcCMV_SOD-2 + AcCMV_BCL-2 injured cells compared to control cells (Figure 6.24); whereas, at 8 hpr there was a significant difference (F (4, 49) = 79.37; p<0.001) in ATP contents between preconditioned AcCMV_SOD-2 injured cells and control cells (Figure 5.7, striped red bar *vs.* solid black bar).

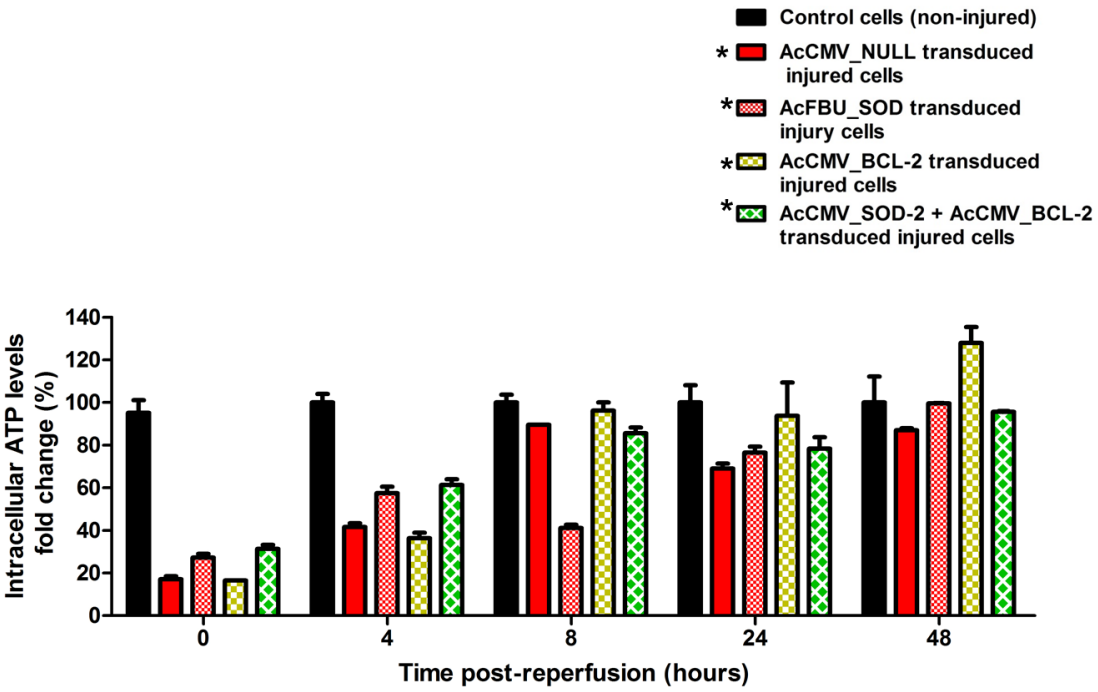

Figure 5.7. Levels of intracellular ATP levels in heat preconditioned transduced I/R injured HK-2 cells. HK-2 cells were transduced with AcCMV_NULL, AcCMV_SOD-2, AcCMV_BCL-2 or with the combination of AcCMV_SOD-2 + AcCMV_BCL-2 at MOI 150. At 24 hpt transduced HK-2 cells were heat preconditioned at 42°C for 20 min. Subsequently, transduced preconditioned cells were subjected to 60 min of simulated ischaemia followed by reperfusion. Intracellular ATP levels were then quantified over-time. Bars represent mean ± SEM (n=3) of a single representative study; *p<0.001 and p<0.05 indicated a significant difference between control cells (non-injured) and preconditioned BacMam transduced injured cells.

In contrast to 8 hpr, at 24 hpr preconditioned AcCMV_NULL transduced injured cells showed ATP levels of 70%, significantly different (F (4, 49) = 79.37; p<0.05) as compared to control cells. Although, in preconditioned AcCMV_SOD-2 + AcCMV_BCL-2 injured cells ATP levels were reduced from 86% to 78% at 24 hpr, there was no significant difference with the ATP levels of control cells (Figure 5.7 striped green bar *vs.* solid black bar).

Increased intracellular levels of ATP were detected in preconditioned AcCMV_SOD-2 injured cells, 76% (Figure 5.7, striped red bar); whilst, ATP contents in preconditioned AcCMV_BCL-2 injured cells were 94%, this was similar to that observed at 8 hpr, 96% (Figure 5.7, striped yellow bar).

As shown in Figure 5.7, at 48 hpr preconditioned AcCMV_SOD-2 (striped red bar) and the virus combination AcCMV_SOD-2 + AcCMV_BCL-2 (striped green bar) injured cells exhibited same high ATP levels of control cells (99% and 95%, respectively, *vs.* 100%). In particular, significantly improved ATP levels were detected in preconditioned AcCMV_BCL-2 injured cells, 128%; these levels were significantly higher when compared to control cells (F (4, 49) = 79.37; p<0.01) and to the preconditioned injured transduced cells with AcCMV_NULL (F (4, 39) = 79.37; p<0.001), AcCMV_SOD-2 (F (4, 49) = 79.37; p<0.05) and with the combination of AcCMVSOD-2 + AcCMV_BCL-2 (F (4, 49) = 79.37; p<0.01). In contrast, compared to control cells, ATP levels were not fully recovered in preconditioned AcCMV_NULL injured cells (87%) after 48 h of reperfusion (Figure 5.7, solid red bar *vs.* solid black bar); however, these decreased ATP levels were not statistically different (F (4, 48) = 81.34; p>0.05) from those of control cells.

5.4.II Caspase-3 activity

Subsequently, it was examined whether the protective effect of BacMam transduction and heat preconditioning in I/R-induced cell injury was associated with reduced apoptosis. As described in Chapter 1, Section 1.3.4.III of this thesis, caspases are cysteine proteases that are responsible for the activation of the apoptotic pathways; therefore, because caspase-3 is released by damaged degenerating cells, in this study the production of activated caspase-3 was quantified over-time (Section 2.2.6). Data from a single experiment are shown as fold change in caspase-3 activity relative to control cells (non-injured) and are illustrated in Figure 5.8.

At 0 hpr, there was no significant changes (F (4, 39)= 41.30; p>0.05) in the levels of caspase-3 activity between control cells and preconditioned injured cells transduced with AcCMV_NULL, AcCMV_SOD-2, AcCMV_BCL-2 and AcCMV_SOD-2 + AcCMV_BCL-2 viruses (Figure 5.8). Following 4 h of reperfusion, the activation of caspase-3 was significantly increased in preconditioned AcCMV_NULL injured cells (F (4, 39)= 41.30; p<0.01) and AcCMV_BCL-2 injured cells (F (4, 39)= 41.30; p<0.05) by approximately two-fold, respectively (Figure 5.8). In contrast, the levels of caspase-3 in the preconditioned injured cells transduced with AcCMV_SOD-2 alone or in combination with AcCMV_BCL-2 were still similar to that in the controls cells (Figure 5.8).

At 8 hpr, the contents of activated caspase-3 in preconditioned transduced injured cells were not significantly different (F (4, 39)= 41.30; p>0.05) from each other and from that observed in control cells (Figure 5.8).

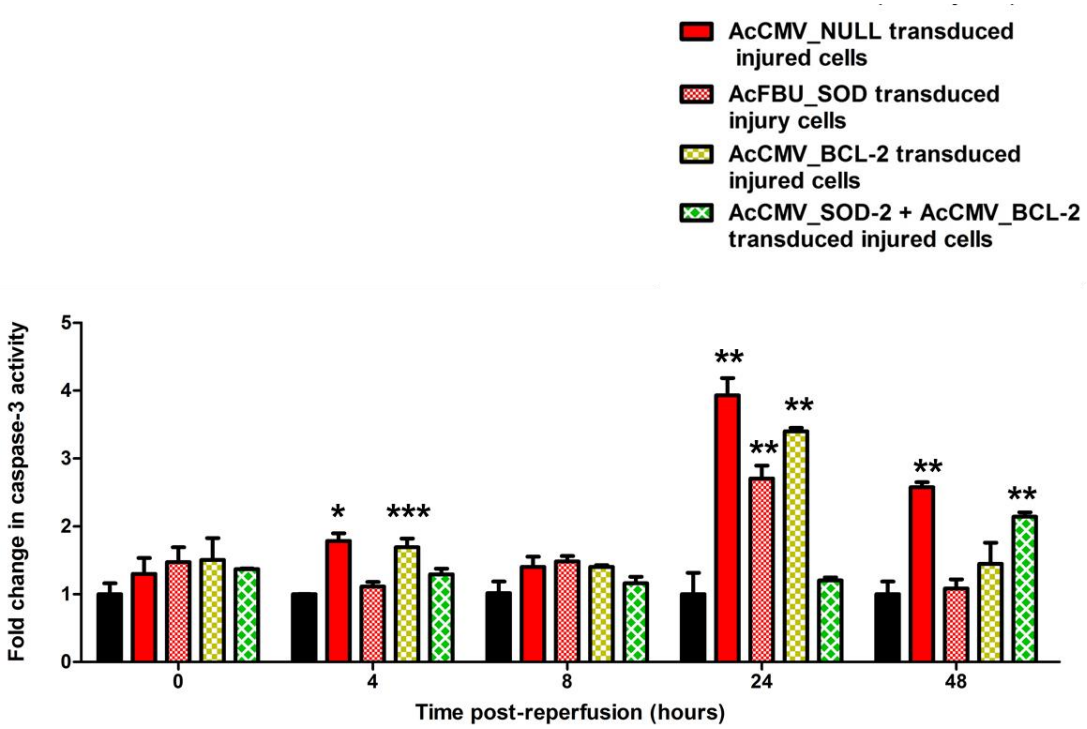

Figure 5.8. Caspase-3 activity in BacMam transduced + preconditioned HK-2 cells after simulated I/R injury. HK-2 cells were transduced with AcCMV_NULL, AcCMV_SOD-2, AcCMV_BCL-2 or with the combination of AcCMV_SOD-2 + AcCMV_BCL-2 at MOI 150. At 24 hpt transduced HK-2 cells were heat preconditioned at 42°C for 20 min. Subsequently, transduced preconditioned cells were subjected to 60 min of simulated ischaemia followed by reperfusion. Caspase-3 assay was performed following the manufacturer guidelines (Chapter 2, Section 2.2.38). Bars represent mean ± SEM (n=3) of results from a single experiment; *p<0.01, **p<0.001 and ***p<0.05 indicated a significant difference between control cells (non-injured) and preconditioned BacMam transduced injured cells.

Compared to control cells (non-injured), at 24 hpr the caspase-3 activity was significantly increased (F (4, 39)= 41.30; p<0.001) in preconditioned injured cells transduced with AcCMV_NULL (approximately four-fold), AcCMV_SOD-2 (approximately three-fold) and in AcCMV_BCL-2 (three-fold); whereas, preconditioned injured cells transduced with the virus combination AcCMV_SOD-2 + AcCMV_BCL-2 showed similar levels of active caspase-3 to that of control cells and caspase-3 activity was significantly attenuated (F (4, 39)= 41.30; p<0.001) compared to preconditioned injured cells transduced with AcCMV_NULL, AcCMV_SO-2 and AcCMV_BCL-2 viruses (Figure 5.8).

As shown in Figure 5.8, following 48 hpr there was still significantly increased (F (4, 39)= 41.30; p<0.001) levels of caspase-3 activity in preconditioned AcCMV_NULL injured cells (approximately three-fold) compared to control cells and both preconditioned AcCMV_SOD-2 and AcCMV_BCL-2 injured cells (Figure 5.8solid red bar *vs.* solid black bar). Levels of caspase-3 activity similar to control cells were detected in preconditioned AcCMV_SOD-2 and in AcCMV_BCL-2 injured cells at 48 hpr; while, caspase-3 activity was significantly induced (F (4, 39)= 41.30; p<0.001) by two-fold above control cells in preconditioned injured cells transduced with the viral combination AcCMV_SOD-2 + AcCMV_BCL-2 (Figure 5.8).

Taken together, these results suggested that heat preconditioning in combination with either AcCMV_SOD-2 or AcCMV_BCL-2 partially protected HK-2 cells from apoptosis induced by I/R injury compared to AcCMV_NULL injured cells. Furthermore, the increased caspase-3 activity observed at 24 and 48 hpr in preconditioned AcCMV_NULL injured cells may contribute to, or may results from, the reduced recovery observed with the intracellular ATP levels (Figures 5.7).

5.4.III Total cellular SOD activity

To determine whether the beneficial effect of BacMam transduction and heat preconditioning on I/R injury was related to the antioxidant capacity, a single experiment was carried out to investigate the inhibition rate of the total cellular SOD activity (Section 2.2.6). The SOD activity assay is based on the inhibition of nitroblue tetrazolium (NBT) which is converted by SOD into a blue tetrazolium salt. The amount required to inhibit the rate of reduction of NBT by 50% is defined as one unit of enzyme activity. SOD activity time course during the reperfusion period is shown in Figure 5.9.

SOD activity following ischaemia (0 hpr) was significantly higher (F (4, 50)= 10.25; p<0.001) in preconditioned AcCMV_NULL injured cells (257%) compared to control cells (100%) and preconditioned injured cells transduced with AcCMV_SOD-2 (153%), AcCMV_BCL-2 (110%) and with the combination of AcCMV_SOD-2 + AcCMV_BCL-2 viruses (144%; Figure 5.9). After 4 hpr, this markedly increased SOD activity in AcCMV_NULL injured cells (Figure 5.9, solid red bar) decreased to 176%; however this was significant higher than control cells (F (4, 50)= 10.25; p<0.05) and preconditioned AcCMV_BCL-2 transduced injured cells (F (4, 50)= 10.25; p<0.001). Indeed, a reduced SOD activity below control cells was detected in preconditioned AcCMV_BCL-2 injured cells (65%).

Compared to control cells, at 4 hpr the SOD activity was significantly higher (F (4, 50)= 10.25; p<0.05) in preconditioned injured cells transduced with AcCMV_SOD-2 alone (180%), but not affected in preconditioned injured cells transduced with the virus combination AcCMV_SOD-2 + AcCMV_BCL-2 (120%).

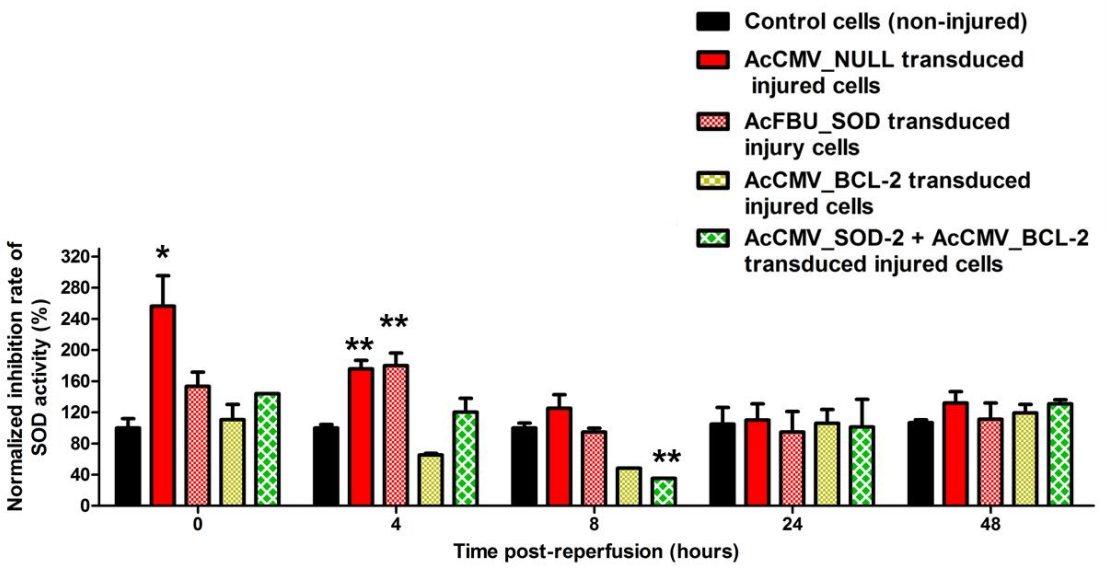

Figure 5.9.Effect of I/R injury on SOD activity in preconditioned BacMam transduced HK-2 cells. Cultures were transduced with AcCMV_NULL, AcCMV_SOD-2, AcCMV_BCL-2 or with the combination of AcCMV_SOD-2 + AcCMV_BCL-2 at MOI 150. At 24 hpt transduced HK-2 cells were heat preconditioned at 42°C for 20 min. Subsequently, transduced preconditioned cells were subjected to 60 min of simulated ischaemia followed by reperfusion. SOD activity assay was performed following the manufacturer guidelines (Chapter 2, Section 2.2.37). Bars represent mean ± SEM (n=3) of results from a single study; *p<0.001 and **p<0.05 indicated a significant difference between control cells (non-injured) and preconditioned BacMam transduced injured cells.

Following 8 hpr, SOD activity in preconditioned AcCMV_NULL (125%) and AcCMV_SOD-2 (95%) injured cells decreased to the levels of control cells (100% Figure 5.9 solid and striped bars *vs.* solid black bar). Furthermore, compared to control cells, a markedly decreased SOD activity was detected in preconditioned AcCMV_BCL-2 and in AcCMV_BCL-2 + AcCMV_SOD-2 injured cells at 8 hpr. As shown in Figure 5.9, at reperfusion times 24 and 48 h the SOD activity amongst all the preconditioned transduced injured cells was not statistically different (F (4, 50)= 10.25; p>0.05) from that of control cells (solid black bars)

5.5 DISCUSSION

I/R injury is one of the most common causes of AKI; indeed, ischaemic AKI represents one of the major problems in transplantation; it is often associated with initial delayed graft function, which likely contributes to long-term graft damage (reviewed by Bellomo *et al.,* 2004; and Heyman *et al.,* 2012).

The pathophysiologic mechanism of ischaemic AKI is complex and is thought to include cell dysfunction (Parikh, 2013), inflammation processes (Akcay *et al.,* 2009) and tubular cellular apoptosis (Bengatta *et al.,* 2009). Despite advances in supportive care and novel therapeutic strategies, there are no currently available approaches that efficiently prevent AKI induced by I/R injury (Kunzendorf *et al.,* 2010; Bauerle *et al.,* 2011). A number of gene therapy strategies have been developed based on information obtained from clinical studies as well as *in vitro* and *in vivo* models of renal injury (reviewed by Basile, 2007). In particular, these approaches have been aimed to understand the molecular, cellular, and physiologic responses of renal I/R injury. A number of reports identified oxidant stress, inflammation, and apoptotic pathways as potential therapeutic targets (reviewed by Basile, 2007). As described in Chapter 1 Sections 1.3.4.II & III of this thesis, *sod-2* and *bcl-2* represent the primary defence against ROS overproduction and apoptosis, respectively, caused by I/R injury. In particular, gene transfer studies have described a beneficial effect of delivering exogenous *sod-2* and *bcl-2*, by using mammalian viruses, on ischaemic tissues such as brain, liver, retinal, heart and kidneys (Chen *et al.,* 2001; 2009; Wu *et al.,* 2009).

Mammalian viruses are generally used as gene delivery systems in gene therapy studies compared to non-viral vectors due to the high gene transfer efficiency and prolonged recombinant gene expression (reviewed by Jin *et al.,* 2014). However, these mammalian viruses often induce a significant inflammatory and immune response upon transduction which compromises their gene transfer ability. Therefore, the ideal gene delivery systems should have high transduction efficiency, low cytotoxicity and exhibits a lower effect on the innate immune response. Amongst all the viral-based delivery systems, BacMam viruses have been widely described as a useful and safe gene delivery system with low cytopathic effects and immune response compared to mammalian viruses; indeed, BacMam are believed to hold great promise for certain gene therapy applications (Paul *et al.,* 2012). In light of these positive results, the current study was designed to investigate the role of *sod-2* and *bcl-2* in an *in vitro* simulated renal I/R injury model using BacMam gene delivery system to overexpress these protective genes.

5.5.I ATP depletion-recovery model in HK-2 cells

A proximal tubular cell line, derived from adult human kidney, was established for the first time by Ryan *et al.* (1994) and was designed HK-2. An extensive number of reports have utilized HK-2 cells for *in vitro* renal physiology and pathology studies. In particular, HK-2 cell response to injury has been reported to be similar to primary cultures of human proximal tubular cells (Janssen *et al.,* 2001) and they are therefore considered to be a good model to study ischaemia. To verify that HK-2 cells were a valid cellular model to study the protective effect of BacMam-mediated *sod-2* delivery in proximal tubule cells, experimental conditions were first optimized and are described in supplementary data CD attached to this thesis (Chapter 5-S2).

Intracellular ATP depletion, fall in tissue oxygen levels with a concomitant rinse in intracellular calcium are the main features of renal I/R injury (Greene & Paller, 1994; Lee & Emala, 2002). Therefore in this study, ATP-depletion protocol was used as an *in vitro* model to study I/R induced injury in HK-2 cells.

Results indicated that following simulated-ischaemic injury, ATP levels were significantly reduced within 30 min of treatment; levels remained markedly low after 45 and 60 min of treatment compared to non-injured cells (Figure 5.1). These results mimicked observations made by Doctor *et al.* (1994); after 30 min of metabolic inhibition with rotenone or antimycin A + 2-deoxyglucose, ATP levels dramatically dropped to 1-4% of control cells in both tested kidney cells, LLC-PK and MDCK. These results were also consistent with Lee & Emala (2002); they examined HK-2 cell death mediated by ATP/glucose depletion as an *in vitro* model of anoxia/ischaemia. By measuring percentage of LDH released into the cell culture media Lee and Emala demonstrated that the ATP-depletion injures model of HK-2 cell was time-dependent manner; the amount of LDH released increased from approximately 40% to 80% within 3 h of ATP-depletion.

Having confirmed that the *in vitro* model of simulated ischaemia induced injury in HK-2 cells, the time points 30 and 60 min were chosen for subsequent optimization studies; these have been included as supplementary data in the CD attached with this thesis (Chapter 5-S3). Findings from these studies suggested that 60 min of simulated ischaemia induced a less severe injury than the shorter time, 30 min; therefore, 60 min of simulated I/R injury was chosen for future experiments.

To validate the optimal conditions and the reproducibility of the protective effect of BacMam-mediated *sod-2* overexpression, HK-2 cultures were transduced for 72 h before I/R injury (60 min of injury and 0 to 72 h of reperfusion).

In accordance with the optimization study, *sod-2* overexpressing-injured cells showed a trend of increasing intracellular ATP levels over-time (from 20% to 140%), with a full ATP recovery observed at 72 h, compared to AcCMV_NULL injured cells, 19% to 86% (Figure 5.2 A). Since the intracellular ATP content is essential for maintaining normal cell functions as well as cellular integrity, it should be noticed that any increase, even small, in ATP content during I/R injury might contribute to the long-term cellular recovery. Although a full ATP recovery was observed at 72 hpr in AcCMV_SOD-2 transduced/injured cells, the increase in ATP contents, observed between 6 and 48 hpr, also exerted a protective effect against I/R injury. These results were consistent with cell viability data; over the course of reperfusion, cell viability in AcCMV_SOD-2 injured cells increased from 83% to 93% by 72 hpr, compared to AcCMV_NULL injured cells (Figure 5.2 B). These observations are also consistent with published models of renal I/R injury in cells overexpressing *sod-2* (Cruthirds *et al.,* 2005; Pisani *et al.,* 2014). Koo *et al.* (2005) generated a stable alveolar epithelial cells line overexpressing *sod-2*; they demonstrated that the overexpression of *sod-2* significantly protected the cells within the first 48 h of hyperoxia exposure and significantly increased the number of viable cells (p<0.05).

5.5.II Potential beneficial effect of sodium butyrate + BacMam-mediated gene delivery

Recently, Machado *et al.* (2012) demonstrated that sodium butyrate prevented the translocation of nuclear factor kappa B (NF-kB) into the nucleus which decreased oxidative damage, inflammatory response, tubular damage and attenuated acute kidney injury. Additionally, more recent studies showed that sodium butyrate reduced inflammatory responses and pulmonary oxidative stress in the lungs of severely burned rats (Liang *et al.,* 2013) and also ameliorated I/R-induced liver injury (Qiao *et al.,* 2014). Thus, based on the information available in the literature, this pilot study aimed was aimed to investigate the possible effects of sodium butyrate in combination with BacMam-mediated gene delivery after simulated I/R injury in HK-2 cells.

Microscopy and Trypan blue exclusion assay revealed that increasing sodium butyrate concentration was associated with loss of cell viability (Figure 5.3 A). Results showed that the optimal concentration of sodium butyrate (low cytotoxicity and high cell viability) in HK-2 cells was below 5 mM as suggested by the increased amount of non-viable cells with sodium butyrate at concentrations of 7 mM and 10 mM (Figure 5.3 B). These data were consistent with Matsumoto *et al.* (2006) study which demonstrated that exposure of renal epithelial HK-2 cells to elevated concentrations of sodium butyrate (0–10 mM), suppressed in a dose-dependent manner both basal and stimulated pro-fibrotic cytokine

transforming growth factor-beta1 (TGF-$^{\beta}$1) synthesis, a key mediator of progressive renal injury. Importantly, they detected a significant reduction of TGF-$^{\beta}$1 synthesis at concentrations of sodium butyrate of 5 mM.

Having determined the optimal sodium butyrate concentration (5 mM), it was next sought to examine its effect in combination with 24 h AcCMV_SOD-2 transduction against simulated I/R injury. Two experiments were conducted in parallel to determine sodium butyrate effect (Figure 5.4): in the experimental protocol 1, HK-2 cells were only transduced for 24 h with AcCMV_SOD-2 virus (no-sodium butyrate).

Kidney cells ATP levels fall to less than 20% of pre-ischaemic values within 1-2 h of ischaemia; depending on the ischaemic interval, ATP levels can return between 60-80% to control values upon reperfusion (Doctor *et al.,* 1994; Lee & Emala, 2002; Cruthirds *et al.,* 2005; Szeto *et al.,* 2011). Results from this study were consistent with these reports. Decreases in ATP levels were detected at 0 hpr in injured cells (31% and 14% respectively; Figure 5.5 A). ATP levels only partially recovered in AcCMV_SOD_2 injured cells (90%) compared to AcCMV_NULL injured cells which a complete recovery of ATP was found after 24 and 48 h of reperfusion (Figure 5.5 A). Consistent with Cruthirds *et al.* (2005) which demonstrated that overexpressing *sod-2* in NRK cells by stable transfection 24 h pre-antimycin A exposure induced a trend of increasing ATP levels; following 2 h of ischaemia, ATP levels were decreased to less than 20% of control values and increased approximately to 70% after 4 h of reperfusion.

In the second approach used in this study, AcCMV_SOD-2 transduced HK-2 cells were treated with 5 mM sodium butyrate for 24 h before simulated I/R injury. The results clearly demonstrated a complete recovery of ATP levels within 6 h of reperfusion in *sod-2* overexpressing-treated injured cells compared to AcCMV_NULL treated injured cells; these ATP levels were still completely restored (114-137%) compared to AcCMV_NULL + sodium butyrate injured cells at 48 hpr (Figure 5.5 B). Results from this study were also consistent with Qiao *et al.* (2014) who demonstrated that pre-treatment with sodium butyrate before 60 min of hepatic ischaemia markedly improved hepatic function and histology at 6 and 24 h after reperfusion, as indicated by reduced transaminase levels. Sun and colleagues demonstrated that administration of sodium butyrate 30 min prior to the daily intraperitoneally injection of gentamicin into rats, attenuated gentamicin-induced nephrotoxicity by enhancing renal antioxidant enzymes activity such as SODs (Sun *et al.,* 2013).

To my knowledge this is the first study on the protective effect of sodium butyrate + BacMam-mediated gene delivery on renal I/R-induced injury.

Although, this pilot study indicated a full recovery of HK-2 cells from I/R injury in the presence of overexpressed *sod-2* and 5 mM sodium butyrate, more studies are needed to further elucidate whether this beneficial effect was due to the burst of *sod-2* expression alone, reduced inflammatory response or because of the combined action of both *sod-2* overexpression and reduced inflammatory response.

5.5.III Thermal preconditioning effect on HK-2 cells I/R induced-injury

Preconditioning has been recognized as a protective strategy to reduce damage that occurs after reperfusion (reviewed by Bonventre, 2002). Tolerance to ischaemia is achieved with this method by exposing cells, tissues or organs to transient and brief periods of injury prior to long-term I/R injury. The protective effect has been linked to various pathways such as reduced cellular apoptosis (Yamasowa *et al.,* 2005), decreased inflammatory response (Jiang *et al.,* 2007) and preservation of intracellular ATP (Halestrap *et al.,* 2009). A number of protocols have been used in different experimental studies induced by ischaemic (Fan *et al.,* 2012), thermal (Huang *et al.,* 2003; Luh *et al.,* 2007) or pharmacologic stimuli (Ferreyra *et al.,* 2013). In particular, thermal preconditioning, which represents changes in the normal physiological temperature (37°C), and has been previously demonstrated to attenuate kidney I/R induced injuries (Jo *et al.,* 2006). The detailed molecular mechanism of thermal preconditioning is still unclear; however, studies have suggested that the protective effect might be mediated by an increased expression of heat shock proteins (HSPs) which are known for their ability to facilitate refolding, assembly, and stabilization of denatured proteins (Kondo *et al.,* 2000; McCormick *et al.,* 2003).

Intracellular ATP levels

In this study, two experimental protocols were designed (Figure 5.6). The effect of preconditioning using the experimental protocol 1 is included in the supplementary data CD attached with this thesis (Chapter 5-S4). Results suggested a full recovery of ATP levels in HK-2 cells from I/R injury in preconditioned injured cells overexpressing *sod-2* and *bcl-2* compared to preconditioned AcCMV_NULL injured cells (Chapter 5-S4).

A temporal analysis, using the experimental protocol 2, showed a trend of increasing ATP levels in *sod-2* and *bcl-2* overexpressing (alone or in combination) preconditioned injured cells compared to preconditioned AcCMV_NULL injured cells (Figure 5.7). It was noteworthy that ATP levels were completely restored by 8 hpr only in preconditioned injured cells transduced with AcCMV_BCL-2 alone (Figure 5.7), these were consistent with data from the experimental protocol 1 (see supplementary data, Chapter 5-S4).

In contrast, ATP levels only partially recovered during the 48 h of reperfusion in preconditioned injured cells transduced with the backbone virus, AcCMV_NULL (Figure 5.7). These data were also consistent with previous reports; thermal preconditioning (43°C for 30 min) reduced cardiocytes cell death as indicated by decreased LDH activity at 18-20 h after stress (Cumming *et al.,* 1996). Furthermore, in this study BacMam-mediated *bcl-2* overexpression within 8 hpr increased ATP levels in preconditioned injured cells. This was consistent with Chien *et al.* (2005) who demonstrated that 24 h adenovirus-mediate *bcl-2* delivery to proximal and distal tubular cells *in vitro* up-regulated *bcl-2* expression and inhibited hypoxia/reoxygenation-induced injury and tubular apoptosis.

Collectively, consistent with the conclusion from experimental protocol 1 (see supplementary data, Chapter 5-S), these results suggested that heat preconditioning before simulated I/R injury ameliorated cell viability by increasing the intracellular ATP levels during 48 h of reperfusion.

Caspase-3 activation

Subsequently, it was hypothesized that *sod-2* and *bcl-2* overexpression might attenuate I/R-induced not only by increasing ATP levels but also by reducing apoptosis. Time-course analysis showed that heat preconditioning in combination with either AcCMV_SOD-2 or AcCMV_BCL-2 (alone or in combination) partially reduced caspase-3 activation and therefore, prevented apoptosis induced by I/R injury at 48 hpr (Figure 5.8). From these data it also appeared that AcCMV_NULL transduction did not attenuate cell death as seen by the increased caspase-3 activity at 4, 24 and 48 hpr. These results are consistent with previous reports which, demonstrated that apoptosis occurs following ATP depletion/reperfusion (Cruthirds *et al.,* 2005; Zhao *et al.,* 2009). Cruthirds *et al.* (2005) demonstrated that there was no increase in caspase-3 activity in the NRK overexpressing *sod-2* cells following ATP depletion/recovery which, was in contrast to what was observed in *sod-2* non-expressing injured NRK cells (approximately four-fold increased caspase-3 levels). Overexpression of *bcl-2* using lentivirus has been shown to significantly reduce caspase-3 activity following hypoxia and ischaemia reperfusion in aorta endothelial cells (Zhao *et al.,* 2009).

SOD activity

Although a number of studies reported reduced endogenous SOD enzymes activity after renal I/R injury (Wang *et al.,* 2010; Collino *et al.,* 2013; Seifi *et al.,* 2014), several other lines of evidence showed that thermal or ischaemic preconditioning augmented various protective proteins and especially SOD-2 (Chen *et al.,* 2003; Yang *et al.,* 2007).

Therefore, in this study, in order to extend previous observations, the enzymatic activity of SOD was measured in control cells and in preconditioned transduced injured cells. Time-course analysis of the total SOD enzymes activity revealed that within 4 h of reperfusion SOD activity significantly increased only in AcCMV_NULL (176%) and AcCMV_SOD-2 (180%) injured cells above control value (Figure 5.9); however, upon longer time of reperfusion (from 8 to 48 h) SOD activity in all preconditioned transduced injured cells returned to levels similar to control values. Rahman *et al.* (2009) administered human *sod-2* in a rat kidney prior renal I/R injury. They showed increased SOD activity following 16 h of reperfusion which improved renal function and reduced tissue injury compared to the *sod-2* non-overexpressing kidneys.

This was the first *in vitro* study to utilize BacMam-mediated gene delivery approach to overexpress protective genes during I/R renal injury. In particular, the investigations conducted in this study demonstrated that (1) using optimized conditions, delivery of s*od-2* prior to the simulated ischaemia, improved cellular resistance to injury with complete recovery of ATP levels within 48 h of reperfusion in HK-2 cells. (2) The addition of sodium butyrate following BacMam transduction might play an important role in SOD-2-mediated early h protection against oxidative-stress in kidney cells, although more studies are need to clarify its effect during I/R injury. (3) Furthermore, to my knowledge, this study reported for the first time an *in vitro* protective effect of the recombinant *sod-2* and *bcl-2* (alone or in combination) and heat preconditioning against subsequent ATP-depletion induced injury in HK-2 cells.

Chapter 6

BacMam transduction *ex vivo* in porcine kidney

6.1 INTRODUCTION

In 1906, Jaboulay was the first to attempt kidney transplantation in two patients by transplanting a goat kidney into one and a pig kidney into the other. However, both transplants failed and the two patients died (reviewed by Morris, 2004). Thirty years later, the first human kidney transplant was performed by Voronoy; nevertheless, this also failed due to the deleterious effects of warm ischaemia (reviewed by Matevossian *et al.,* 2009). The first successful long-term transplant was performed by Murray *et al.* (1954) between identical twins one in good health and the other dying of kidney disease; however, the transplant recipient died eight years after transplantation.

The main purpose of kidney preservation is to maintain the organ in a viable state from the time of retrieval until transplantation. Hypothermic preservation solutions such as UW solution were developed in the late 1980s to maintain kidney tissue viability by reducing metabolic activity and accumulation of toxic substances during the obligatory cold storage period (Koo *et al.,* 1998; reviewed by Watson & Dark, 2012). During transplantation, organs undergo hypoxic ischaemic and reperfusion injury due to the cold storage and cold perfusion re-oxygenation. Indeed, to date I/R injury represents a major limiting factor in kidney transplantation which contributes to delayed graft function and subsequent chronic graft deterioration (reviewed by Ponticelli, 2013; and Akhtar *et al.,* 2014). Therefore, emerging strategies have aimed to prevent the initial renal I/R injury which would improve short- and long-term outcomes of kidney transplantation; in particular, these have included approaches that can be applied *ex vivo* to the organ during preservation such as static and machine perfusion as well as preservation solutions supplemented with pharmacological agents (reviewed by Bon *et al.,* 2012; and Akhtar *et al.,* 2014).

As described in Chapter 5 of this thesis, overexpressing *sod-2* appeared to protect against I/R injury in HK-2 cells *in vitro* renal models. Therefore, to extend the *in vitro* observations, in this preliminary study an *ex vivo* kidney perfusion method was developed and evaluated for highly efficient BacMam-mediated gene transfer using porcine kidney as experimental model. Importantly, it was hypothesized that augmentation of BacMam-mediated *sod-2* gene transfer (AcCMV_SOD-2) might improve I/R induced renal injury during cold preservation. It should be noticed that this was a pilot study and therefore, all the experiments described in this thesis Chapter were only carried out once.

6.2 BACMAM GENE TRANSFER DURING *EX VIVO* KIDNEY PERFUSION

Five porcine kidneys (Figure 6.1 A) obtained from a local abattoir within 10 min after death, were flushed *in situ* with 3 litres of soltran kidney perfusion fluid to remove impurity and blood (Section 2.1.8). As can be seen from Figure 6.1 B, a red coloured solution was collected after the first flush which gradually became colourless after the third flush indicating the removal of most of the blood present in the kidneys. Immediately after the kidneys arrived in the laboratory, they were measured, weighed (Table 6.1) and placed in Belzer UW® cold perfusion solution at 4°C. All the virus stocks used in this study were also resuspended in BELZER UW® cold preservation solution (Bridge To Life Ltd.) after concentration by low-speed centrifugation (Section 4.3).Two protocols were developed and evaluated using five experimental groups of kidneys.

6.2.I Experimental protocol 1

In experimental group I, one kidney was incubated with cold BELZER UW® solution (206 ml) and no virus was added to the preservation solution; this represented the control group (Figure 6.2 A). The second kidney was transduced *ex vivo* (experimental group II) with BELZER UW® solution (206 ml) supplemented with AcCMV_EGFP BacMam to a final concentration of $3x10^8$ pfu/ml (Figure 6.2 B). Similarly, in experimental group III, one kidney was transduced *ex vivo* by incubation with BELZER UW® solution (206 ml) supplemented with AcCMV_lacZ BacMam to a final concentration of $1x10^9$ pfu/ml (Figure 6.2 C). Control and BacMam transduced kidneys were incubated on a rocking platform (Figure 6.2 D) at 4°C for 24 h. The ability of BacMam to transfer the reporter gene *egfp* into kidney was then evaluated using a fluorescence plate reader (Section 2.2.7.II), whilst *lacZ* expression was detected by X-gal staining (Section 2.2.6). Cytotoxicity was monitored by microscopy using paraffin-embedded sections (Section 2.2.5.IV) after hematoxylin and eosin (H&E) and periodic acid-Schiff (PAS) staining (Sections 2.2.5.V and VI).

6.2.I.I *Egfp* expression

The distribution of e*gfp* fluorescence 24 hpt was initially evaluated using a Bio-Rad ChemiDoc™ MP system and Epi-green illumination (exposure time= 2.7 seconds; emission filter= 605/50) and representative images of fluorescence distribution patterns in control and AcCMV_EGFP kidney sections are shown in Figure 7.3.

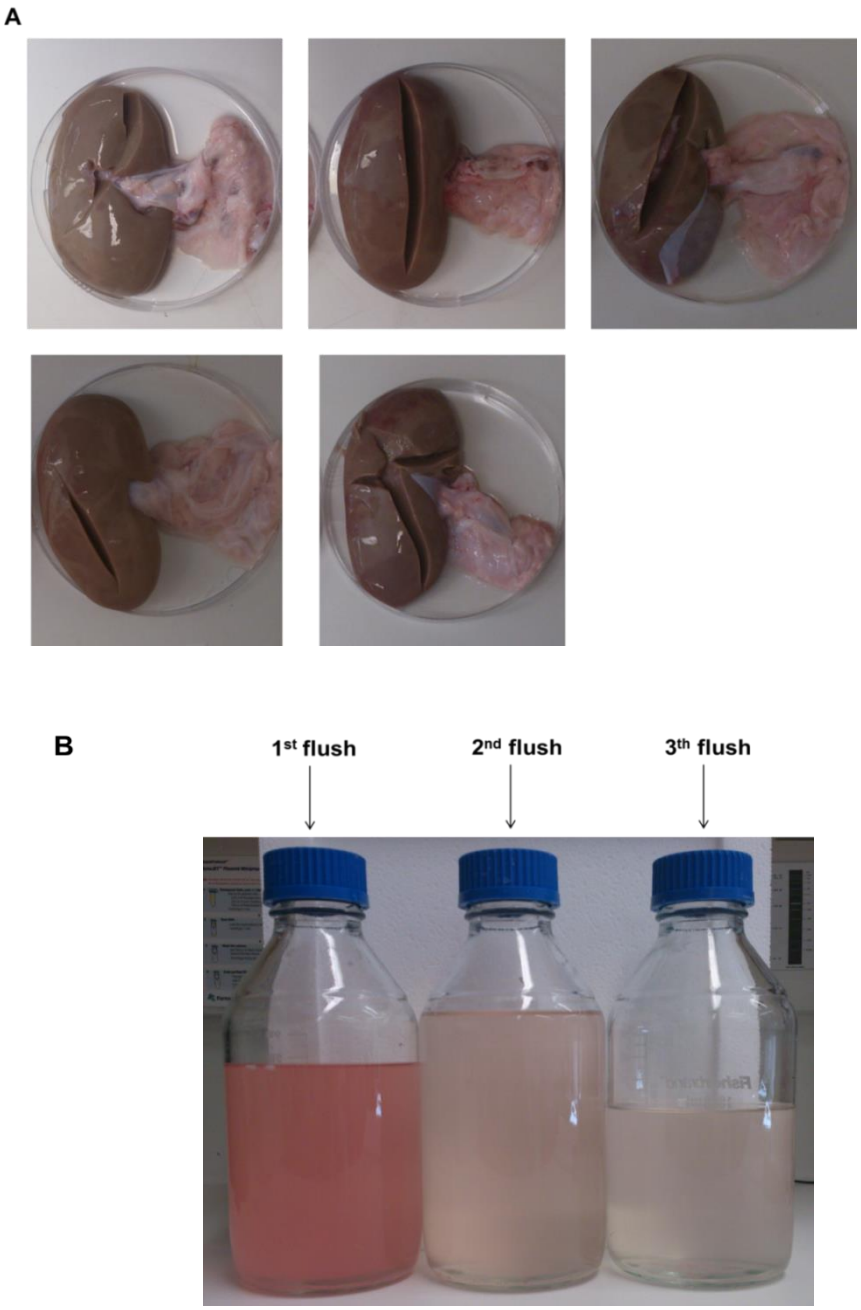

Figure 6.1. Flushing kidneys. (**A**) Representative images of porcine kidneys. Kidneys were incised at the slaughter house as part of the food security act (FSA) inspection process. (**B**) Kidneys were then flushed using soltran solution and three representative bottles rare shown containing three sequential flushes of kidneys.

Table 6.1. Comparison of kidney length, width and weight between control and BacMam transduced groups.

Experimental groups	Length (cm^1)	Width (cm)*	Weight (Kg^2)
Control group (I)	12	7	168
AcCMV_EGFP group (II)	12.5	6.5	166
AcCMV_lacZ group (III)	12	6.5	173
Control group perfused (IV)	13	7	166
AcCMV_lacZ group perfused (V)	11.5	7	182

[1] cm: centimetre.
[2] Kg: kilograms.
* Width was measured from under the ureter.

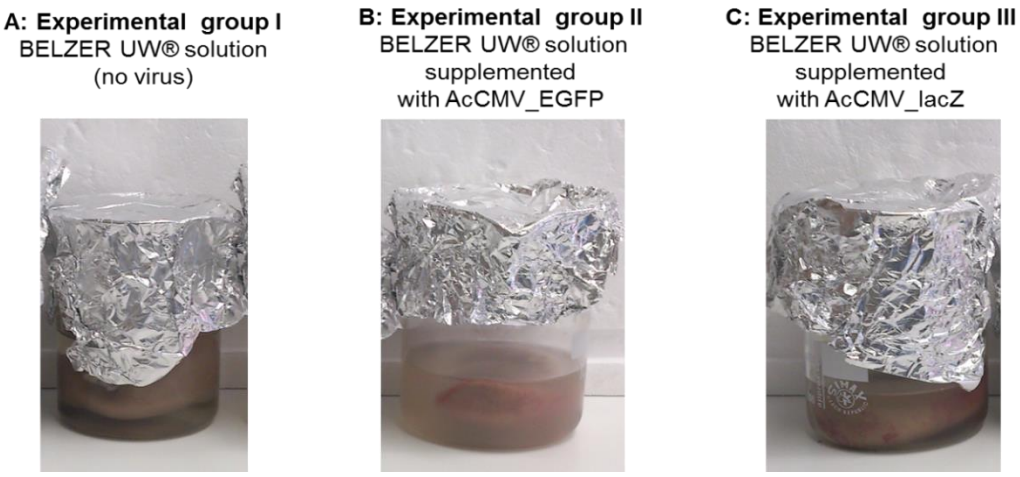

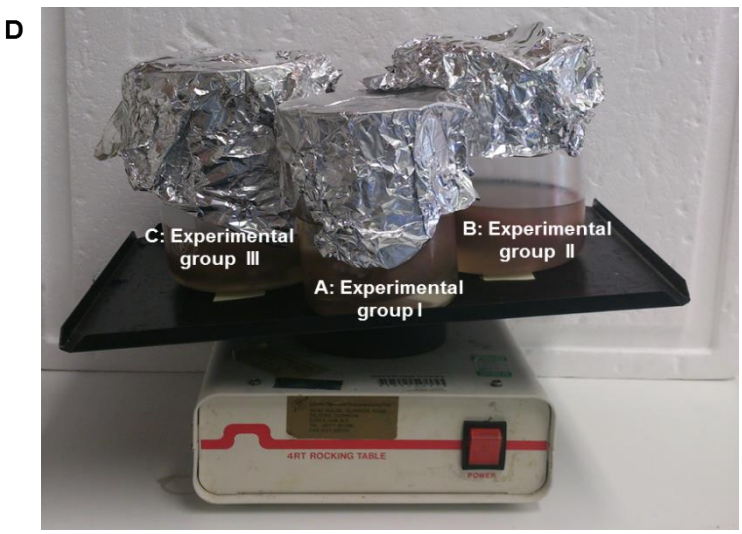

Figure 6.2. Experimental protocol 1. (**A**) Control group (no-virus). In the BacMam *ex vivo* transduced groups, kidneys were incubated in cold BELZER UW® containing either (**B**) AcCMV_EGFP or (**C**) AcCMV_lacZ. (**D**) The experimental groups which were incubated at 4°C for 24 h with gentle rocking.

Kidneys were divided vertically in half and then one half cross sectioned to yield one external and one internal section, for fluorescence analysis. As shown in Figure 6.3 B, dark regions and small black dots (highlighted by white arrows) indicative of EGFP were observed in the AcCMV_EGFP transduced kidney (experimental group II) but were absent in the control group, which was uniformly coloured (Figure 6.3 A). In particular, it appeared that more dark areas with tiny black dots were present in the external section (highlighted by three arrows) of experimental group II, which represented the region of transduced kidneys immediately in contact with the AcCMV_EGFP virus (Figures 6.3 B and 6.3 B1). To confirm these observations, sections were then divided into 6 segments, as illustrated in Figure 6.4, and tissues enzymatically dissociated to single cells by collagenase incubation (Section 2.2.5.IV). These samples were then analysed by fluorescence microscopy (Figure 6.5).

Increased fluorescence intensity, was detected in cells dissociated from AcCMV_EGFP transduced kidney for both external (between two- and six-fold) and internal (between two- and four-fold) segments. As expected, the highest fluorescence intensity of *egfp* expression was obtained in cells dissociated from the external sections (E1 and E2) with an increase of approximately four- and six-fold, respectively, above control group (Figure 6.5). The fluorescence fold changes between AcCMV_EGFP E1 and E2 and control E1 and E2 regions were significantly different from each other (F (11, 48)= 819.1; p<0.001).

Compared to cells obtained from regions E3, E4 and E5 of the control group, a two-fold increase in *egfp* fluorescence intensity was detected in AcCMV_EGFP transduced E3, E4 and E5 regions of the external section (Figure 6.5); these fluorescence intensity differences were statistically significant (F (11, 48)= 819.1; p<0.001). Consistent with previous observations (Figure 6.3, highlighted by the arrow), a significant increase in *egfp* fluorescence (F (11, 48)= 819.1; p<0.001) of approximately four-fold was detected in AcCMV_EGFP E6 compared to control E6 (Figure 6.5).

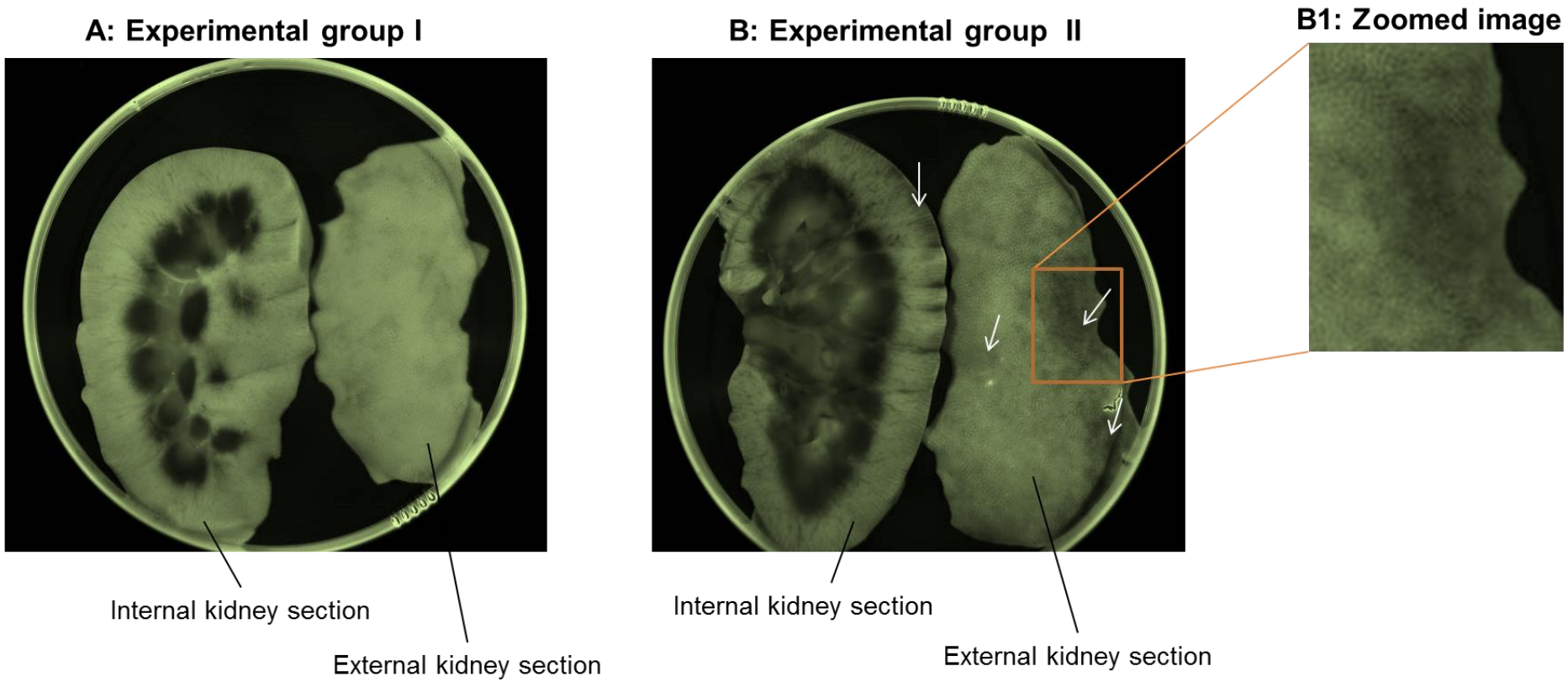

Figure 6.3. Visualization of kidney cross sections in experimental groups I & II. Kidneys, incubated for 24 h at 4°C with BELZER UW® solution supplemented with or without AcCMV_EGFP virus, were cross sectioned and imaged on a Bio-Rad ChemiDoc MP system using Epi-green illumination. False colour images of (**A**) control group (no-virus) and (**B**) AcCMV_EGFP transduced group. (**B1**) Zoom image shows a dark area with tiny black dots in AcCMV_EGFP transduced kidney.

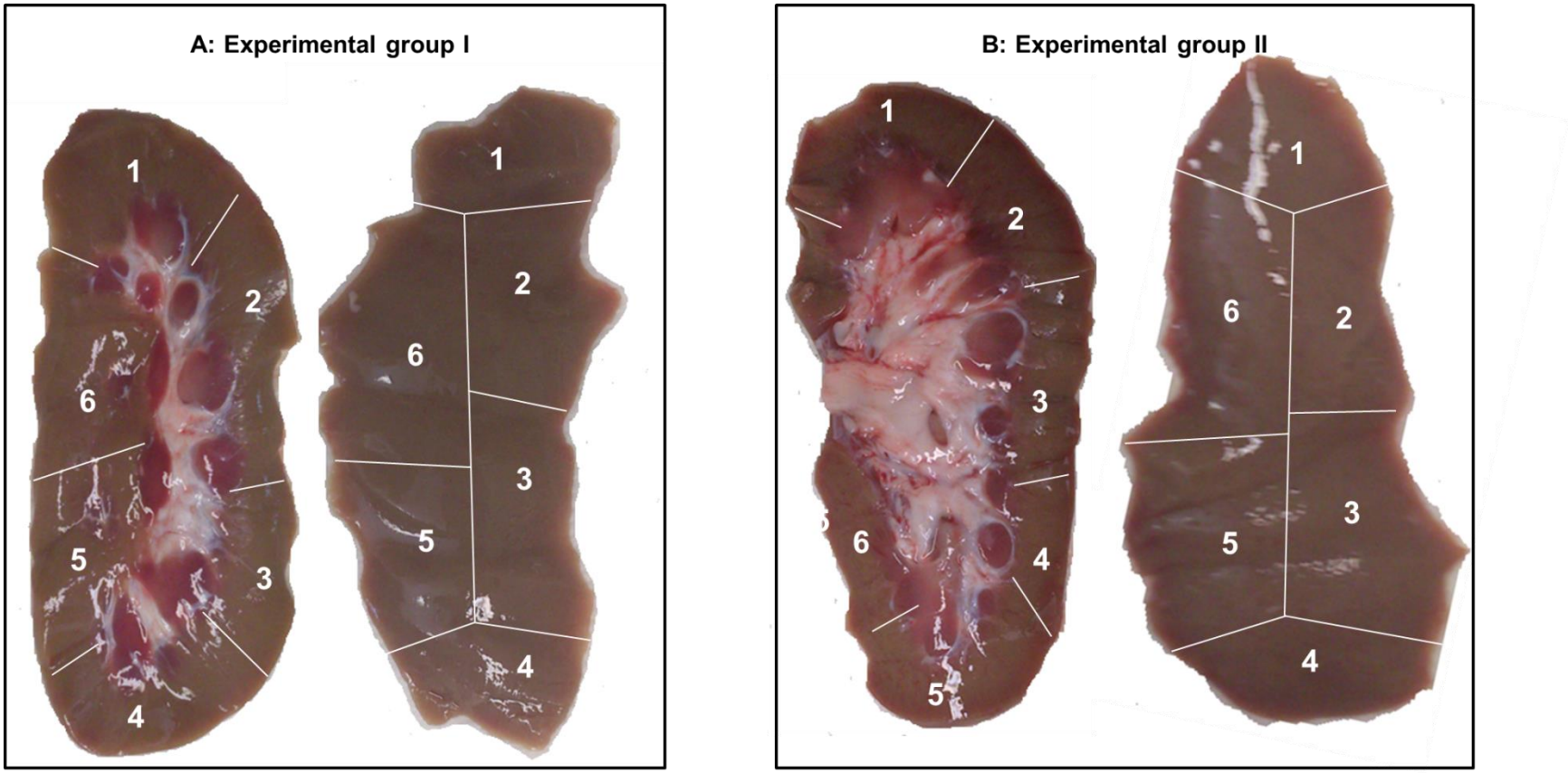

Figure 6.4. Schematic representations of kidney regions dissociated enzymatically to obtain single cells. (**A**) Control group and (**B**) AcCMV_EGFP transduced kidney. These were the same kidneys represented in Figure 6.3.

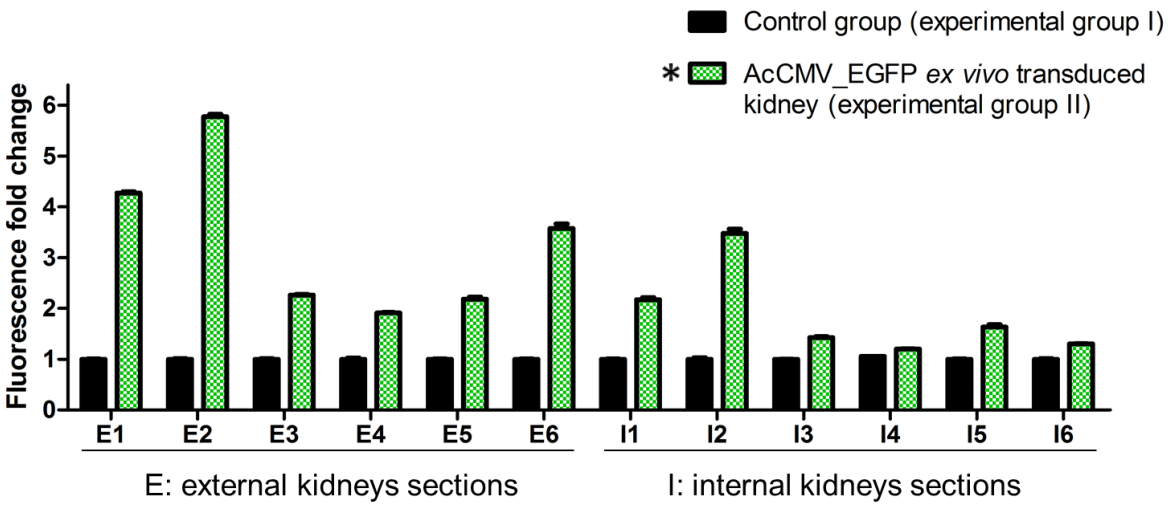

Figure 6.5. EGFP fluorescence in control and BacMam transduced kidneys. Kidneys were incubated in BELZER UW® solution with or without AcCMV_EGFP virus for 24 h at 4°C. Two cross sections for each kidney were prepared and then divided into 6 internal or external regions (Figure 7.4). Tissues were dissociated and fluorescence intensity was quantified using a plate reader. The bar graph represents the fold change in EGFP fluorescence which was calculated by dividing the average fluorescence of AcCMV_EGFP dissociated kidney cells with that of the control group. Bars represent mean ± standard deviations (n=3); *p<0.0001 indicated a significant difference between experimental group I and AcCMV_EGFP transduced kidney (Two-way ANOVA).

As shown in Figure 6.5, a significant increase in fluorescence (F (11, 48)= 819.1; p<0.001) was observed in cells obtained from the internal section of AcCMV_EGFP transduced kidney, I1, I2 and I3 (two-, three and approximately two-fold, respectively) compared to control cells. A significant increase in *egfp* fluorescence approximately two-fold above control group was also detected in AcCMV_EGFP I5 (Figure 6.5). However, the fluorescence intensity in AcCMV_EGFP I4 and I6 was only slightly higher than the control group (Figure 6.5).

6.2.I.II *LacZ* expression

BacMam transduction into whole kidneys was further evaluated using *lac*Z. Kidneys were sectioned and transferred into large Petri dishes containing 30 ml of PBS supplemented with 2% X-gal. PBS with X-gal alone (no-kidney section) was used as a negative control. Transduction was carried out using AcCMV_lacZ by gently rocking the kidney with the virus at 4°C for 24 h. Subsequent X-gal staining resulted in strong β-galactosidase production in both external and internal sections compared to control group (Figure 6.6 A, A3 *vs.* A2). Overall, these findings demonstrated successful *ex vivo* BacMam-mediated gene transfer into kidneys.

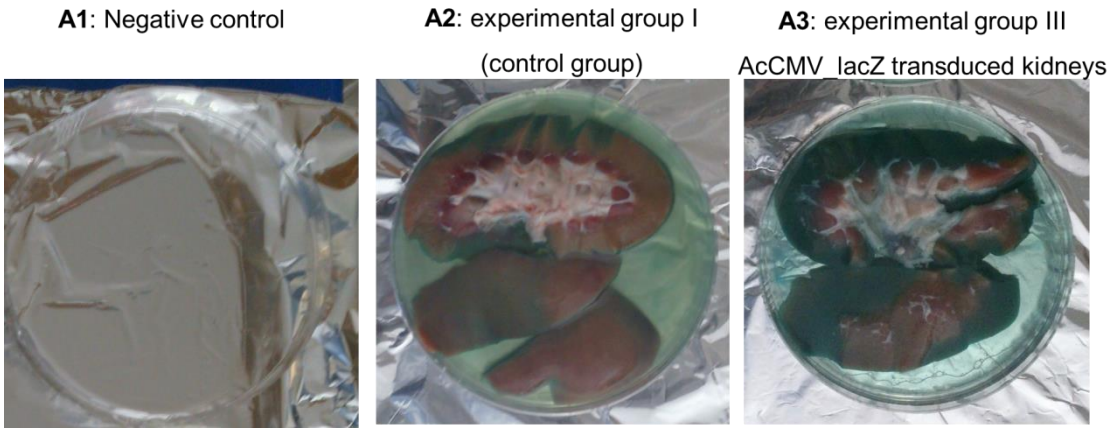

Figure 6.6. Expression of *lacZ* gene in cross sectioned porcine kidney. (**A1**) Experimental group I, non-transduced kidney and (**A2**) AcCMV_lacZ transduced kidney.

6.2.I.III Histological evaluation of kidney tissues

H&E and PAS staining were used to evaluate morphological changes due to BacMam transduction. The remaining half of each of the vertically sectioned kidneys from experimental groups I and II (section 6.2.I.I) were used for this purpose. As illustrated in Figure 6.7, kidneys from experimental group I and II were first divided in two halves vertically; one half was cross sectioned and then sub-divided in two equal parts. The top part of the cross section was further divided into four sections, and each section was then segmented into five smaller pieces (Figure 6.7); these kidney tissue samples were then paraffin embedded (Section 2.2.5.IV) for immunopathologic staining. Representative stained images are shown in Figure 6.8. Evaluation of tissue histology with H&E showed that both control group and AcCMV_EGFP transduced kidney glomerular and tubular structures had similar morphology (Figure 6.8 A). The H&E staining also showed some proximal tubule brush-border damage, interstitial inflammation and tubular dilation in both transduced and non-transduced tissues (Figure 6.8 A, highlighted by the star). These observations were further confirmed in sections of kidney stained with PAS (Figure 6.8 B). In conclusion, AcCMV_EGFP transduced kidney did not differ morphologically from experimental group I (Figure 6.8 B).

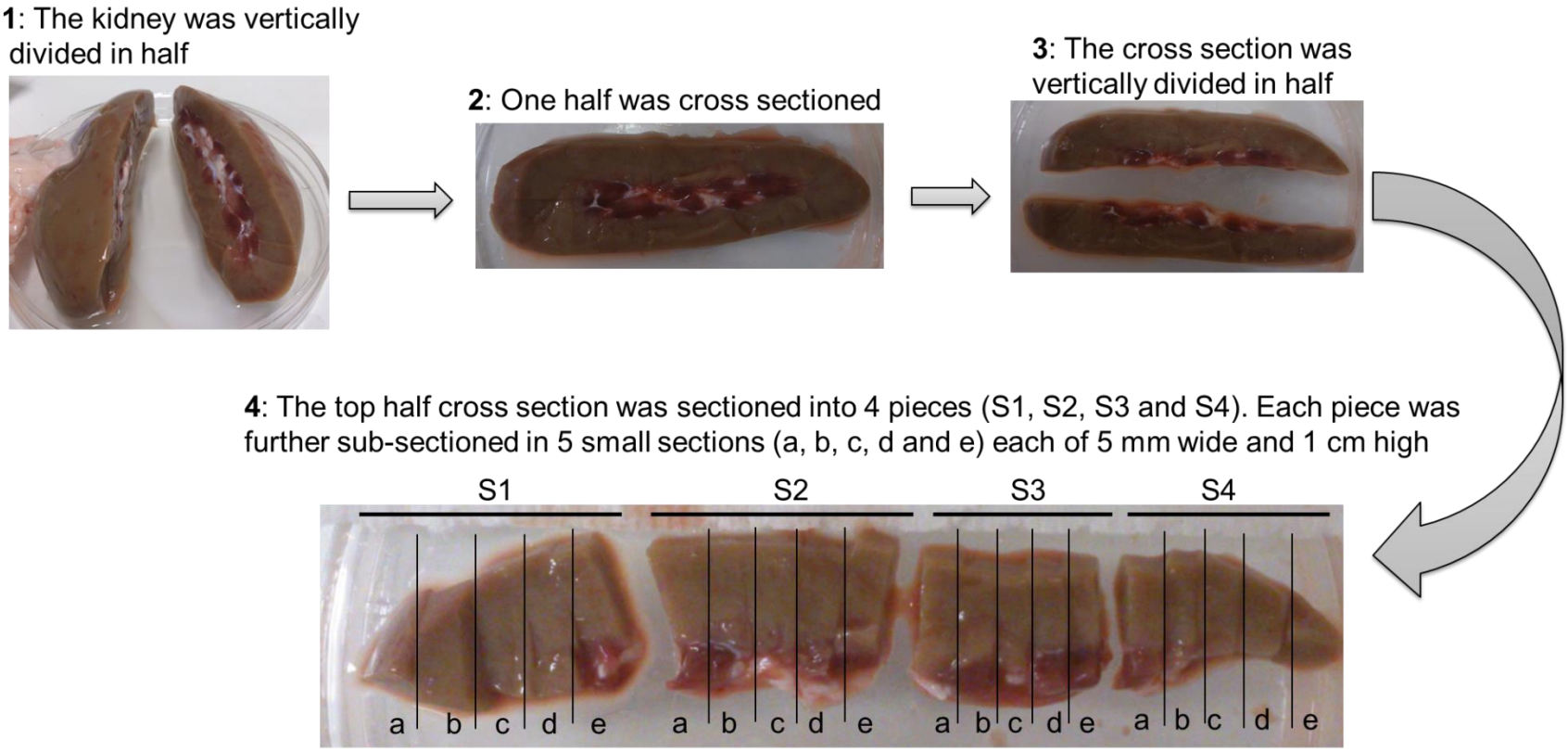

Figure 6.7. Schematic representation of kidneys sampled at 24 hpt. The same procedure was used for experimental group I and II. Small sections were processed and paraffin-embedded for histological analysis.

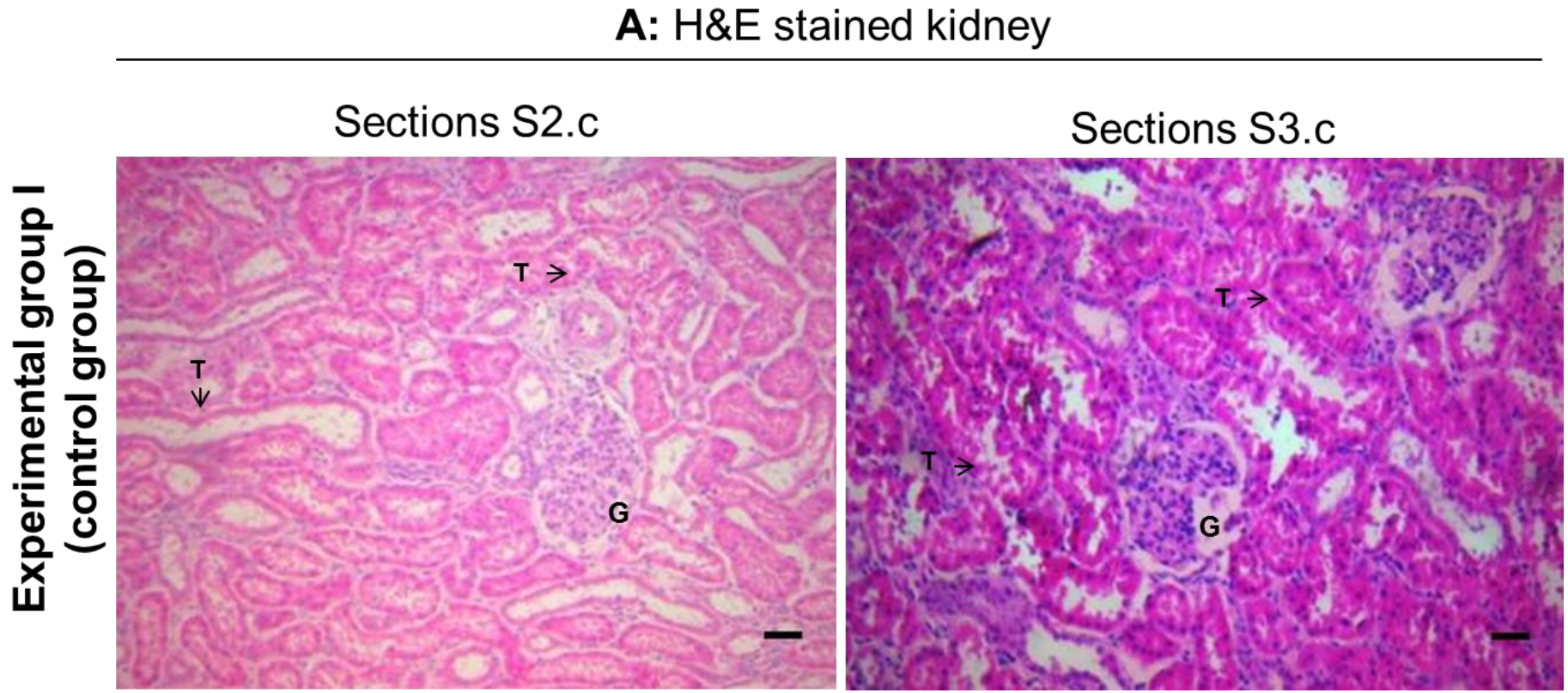
A: H&E stained kidney
Sections S2.c
Sections S3.c
Experimental group I
(control group)
T
T
G
T
T
G

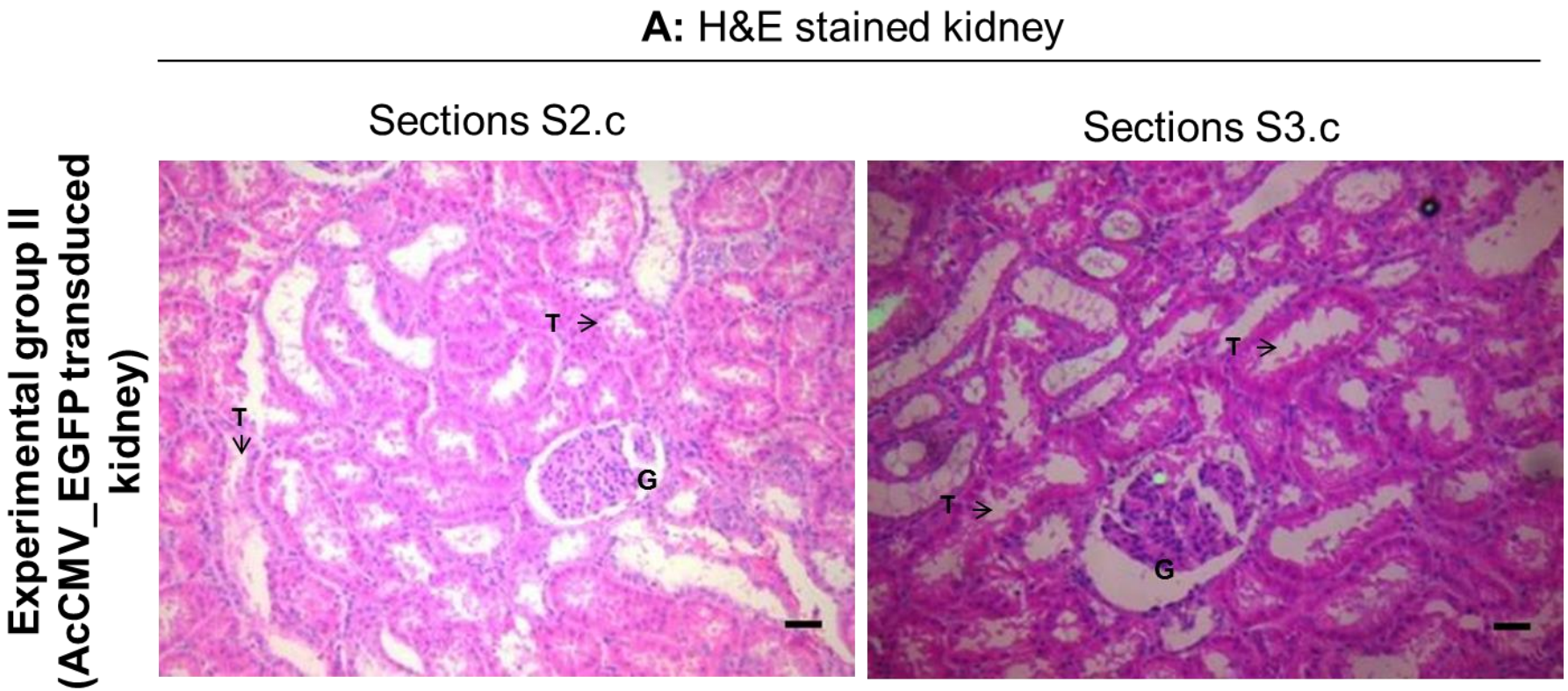
A: H&E stained kidney
Sections S2.c
Sections S3.c
Experimental group II
(AcCMV_EGFP transduced
kidney)
T
T
G
T
T
G

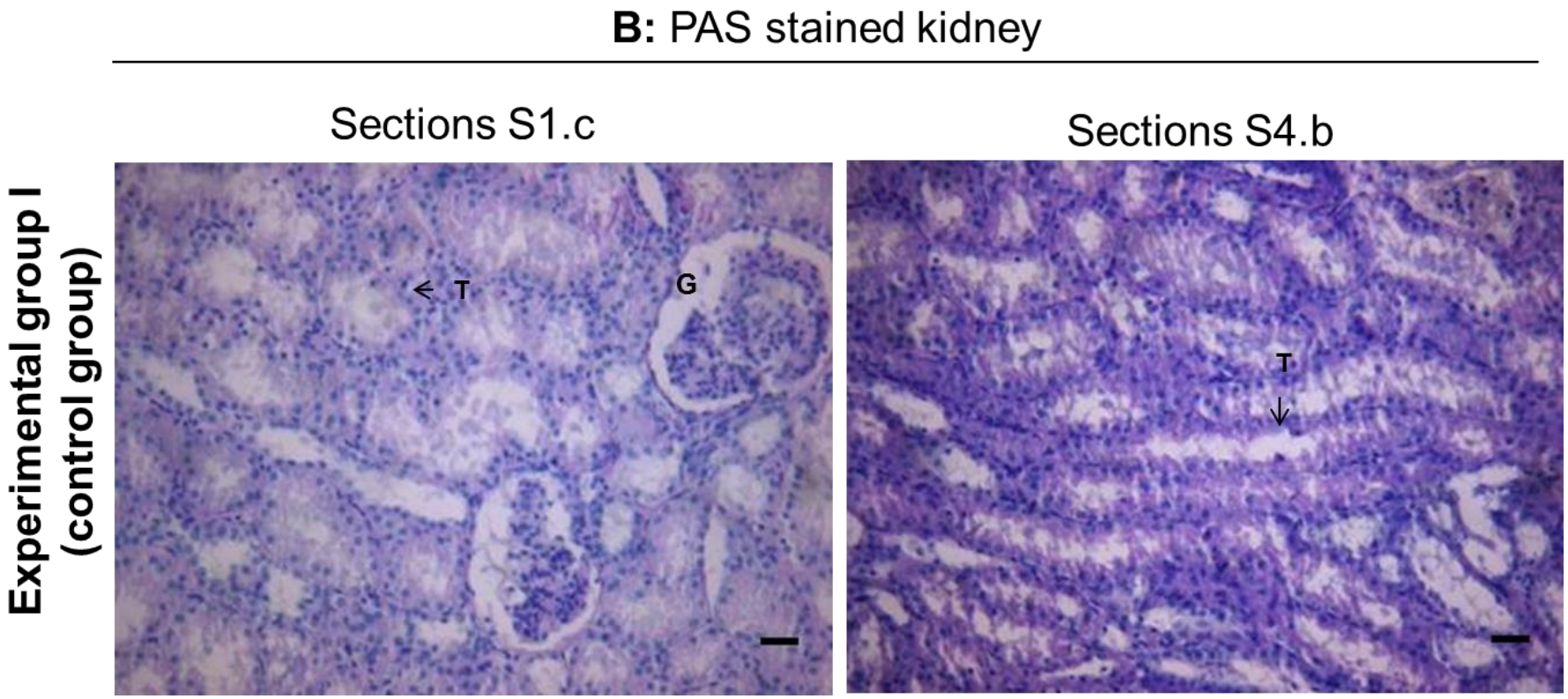
B: PAS stained kidney
Sections S1.c
Sections S4.b
Experimental group I
(control group)
T
G
T

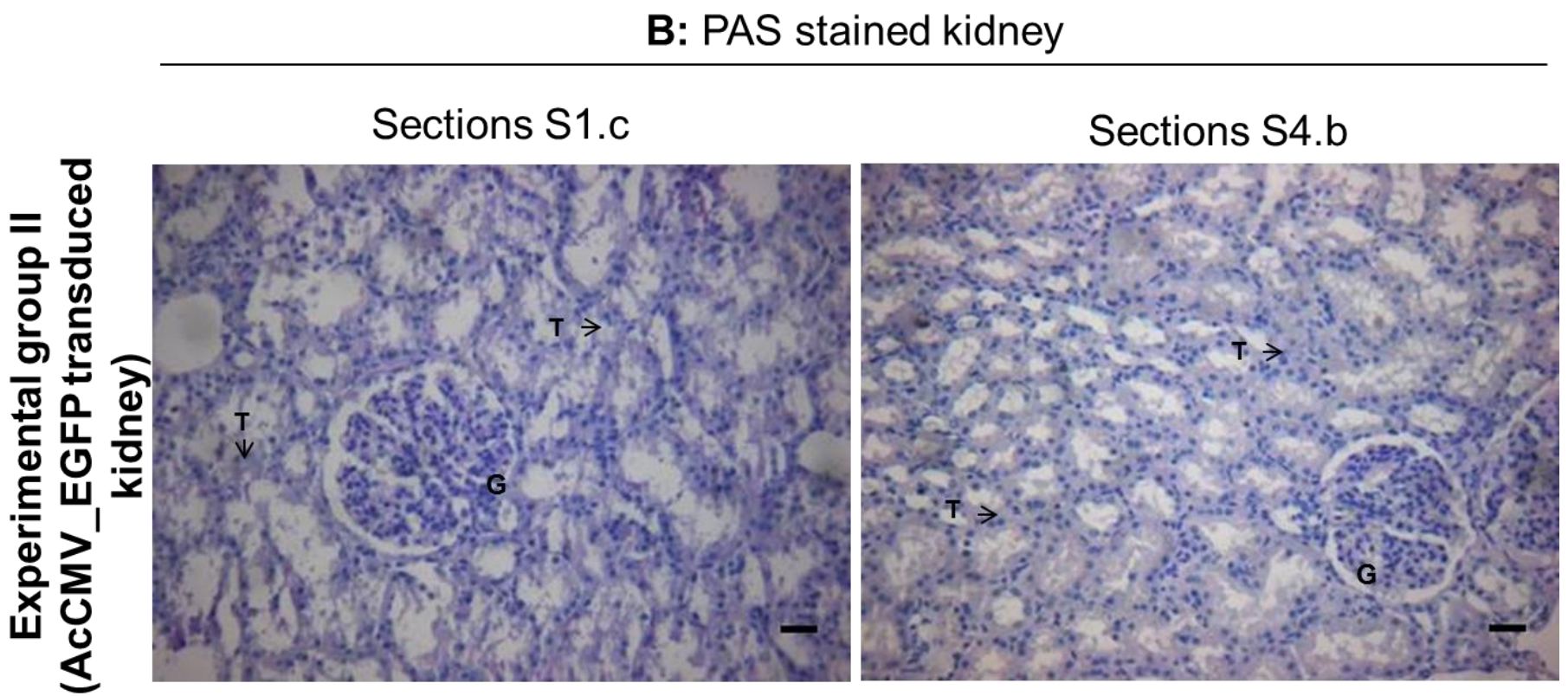
B: PAS stained kidney
Sections S1.c
Sections S4.b
Experimental group II
(AcCMV_EGFP transduced
kidney)
T
T
G
T
T
G

Figure 6.8. Histological examination of control and BacMam transduced porcine kidneys. Representative tissue images obtained using a light microscope (objective 10X) with H&E (**A**) and PAS (**B**) showing glomeruli (G) and tubule (T). Scale bar= 10μm.

Tubular cell dilatation and loss of brush border were observed in tissue from both groups I and II. Therefore, these observations suggested that the observed changes were most likely the result of the procedure and not a consequence of virus administration or an adverse immune response to BacMam. Furthermore, these results also indicated that the viral dose used here did not cause any significant morphological damage.

6.2.I.IV *Egfp* expression in kidney S3.c sections

To further confirm the observations in Section 6.2.I.I, *egfp* expression was monitored by confocal microscopy (Section 2.2.5.II). The paraffin-embedded kidney sections S3.c (Figure 6.7), from both experimental groups I and II, were arbitrary chosen for this experiment. The kidney sections were fixed with paraformaldehyde, immunofluorescently stained for *egfp* and then labelled red with Alexa Fluor®-568 conjugated phalloidin secondary antibody (Section 2.1.6). Panels A1 and B1 in Figure 6.9, shows bright field images of proximal tubular kidney cells of both control and transduced kidneys, respectively. Confocal microscopy observations revealed that *egfp* was highly expressed in the tubular cells of the S3.c section obtained from the AcCMV_EGFP transduced kidney (Figure 6.9 B2) but not in control kidney (Figure 6.9 A2). In Figure 6.9, a representative single kidney tubule is shown in both zoomed A2 and B2 images; *egfp* was highly expressed in the S3.c sections from experimental group II and was undetectable in S3.c from experimental control group I (Figure 6.9 B2 *vs.* A2).

Control included primary antibody only, secondary antibody only and no antibodies. As shown in Figure 6.10 A, background fluorescence was detected as a faint red signal in the control S3.c kidney sections incubated either with primary (1) or secondary antibody (2) alone; this background fluorescence was not observed in S3.c sections of the experimental group II labelled with either primary or secondary antibodies (Figure 6.10 B 1 and 2).

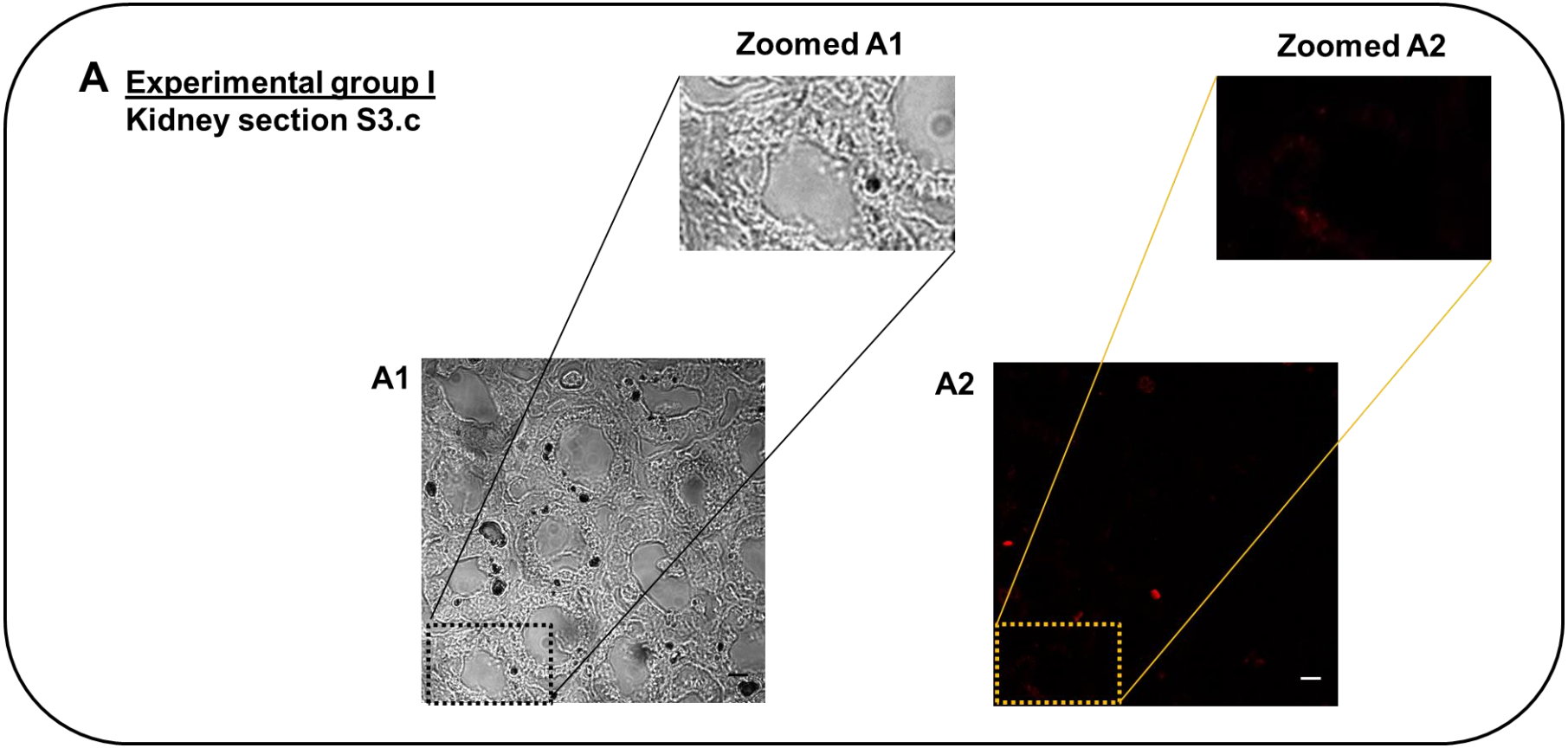
A
Experimental group I
Kidney section S3.c
Zoomed A1
Zoomed A2
A1
A2

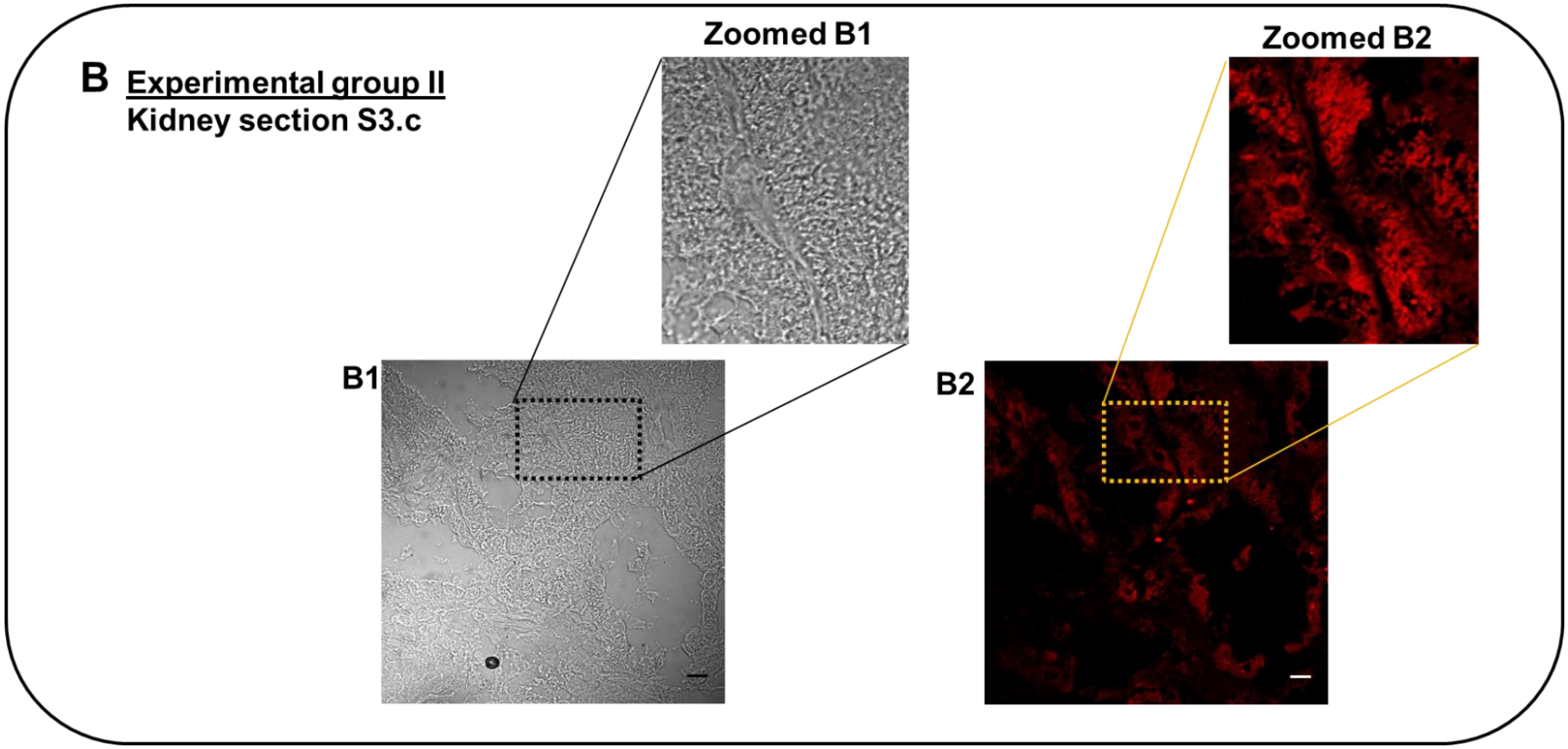

Figure 6.9. *Egfp* expression in S3.c sections of control and BacMam transduced kidneys. Kidneys were incubated in BELZER UW® solution supplemented with or without AcCMV_EGFP virus and incubated at 4°C for 24 h. (**A**) Control and (**B**) BacMam transduced kidneys were cross sectioned, sub-divided into 4 regions and each region sectioned into 5 small pieces. Tissues were paraffin-embedded and *egfp* fluorescence analysed by confocal microscopy. Bright field images are shown in A1 and B1 panels; whilst, fluorescence images are shown in A2 and B2 panels (oil immersion x63 objective). The arrow in panel B1 indicates the presence of air bubbles trapped in the mounting medium. Brightness of the images was modified to enhance definition of the red fluorescence signal. Scale bar=10µm.

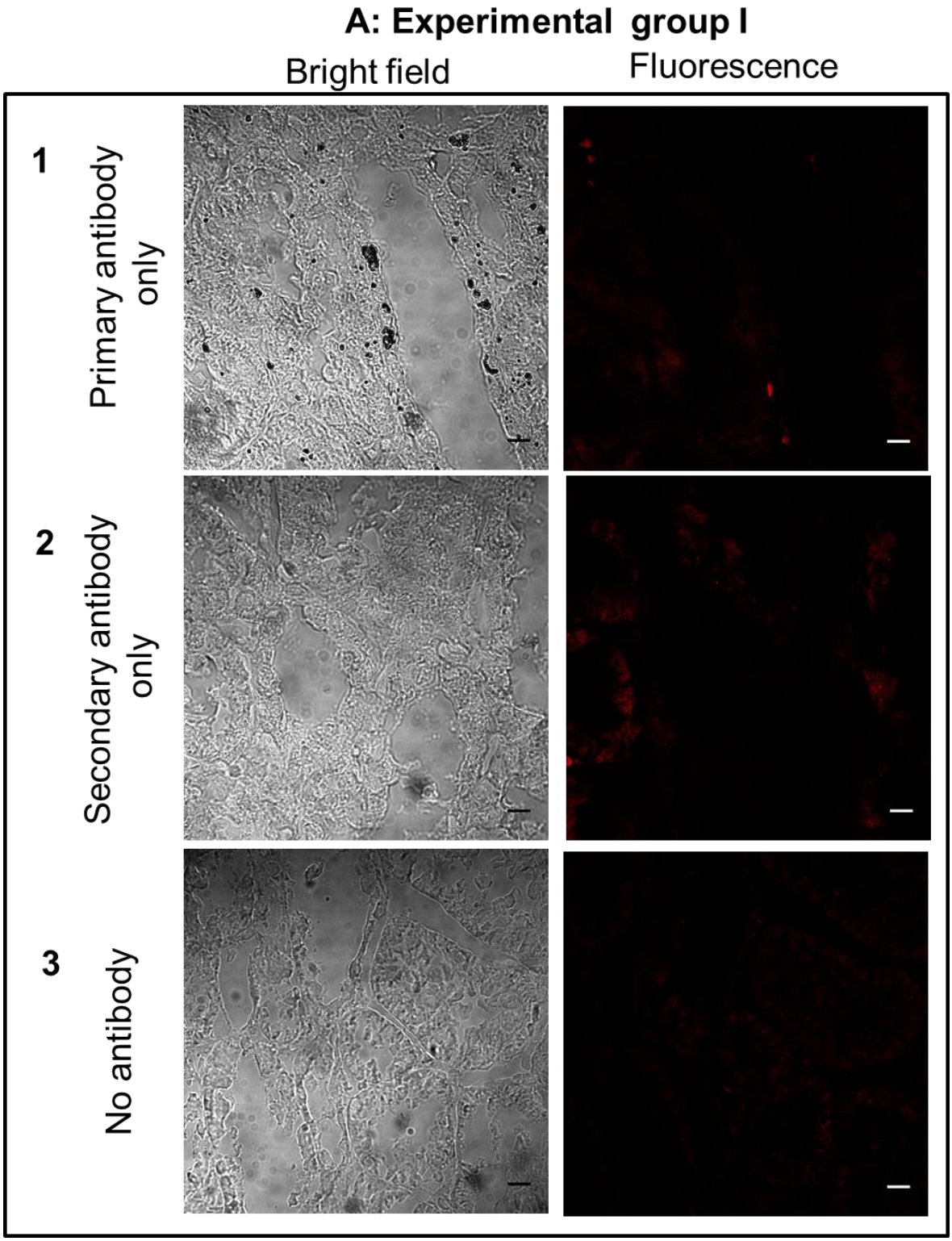
A: Experimental group I
Bright field
Fluorescence
1
Primary antibody only
2
Secondary antibody only
3
No antibody

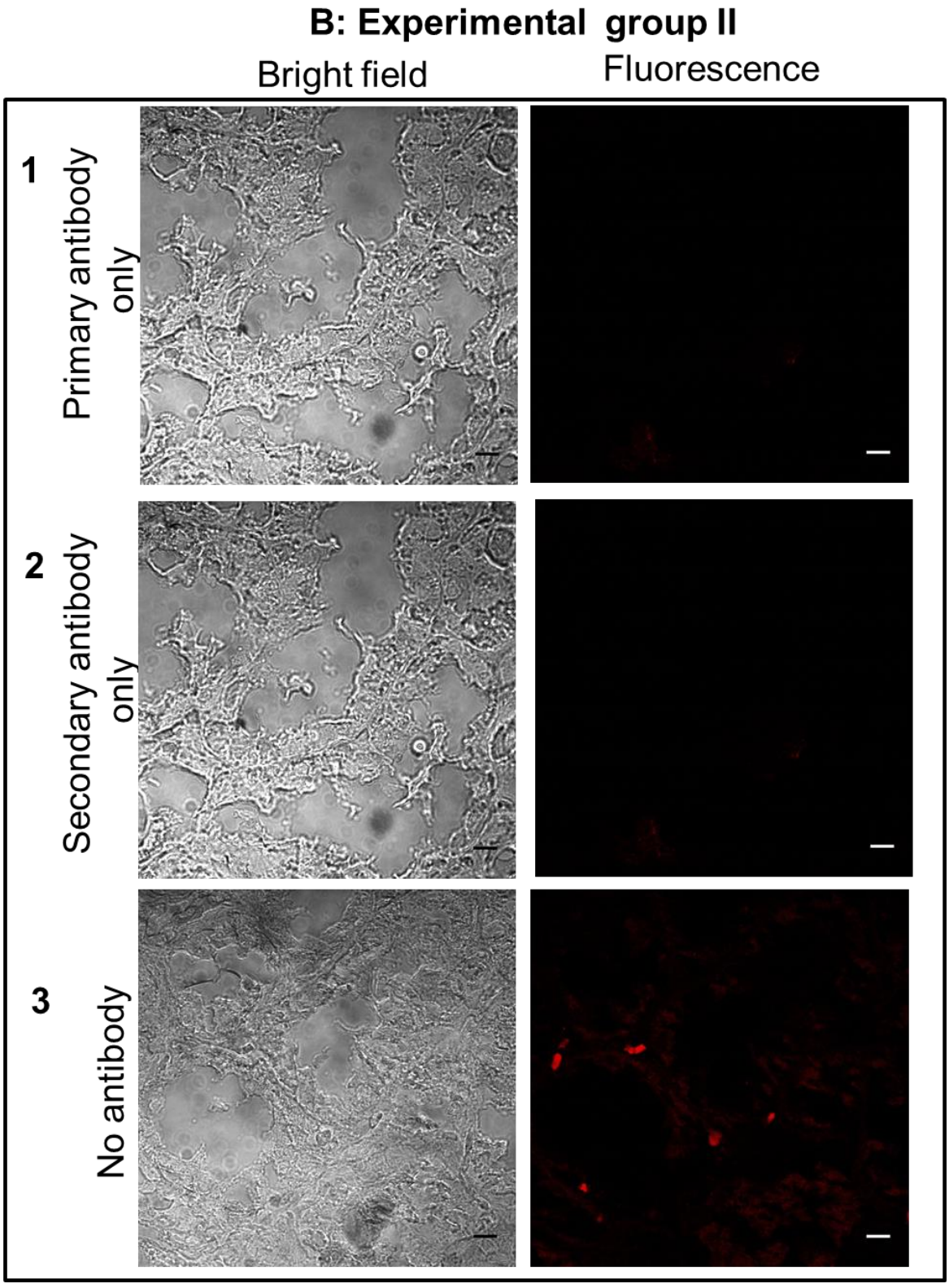

Figure 6.10. Kidney S3.c antibodies control sections. Representative images of s3.c sections from control kidney (**A**) and AcCMV_EGFP transduced kidney (**B**). Kidney sections were either incubated with (1) primary antibody only; (2) secondary antibody alone and (3) no antibody (no-primary and no-secondary). Brightness of the mages was modified to enhance definition of the red fluorescence signal (oil immersion x63 objective). Scale bar= 10µm.

A very faint red signal indicative of auto-fluorescence was observed in S3.c sections from experimental group I (control kidney) with no-antibody staining (Figure 6.10 A 3). In contrast, as shown in Figure 6.10 B 3, a visible red fluorescence signal, which shows the border of the tubules, was detected in S3.c sections from experimental group II incubated with no-antibodies. This staining distribution can be explained as a reflection of the spectral overlap between the emission wavelength of EGFP and the absorbance of the Alexa Fluor®-568 antibody.

6.2.II Experimental protocol 2

A closed-circuit perfusion system for continuous circulation of BacMam in a whole kidney *ex vivo* was developed for this study. This system consisted of a reservoir containing the kidney to be perfused and a peristaltic pump (at a constant speed of 10 rpm) connected to the kidney using silicon tubing of different diameters. The kidney was attached to the perfusion system by cannulating the renal artery with a small silicon tube (Figure 6.11 A). Two experimental groups were used in this protocol; one kidney was perfused with cold Belzer UW® solution (206 ml) containing no virus (Figure 6.11 A 1); this represented experimental group IV (control group). Whereas, the second kidney was perfused and transduced (experimental group V) with Belzer UW® solution (206 ml) containing AcCMV_lacZ as described in protocol 1 (Figure 6.11 A 2). Experimental groups were perfused as shown in Figure 6.11 B, for 24 h at 4°C.

LacZ gene expression

In order to validate this BacMam based perfusion system *lacZ* expression was examined by β-galactosidase staining (Figure 6.12). After 24 h post-perfusion (hpp), over expression of β-galalctosidase was detected in the transduced kidney compared to sections obtained from the control group (Figure 6.12). Furthermore, as shown in Figure 6.12, considerably higher efficiency of BacMam transduction was observed in kidney transduced using the cold closed-circuit perfusion system compared to the results observed for kidneys transduced using the rocking method (Figures 6.12 *vs.* 6.6). Consequently, experimental protocol 2 was chosen for subsequent studies because (1) it more closely mimics *in vivo* conditions, compared to protocol 1 (2) showed the highest BacMam transduction efficiency and (3) highest transgene expression.

6.3 PROTECTIVE ROLE OF BACMAM-MEDIATED SOD-2 GENE TRANSFER ON CELL VIABILITY AND APOPTOSIS DURING *EX VIVO* KIDNEY COLD PERFUSION

Previous studies indicated that virus-mediated *sod-2* transfer conferred anti-oxidant and anti-apoptotic resistance against oxidative stress (Bertera *et al.,* 2003; Duffy *et al.,* 2010; reviewed by Fukai & Ushio-Fukai, 2011; Liu *et al.,* 2012). Therefore, in this study the effect of AcCMV_SOD-2 administration on cell viability and apoptosis were evaluated using a cold closed-circuit perfusion system. Four fresh porcine kidneys (two left and two right) were obtained from the local abattoir, flushed *in situ* and transported to the laboratory for analysis. As shown in Figure 6.13, kidneys were divided into two experimental groups: group I (perfused control kidneys, no-virus) and group II (AcCMV_SOD-2 transduced and perfused kidneys); each group contained a paired kidney (one left and one right) excised from the same pig.

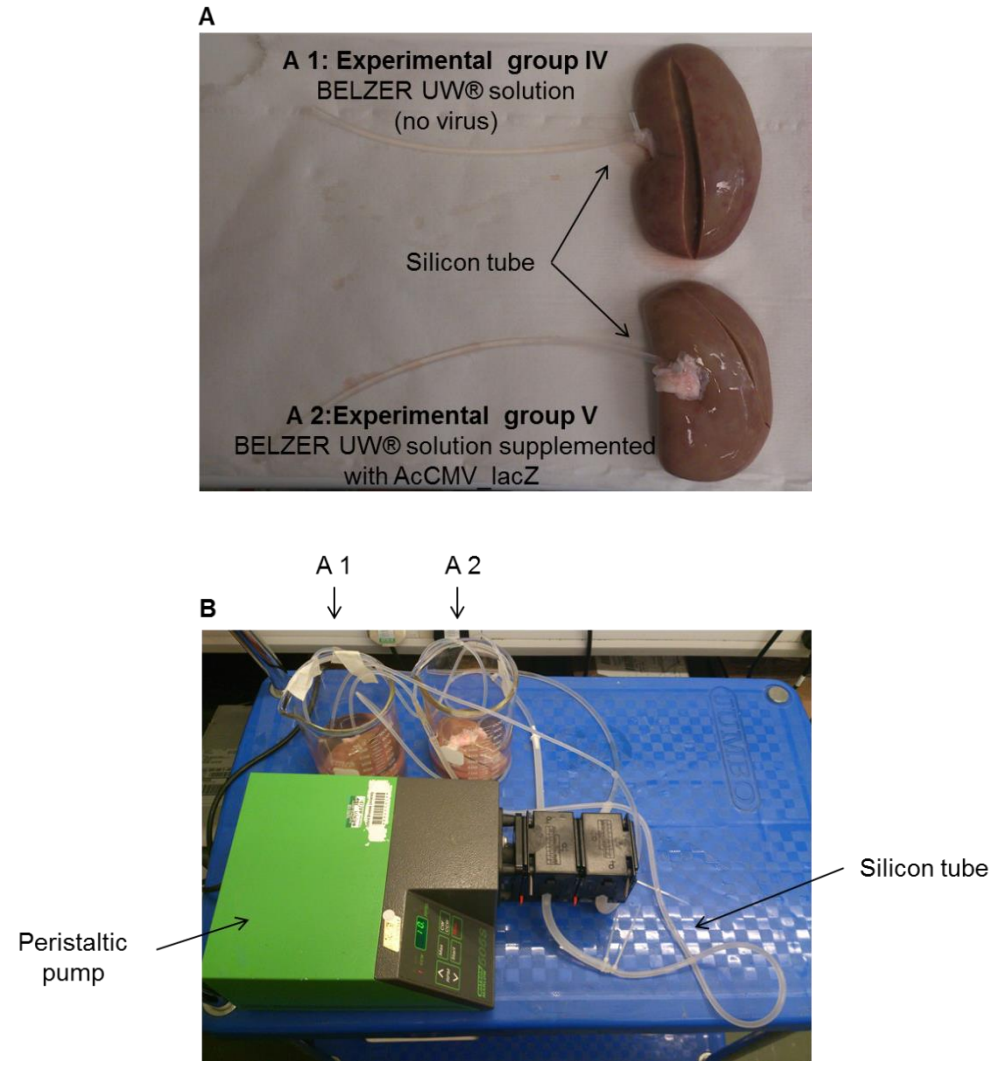

Figure 6.11. Experimental protocol 2. (**A**) Cannulated kidneys with a small silicon tube; A1: Control group (no-virus) and A2: AcCMV_lacZ transduced kidney. (**B**) *Ex vivo* perfusion system maintained at 4°C.

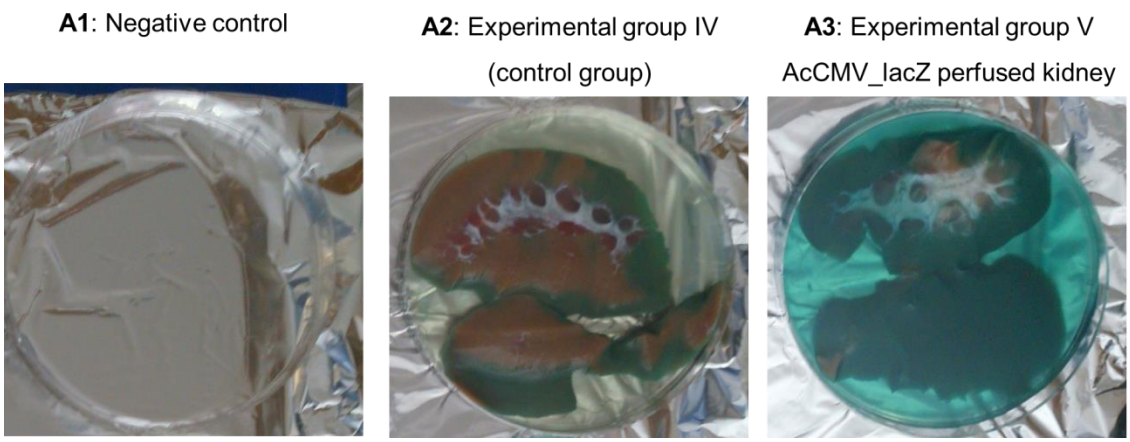

Figure 6.12. Expression of *lacZ* in porcine kidney after 24 h of *ex vivo* closed-circuit perfusion with or without BacMam. (**A1**) Negative control containing PBS (30 ml) with 2% X-gal. (**A2**) Experimental group IV, non-transduced perfused kidney and (**A3**) AcCMV_lacZ transduced kidney.

Kidneys were measured and weighed before perfusion and data are shown in Table 6.2. Left and right kidneys were the same length and width, with slight differences in weight the two experimental group, albeit not significant (F (4, 16)= 0.0; p=1.0000). Subsequently, both groups of kidneys were cannulated and perfused at 4°C for 24 h using the closed-circuit perfusion system (10 rpm) with 200 ml of BELZER UW® cold solution containing either no-virus (experimental group I) or with AcCMV_SOD-2 (virus stock 1.09×10^9 pfu/ml) at a final concentration of 3.3×10^8 pfu/ml.

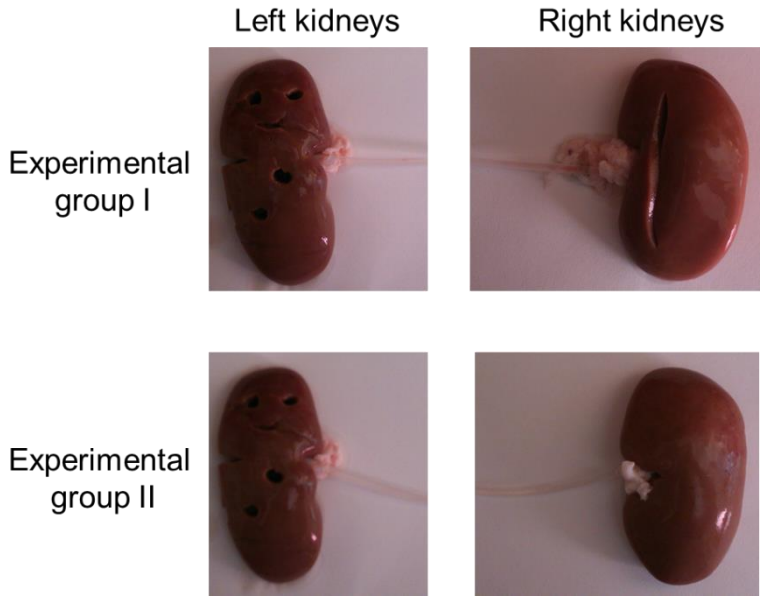

Figure 6.13. Representative images of porcine kidneys. Four kidneys were obtained from the local abattoir and flushed *in situ* with SOLTRAN solution. Holes in both left kidneys are where samples were taken for analysis at 0 h. Kidneys were incised *in situ* as part of the food security act (FSA) inspection process.

Table 6.2. Length, width and weight of control and BacMam transduced kidneys

Experimental groups	Side	Length (cm)	Width (cm)*	Weight (Kg)
Experimental group I (control group)	Left	13	6	199.10
	Right	12	6.8	214
Experimental group II (AcCMV_SOD-2 transduced kidney)	Left	13	6	200
	Right	13	6.3	179

* Width was measured from under the ureter.

During the 24 h period of perfusion/transduction, tissue samples were collected from kidneys of both experimental groups I and II (Figure 6.14 A) using a modified plastic syringe barrel (Figure 6.14 B). As shown in Figure 6.14 B, in order to allow the collection of small kidney samples the syringe barrel head was removed (where the needle hub attaches). Samples from the left kidney of both experimental groups were collected at 0, 2, 4 and 24 hpp, weighed and enzymatically dissociated into single cells, using collagenase, for cell viability analysis. Whereas, tissue samples from the right kidneys were collected at 0, 2, 4, and 24, dissociated and used for (1) the detection of *sod-2* expression, (2) induction of *hsp70* expression and (3) caspase-3 activity (only samples collected at 24 hpp).

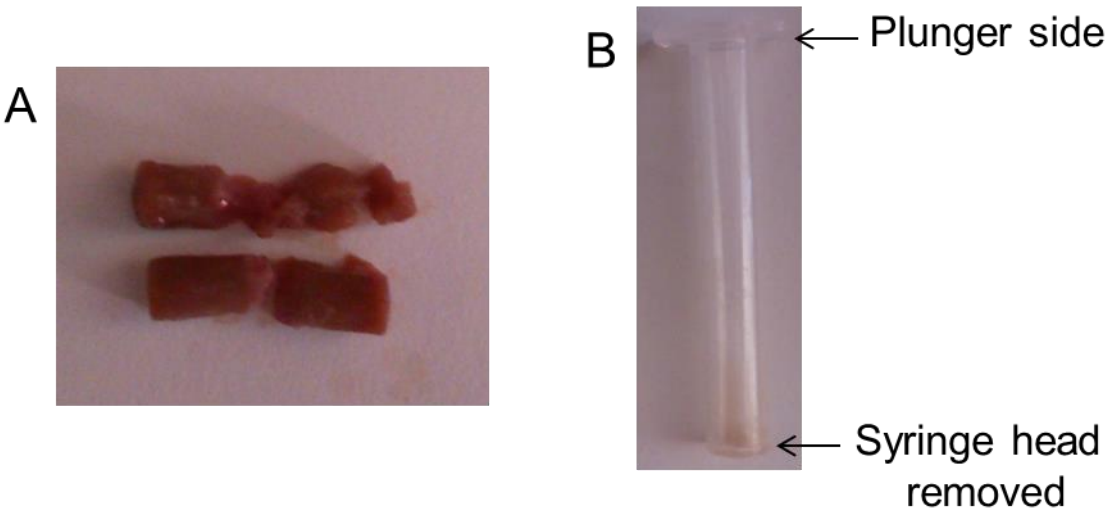

Figure 6.14. Representative kidney tissue samples (A) and modified syringe used to collect them (B).

6.3.I Intracellular ATP levels

Dissociated cells from the left kidneys of group I and II were used to quantify intracellular ATP levels which are a marker of cell viability. The ATP levels were normalized against the average weight of the tissue samples used (668.5 milligrams) and plotted as normalized relative luciferase units (RLU) against time (Figure 6.15). Results showed that at 0 hpp similar ATP levels (F (2, 17)= 3.760; p>0.05) were detected between the control group (no-virus) and the AcCMV_SOD-2 perfused/transduced kidneys (Figure 6.15, solid black bar *vs.* striped red bar). Decreased ATP levels were detected at 2 hpp in both the control perfused kidney and in AcCMV_SOD-2 perfused/transduced kidneys (Figure 6.15). However, increased ATP levels were detected following 4 h of perfusion; slightly higher levels were found in cells dissociated from the AcCMV_SOD-2 perfused/transduced kidney samples (23453 RLU) compared to those detected in control kidney cells (14651 RLU) (Figure 6.15, striped red bar *vs.* solid black bar); although there was no statistical difference (F (2, 17)= 3.760; p>0.05).

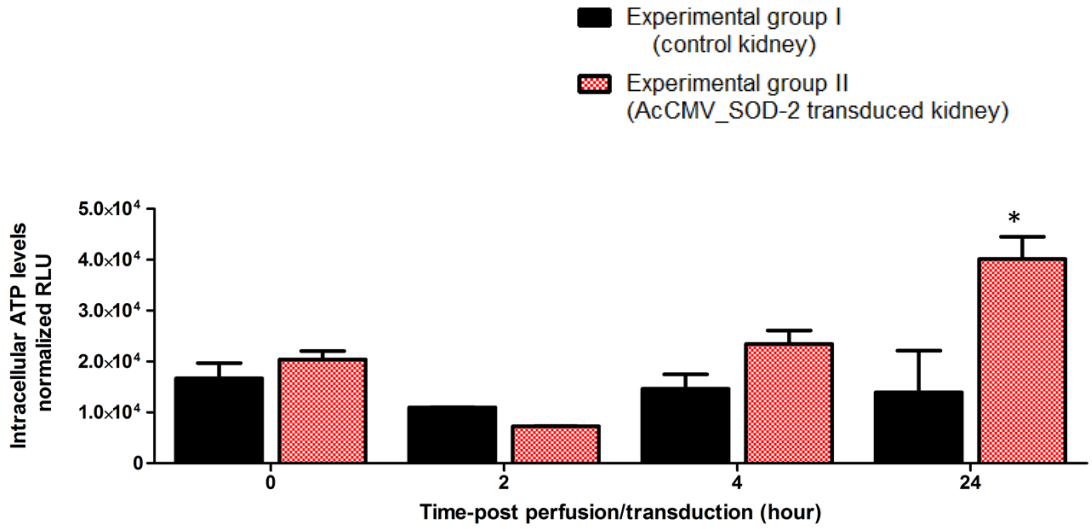

Figure 6.15. Intracellular ATP levels in perfused porcine kidneys. Tissue kidney samples were collected over-time from the left perfused kidney of control group (experimental group I) and AcCMV_SOD-2 transduced group (experimental group II). Kidney samples were enzymatically dissociated into single cells and ATP levels measured over-time. *p<0.01 indicated a significant difference between the ATP levels of AcCMV_SOD-2 transduced kidney and control kidney.

As shown in Figure 6.15, a significant increase (F (2, 17)= 3.760; p<0.01) of approximately three-fold in ATP levels was detected at 24 h of perfusion in cells derived from AcCMV_SOD-2 transduced kidney samples (40166 RLU) compared to cells dissociated from control perfused kidney containing no-BacMam (13945 RLU).

6.3.II Detection of *sod-2* transgene

Western blot analysis (Section 2.2.4.IV) was used to detect the presence of *sod-2* in dissociated control cells and AcCMV_SOD-2 transduced kidney cells. Perfused kidney samples were collected at 0, 2, 4 and 24 h and processed for SDS-PAGE (Sections 2.2.4.I and II). Proteins were transferred and immunoblotted using anti-SOD-2 antibody (Tables 2.7 and 2.8). Whole cell lysate of AcCMV_SOD-2 transduced HEK293 cells was included as a positive control. Results confirmed the presence of *sod-2* with the correct molecular weight ~23 kDa in both perfused/transduced kidney and AcCMV_SOD-2 transduced HEK293 cells (Figure 6.16 B, highlighted by the arrow). Furthermore, due to the high specificity and sensitivity of the antibody towards the endogenous SOD-2 protein, bands were also detected in perfused/non-transduced kidney cells (Figure 6.16 A).

Densitometry analysis of SOD-2 bands indicated that the expression levels at 0 hpp were similar (F (13, 41)= 123.5; p>0.05) between control kidney cells (Figure 6.16 A) and AcCMV_SOD-2 perfused/transduced cells (Figure 6.16 B), 17% and approximately 18%, respectively. Significantly decreased SOD-2 protein levels (F (13, 41)= 123.5; p<0.001) were observed at 2 hpp in cells dissociated from both experimental groups I and II (Figure 6.16); these observations were consisted with low levels of ATP detected in the previous experiment (Figure 6.15).

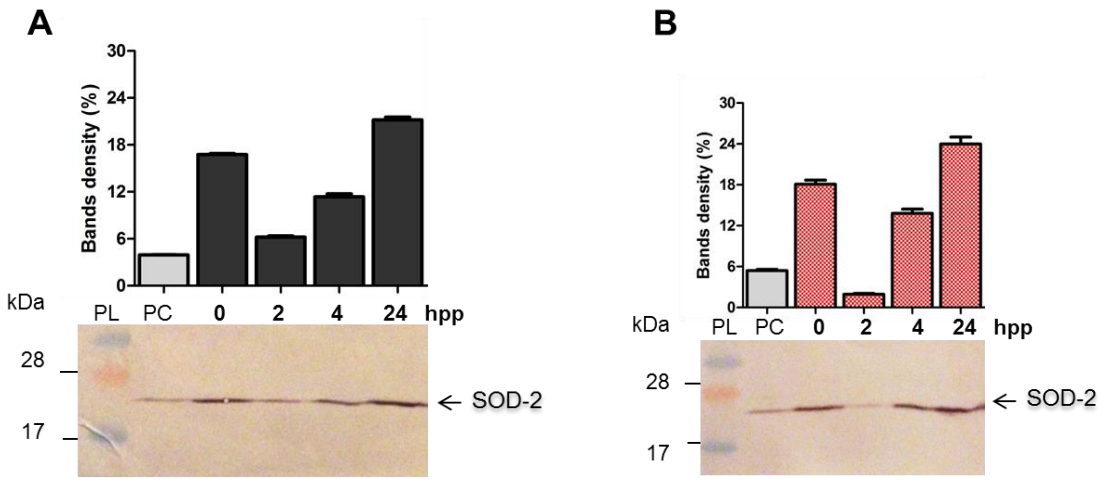

Figure 6.16.Time course of *sod-2* expression in perfused porcine kidneys. Kidney tissue samples were collected and dissociated into single cells. (**A**) Expression levels of SOD-2 in perfused/non-transduced kidney (experimental group I) and (**B**) *sod-2* expression levels in AcCMV_SOD-2 perfused/transduced kidney cells. Lane PL, PageRuler Plus Prestained Protein Ladder and lane PC, positive control (AcCMV_SOD-2 transduced HEK293 cells). Lanes from 0 to 24 represent the time of sample collection (hpp). Densitometry analysis of western blot results (n=3) was performed and data are shown as means ± SE (above western blot).

Compared to cells from perfused/non-transduced kidney (Figure 6.16 A), higher levels of SOD-2 were detected in AcCMV_SOD-2 perfused/transduced kidney cells at 4 hpp (11% and 14%, respectively) and 24 hpp (21% and 24%, respectively) (Figure 6.16 B); however these differences in band intensity were not statistically significant (F (13, 41)= 123.5; p>0.05).

6.3.III Apoptosis

Caspase-3 is known to be the main effector molecule of apoptosis (Kunduzova *et al.,* 2003) and its activity in kidney tissues was evaluated after 24 h of perfusion/transduction. As shown in Figure 6.17, caspase-3 activity increased in non-transduced kidney subjected to cold perfusion (solid black bar) compared to AcCMV_SOD-2 perfused/transduced kidney (striped red bar) which showed slightly decreased, but not significantly different (F (1,21)= 1.254; p=0.2754), caspase-3 levels. These decreased levels of caspase-3 in the transduced kidney were correlated with increased levels of ATP at 24 hpp (Figure 6.15).

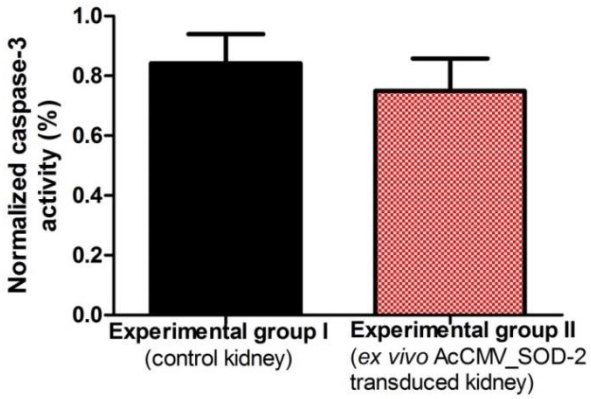

Figure 6.17. Caspase-3 activity in porcine kidney cold perfused. Tissue samples of the right perfused kidney with no-virus or with AcCMV_SOD-2 were collected at 24 hpp. Samples were enzymatically dissociated and caspase-3 assay was performed following the manufacturer guidelines (Chapter 2, Section 2.2.38). Bars represent mean ± SEM (n=4).

6.4 EFFECT OF ADDING HYDROXYUREA + SODIUM BUTYRATE DURING COLD KIDNEY PRESERVATION

A number of published studies have shown the beneficial use of chemical compound such as hydroxyurea and sodium butyrate (Lui *et al,.* 2010; Machado *et al.,* 2012) against oxidative stress injury. Indeed, Lui *et al.* (2010) and de Souza Torres *et al.* (2012) demonstrated that hydroxyurea has an antioxidant activity; hydroxyurea treatment was associated with less oxidative stress damage. Therefore, based on published reports and on the *in vitro* data described in Chapter 4 of this thesis, the chemical combination

hydroxyurea +sodium butyrate was chosen to evaluate their potential protective effect during *ex vivo* cold kidney preservation.

For this study, six kidneys were obtained from a local abattoir (Figure 6.18 A) and flushed three times with cold SOLTRAN solution. Figure 6.18 B, shows the solution obtained after kidney flushes; in the 1st bottle the red colour indicated the presence of blood which gradually decreased showing a light rose colour after flushing three times. Four experimental groups were assigned and dimensions and weights of the kidneys are shown in Table 6.3.

As shown in Table 6.3, the length and width of the six kidneys were similar (12-13 cm, and 6-7.2 cm, respectively). The weight of the kidneys assigned to experimental groups I.a, II.a, II.b and IV was between 213 and 233 Kg; whilst, the weight of the kidneys allocated to experimental groups I.b and III were lower (126-163 kg).

In Chapter 4 hydroxyurea and sodium butyrate were used at concentrations of 40 mM and 10 mM, respectively for HEK293 cell cultures. Therefore, the concentrations used for a whole kidney in this study were obtained by correlating the weight of HEK293 cell pellets (36 mg) with the weight of kidney tissue sample collected at 0 hpp (96 mg). Thus, whole kidneys were first treated with 107 mM of hydroxyurea for 4 h at 4°C and then with 27 mM of sodium butyrate; incubation was continued for an extra 20 h at 4°C. Additionally, kidney cross sections were also incubated for the same time period as the whole kidneys but using the same concentration for cell culture (40 mM of hydroxyurea and 10 mM sodium butyrate).

As shown in Figure 6.19 A, experimental groups I.a and I.b (non-transduced control kidneys) were perfused by gently rocking in 230 ml of BELZER UW® solution (containing no BacMam), at 4°C for 24 h.

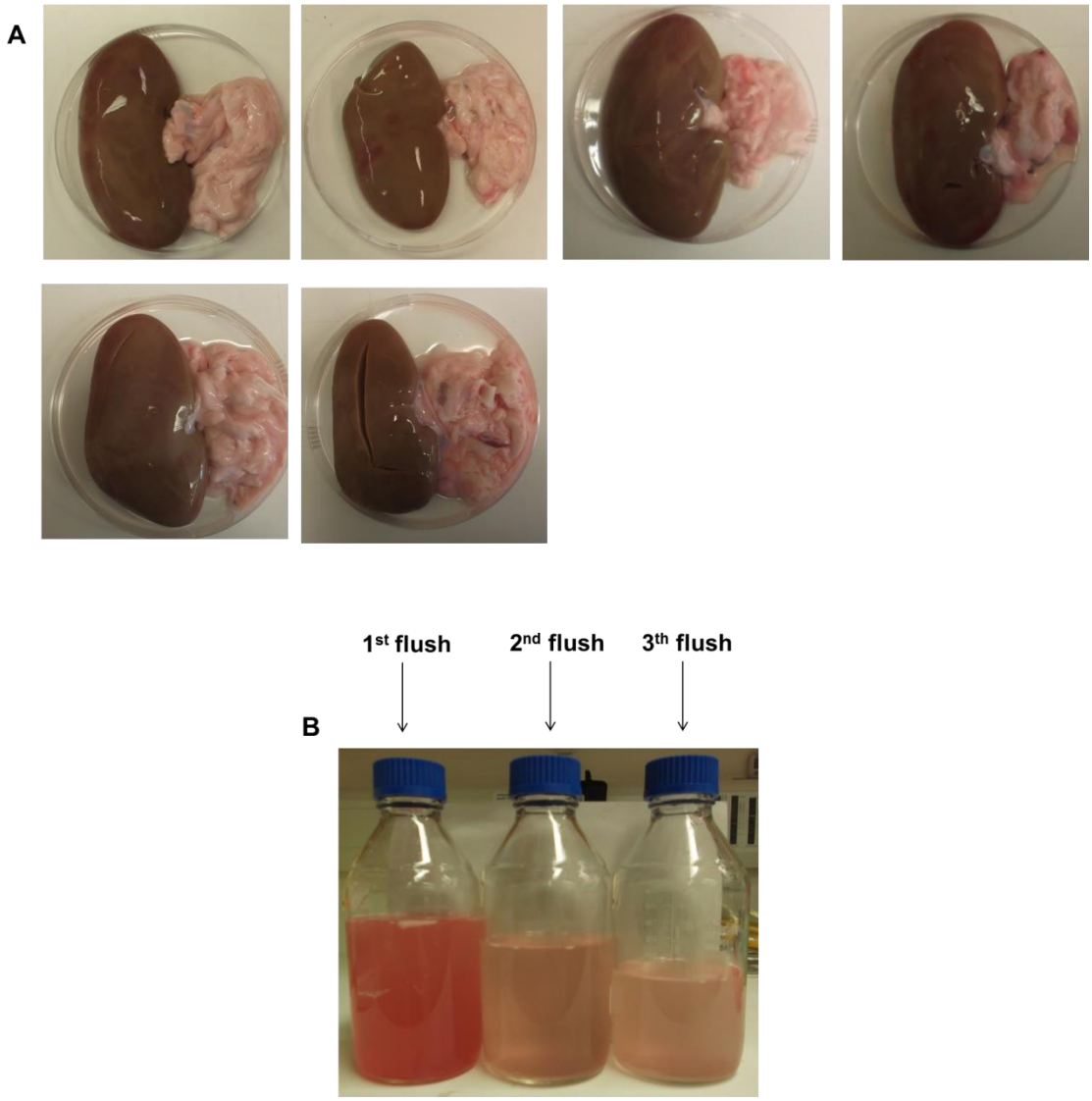

Figure 6.18. Representative images of kidneys and flushing solutions. (**A**) six porcine kidneys obtained from a local abattoir. Kidneys were incised as part of the food security act (FSA) inspection process. (**B**) Three bottles containing SOLTRAN solution after flushing kidneys within10 min of their collection.

Table 7.3. Weight and dimensions of non-transduced controls and BacMam transduced kidneys

Experimental groups	Length (cm)	Width (cm)*	Weight (Kg)
Experimental group I.a (control group)	13	7	233
Experimental group I.b (control group)	12	6	163
Experimental group II.a (AcCMV_EGFP transduced kidney)	13	7	213
Experimental group II.b (AcCMV_EGFP transduced kidney)	13	7.2	214
Experimental group III (AcCMV_lacZ transduced kidney)	12	6.5	126
Experimental group IV (AcCMV_EGFP transduced kidney)	12	7	214

* Width was measured from under the ureter.

The experimental group I.a was incubated with the perfusion solution alone; whilst, the kidney for experimental group I.b was treated with hydroxyurea + sodium butyrate. These perfused kidneys were then used as a control for the experimental groups comprising BacMam transduced kidneys in the presence or absence of chemicals. As illustrated in Figure 6.19 B, only the AcCMV_SOD-2 transduced kidneys were perfused using the closed-circuit system due to the limited number of peristaltic pumps available.

Similarly, one kidney (experimental group II.a) was incubated with 230 ml of perfusion solution supplemented with AcCMV_SOD-2 (virus stock $1.09x10^9$ pfu/ml) at a final concentration of $2.5x10^8$ pfu/ml. Whereas, the second kidney (experimental group II.b) was incubated with the same AcCMV_SOD-2 virus concentration but in the presence of hydroxyurea + sodium butyrate. Kidneys from experimental groups III and IV were cut vertically in half and then four cross sections were obtained (Figure 6.19 C and D). For both groups, two cross sections were also transduced in 60 ml of BELZER UW® solution with either AcCMV_lacZ (final concentration of $6.7x10^8$ pfu/ml) or AcCMV_EGFP (final concentration of $7x10^8$ pfu/ml), with and without hydroxyurea + sodium butyrate.

6.4.I Intracellular ATP levels in perfused/transduced kidneys with AcCMV_lacZ or AcCMV_EGFP in the presence or absence of hydroxyurea + sodium butyrate

Intracellular ATP levels in AcCMV_lacZ and AcCMV_EGFP perfused/transduced kidneys, with or without chemical compounds, were quantified over-time. Kidney tissue samples were collected at 0, 4 and 24 hpp from experimental groups I.a, I.b, III.a and III.b, as described in Section 6.3, and enzymatically dissociated into single cells. Intracellular ATP levels were normalized as described previously and plotted as RLU against time (Figure 6.20). As shown in Figure 6.20 A, ATP levels in AcCMV_lacZ perfused/transduced kidney, not chemically treated (striped blue bar), at 0 hpp were slightly higher and significantly different (F (2, 24)= 154.6; p<0.05) from those of the experimental control group I.a (solid black bar), 8666 and 6644 RLU, respectively. These levels decreased significantly (F (2, 23)= 154.6; p<0.0.01) to 5659 RLU and 2387 RLU at 4 and 24 hpp, respectively, in the experimental group III.a (no-chemicals) compared to 15417 and 9955 RLU, respectively, detected in control group I.a (Figure 6.20 A, striped blue bar *vs.* solid black bar).

Unexpectedly, at 0 hpp the ATP levels in AcCMV_lacZ transduced kidney treated with the chemical combination (experimental group III.b) were significantly higher (F (2, 24)= 154.6; p<0.00.1) than in any of the other 3 experimental groups (Figure 6.21 A, striped purple bar).

However, these ATP levels decreased but not significantly (F (2, 24)= 154.6; p>0.05) when compared to the experimental group I.b after 4 h of perfusion (Figure 7.21 A, striped purple bar *vs.* solid grey bar).

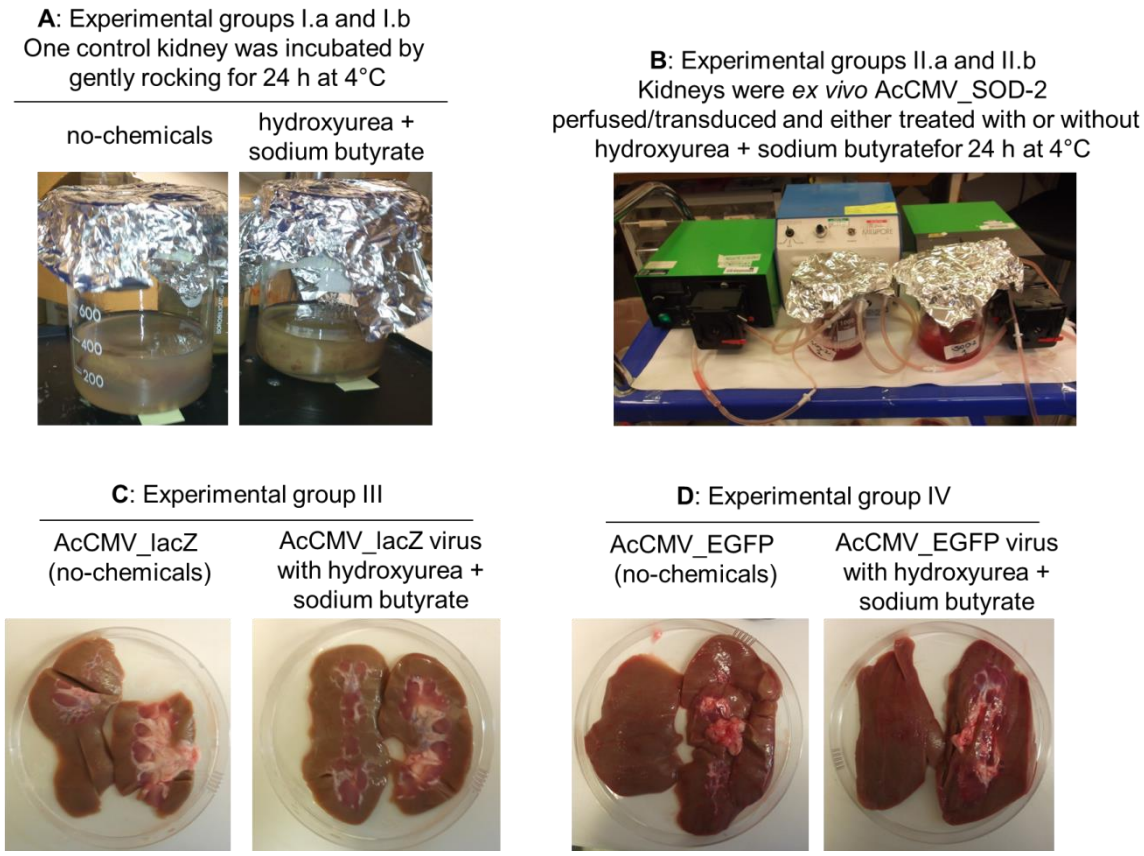

Figure 6.19. Experimental protocols. (**A**) Experimental groups I.a and I.b were rocked gently for 24 h at 4°C. (**B**) Kidneys cannulated with a small silicon tube for AcCMV_SOD-2 perfusion/transduction. (**C**) Kidney cross sections transduced with AcCMV_lacZ and (**D**) with AcCMV_EGFP. Controls and transduced kidneys were treated with or without hydroxyurea + sodium butyrate.

As shown in Figure 6.20 A, by 24 h of perfusion, ATP levels were considerable decreased in both AcCMV_lacZ perfused/transduced kidney chemically treated with hydroxyurea + sodium butyrate (striped purple bar) and control treated kidney sections (solid grey bar) compared to control untreated kidneys (Figure 6.20 A, solid black bar). As shown in Figure 6.20 B, ATP levels were modestly but significantly increased (F (2, 24)= 50.66; p<0.05) at 0 and 24 hpp in AcCMV_EGFP perfused/transduced and untreated kidney, 9062 RLU (Figure 6.20 B, striped green bar) compared to those of control kidney group I.a, 6643 RLU (solid black bar).

However, as expected, the intracellular ATP levels did not recover significantly (F (2, 24)= 50.66; p<0.001) at 24 hpp between the experimental control groups (I.a and I.b) and the BacMam transduced groups (II.a and II.b).

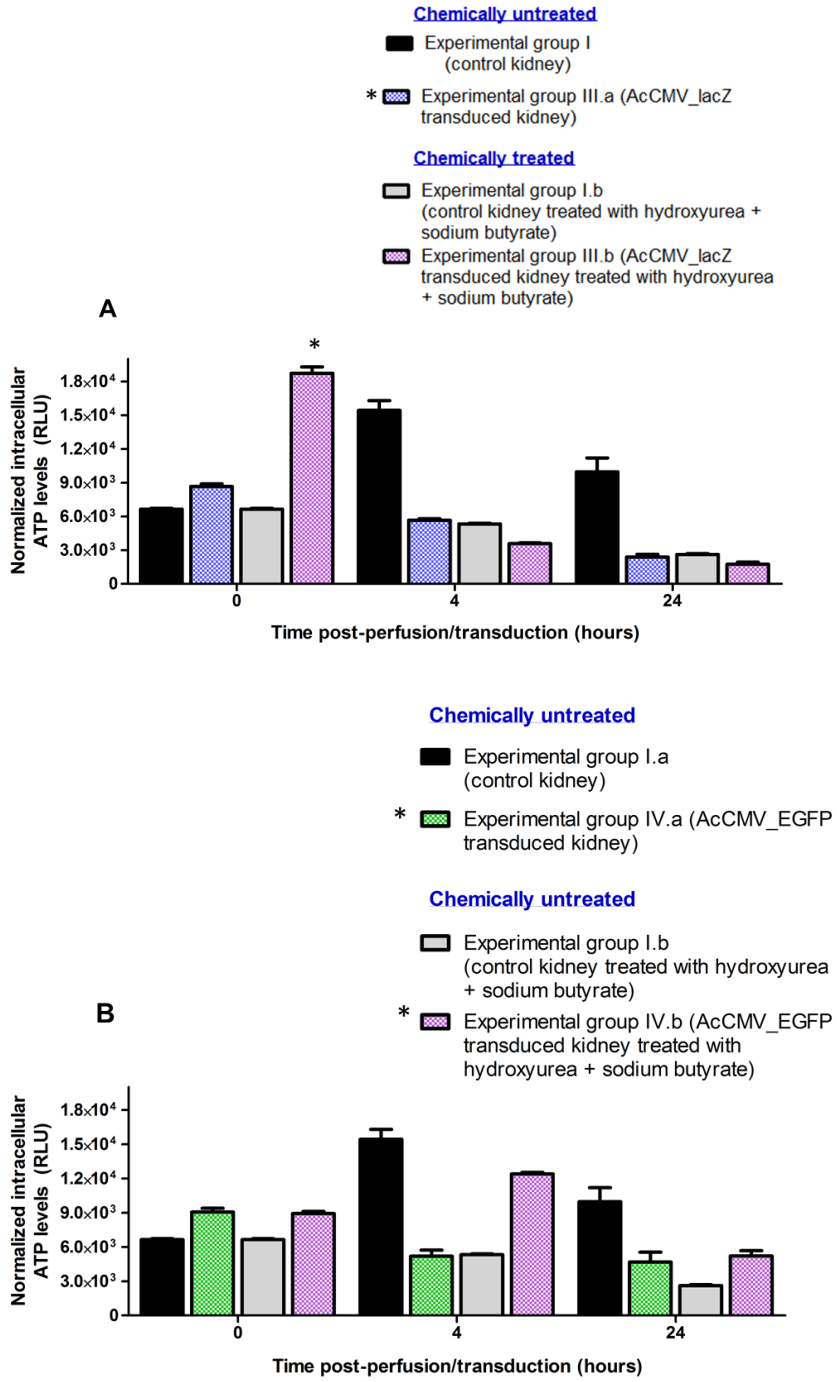

Figure 6.20. Intracellular ATP levels in non-transduced and BacMam perfused/transduced porcine kidneys, with or without chemicals. Tissue kidney samples were collected over-time from control groups (experimental group I.a and I.b) and AcCMV_lacZ (experimental groups III.a and III.b) or AcCMV_EGFP (experimental group IV.a and IV.b) transduced groups. Experimental groups I.b, III.b and IV.b were treated with hydroxyurea + sodium butyrate. Kidney samples were enzymatically dissociated in single cells and ATP level measured over-time. *p<0.05 and **p<0.001 indicated a significant difference between the ATP levels of perfused/non-transduced and BacMam perfused/transduced kidneys.

6.4.II Intracellular ATP levels in AcCMV_SOD-2 perfused/transduced kidneys in the presence or absence of hydroxyurea + sodium butyrate

Kidney tissue samples were collected and processed as described in Section 6.3. ATP levels detected at 0 hpp in AcCMV_SOD-2 transduced kidneys (6320 RLU), were not significant different (F (2, 22)= 85.71; p>0.05) compared to the ATP levels of the experimental group I.a, 6641 RLU (Figure 6.21, striped red bar *vs.* solid black bar). While, increased ATP levels were found at 0 hpp in experimental group II.b, treated with hydroxyurea + sodium butyrate (10131 RLU); these levels were significantly different (F (2, 22)= 85.71; p<0.05) from those of control group I.b, 6641 RLU (Figure 6.21, striped orange bar *vs.* solid grey bar).

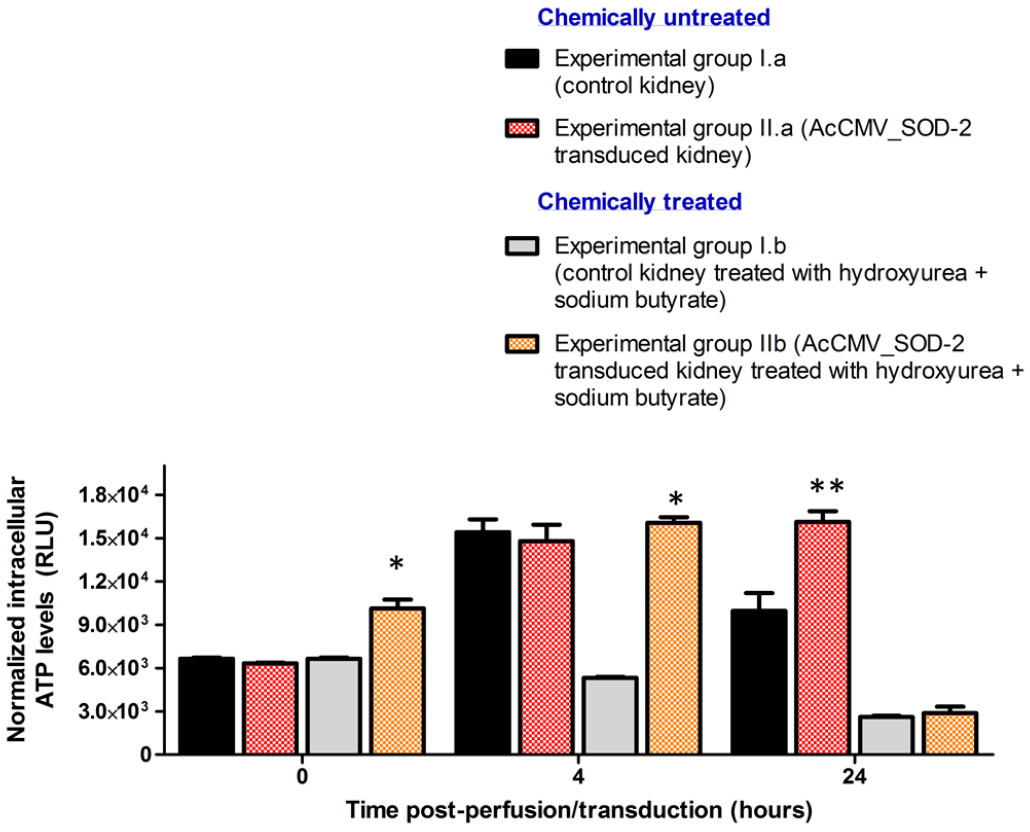

Figure 6.21. Intracellular ATP levels in non-transduced and AcCMV_SOD-2 perfused/transduced porcine kidneys, with or without chemicals. Tissue kidney samples were collected over-time from control groups (experimental group I.a and I.b) and AcCMV_SOD-2 transduced groups (experimental groups II.a and II.b). Experimental groups I.b and II.b were treated with hydroxyurea + sodium butyrate. Kidney samples were enzymatically dissociated in single cells and ATP level measured over-time. *p<0.001 indicated a significant difference between the ATP levels of perfused/non-transduced kidney and AcCMV_SOD-2 perfused/transduced kidney.

Increased ATP levels were detected at 4 hpp in both AcCMV_SOD-2 perfused/transduced kidney with (16052 RLU) and without (14795 RLU) chemical compounds compared to those detected at 0 hpp (Figure 6.21, striped red and orange bars). However, ATP levels in non-treated transduced cells were similar and not significantly different (F (2, 22)= 85.71; p>0.05) to those of the experimental control group I.a (15415 RLU), while levels in treated transduced cells were significantly higher (F (2, 22)= 85.71; p<0.001) than control group I.b (5318 RLU). As shown in Figure 6.21, a marked and significant increase (F (2, 22)= 85.71; p<0.001) in ATP levels was detected at 24 hpp in cells derived from AcCMV_SOD-2 transduced but chemically untreated kidney samples (16127 RLU) compared to the ATP levels observed in the experimental control group I.a (striped red bar *vs.* solid black bar). This approximately two-fold increase in ATP levels was consistent with the previous experiment (Figure 6.15). In contrast, intracellular ATP levels significantly decreased (F (2, 22)= 85.71; p<0.001) in both control group I.b and transduced kidney treated with hydroxyurea + sodium butyrate (experimental group II.b) compared to the untreated transduced kidneys (Figure 6.21, striped orange bar *vs.* striped red bar).

Overall, these preliminary observations suggested that BacMam-mediated *sod-2* overexpression during cold perfusion, might protect against cold preservation damage by enhancing the recovery of ATP levels at 24 hpp.

6.5 Discussion

The primary cause of ischemia in the kidneys is reduced blood flow due to the clamping of the renal arteries which may occur during the surgical procedure of renal transplantation (reviewed by Watson & Dark, 2012). Accumulation of toxic metabolites, cell membrane depolarization and loss of cellular integrity are all events caused by a lack of ATP (reviewed by Watson & Dark, 2012). Therefore, strategies for organ preservation are fundamentally based on the prevention or suppression of these changes as quickly as possible; this is usually achieved by hypothermia, between 0−5˚C, which reduces the cells metabolic rate (reviewed by Watson & Dark, 2012). Two main methods have been used for renal preservation during kidney transplantation; (1) hypothermic static storage and (2) continuous hypothermic perfusion (reviewed by Toledo‑Pereyra *et al.,* 2010). Although a large number of perfusion solutions have been developed to use in these two perfusion systems, they are not sufficiently effective to prevent preservation-induced injury of the tissues (Mangino *et al.,* 2004; Lee *et al.,* 2009).

The application of *ex vivo* gene transfer technology to the field of transplantation offers the unique opportunity to modify the donor kidney before implantation by specifically targeting I/R cold-preservation induced injury (reviewed by Kelley & Sukhatme, 1999). Numerous studies have demonstrated that exogenous administration of SOD markedly reduced ATP failure and tissue damage associated with renal I/R injury (Yin *et al.,* 2002; Cruthirds *et al.,* 2005; Chen *et al.,* 2009). Several different delivery systems have been used to overexpress *sod* genes *in vivo* or *ex vivo* in kidneys, and have included viral-based vectors *e.g.* adeno-associated virus (Chen *et al.,* 2003; Chung *et al.,* 2011), adenovirus (Yin *et al.,* 2001) and BacMam (Murguía-Meca *et al.,* 2011). However, it is crucial for long-term beneficial effects that the vector over-expresses the transgene for a prolonged period of time, induces low pathogenicity and has the ability to circumvent the host immune response. Although adeno-associated virus and adenovirus transduce various tissues with high efficiency and can persist for long periods of time, they are of limited utility in *in vivo* / *ex vivo* gene transfer due to their high pathogenicity as well as immunogenicity (reviewed by Kost & Condreay, 2002). Therefore, BacMam are believed to hold great promise for gene therapy applications (Paul *et al.,* 2012, reviewed by Airenne *et al.,* 2013).

Previously, members of our research group demonstrated baculovirus delivery of *egfp* fused to a baculovirus envelope gene (*vp39*) into whole kidneys (Murguía-Meca *et al.,* 2011). They also constructed a BacMam containing Ds-Red but were unable to observe fluorescence in transduced tissues, although expression was confirmed by rt-PCR. It was speculated that unfavourable cell conditions during cold storage may have precluded protein production by reducing promoter activity or that the promoter itself may have been problematic. This previous work was carried out using early generation virus vectors, containing different promoter and coding sequences, compared to the vectors used in this study. Therefore, we initially wanted to confirm *ex vivo* delivery and expression into porcine kidney using the vector constructed for this study. Subsequently, the main objective was to investigate the hypothesis that BacMam-mediated *sod-2* gene transfer could minimize renal injury associated with prolonged cold kidney preservation, as suggested by the *in vitro* model described in Chapter 5.

6.5.I Expression of reporter genes after *ex vivo* kidney transduction

Experimental protocol I

Initial experiments demonstrated the feasibility of *ex vivo* gene transfer into a whole kidney during cold preservation using BacMam supplemented in the perfusion solution. *Egfp* expression in cross sections of kidney was initially detected using a Bio-Rad ChemiDoc™ MP system and then confirmed and quantified using a plate reader.

After 24 h of gene transfer, *egfp* fluorescence intensity was between two- and six-fold higher in the external section and between two- to four-fold higher in the internal section of AcCMV_EGFP kidney compared to the experimental group I (Figure 6.5). These observations were consistent with published studies which used mammalian-based viruses to transfer genes into kidneys. Chen *et al.* (2003) evaluated *gfp* expression in rat kidney after intra-renal arterial infusion of a recombinant adeno-associated virus, rAAV2-GFP. They showed time-dependent expression of *gfp* in the S3 segment of the proximal tubule of kidneys transduced with rAAV2-GFP up to 6 weeks post-transduction. Importantly, results from the study described in this thesis were also consistent with observations made by Murguía-Meca *et al.* (2011) who observed after 2 and 8 h of perfusion green fluorescence virus particles in *ex vivo* kidney sections perfused with UW solution containing a baculovirus (AcVP39-eGFP).

AcCMV_lacZ virus was also used to transduce whole-kidney during cold storage. AcCMV_lacZ kidney sections stained positive for β-galactosidase expression as evident from the diffuse blue colour in both sections, following X-gal staining (Figure 6.6). A four-fold increase in β-galactosidase activity was observed in adult female Sprague-Dawley rat kidneys transduced by injection into the iliac vein *via* a local incision with adenovirus carrying *lacZ* (Yin *et al.,* 2001). In this study, the control kidney sections (no-BacMam) also showed some β-galactosidase activity (Figure 6.6 A3 *vs.* A2) which was not unexpected; previous have been demonstrated that kidneys express endogenous levels of β-galactosidase activity (Weiss *et al.,* 1999; Bolon *et al.,* 2008).

Subsequently, pathological changes in kidney structure were analysed by H&E and PAS staining after 24 h of *ex vivo* transduction and cold storage. Due to the presence of endogenous β-galactosidase expression in kidneys, it was decided to use sections from AcCMV_EGFP transduced kidney. Although some tubule damage and some signs of inflammation were revealed by histologic analysis in both experimental groups I and II, no major morphological differences were observed following transduction, when compared to non-transduced tissues (Figure 6.8). Yin *et al.* (2001) analysed the effects of β-galactosidase delivered by Ad-LacZ; 2 weeks after I/R injury they found that kidneys from rats that received Ad-LacZ exhibited tubular cell swelling, loss of brush border, and cast formation.

These data were consistent with observations made by Chen *et al.* (2003); they observed chronic interstitial infiltration with mononuclear cells, tubular atrophy, and scar formation in H&E–stained sections of the left kidney transduced with either saline solution (control kidney section) or rAAV2-GFP virus.

They concluded that these changes were caused by ischemia injury associated with the procedure and not as a consequence of adeno-associated virus administration. Results from the present study are in agreement with those of Murguía-Meca *et al.* (2011) who examined kidney sections by H&E staining for loss of brush border, dilatation, vascularization and necrosis of proximal tubules; they reported no differences in these morphological features between transduced and non-trasduced tissues at 0 or 8 hpp.

In order to further assess BacMam transduction *ex vivo*, *egfp* expression was analysed by confocal microscopy using paraffin-embedded S3.c kidney sections from non-transduced and AcCMV_EGFP transduced experimental groups. Immuno-detection showed *egfp*-specific staining in AcCMV_EGFP transduced kidney tissues (Figure 6.9 B2) and no *egfp* expression was detected in kidneys incubated with BELZER UW® solution alone (Figure 6.9 A2). Expression of BacMam delivered *egfp* by was predominantly observed in the proximal tubules (Figure 6.9 B). No *egfp* fluorescence was detected in any controls with the exception of the AcCMV_EGFP S3.c section incubated with no antibodies (Figure 6.10). The presence of a red fluorescent signal in the no antibodies control can be explained as the results of two spectra overlapping. An alternative explanation of this staining pattern, previously reported by Elowitz *et al.* (1997), is photo-activation of GFP. Elowitz and colleagues demonstrated that under low oxygen conditions, the GFP fluorescence spectrum changes and begins to absorb green light and emit red light. This explanation appears consistent with results from this study as low oxygen concentrations represents one of main causes of injury induced by the loss of intracellular ATP during *ex vivo* organ preservation.

The identification and distribution of *egfp* in this present study was in accordance with previous results obtained by *in vivo* adenovirus and lentivirus gene transfer into kidneys. Gusella *et al.* (2002) demonstrated by immunohistochemistry *egfp* fluorescence after *in vivo* intraureteral injection of lentivirus ($5x10^8$ transduction units) in mice left kidney but not in control contralateral kidney or in kidneys infused with PBS only. They also observed localization predominantly in the cortico-medullary junction, particularly in the proximal tubules. Similarly, Ortiz *et al.* (2003), using confocal microscopy, reported *gfp* expression only in tubules of the thick ascending limb of the loop of Henle but not in any cortical or inner medullary structures. This was five days after injecting a recombinant adenovirus, Ad-CMVGFP, into the outer medullary interstitium of Sprague-Dawley rat kidneys.

Experimental protocol II

In this study, an *ex vivo* porcine kidney perfusion system was developed and established to mimic *in vivo* kidney conditions as closely as was possible with the materials available. Based on literature reviews, roller and peristaltic pumps have been widely used for *ex vivo* organ perfusion (Heikkila *et al.,* 1996; Khalfoun *et al.,* 2000; Miyakawa *et al.,* 2008; Schreiter *et al.,* 2012). In line with these studies, a peristaltic pump was used in this study for the bidirectional transport of the perfusion medium supplemented with AcCMV_lacZ virus (Figure 6.11 B). Following 24 h of perfusion/transduction kidneys were cross sectioned and very strong β-galactosidase expression was observed in AcCMV_lacZ kidney sections (Figure 6.12 A3). Whereas, only low levels of endogenous β-galactosidase expression were detected in the control kidney (Figure 6.12 A2); this was consistent with the hypothermic cold storage observations (Figure 6.6 A2). This *ex vivo* perfusion/transduction approach proved to be more efficient for gene transfer as observed by the more intense blue staining compared to transduced cold stored kidneys. These observations were consistent with the study of Heikkila *et al.* (1996) who perfused *ex vivo* porcine kidneys for 12 h with a solution containing adenovirus using a peristaltic pump. They demonstrated the presence of high levels of β-galactosidase with approximately 85% of the glomeruli positive for *lacZ*.

6.5.II *Ex vivo* gene transfer of *sod-2* during hypothermic kidney perfusion

Cold preservation has facilitated the use of cadaveric organs including kidneys for renal transplantation; however, severe damage can occur during the preservation process and the reperfusion phase after transplantation (Henke *et al.,* 1995; Saba *et al.,* 2008). A number of reports demonstrated that administration of *sod-2 d*uring perfusion, ameliorated reperfusion-associated injury in cold-preserved ischemic kidneys (Yin *et al.,* 2001; Fennell *et al.,* 2002; Kim *et al.,* 2006; Schneider *et al.,* 2010;). In an *in vitro* study, Salahudeen *et al.* (2000) indicated that cold-storage (4°C) of human renal tubular cells in UW perfusion solution, induced an increase in *sod-2* expression but not *sod-1* or *sod-3*. Furthermore, in a recent study, Saba *et al.* (2008) demonstrated that short-term cold kidney preservation (40 min of cold preservation plus 18 h of reperfusion) resulted in the inactivation of *sod-2,* which induced the inhibition of mitochondrial complexes and subsequent renal injury in an *in vivo* rodent model. Therefore, in this present study the protective role of *sod-2* to improve cell viability and reduce apoptosis was investigated during prolonged cold preservation. Paired kidneys (left and right) were subjected to 24 h of either control perfusion (no-BacMam) or AcCMV_SOD-2 perfusion/transduction.

Renal tissues were harvested over-time and cells analysed for cellular ATP concentration, transgene expression as well as for caspase-3 activity.

Intracellular ATP levels were slightly increased but not statistically different from control kidney at 0 hpp in AcCMV_SOD-2 perfused/transduced kidney (Figure 6.15). A rapid decrease in ATP levels was observed after 2 h of perfusion in experimental groups I and II; this was followed by a progressive and significant increase in ATP concentration between 4 and 24 hpp in kidneys overexpressing *sod-2* (experimental group II) but not in control kidneys where ATP levels remained similar (Figure 6.15). The results suggested that overexpressing *sod-2* induced a significant recovery of ATP levels which is crucial to maintain cell integrity and viability. Although different conditions were used for the *ex vivo* AcCMV_SOD-2 perfusion model and the *in vitro* experiments described in Chapter 5 of this thesis (Section 5.2.II); both data showed a pattern of increased intracellular ATP levels at 24 h following reperfusion/perfusion.

It was previously reported that during a clinical trial recombinant human *sod-2* (rh-SOD) exerted a beneficial effect on early irreversible and acute kidney rejection events in rh-SOD-treated patients (given in a dose of 200 mg intravenously) compared to the control group; this positive effect was assumed to be related to its antioxidant action on I/R injury of the renal allograft (Land *et al.,* 1994). Yin *et al.* (2001) examined whether adenovirus encoding for *sod-1* could protect against I/R–induced renal injury in an *in vivo* rat model. Although they used a different SOD isoform from the one used in this study, they demonstrated that *sod-1* overexpression provided protection against renal I/R injury by significantly reducing LDH levels compared to control kidneys that received *lacZ* gene.

Western blot analysis of cell lysates harvested from AcCMV_SOD-2 perfused/transduced kidneys revealed efficient production of the 23 kDa SOD-2 protein (Figure 6.16 B). Moreover, endogenous SOD-2 protein was also detected by the anti-SOD-2 antibody (Figure 6.16 A). Density scanning of these immunoblots showed that the relative expression of *sod-2* after 4 and 24 h of perfusion in *ex vivo* AcCMV_SOD-2 transduced kidney cells were approximately 4% higher than endogenous levels observed in the control cells (Figure 6.16 B *vs.* A). Yin *et al.* (2001) evaluated SOD-1 protein expression in rat kidneys by western blot analysis 3 days after *in vivo* adenovirus transduction. They observed increased levels of human SOD-1 protein in rats that received Ad-SOD; however they also detected very low levels of SOD-1 protein in Ad-LacZ transduced kidney cells which corresponded to endogenous *sod-1* gene expression. These data were also consistent with other studies which overexpressed *sod-2* by viral vectors in different organs (Knobil *et al.,* 1998; Zanetti *et al.,* 2001; Baud *et al.,* 2004).

In contrast with these observations, Fennell *et al.* (2002) assessed in an *in vitro* / *in vivo* study the endogenous expression of *sod-2* as well as the levels evoked by adenovirus-mediated *sod-2* overexpression. They demonstrated the presence of a 22 kDa protein corresponding to the recombinant human sod-2 in transduced cells but not in the endothelial cells transduced with either β-galactosidase expressing adenovirus or in control cells.

Subsequently, to determine whether the protective effect of *sod-2* overexpression detected at 24 h of perfusion was associated with decreased apoptosis, caspase-3 activity was measured in control and AcCMV_SOD-2 kidneys. The number of apoptotic cells was much greater in control perfused kidney (experimental group I) than in cell derived from AcCMV_SOD-2 transduced kidney (experimental group II), in which the SOD-2 level was 4% and ATP three-fold higher than control kidney (Figure 6.17). Overall, the kidney overexpressing *sod-2* had a partial protective effect against apoptosis induced by prolonged hypothermic perfusion than control kidney. This is consistent with other reports in the literature that have demonstrated that exogenous *sod-2* protected against apoptosis *e.g.* Linag *et al.,* 2008. Liang and colleagues showed that *in vivo* overexpression of a SOD mimetic (mimetic manganese (III) tetrakis(1-methyl-4-pyridyl)porphyrin) was able to partially reduced caspase-3 activity in male Sprague-Dawley rat kidneys that underwent to a bilateral clamping of the renal arteries for 45 min followed by reperfusion for 24 h.

This single pilot study suggested a potential protective effect of ex vivo BacMam-mediated delivery of sod-2 against long cold kidney preservation injury. It should be noted that the study described in this thesis was a small pilot experiment and triplicate samples were harvested only from one control kidney and one transduced kidney. Furthermore, this study has focused on the role of overexpressing sod-2 and its beneficial effect, however, there are clearly limitations inherent to the ex vivo cold perfusion model used in this experiment that need to be addressed in future.

The main limitation of the perfused ex-vivo model is the limited lifespan of the organ perfused and knowing when valid data can be extracted during this lifespan (reviewed by Ong *et al.,* 2013). Moreover, the interaction of either physiological perfusion solution or autologous blood with the non-biological surfaces of the perfusion circuit might activate biological pathways producing an inflammation or immune response (reviewed by Ong *et al.,* 2013). Ex vivo cold perfusion models are also limited by the fact that hypothermic preservation can significantly decrease the organ metabolic functions, which can preclude full recovery (St Peter *et al.,* 2002).

Therefore, further studies are needed to more fully investigate the potential beneficial effects of overexpressing sod-2 during ex vivo cold kidney perfusion and to provide new experimental approach to overcome limitations of the model.

6.5.III *Ex vivo* application of Hydroxyurea + sodium butyrate during kidney cold preservation

The chemotherapeutic agent, hydroxyurea is the only disease-modifying therapy approved for sickles cell disorders; the main effect of this chemical compound is to enhance the antioxidant enzyme activity of sickle erythrocytes such as glutathione peroxidase 1, catalase or flavin reductase (reviewed by Silva *et al.,* 2013). Recently, Teixeira Neto *et al.* (2011) reported a possible role of hydroxyurea as an antioxidant drug acting by increasing the glutathione levels which controls concentrations of lipid hydroperoxides and therefore prevents cell damage by free radicals. Sodium butyrate has been considered to possess a potential anticancer activity; however, recently a few studies have also demonstrated an anti-inflammatory and immunomodulatory effects (Hinnebusch *et al.,* 2002; Meijer *et al.,* 2010). Indeed published reports have shown that sodium butyrate exerted a protective effect in a rat ischemic model of stroke (Zhang *et al.,* 2007; Hu *et al.,* 2014) as well as protected against hepatic I/R injury (Qiao *et al.,* 2014). Hence, this present study aimed to evaluate the injury profile, by measuring the intracellular ATP levels, in control and transduced kidneys treated with or without hydroxyurea + sodium butyrate and thus assess the benefit of these chemicals in improving kidney recovery.

The results of this second pilot study showed a significant difference over-time in the recovery of the ATP levels between control kidneys and kidney transduced with BacMam carrying reporter genes compared to untreated AcCMV_SOD-2 kidneys; these data were in line with the results of the previous experiment (Section 6.3). These data also showed a significant and consistent negative effect of hydroxyurea + sodium butyrate in all 3 experiments with markedly reduced levels of intracellular ATP at 24 hpp (Figures 6.20 and 6.21). Although, published reports evaluated sodium butyrate or hydroxuyrea alone using different approaches, results from this study were not consistent with those from literature (Teixeira Neto *et al.,* 2011; Hu *et al.,* 2014; Qiao *et al.,* 2014). Hu and colleagues examined the preconditioning effect of sodium butyrate during *in vivo* myocardial I/R injury in a rat model. They showed that following 4 h of reperfusion, the LDH levels in the ischaemic group were significantly increased compared with the experimental group that received high dose of sodium butyrate (300 mg/kg) which significantly inhibited the release of LDH.

Similarly, Qiao *et al.* (2014) investigated the protective effect of sodium butyrate preconditioning against hepatic I/R injury in rats and suggested that sodium butyrate improved I/R-induced liver injury by reducing transaminase levels, tissue pathologic changes and possible by suppressing inflammatory factors production and preventing NF-kB activation in Kupffer cells.

A number of studies have confirmed that the direct assessment of ATP content in organs represents a suitable parameter for demonstrating ex vivo organ viability (Lietzenmayer *et al.,* 1991; von Elverfeldt *et al.,* 2007; Buchs *et al.,* 2014). However, attempting to precisely quantify ATP within kidney tissue is a very challenging process due its structural and functional heterogeneity (reviewed by Palygin & Staruschenko, 2013). The luciferin-luciferase reaction was utilized to monitor intracellular ATP levels in this pilot study; however, it should be noted that preliminary results were given as normalized relative luciferase units (RLU), after background correction because of the superior sensitivity of the GloMax® 20/20 luminometer (Promega) used (detection limit: 1 x 10^{-21} moles of luciferase enzyme). Boudjema *et al.* (1990) and Clavien and colleagus (1992) demonstrated that during hypothermic preservation, whilst kidney cell metabolism slowed (approximately two-fold less for every 10°C drop in temperature) there was still considerable activity at 1°C; they also demonstrated that after 6 h of cold preservation intracellular ATP levels dropped by 84%. However, Lazeyras *et al.* (2009) demonstrated that ATP was re-synthesized immediately after hypothermic perfusion (10 h) in the presence of oxygen (pO2 ≥ 100kPa), in comparison to a kidney group where no perfusion was applied. This study was recently confirmed by Buchs *et al.* (2014) who demonstrated, using magnetic resonance imaging, ATP re-synthesis in 14 kidneys perfused with oxygenation at 4°C. In particular, the Buches *et al.* (2014) study demonstrated viability of 93% in ex vivo kidneys oxygenated during hypothermic perfusion.

In summary, this pilot study demonstrated for the first time the successful transfer and expression of reporter genes using BacMam gene transfer approach *ex vivo* in kidneys. The results from the present study also provided the first evidence of *ex vivo* BacMam-mediated *sod-2* expression in a kidney, findings that have not been previously reported with BacMam gene transfer. Importantly, this pilot study suggested that overexpressing *sod-2* in kidneys might provide protection against cold preservation-induced injury which may be associated with reduced apoptosis and the recovery of the intracellular ATP levels.

Therefore, future experiments should aim to calculate, from standard curves, the concentration of ATP present in each perfusate used during experiments; this will allow a

better understanding of whether kidneys preserved in the presence of *sod-2* generated higher concentrations of ATP during the 24 h of hypothermic perfusion than kidneys preserved in the absence of *sod-2*.

Chapter 7
Final discussion
and
Future work

The discovery that baculovirus can transduce mammalian cells has greatly increased their utility beyond recombinant protein expression and their application towards gene therapy has become increasingly popular. This study set out to expand upon previous work by the IVRG where baculovirus was used to deliver a reporter gene into whole kidneys. Although it had been demonstrated that baculovirus could deliver *egfp* into a porcine kidney, I sought to expand upon these studies by developing BacMam as a tool to deliver and over-express protective genes against I/R injury.

In this study, a range of transfer vectors and BacMam viruses were constructed. Vector integrity was confirmed by sequencing and BacMam expression was observed by microscopy, reporter assays and western blot. These vectors contained reporter genes (*egfp* and *lacZ*), for easy transgene detection during optimization experiments, but also the protective genes *sod-2* or *bcl-2* however, for future studies a greater range of vectors could be constructed to include other genes that may have a protective function against I/R injury, such as heme oxygenase-1 (HO-1), glutathione or hypoxia inducible factors (HIF1-3). Studies have demonstrated that overexpression of HO-1 or glutathione exert a protective function in organs against I/R injury (Xue *et al.,* 2008; reviewed by Ferenbach *et al.,* 2010). A more recent report showed that *in vivo* electroporation-mediated delivery of HIF-1α plasmid DNA improved neovascularization in a mouse model of limb ischaemia (Ouma *et al.,* 2014). Multiple BacMam vectors could also be transduced into the same organ. The advantage of this approach would be that several different stages in the I/R injury pathway could be engaged during the same period. This approach has been used previously by Durand *et al.* (2005); they evaluated the combined effect of adenovirus-mediated gene transfer of *sod-1* and catalase on ROS production and inflammation after ballon angioplasty. Liang *et al.* (2010) also evaluated the effect of lentivirus-mediated *sod-1* delivery together with the administration of MitoTEMPO (a mitochondria-targeted antioxidant), on mitochondrial function and signalling pathways in an *in vitro* ATP depletion/recovery injury of porcine kidney cells. Bicistronic vectors could also be produced, overexpressing multiple genes from a single BacMam, possibly under different promoters to control timing and strength of expression. This multi-gene approach would initially require optimisation of a wider range of single gene expression studies to ensure the genes used indeed had a protective effect and that they then worked synergistically to improve individual gene effects.

In Chapter 3, I speculated that in order to see any beneficial effect after transducing a whole kidney it would likely require transduction with high concentrations of purified virus, expressing maximal levels of the delivered gene. Therefore, these studies were aimed at determining the most efficient way to produce BacMam viruses at high concentration.

Initially, different methods of concentrating baculovirus were compared, including centrifugation at different speeds, spin filters and chromatography. Ideally, the method chosen would be reproducible and simple to use, able to accommodate different volumes and cheap to implement. Amongst the methods tested, centrifugation most closely matched all of these requirements and despite initial concerns that it may produce aggregated virus particles, potentially reducing transduction efficiency, it actually proved to be the most reliable process. Future work should aim to determine diameter and morphology of the concentrated BacMam particles; this will involve using techniques such as transmission electron microscopy. Electron microscopy study will further characterize the intact rod-shaped structure and size value of the BacMam particles following concentration. Furthermore, flow cytometry analysis could be used to detect viral particle aggregates by using BacMam virus carrying reporter genes. The presence of aggregates will be associated with fluorescence intensity and used as an indicator of the mean aggregate size. Aiming for maximum product purity, future work may explore purification steps that would yield highly purified BacMam particles for gene therapy applications.

Although BacMam transduction and expression is relatively high compared to other virus vector systems, we sought to enhance it further to offset potentially low transduction efficiencies when using whole organs; this study was reported in Chapter 4. Literature searches of the public databases identified a number of reagents reported to enhance mammalian viral delivery, including different lipids and chemicals. Generally, in this study the lipids gave little improvement in transduction efficiency and as such were discontinued. However, the addition of certain chemicals both alone and in combination did show improved expression and these were included in subsequent I/R injury experiments. As a continuation of the research presented in Chapter 4, the following areas of investigation should be considered: (1) further analysis of the effect of chemicals on cell viability, since this is an important factor in achieving an effective gene transfer for gene therapy study; experiments would be conducted for all combinations of chemical via MTT or LDH assay as well as quantification of active caspase-3 by using fluorimetric-based assay. (2) Understanding the biological consequences of altering DNA replication, histone acetylation and topoisomerase activity may provide insight to maximize the utility of these compounds during BacMam *ex vivo* / *in vivo* transduction of whole organs. Therefore, further studies should include DNA microarrays; the comparison of the transcriptomes of untransduced cells and transduced cells cultured either with or without chemicals may provide information about the genetic regulation of gene expression in the treated transduced samples. (3) In addition, large-scale studies should also be carried out

to determine whether enhanced transgene expression can still be obtained at scales more typical of a real bioprocess.

Chapter 5 reported the optimisation of an *in vitro* IRI model using mammalian cells. Initially the model was developed in HEK293 cells, but was then extended to HK-2 cells. Initial, results were not conclusive using either short (15 min) or long (120 min) periods of ATP-depletion followed by BacMam transduction. However, after incorporating the BacMam transduction as a pre-step into the process we were able to show partially improved ATP levels over-time in HEK293 cells and a full recovery of cellular ATP in HK-2 cells. This work was an important step towards transducing BacMam into whole organs. Clearly overexpression of a single protective gene in vitro may not be representative of the likely success of an in vivo approach, perhaps because of the complexity of the I/R injury process. Therefore, future experiments should aim to identify novel protective components by reviewing current literature as well as by evaluating mRNA from ischaemic cells following BacMam transduction using GeneChip expression analysis; microarray assay will allow the identification of differentially regulated genes during renal I/R injury and may lead to the development a more successful BacMam multi-gene delivery approach. Using the learning gained from Chapter 3 and 4, it was decided to include the chemical sodium butyrate;preconditioning with sodium butyrate BacMam transduced cells improved cell viability at early time point of reperfusion. However, this was a single pilot study and was not obtained enough data to elucidate the role of sodium butyrate in renal I/R injury; therefore further studies are needed to confirm this hypothesis. Importantly, further studies should identify sodium butyrate-targeted genes and pathways involved in its protection and to assess in detail safety and pharmacotoxicity with regard to renal I/R injury. Additionally, future experiments should also assess the therapeutic benefits of using compounds, such as hydroxyurea and etoposide, against renal I/R injury.

Chapter 6 described the use of BacMam to deliver reporter and protective genes into a whole kidney. This work was a culmination of the studies carried out in previous Chapters and although it was a preliminary experiment, it demonstrated BacMam expression in the kidney and ATP assays suggested that overexpression of *sod-2* could have a beneficial effect *ex vivo*. As mentioned above, this was a preliminary study and going forward this *ex vivo* model needs to be optimised further, including determining the optimum amount of BacMam virus and chemical concentrations. Future studies could also be directed towards transducing organs with multiple vector/gene combinations. BacMam virus expression appeared to concentrate in certain areas of the organ and future work should seek to identify more clearly the virus localisation areas within the organ. This will ensure a more targeted and hence more efficient delivery system.

Additionally, more work should also be carried out on determining the immune response of the tissues. Although no apparent damage has been observed after transducing BacMam viruses into kidneys, it is likely that there are immunological responses that are below the levels of detection used in this study. Certainly, as described in the supplementary data in the CD attached to this thesis (virus construction & transgene expression test, S2), it was observed up-regulation of a number of cytokines and other immune response genes by RT^2 profiler PCR array, after BacMam transduction into HEK293 cells, and a similar approach should be considered for future organ studies. Future experiments should consider different approaches for the detection of intracellular ATP including (1) real-time electrochemical detection of ATP; this method represents a unique approach for the real-time monitoring of the changes in ATP levels in whole kidney. (2) Chromatographic methods such as ion-exchange chromatography or high-performance liquid chromatography (HPLC). Furthermore, ^{31}P magnetic resonance spectroscopy should also be considered if kidneys will be perfused with oxygenated hypothermic pulsatile perfusion; this technique allows direct assessment of ATP concentration, which provides a reliable indicator for organ bioenergetics and viability.

In conclusion this study has 1) optimised an *in vitro* I/R injury model in human kidney 2 (HK-2) cells for BacMam, 2) shown that BacMam delivery of *bcl-2* and *sod-2*, alone or in combination, into ischaemic HK-2 cells ameliorated the effects of I/R injury *in vitro* and 3) clearly demonstrated the potential of using BacMam viruses for ameliorating I/R injury *ex vivo* by delivering and overexpressing *sod-2* in whole porcine kidneys.

References

Abu Jawdeh, B. G. and Rabb, H. (2011) 'Delayed kidney allograft function - what does it tell us about acute kidney injury?', *Contrib Nephrol,* 174, 173-81.

Acker, C. G., Singh, A. R., Flick, R. P., Bernardini, J., Greenberg, A. and Johnson, J. P. (2000) 'A trial of thyroxine in acute renal failure', *Kidney Int,* 57(1), 293-8.

Airenne, K. J., Hiltunen, M. O., Turunen, M. P., Turunen, A. M., Laitinen, O. H., Kulomaa, M. S. and Ylä-Herttuala, S. (2000) 'Baculovirus-mediated periadventitial gene transfer to rabbit carotid artery', *Gene Ther,* 7(17), 1499-504.

Airenne, K. J., Hu, Y. C., Kost, T. A., Smith, R. H., Kotin, R. M., Ono, C., Matsuura, Y., Wang, S. and Ylä-Herttuala, S. (2013) 'Baculovirus: an insect-derived vector for diverse gene transfer applications', *Mol Ther,* 21(4), 739-49.

Airenne, K. J., Makkonen, K. E., Mähönen, A. J. and Ylä-Herttuala, S. (2010) '*In vivo* application and tracking of baculovirus', *Curr Gene Ther,* 10(3), 187-94.

Akcay, A., Nguyen, Q. and Edelstein, C. L. (2009) 'Mediators of inflammation in acute kidney injury', *Mediators Inflamm,* 2009, 137072.

Akhtar, M. Z., Sutherland, A. I., Huang, H., Ploeg, R. J. and Pugh, C. W. (2014) 'The role of hypoxia-inducible factors in organ donation and transplantation: the current perspective and future opportunities', *Am J Transplant,* 14(7), 1481-7.

Aouacheria, A., Arnaud, E., Venet, S., Lalle, P., Gouy, M., Rigal, D. and Gillet, G. (2001) 'Nrh, a human homologue of Nr-13 associates with Bcl-Xs and is an inhibitor of apoptosis', *Oncogene,* 20(41), 5846-55.

Archer, S. Y. and Hodin, R. A. (1999) 'Histone acetylation and cancer', *Curr Opin Genet Dev,* 9(2), 171-4.

Assenberg, R., Wan, P. T., Geisse, S. and Mayr, L. M. (2013) 'Advances in recombinant protein expression for use in pharmaceutical research', *Curr Opin Struct Biol,* 23(3), 393-402.

Au, S., Wu, W. and Panté, N. (2013) 'Baculovirus nuclear import: open, nuclear pore complex (NPC) sesame', *Viruses,* 5(7), 1885-900.

Aucoin, M. G., Mena, J. A. and Kamen, A. A. (2010) 'Bioprocessing of baculovirus vectors: a review', *Curr Gene Ther,* 10(3), 174-86.

Avery, O. T., Macleod, C. M. and McCarty, M. (1944) 'studies on the chemical nature of the substance inducing transformation of pneumococcal types: induction of transformation by a desoxyribonucleic acid fraction isolated from pneumococcus type III', *J Exp Med,* 79(2), 137-58.

Ayres, M. D., Howard, S. C., Kuzio, J., Lopez-Ferber, M. and Possee, R. D. (1994) 'The complete DNA sequence of Autographa californica nuclear polyhedrosis virus.', *Virology,* 202(2), 586-605.

Backliwal, G., Hildinger, M., Kuettel, I., Delegrange, F., Hacker, D. L. and Wurm, F. M. (2008) 'Valproic acid: a viable alternative to sodium butyrate for enhancing protein expression in mammalian cell cultures', *Biotechnol Bioeng,* 101(1), 182-9.

Bak, X. Y., Lam, D. H., Yang, J., Ye, K., Wei, E. L., Lim, S. K. and Wang, S. (2011) 'Human embryonic stem cell-derived mesenchymal stem cells as cellular delivery vehicles for prodrug gene therapy of glioblastoma', *Hum Gene Ther,* 22(11), 1365-77.

Bakhshi, A., Jensen, J. P., Goldman, P., Wright, J. J., McBride, O. W., Epstein, A. L. and Korsmeyer, S. J. (1985) 'Cloning the chromosomal breakpoint of t(14;18) human lymphomas: clustering around JH on chromosome 14 and near a transcriptional unit on 18', *Cell,* 41(3), 899-906.

Bank, A. (1996) 'Human somatic cell gene therapy', *Bioessays,* 18(12), 999-1007.

Barra, D., Schinina, M. E., Simmaco, M., Bannister, J. V., Bannister, W. H., Rotilio, G. and Bossa, F. (1984) 'The primary structure of human liver manganese superoxide dismutase', *J Biol Chem,* 259(20), 12595-601.

Barsoum, J. (1999) 'Concentration of recombinant baculovirus by cation-exchange chromatography', *Biotechniques,* 26(5), 834-6, 838, 840.

Basile, D. P. (2007) 'The endothelial cell in ischemic acute kidney injury: implications for acute and chronic function', *Kidney Int,* 72(2), 151-6.

Baud, O., Haynes, R. F., Wang, H., Folkerth, R. D., Li, J., Volpe, J. J. and Rosenberg, P. A. (2004) 'Developmental up-regulation of MnSOD in rat oligodendrocytes confers protection against oxidative injury', *Eur J Neurosci,* 20(1), 29-40.

Bauerle, J. D., Grenz, A., Kim, J. H., Lee, H. T. and Eltzschig, H. K. (2011) 'Adenosine generation and signaling during acute kidney injury', *J Am Soc Nephrol,* 22(1), 14-20.

Bayati, A., Källskog, O., Odlind, B. and Wolgast, M. (1988) 'Plasma elimination kinetics and renal handling of copper/zinc superoxide dismutase in the rat', *Acta Physiol Scand,* 134(1), 65-74.

Becker, L. B. (2004) 'New concepts in reactive oxygen species and cardiovascular reperfusion physiology', *Cardiovasc Res,* 61(3), 461-70.

Beckman, J. S. and Koppenol, W. H. (1996) 'Nitric oxide, superoxide, and peroxynitrite: the good, the bad, and ugly', *Am J Physiol,* 271(5 Pt 1), C1424-37.

Bellomo, R., May, C. and Wan, L. (2004) 'Acute renal failure and sepsis', *N Engl J Med,* 351(22), 2347-9; author reply 2347-9.

Belyavskyi, M., Braunagel, S. C. and Summers, M. D. (1998) 'The structural protein ODV-EC27 of Autographa californica nucleopolyhedrovirus is a multifunctional viral cyclin', *Proc Natl Acad Sci U S A,* 95(19), 11205-10.

Bengatta, S., Arnould, C., Letavernier, E., Monge, M., de Préneuf, H. M., Werb, Z., Ronco, P. and Lelongt, B. (2009) 'MMP9 and SCF protect from apoptosis in acute kidney injury', *J Am Soc Nephrol,* 20(4), 787-97.

Berridge, M. J. (2012) 'Calcium signalling remodelling and disease', *Biochem Soc Trans,* 40(2), 297-309.

Bertera, S., Crawford, M. L., Alexander, A. M., Papworth, G. D., Watkins, S. C., Robbins, P. D. and Trucco, M. (2003) 'Gene transfer of manganese superoxide dismutase extends islet graft function in a mouse model of autoimmune diabetes', *Diabetes,* 52(2), 387-93.

Bilbao, G., Contreras, J. L., Eckhoff, D. E., Mikheeva, G., Krasnykh, V., Douglas, J. T., Thomas, F. T., Thomas, J. M. and Curiel, D. T. (1999) 'Reduction of ischemia-reperfusion injury of the liver by in vivo adenovirus-mediated gene transfer of the antiapoptotic Bcl-2 gene', *Ann Surg,* 230(2), 185-93.

Blissard, G. W. and Rohrmann, G. F. (1990) 'Baculovirus diversity and molecular biology.', *Annu Rev Entomol,* 35, 127-55.

Boise, L. H., González-García, M., Postema, C. E., Ding, L., Lindsten, T., Turka, L. A., Mao, X., Nuñez, G. and Thompson, C. B. (1993) 'bcl-x, a bcl-2-related gene that functions as a dominant regulator of apoptotic cell death', *Cell,* 74(4), 597-608.

Bolon, B. (2008) 'Whole mount enzyme histochemistry as a rapid screen at necropsy for expression of beta-galactosidase (LacZ)-bearing transgenes: considerations for

separating specific LacZ activity from nonspecific (endogenous) galactosidase activity', *Toxicol Pathol,* 36(2), 265-76.

Bon, D., Chatauret, N., Giraud, S., Thuillier, R., Favreau, F. and Hauet, T. (2012) 'New strategies to optimize kidney recovery and preservation in transplantation', *Nat Rev Nephrol,* 8(6), 339-47.

Bonegio, R. and Lieberthal, W. (2002) 'Role of apoptosis in the pathogenesis of acute renal failure', *Curr Opin Nephrol Hypertens,* 11(3), 301-8.

Bonning, B. C. (2005) *Baculoviruses: biology, biochemistry and molecular biology., In Comprehensive Molecular Insect Science*.

Bonning, B. C. and Hammock, B. D. (1992) 'Development and potential of genetically engineered viral insecticides.', *Biotechnol Genet Eng Rev,* 10, 455-89.

Bonventre, J. V. (2002) 'Kidney ischemic preconditioning', *Curr Opin Nephrol Hypertens,* 11(1), 43-8.

Bonventre, J. V. and Yang, L. (2011) 'Cellular pathophysiology of ischemic acute kidney injury', *J Clin Invest,* 121(11), 4210-21.

Bouard, D., Alazard-Dany, D. and Cosset, F. L. (2009) 'Viral vectors: from virology to transgene expression', *Br J Pharmacol,* 157(2), 153-65.

Boyce, F. M. and Bucher, N. L. (1996) 'Baculovirus-mediated gene transfer into mammalian cells.', *Proc Natl Acad Sci U S A,* 93(6), 2348-52.

Braunagel, S. C., Parr, R., Belyavskyi, M. and Summers, M. D. (1998) 'Autographa californica nucleopolyhedrovirus infection results in Sf9 cell cycle arrest at G2/M phase', *Virology,* 244(1), 195-211.

Breggia, A. C. and Himmelfarb, J. (2008) 'Primary mouse renal tubular epithelial cells have variable injury tolerance to ischemic and chemical mediators of oxidative stress', *Oxid Med Cell Longev,* 1(1), 33-8.

Brown, S. W. and Mehtali, M. (2010) 'The Avian EB66(R) Cell Line, Application to Vaccines, and Therapeutic Protein Production', *PDA J Pharm Sci Technol,* 64(5), 419-25.

Brüne, B., Zhou, J. and von Knethen, A. (2003) 'Nitric oxide, oxidative stress, and apoptosis', *Kidney Int Suppl,* (84), S22-4.

Cai, Y., Martens, G. A., Hinke, S. A., Heimberg, H., Pipeleers, D. and Van de Casteele, M. (2007) 'Increased oxygen radical formation and mitochondrial dysfunction mediate beta cell apoptosis under conditions of AMP-activated protein kinase stimulation', *Free Radic Biol Med,* 42(1), 64-78.

Carbonell, L. F., Klowden, M. J. and Miller, L. K. (1985) 'Baculovirus-mediated expression of bacterial genes in dipteran and mammalian cells.', *J Virol,* 56(1), 153-60.

Carstens, E. B., Ye, L. B. and Faulkner, P. (1987) 'A point mutation in the polyhedrin gene of a baculovirus, Autographa californica MNPV, prevents crystallization of occlusion bodies', *J Gen Virol,* 68 (Pt 3), 901-5.

Cassis, P., Solini, S., Azzollini, N., Aiello, S., Rocchetta, F., Conti, S., Novelli, R., Gagliardini, E., Mister, M., Rapezzi, F., Rapezzi, S., Benigni, A., Remuzzi, G., Conway, E. M. and Noris, M. (2014) 'An unanticipated role for survivin in organ transplant damage', *Am J Transplant,* 14(5), 1046-60.

Cavazzana-Calvo, M. and Fischer, A. (2004) 'Efficacy of gene therapy for SCID is being confirmed', *Lancet,* 364(9452), 2155-6.

Chan, P. H. (2001) 'Reactive oxygen radicals in signaling and damage in the ischemic brain', *J Cereb Blood Flow Metab,* 21(1), 2-14.

Charlton, C. A. and Volkman, L. E. (1993) 'Penetration of Autographa californica nuclear polyhedrosis virus nucleocapsids into IPLB Sf 21 cells induces actin cable formation', *Virology,* 197(1), 245-54.

Chatterjee, A., Xiao, H., Bollong, M., Ai, H. W. and Schultz, P. G. (2013) 'Efficient viral delivery system for unnatural amino acid mutagenesis in mammalian cells', *Proc Natl Acad Sci U S A,* 110(29), 11803-8.

Chen, C. Y., Lin, C. Y., Chen, G. Y. and Hu, Y. C. (2011) 'Baculovirus as a gene delivery vector: recent understandings of molecular alterations in transduced cells and latest applications', *Biotechnol Adv,* 29(6), 618-31.

Chen, G. Y., Chen, C. Y., Chang, M. D., Matsuura, Y. and Hu, Y. C. (2009) 'Concanavalin A affinity chromatography for efficient baculovirus purification', *Biotechnol Prog,* 25(6), 1669-77.

Chen, H. C., Sung, L. Y., Lo, W. H., Chuang, C. K., Wang, Y. H., Lin, J. L. and Hu, Y. C. (2008) 'Combination of baculovirus-expressed BMP-2 and rotating-shaft bioreactor culture synergistically enhances cartilage formation', *Gene Ther,* 15(4), 309-17.

Chen, R. L., Nagel, S., Papadakis, M., Bishop, T., Pollard, P., Ratcliffe, P. J., Pugh, C. W. and Buchan, A. M. (2012) 'Roles of individual prolyl-4-hydroxylase isoforms in the first 24 hours following transient focal cerebral ischaemia: insights from genetically modified mice', *J Physiol,* 590(Pt 16), 4079-91.

Chen, W. Y., Bailey, E. C., McCune, S. L., Dong, J. Y. and Townes, T. M. (1997) 'Reactivation of silenced, virally transduced genes by inhibitors of histone deacetylase', *Proc Natl Acad Sci U S A,* 94(11), 5798-803.

Chen, Y. F., Li, P. L. and Zou, A. P. (2001) 'Oxidative stress enhances the production and actions of adenosine in the kidney', *Am J Physiol Regul Integr Comp Physiol,* 281(6), R1808-16.

Chen, Z., Siu, B., Ho, Y. S., Vincent, R., Chua, C. C., Hamdy, R. C. and Chua, B. H. (1998) 'Overexpression of MnSOD protects against myocardial ischemia/reperfusion injury in transgenic mice', *J Mol Cell Cardiol,* 30(11), 2281-9.

Chen, Z. C., Wu, W. S., Lin, M. T. and Hsu, C. C. (2009) 'Protective effect of transgenic expression of porcine heat shock protein 70 on hypothalamic ischemic and oxidative damage in a mouse model of heatstroke', *BMC Neurosci,* 10, 111.

Cheng, X. H., Hillman, C. C., Zhang, C. X. and Cheng, X. W. (2013) 'Reduction of polyhedrin mRNA and protein expression levels in Sf9 and Hi5 cell lines, but not in Sf21 cells, infected with Autographa californica multiple nucleopolyhedrovirus fp25k mutants', *J Gen Virol,* 94(Pt 1), 166-76.

Chernyak, B. V. (1997) 'Redox regulation of the mitochondrial permeability transition pore', *Biosci Rep,* 17(3), 293-302.

Chien, C. T., Chiang-Ting, C., Chang, T. C., Tzu-Ching, C., Tsai, C. Y., Ching-Yi, T., Shyue, S. K., Song-Kuen, S., Lai, M. K. and Ming-Kuen, L. (2005) 'Adenovirus-mediated bcl-2 gene transfer inhibits renal ischemia/reperfusion induced tubular oxidative stress and apoptosis', *Am J Transplant,* 5(6), 1194-203.

Christensen, E. I., Wagner, C. A. and Kaissling, B. (2012) 'Uriniferous tubule: structural and functional organization', *Compr Physiol,* 2(2), 805-61.

Chuang, C. K., Lin, K. J., Lin, C. Y., Chang, Y. H., Yen, T. C., Hwang, S. M., Sung, L. Y., Chen, H. C. and Hu, Y. C. (2010) 'Xenotransplantation of human mesenchymal stem cells into immunocompetent rats for calvarial bone repair', *Tissue Eng Part A,* 16(2), 479-88.

Collino, M., Pini, A., Mugelli, N., Mastroianni, R., Bani, D., Fantozzi, R., Papucci, L., Fazi, M. and Masini, E. (2013) 'Beneficial effect of prolonged heme oxygenase 1 activation in a rat model of chronic heart failure', *Dis Model Mech,* 6(4), 1012-20.

Condreay, J. P., Witherspoon, S. M., Clay, W. C. and Kost, T. A. (1999) 'Transient and stable gene expression in mammalian cells transduced with a recombinant baculovirus vector', *Proc Natl Acad Sci U S A,* 96(1), 127-32.

Constantinou, C. E. and Hrynczuk, J. R. (1976) 'Renal pelivic pacemaker arrhythmias induced by pentothal anesthesia', *Urol Int,* 31(6), 489-500.

Cory, S. and Adams, J. M. (2002) 'The Bcl2 family: regulators of the cellular life-or-death switch', *Nat Rev Cancer,* 2(9), 647-56.

Cory, S., Huang, D. C. and Adams, J. M. (2003) 'The Bcl-2 family: roles in cell survival and oncogenesis', *Oncogene,* 22(53), 8590-607.

Cox, M. M. (2012) 'Recombinant protein vaccines produced in insect cells', *Vaccine,* 30(10), 1759-66.

Cruthirds, D. L., Saba, H. and MacMillan-Crow, L. A. (2005) 'Overexpression of manganese superoxide dismutase protects against ATP depletion-mediated cell death of proximal tubule cells', *Arch Biochem Biophys,* 437(1), 96-105.

Cumming, D. V., Heads, R. J., Brand, N. J., Yellon, D. M. and Latchman, D. S. (1996) 'The ability of heat stress and metabolic preconditioning to protect primary rat cardiac myocytes', *Basic Res Cardiol,* 91(1), 79-85.

Czabotar, P. E., Lessene, G., Strasser, A. and Adams, J. M. (2014) 'Control of apoptosis by the BCL-2 protein family: implications for physiology and therapy', *Nat Rev Mol Cell Biol,* 15(1), 49-63.

Derossi, R., Medeiros, U., de Almeida, R. G., Righetto, F. R. and Frazílio, F. O. (2008) 'Meperidine prolongs lidocaine caudal epidural anaesthesia in the horse', *Vet J,* 178(2), 294-7.

Devarajan, P. (2005) 'Cellular and molecular derangements in acute tubular necrosis', *Curr Opin Pediatr,* 17(2), 193-9.

Doctor, R. B., Bacallao, R. and Mandel, L. J. (1994) 'Method for recovering ATP content and mitochondrial function after chemical anoxia in renal cell cultures', *Am J Physiol,* 266(6 Pt 1), C1803-11.

Dröge, W. (2002) 'Free radicals in the physiological control of cell function', *Physiol Rev,* 82(1), 47-95.

Duffy, A. M., O'Brien, T. and McMahon, J. M. (2010) 'Generation of antioxidant adenovirus gene transfer vectors encoding CuZnSOD, MnSOD, and catalase', *Methods Mol Biol,* 594, 381-93.

Duisit, G., Saleun, S., Douthe, S., Barsoum, J., Chadeuf, G. and Moullier, P. (1999) 'Baculovirus vector requires electrostatic interactions including heparan sulfate for efficient gene transfer in mammalian cells', *J Gene Med,* 1(2), 93-102.

Durand, E., Al Haj Zen, A., Addad, F., Brasselet, C., Caligiuri, G., Vinchon, F., Lemarchand, P., Desnos, M., Bruneval, P. and Lafont, A. (2005) 'Adenovirus-mediated gene transfer of superoxide dismutase and catalase decreases restenosis after balloon angioplasty', *J Vasc Res,* 42(3), 255-65.

Elowitz, M. B., Surette, M. G., Wolf, P. E., Stock, J. and Leibler, S. (1997) 'Photoactivation turns green fluorescent protein red', *Curr Biol,* 7(10), 809-12.

Fan, L. H., He, L., Cao, Z. Q., Xiang, B. and Liu, L. (2012) 'Effect of ischemia preconditioning on renal ischemia/reperfusion injury in rats', *Int Braz J Urol,* 38(6), 842-54.

Faulkner, P., Kuzio, J., Williams, G. V. and Wilson, J. A. (1997) 'Analysis of p74, a PDV envelope protein of Autographa californica nucleopolyhedrovirus required for occlusion body infectivity in vivo.', *J Gen Virol,* 78 (Pt 12), 3091-100.

Federici, B. A. and Hice, R. H. (1997) 'Organization and molecular characterization of genes in the polyhedrin region of the Anagrapha falcifera multinucleocapsid NPV.', *Arch Virol,* 142(2), 333-48.

Feldherr, C. M., Akin, D. and Cohen, R. J. (2001) 'Regulation of functional nuclear pore size in fibroblasts', *J Cell Sci,* 114(Pt 24), 4621-7.

Fennell, J. P., Brosnan, M. J., Frater, A. J., Hamilton, C. A., Alexander, M. Y., Nicklin, S. A., Heistad, D. D., Baker, A. H. and Dominiczak, A. F. (2002) 'Adenovirus-mediated overexpression of extracellular superoxide dismutase improves endothelial dysfunction in a rat model of hypertension', *Gene Ther,* 9(2), 110-7.

Ferenbach, D. A., Kluth, D. C. and Hughes, J. (2010) 'Hemeoxygenase-1 and renal ischaemia-reperfusion injury', *Nephron Exp Nephrol,* 115(3), e33-7.

Ferreyra, C., Vargas, F., Rodríguez-Gómez, I., Pérez-Abud, R., O'Valle, F. and Osuna, A. (2013) 'Preconditioning with triiodothyronine improves the clinical signs and acute tubular necrosis induced by ischemia/reperfusion in rats', *PLoS One,* 8(9), e74960.

Fraser, M. J., Brusca, J. S., Smith, G. E. and Summers, M. D. (1985) 'Transposon-mediated mutagenesis of a baculovirus', *Virology,* 145(2), 356-61.

Fraser, M. J., Smith, G. E. and Summers, M. D. (1983) 'Acquisition of host cell DNA sequences by baculoviruses: relationship between host DNA insertions and FP mutants of Autographa cMifornica and Galleria mellonella nuclear polyhedrosis viruses. ', *Journal of Virology* 47, 287-300.

Fuchs, L. Y., Woods, M. S. and Weaver, R. F. (1983) 'Viral Transcription During Autographa californica Nuclear Polyhedrosis Virus Infection: a Novel RNA Polymerase Induced in Infected Spodoptera frugiperda Cells.', *J Virol,* 48(3), 641-6.

Fukai, T. and Ushio-Fukai, M. (2011) 'Superoxide dismutases: role in redox signaling, vascular function, and diseases', *Antioxid Redox Signal,* 15(6), 1583-606.

Fukui, M. and Zhu, B. T. (2010) 'Mitochondrial superoxide dismutase SOD2, but not cytosolic SOD1, plays a critical role in protection against glutamate-induced oxidative stress and cell death in HT22 neuronal cells', *Free Radic Biol Med,* 48(6), 821-30.

Funk, C. J., Braunagel, S. C. and Rohrmann, G. F. (1997) *Baculovirus structure,* In *The Baculoviruses*.

Geisler, C. and Jarvis, D. L. (2010) 'Identification of genes encoding N-glycan processing beta-N-acetylglucosaminidases in Trichoplusia ni and Bombyx mori: Implications for glycoengineering of bac5ulovirus expression systems', *Biotechnol Prog,* 26(1), 34-44.

Geisse, S. and Voedisch, B. (2012) 'Transient expression technologies: past, present, and future', *Methods Mol Biol,* 899, 203-19.

Gentilomi, G., Lelli, R., D'Angelo, M., Langella, V., Monaco, F., Portanti, O., Luciani, M., Mirasoli, M., Roda, A., Zerbini, M. and Musiani, M. (2006) 'Expression of bioactive recombinant bovine interferon-gamma using baculovirus', *New Microbiol,* 29(1), 19-24.

Georgopoulos, L. J., Elgue, G., Sanchez, J., Dussupt, V., Magotti, P., Lambris, J. D., Tötterman, T. H., Maitland, N. J. and Nilsson, B. (2009) 'Preclinical evaluation of innate

immunity to baculovirus gene therapy vectors in whole human blood', *Mol Immunol,* 46(15), 2911-7.

Gerster, P., Kopecky, E. M., Hammerschmidt, N., Klausberger, M., Krammer, F., Grabherr, R., Mersich, C., Urbas, L., Kramberger, P., Paril, T., Schreiner, M., Nöbauer, K., Razzazi-Fazeli, E. and Jungbauer, A. (2013) 'Purification of infective baculoviruses by monoliths', *J Chromatogr A,* 1290, 36-45.

Ghadiani, M. H., Peyrovi, S., Mousavinasab, S. N. and Jalalzadeh, M. (2012) 'Delayed graft function, allograft and patient srvival in kidney transplantation', *Arab J Nephrol Transplant,* 5(1), 19-24.

Ghosh, M. K., Borca, M. V. and Roy, P. (2002) 'Virus-derived tubular structure displaying foreign sequences on the surface elicit CD4+ Th cell and protective humoral responses', *Virology,* 302(2), 383-92.

Giacca, M. and Zacchigna, S. (2012) 'Virus-mediated gene delivery for human gene therapy', *J Control Release,* 161(2), 377-88.

Giraud, S., Favreau, F., Chatauret, N., Thuillier, R., Maiga, S. and Hauet, T. (2011) 'Contribution of large pig for renal ischemia-reperfusion and transplantation studies: the preclinical model', *J Biomed Biotechnol,* 2011, 532127.

Gobé, G., Zhang, X. J., Willgoss, D. A., Schoch, E., Hogg, N. A. and Endre, Z. H. (2000) 'Relationship between expression of Bcl-2 genes and growth factors in ischemic acute renal failure in the rat', *J Am Soc Nephrol,* 11(3), 454-67.

Gombart, A. F., Pearson, M. N., Rohrmann, G. F. and Beaudreau, G. S. (1989) 'A baculovirus polyhedral envelope-associated protein: genetic location, nucleotide sequence, and immunocytochemical characterization.', *Virology,* 169(1), 182-93.

Goode, N. P., Shires, M. and Davison, A. M. (1996) 'The glomerular basement membrane charge-selectivity barrier: an oversimplified concept?', *Nephrol Dial Transplant,* 11(9), 1714-6.

Gorman, C. M., Howard, B. H. and Reeves, R. (1983) 'Expression of recombinant plasmids in mammalian cells is enhanced by sodium butyrate', *Nucleic Acids Res,* 11(21), 7631-48.

Gosnell, H., Kasman, L. M., Potta, T., Vu, L., Garrett-Mayer, E., Rege, K. and Voelkel-Johnson, C. (2014) 'Polymer-enhanced delivery increases adenoviral gene expression in an orthotopic model of bladder cancer', *J Control Release,* 176, 35-43.

Goswami, M., Mangoli, S. H. and Jawali, N. (2007) 'Effects of glutathione and ascorbic acid on streptomycin sensitivity of Escherichia coli', *Antimicrob Agents Chemother,* 51(3), 1119-22.

Grabherr, R. and Ernst, W. (2001) 'The baculovirus expression system as a tool for generating diversity by viral surface display', *Comb Chem High Throughput Screen,* 4(2), 185-92.

Granados, R. R., Li, G. X., Derksen, A. C. G. and McKenna, K. A. (1994) 'A new insect cell line from Trichoplusia ni (BTI-Tn-5B1-4) susceptible to Trichoplusia ni single enveloped nuclear polyhedrosis virus. ', *Journal of Invertebrate Pathology* 64, 260-266.

Greene, E. L. and Paller, M. S. (1992) 'Xanthine oxidase produces O2-. in posthypoxic injury of renal epithelial cells', *Am J Physiol,* 263(2 Pt 2), F251-5.

Greene, E. L. and Paller, M. S. (1994) 'Calcium and free radicals in hypoxia/reoxygenation injury of renal epithelial cells', *Am J Physiol,* 266(1 Pt 2), F13-20.

Greger, R. (1985) 'Ion transport mechanisms in thick ascending limb of Henle's loop of mammalian nephron', *Physiol Rev,* 65(3), 760-97.

Grein, T. A., Michalsky, R., Vega López, M. and Czermak, P. (2012) 'Purification of a recombinant baculovirus of Autographa californica M nucleopolyhedrovirus by ion exchange membrane chromatography', *J Virol Methods,* 183(2), 117-24.

Gröner, A., Granados, R. R. and Burand, J. P. (1984) 'Interaction of Autographa californica nuclear polyhedrosis virus with two nonpermissive cell lines', *Intervirology,* 21(4), 203-9.

Guarino, L. A. and Smith, M. W. (1990) 'Nucleotide sequence and characterization of the 39K gene region of Autographa californica nuclear polyhedrosis virus', *Virology,* 179(1), 1-8.

Guo, R., Zhang, Y., Liang, S., Xu, H., Zhang, M. and Li, B. (2010) 'Sodium butyrate enhances the expression of baculovirus-mediated sodium/iodide symporter gene in A549 lung adenocarcinoma cells', *Nucl Med Commun,* 31(10), 916-21.

Gusella, G. L., Fedorova, E., Marras, D., Klotman, P. E. and Klotman, M. E. (2002) 'In vivo gene transfer to kidney by lentiviral vector', *Kidney Int,* 61(1 Suppl), S32-6.

Guyton, A. C. (1991) 'Abnormal renal function and autoregulation in essential hypertension', *Hypertension,* 18(5 Suppl), III49-53.

Halestrap, A. P. and Pasdois, P. (2009) 'The role of the mitochondrial permeability transition pore in heart disease', *Biochim Biophys Acta,* 1787(11), 1402-15.

Harrison, R. L. and Jarvis, D. L. (2006) 'Protein N-glycosylation in the baculovirus-insect cell expression system and engineering of insect cells to produce "mammalianized" recombinant glycoproteins', *Adv Virus Res,* 68, 159-91.

Heikkila, P., Parpala, T., Lukkarinen, O., Weber, M. and Tryggvason, K. (1996) 'Adenovirus-mediated gene transfer into kidney glomeruli using an ex vivo and in vivo kidney perfusion system - first steps towards gene therapy of Alport syndrome', *Gene Ther,* 3(1), 21-7.

Heikura, T., Nieminen, T., Roschier, M. M., Karvinen, H., Kaikkonen, M. U., Mähönen, A. J., Lesch, H. P., Rissanen, T. T., Laitinen, O. H., Airenne, K. J. and Ylä-Herttuala, S. (2012) 'Baculovirus-mediated vascular endothelial growth factor-D(ΔNΔC) gene transfer induces angiogenesis in rabbit skeletal muscle', *J Gene Med,* 14(1), 35-43.

Hendrick, V., Winnepenninckx, P., Abdelkafi, C., Vandeputte, O., Cherlet, M., Marique, T., Renemann, G., Loa, A., Kretzmer, G. and Werenne, J. (2001) 'Increased productivity of recombinant tissular plasminogen activator (t-PA) by butyrate and shift of temperature: a cell cycle phases analysis', *Cytotechnology,* 36(1-3), 71-83.

Henke, W., Jung, K. and Polster, F. (1995) 'Effects of preservation solutions on cortical and medullary mitochondria of rat kidney', *Cell Mol Biol (Noisy-le-grand),* 41(2), 319-26.

Herniou, E. A. and Jehle, J. A. (2007) 'Baculovirus phylogeny and evolution', *Curr Drug Targets,* 8(10), 1043-50.

Hervas-Stubbs, S., Rueda, P., Lopez, L. and Leclerc, C. (2007) 'Insect baculoviruses strongly potentiate adaptive immune responses by inducing type I IFN', *J Immunol,* 178(4), 2361-9.

Heyman, S. N., Evans, R. G., Rosen, S. and Rosenberger, C. (2012) 'Cellular adaptive changes in AKI: mitigating renal hypoxic injury', *Nephrol Dial Transplant,* 27(5), 1721-8.

Hillar, A. and Jarvis, D. L. (2010) 'Re-visiting the endogenous capacity for recombinant glycoprotein sialylation by baculovirus-infected Tn-4h and DpN1 cells', *Glycobiology,* 20(10), 1323-30.

Hinnebusch, B. F., Meng, S., Wu, J. T., Archer, S. Y. and Hodin, R. A. (2002) 'The effects of short-chain fatty acids on human colon cancer cell phenotype are associated with histone hyperacetylation', *J Nutr,* 132(5), 1012-7.

Hitchman, R. B., Locanto, E., Possee, R. D. and King, L. A. (2011) 'Optimizing the baculovirus expression vector system', *Methods,* 55(1), 52-7.

Hitchman, R. B., Possee, R. D., Crombie, A. T., Chambers, A., Ho, K., Siaterli, E., Lissina, O., Sternard, H., Novy, R., Loomis, K., Bird, L. E., Owens, R. J. and King, L. A. (2010) 'Genetic modification of a baculovirus vector for increased expression in insect cells', *Cell Biol Toxicol,* 26(1), 57-68.

Hochhauser, E., Kivity, S., Offen, D., Maulik, N., Otani, H., Barhum, Y., Pannet, H., Shneyvays, V., Shainberg, A., Goldshtaub, V., Tobar, A. and Vidne, B. A. (2003) 'Bax ablation protects against myocardial ischemia-reperfusion injury in transgenic mice', *Am J Physiol Heart Circ Physiol,* 284(6), H2351-9.

Hoeberichts, F. A. and Woltering, E. J. (2003) 'Multiple mediators of plant programmed cell death: interplay of conserved cell death mechanisms and plant-specific regulators', *Bioessays,* 25(1), 47-57.

Hofmann, C., Sandig, V., Jennings, G., Rudolph, M., Schlag, P. and Strauss, M. (1995) 'Efficient gene transfer into human hepatocytes by baculovirus vectors.', *Proc Natl Acad Sci U S A,* 92(22), 10099-103.

Hohsfield, L. A., Geley, S., Reindl, M. and Humpel, C. (2013) 'The generation of NGF-secreting primary rat monocytes: a comparison of different transfer methods', *J Immunol Methods,* 391(1-2), 112-24.

Hosgood, S. A., Patel, M. and Nicholson, M. L. (2013) 'The conditioning effect of ex vivo normothermic perfusion in an experimental kidney model', *J Surg Res,* 182(1), 153-60.

Hu, J., Luo, C. X., Chu, W. H., Shan, Y. A., Qian, Z. M., Zhu, G., Yu, Y. B. and Feng, H. (2012) '20-Hydroxyecdysone protects against oxidative stress-induced neuronal injury by scavenging free radicals and modulating NF-κB and JNK pathways', *PLoS One,* 7(12), e50764.

Hu, X., Xu, C., Zhou, X., He, B., Wu, L., Cui, B., Lu, Z. and Jiang, H. (2010) 'WITHDRAWN: Sodium butyrate protects against myocardial ischemia and reperfusion injury by inhibiting high mobility group box 1 protein in rats', *Biomed Pharmacother*.

Hu, Y. C., Tsai, C. T., Chang, Y. J. and Huang, J. H. (2003) 'Enhancement and prolongation of baculovirus-mediated expression in mammalian cells: focuses on strategic infection and feeding', *Biotechnol Prog,* 19(2), 373-9.

Huang, K. L., Wu, C. P., Chen, Y. L., Kang, B. H. and Lin, Y. C. (2003) 'Heat stress attenuates air bubble-induced acute lung injury: a novel mechanism of diving acclimatization', *J Appl Physiol (1985),* 94(4), 1485-90.

Huang, S. and Kamihira, M. (2013) 'Development of hybrid viral vectors for gene therapy', *Biotechnol Adv,* 31(2), 208-23.

Huang, T. T., Carlson, E. J., Kozy, H. M., Mantha, S., Goodman, S. I., Ursell, P. C. and Epstein, C. J. (2001) 'Genetic modification of prenatal lethality and dilated cardiomyopathy in Mn superoxide dismutase mutant mice', *Free Radic Biol Med,* 31(9), 1101-10.

Hull, R. N., Cherry, W. R. and Weaver, G. W. (1976) 'The origin and characteristics of a pig kidney cell strain, LLC-PK', *In Vitro,* 12(10), 670-7.

Hüser, A., Rudolph, M. and Hofmann, C. (2001) 'Incorporation of decay-accelerating factor into the baculovirus envelope generates complement-resistant gene transfer vectors', *Nat Biotechnol,* 19(5), 451-5.

Ilizarov, B. S. (2000) '[Stalin: illnesses, death, and "immortality"]', *Nov Novejsaja Istor,* (6), 125-45.

Isaka, Y., Suzuki, C., Abe, T., Okumi, M., Ichimaru, N., Imamura, R., Kakuta, Y., Matsui, I., Takabatake, Y., Rakugi, H., Shimizu, S. and Takahara, S. (2009) 'Bcl-2 protects tubular epithelial cells from ischemia/reperfusion injury by dual mechanisms', *Transplant Proc,* 41(1), 52-4.

Iwata, M., Herrington, J. and Zager, R. A. (1995) 'Protein synthesis inhibition induces cytoresistance in cultured human proximal tubular (HK-2) cells', *Am J Physiol,* 268(6 Pt 2), F1154-63.

Janssen, U., Thomas, G., Glant, T. and Phillips, A. (2001) 'Expression of inter-alpha-trypsin inhibitor and tumor necrosis factor-stimulated gene 6 in renal proximal tubular epithelial cells', *Kidney Int,* 60(1), 126-36.

Jarad, G. and Miner, J. H. (2009) 'Update on the glomerular filtration barrier', *Curr Opin Nephrol Hypertens,* 18(3), 226-32.

Jehle, J. A., Blissard, G. W., Bonning, B. C., Cory, J. S., Herniou, E. A., Rohrmann, G. F., Theilmann, D. A., Thiem, S. M. and Vlak, J. M. (2006) 'On the classification and nomenclature of baculoviruses: a proposal for revision', *Arch Virol,* 151(7), 1257-66.

Jiang, S. H., Liu, C. F., Zhang, X. L., Xu, X. H., Zou, J. Z., Fang, Y. and Ding, X. Q. (2007) 'Renal protection by delayed ischaemic preconditioning is associated with inhibition of the inflammatory response and NF-kappaB activation', *Cell Biochem Funct,* 25(3), 335-43.

Jin, Y. Y., Yu, X. N., Qu, Z. Y., Zhang, A. A., Xing, Y. L., Jiang, L. X., Shang, L. and Wang, Y. C. (2014) 'Adenovirus type 3 induces platelet activation in vitro', *Mol Med Rep,* 9(1), 370-4.

Jo, S. K., Ko, G. J., Boo, C. S., Cho, W. Y. and Kim, H. K. (2006) 'Heat preconditioning attenuates renal injury in ischemic ARF in rats: role of heat-shock protein 70 on NF-kappaB-mediated inflammation and on tubular cell injury', *J Am Soc Nephrol,* 17(11), 3082-92.

Johnson, F. and Giulivi, C. (2005) 'Superoxide dismutases and their impact upon human health', *Mol Aspects Med,* 26(4-5), 340-52.

Johnson, J. E., Choksi, K. and Widger, W. R. (2003) 'NADH-Ubiquinone oxidoreductase: substrate-dependent oxygen turnover to superoxide anion as a function of flavin mononucleotide', *Mitochondrion,* 3(2), 97-110.

Ju, X. D., Lou, S. Q., Wang, W. G., Peng, J. Q. and Tian, H. (2004) 'Effect of hydroxyurea and etoposide on transduction of human bone marrow mesenchymal stem and progenitor cell by adeno-associated virus vectors', *Acta Pharmacol Sin,* 25(2), 196-202.

Kaikkonen, M. U., Maatta, A. I., Ylä-Herttuala, S. and Airenne, K. J. (2010) 'Screening of complement inhibitors: shielded baculoviruses increase the safety and efficacy of gene delivery', *Mol Ther,* 18(5), 987-92.

Kaname, Y., Tani, H., Kataoka, C., Shiokawa, M., Taguwa, S., Abe, T., Moriishi, K., Kinoshita, T. and Matsuura, Y. (2010) 'Acquisition of complement resistance through incorporation of CD55/decay-accelerating factor into viral particles bearing baculovirus GP64', *J Virol,* 84(7), 3210-9.

Kasahara, E., Lin, L. R., Ho, Y. S. and Reddy, V. N. (2005) 'SOD2 protects against oxidation-induced apoptosis in mouse retinal pigment epithelium: implications for age-related macular degeneration', *Invest Ophthalmol Vis Sci,* 46(9), 3426-34.

Kataoka, C., Kaname, Y., Taguwa, S., Abe, T., Fukuhara, T., Tani, H., Moriishi, K. and Matsuura, Y. (2012) 'Baculovirus GP64-mediated entry into mammalian cells', *J Virol,* 86(5), 2610-20.

Kato, T., Suzuki, F. and Park, E. Y. (2011) 'Purification of functional baculovirus particles from silkworm larval hemolymph and their use as nanoparticles for the detection of human prorenin receptor (PRR) binding', *BMC Biotechnol,* 11, 60.

Kawahara, M. and Takaku, H. (2013) 'Intradermal immunization with combined baculovirus and tumor cell lysate induces effective antitumor immunity in mice', *Int J Oncol,* 43(6), 2023-30.

Kelley, V. R. and Sukhatme, V. P. (1999) 'Gene transfer in the kidney', *Am J Physiol,* 276(1 Pt 2), F1-9.

Kennedy, S. E. and Erlich, J. H. (2008) 'Murine renal ischaemia-reperfusion injury', *Nephrology (Carlton),* 13(5), 390-6.

Khalfoun, B., Barrat, D., Watier, H., Machet, M. C., Arbeille-Brassart, B., Riess, J. G., Salmon, H., Gruel, Y., Bardos, P. and Lebranchu, Y. (2000) 'Development of an ex vivo model of pig kidney perfused with human lymphocytes. Analysis of xenogeneic cellular reactions', *Surgery,* 128(3), 447-57.

Kim, S. M., Ahn, S., Min, S. I., Park, D., Park, T., Min, S. K., Kim, S. J. and Ha, J. (2013) 'Cold ischemic time is critical in outcomes of expanded criteria donor renal transplantation', *Clin Transplant,* 27(1), 132-9.

Kioukia, N., Nienow, A. W., Emery, A. N. and al-Rubeai, M. (1995) 'Physiological and environmental factors affecting the growth of insect cells and infection with baculovirus', *J Biotechnol,* 38(3), 243-51.

Kitts, P. A., Ayres, M. D. and Possee, R. D. (1990) 'Linearization of baculovirus DNA enhances the recovery of recombinant virus expression vectors.', *Nucleic Acids Res,* 18(19), 5667-72.

Kitts, P. A. and Possee, R. D. (1993) 'A method for producing recombinant baculovirus expression vectors at high frequency.', *Biotechniques,* 14(5), 810-7.

Knobil, K., Choi, A. M., Weigand, G. W. and Jacoby, D. B. (1998) 'Role of oxidants in influenza virus-induced gene expression', *Am J Physiol,* 274(1 Pt 1), L134-42.

Kokko, J. P. (1970) 'Sodium chloride and water transport in the descending limb of Henle', *J Clin Invest,* 49(10), 1838-46.

Kondo, T., Matsuda, T., Tashima, M., Umehara, H., Domae, N., Yokoyama, K., Uchiyama, T. and Okazaki, T. (2000) 'Suppression of heat shock protein-70 by ceramide in heat shock-induced HL-60 cell apoptosis', *J Biol Chem,* 275(12), 8872-9.

Koo, H. C., Davis, J. M., Li, Y., Hatzis, D., Opsimos, H., Pollack, S., Strayer, M. S., Ballard, P. L. and Kazzaz, J. A. (2005) 'Effects of transgene expression of superoxide dismutase and glutathione peroxidase on pulmonary epithelial cell growth in hyperoxia', *Am J Physiol Lung Cell Mol Physiol,* 288(4), L718-26.

Koo, H. P., Bunchman, T. E., Flynn, J. T., Punch, J. D., Schwartz, A. C. and Bloom, D. A. (1999) 'Renal transplantation in children with severe lower urinary tract dysfunction', *J Urol,* 161(1), 240-5.

Kool, M., Voncken, J. W., van Lier, F. L., Tramper, J. and Vlak, J. M. (1991) 'Detection and analysis of Autographa californica nuclear polyhedrosis virus mutants with defective interfering properties', *Virology,* 183(2), 739-46.

Kost, T. A. and Condreay, J. P. (2002) 'Recombinant baculoviruses as mammalian cell gene-delivery vectors', *Trends Biotechnol,* 20(4), 173-80.

Kost, T. A., Condreay, J. P. and Ames, R. S. (2010) 'Baculovirus gene delivery: a flexible assay development tool', *Curr Gene Ther,* 10(3), 168-73.

Kost, T. A., Condreay, J. P. and Jarvis, D. L. (2005) 'Baculovirus as versatile vectors for protein expression in insect and mammalian cells.', *Nat Biotechnol,* 23(5), 567-75.

Kozopas, K. M., Yang, T., Buchan, H. L., Zhou, P. and Craig, R. W. (1993) 'MCL1, a gene expressed in programmed myeloid cell differentiation, has sequence similarity to BCL2', *Proc Natl Acad Sci U S A,* 90(8), 3516-20.

Kulah, E., Tascilar, O., Acikgoz, S., Tekin, I. O., Karadeniz, G., Can, M., Gun, B., Barut, F. and Comert, M. (2007) 'Oxidized LDL accumulation in experimental renal ischemia reperfusion injury model', *Ren Fail,* 29(4), 409-15.

Kumar, S., Allen, D. A., Kieswich, J. E., Patel, N. S., Harwood, S., Mazzon, E., Cuzzocrea, S., Raftery, M. J., Thiemermann, C. and Yaqoob, M. M. (2009) 'Dexamethasone ameliorates renal ischemia-reperfusion injury', *J Am Soc Nephrol,* 20(11), 2412-25.

Kunzendorf, U., Haase, M., Rölver, L. and Haase-Fielitz, A. (2010) 'Novel aspects of pharmacological therapies for acute renal failure', *Drugs,* 70(9), 1099-114.

Kuzmuk. KN. Schook, LB. (2011) 'Pigs as a Model for Biomedical Sciences', *CAB International. The Genetics of the Pig*, 426-444.

Laakkonen, J. P., Mäkelä, A. R., Kakkonen, E., Turkki, P., Kukkonen, S., Peränen, J., Ylä-Herttuala, S., Airenne, K. J., Oker-Blom, C., Vihinen-Ranta, M. and Marjomäki, V. (2009) 'Clathrin-independent entry of baculovirus triggers uptake of E. coli in non-phagocytic human cells', *PLoS One,* 4(4), e5093.

Lameire, N. (2013) 'The definitions and staging systems of acute kidney injury and their limitations in practice', *Arab J Nephrol Transplant,* 6(3), 145-52.

Land, W., Schneeberger, H., Schleibner, S., Illner, W. D., Abendroth, D., Rutili, G., Arfors, K. E. and Messmer, K. (1994) 'The beneficial effect of human recombinant superoxide dismutase on acute and chronic rejection events in recipients of cadaveric renal transplants', *Transplantation,* 57(2), 211-7.

Lanuti, M., Kouri, C. E., Force, S., Chang, M., Amin, K., Xu, K., Blair, I., Kaiser, L. and Albelda, S. (1999) 'Use of protamine to augment adenovirus-mediated cancer gene therapy', *Gene Ther,* 6(9), 1600-10.

Lawrence, M. S., Ho, D. Y., Sun, G. H., Steinberg, G. K. and Sapolsky, R. M. (1996) 'Overexpression of Bcl-2 with herpes simplex virus vectors protects CNS neurons against neurological insults in vitro and in vivo', *J Neurosci,* 16(2), 486-96.

Lee, C. Y. and Mangino, M. J. (2009) 'Preservation methods for kidney and liver', *Organogenesis,* 5(3), 105-12.

Lee, H. and Krell, P. J. (1994) 'Reiterated DNA fragments in defective genomes of Autographa californica nuclear polyhedrosis virus are competent for AcMNPV-dependent DNA replication', *Virology,* 202(1), 418-29.

Lee, H. T. and Emala, C. W. (2002) 'Characterization of adenosine receptors in human kidney proximal tubule (HK-2) cells', *Exp Nephrol,* 10(5-6), 383-92.

Levine, B. L., Humeau, L. M., Boyer, J., MacGregor, R. R., Rebello, T., Lu, X., Binder, G. K., Slepushkin, V., Lemiale, F., Mascola, J. R., Bushman, F. D., Dropulic, B. and June, C. H. (2006) 'Gene transfer in humans using a conditionally replicating lentiviral vector', *Proc Natl Acad Sci U S A,* 103(46), 17372-7.

Levonen, A. L., Vähäkangas, E., Koponen, J. K. and Ylä-Herttuala, S. (2008) 'Antioxidant gene therapy for cardiovascular disease: current status and future perspectives', *Circulation,* 117(16), 2142-50.

Li, S. F., Wang, H. L., Hu, Z. H. and Deng, F. (2012) 'Genetic modification of baculovirus expression vectors', *Virol Sin,* 27(2), 71-82.

Liang, H. L., Hilton, G., Mortensen, J., Regner, K., Johnson, C. P. and Nilakantan, V. (2009) 'MnTMPyP, a cell-permeant SOD mimetic, reduces oxidative stress and apoptosis following renal ischemia-reperfusion', *Am J Physiol Renal Physiol,* 296(2), F266-76.

Liang, Q., Yu, X., Qu, S., Xu, H. and Sui, D. (2010) 'Acanthopanax senticosides B ameliorates oxidative damage induced by hydrogen peroxide in cultured neonatal rat cardiomyocytes', *Eur J Pharmacol,* 627(1-3), 209-15.

Liang, X., Wang, R. S., Wang, F., Liu, S., Guo, F., Sun, L., Wang, Y. J., Sun, Y. X. and Chen, X. L. (2013) 'Sodium butyrate protects against severe burn-induced remote acute lung injury in rats', *PLoS One,* 8(7), e68786.

Licari, P. and Bailey, J. E. (1991) 'Factors influencing recombinant protein yields in an insect cell-bacuiovirus expression system: multiplicity of infection and intracellular protein degradation', *Biotechnol Bioeng,* 37(3), 238-46.

Linkermann, A., De Zen, F., Weinberg, J., Kunzendorf, U. and Krautwald, S. (2012) 'Programmed necrosis in acute kidney injury', *Nephrol Dial Transplant,* 27(9), 3412-9.

Liochev, S. I. and Fridovich, I. (1999) 'The relative importance of HO* and ONOO- in mediating the toxicity of O*-', *Free Radic Biol Med,* 26(5-6), 777-8.

Liu, H., McTaggart, S. J., Johnson, D. W. and Gobe, G. C. (2012) 'Original article anti-oxidant pathways are stimulated by mesenchymal stromal cells in renal repair after ischemic injury', *Cytotherapy,* 14(2), 162-72.

Long, G., Pan, X., Kormelink, R. and Vlak, J. M. (2006) 'Functional entry of baculovirus into insect and mammalian cells is dependent on clathrin-mediated endocytosis', *J Virol,* 80(17), 8830-3.

Lorenzen, N. D., Stilling, M., Ulrich-Vinther, M., Trolle-Andersen, N., Prynø, T., Søballe, K. and Birke-Sørensen, H. (2013) 'Increased post-operative ischemia in the femoral head found by microdialysis by the posterior surgical approach: a randomized clinical trial comparing surgical approaches in hip resurfacing arthroplasty', *Arch Orthop Trauma Surg,* 133(12), 1735-45.

Lu, A. and Carstens, E. B. (1992) 'Nucleotide sequence and transcriptional analysis of the p80 gene of Autographa californica nuclear polyhedrosis virus: a homologue of the Orgyia pseudotsugata nuclear polyhedrosis virus capsid-associated gene', *Virology,* 190(1), 201-9.

Luckow, V. A., Lee, S. C., Barry, G. F. and Olins, P. O. (1993) 'Efficient generation of infectious recombinant baculoviruses by site-specific transposon-mediated insertion of foreign genes into a baculovirus genome propagated in Escherichia coli', *J Virol,* 67(8), 4566-79.

Luh, S. P., Kuo, P. H., Kuo, T. F., Tsai, T. P., Tsao, T. C., Chen, J. Y., Tsai, C. H. and Yang, P. C. (2007) 'Effects of thermal preconditioning on the ischemia-reperfusion-induced acute lung injury in minipigs', *Shock,* 28(5), 615-22.

Luo, P., Wang, N., He, E., Eriksson, S., Zhou, J., Hu, G., Zhang, J. and Skog, S. (2010) 'The proliferation marker thymidine kinase 1 level is high in normal kidney tubule cells compared to other normal and malignant renal cells', *Pathol Oncol Res,* 16(2), 277-83.

Luo, W. Y., Shih, Y. S., Hung, C. L., Lo, K. W., Chiang, C. S., Lo, W. H., Huang, S. F., Wang, S. C., Yu, C. F., Chien, C. H. and Hu, Y. C. (2012) 'Development of the hybrid Sleeping Beauty: baculovirus vector for sustained gene expression and cancer therapy', *Gene Ther,* 19(8), 844-51.

Lynn, D. E. (2003) 'Comparative susceptibilities of insect cell lines to infection by the occlusion-body derived phenotype of baculoviruses', *J Invertebr Pathol,* 83(3), 215-22.

Lynn, D. E. and Hink, W. F. (1978) 'Cell cycle analysis and synchronization of the TN-368 insect cell line', *In Vitro,* 14(2), 236-8.

Machado, R. A., Constantino, L. e. S., Tomasi, C. D., Rojas, H. A., Vuolo, F. S., Vitto, M. F., Cesconetto, P. A., de Souza, C. T., Ritter, C. and Dal-Pizzol, F. (2012) 'Sodium butyrate decreases the activation of NF-κB reducing inflammation and oxidative damage in the kidney of rats subjected to contrast-induced nephropathy', *Nephrol Dial Transplant,* 27(8), 3136-40.

Majors, B. S., Betenbaugh, M. J., Pederson, N. E. and Chiang, G. G. (2008) 'Enhancement of transient gene expression and culture viability using Chinese hamster ovary cells overexpressing Bcl-x(L)', *Biotechnol Bioeng,* 101(3), 567-78.

Makkonen, K. E., Turkki, P., Laakkonen, J. P., Ylä-Herttuala, S., Marjomäki, V. and Airenne, K. J. (2013) '6-o- and N-sulfated syndecan-1 promotes baculovirus binding and entry into Mammalian cells', *J Virol,* 87(20), 11148-59.

Mancuso, K., Hauswirth, W. W., Li, Q., Connor, T. B., Kuchenbecker, J. A., Mauck, M. C., Neitz, J. and Neitz, M. (2009) 'Gene therapy for red-green colour blindness in adult primates', *Nature,* 461(7265), 784-7.

Mangino, M. J., Ametani, M., Szabó, C. and Southard, J. H. (2004) 'Poly(ADP-ribose) polymerase and renal hypothermic preservation injury', *Am J Physiol Renal Physiol,* 286(5), F838-47.

Mao, G. D., Thomas, P. D., Lopaschuk, G. D. and Poznansky, M. J. (1993) 'Superoxide dismutase (SOD)-catalase conjugates. Role of hydrogen peroxide and the Fenton reaction in SOD toxicity', *J Biol Chem,* 268(1), 416-20.

Matevossian, E., Kern, H., Hüser, N., Doll, D., Snopok, Y., Nährig, J., Altomonte, J., Sinicina, I., Friess, H. and Thorban, S. (2009) 'Surgeon Yurii Voronoy (1895-1961) - a pioneer in the history of clinical transplantation: in memoriam at the 75th anniversary of the first human kidney transplantation', *Transpl Int,* 22(12), 1132-9.

Matilainen, H., Rinne, J., Gilbert, L., Marjomäki, V., Reunanen, H. and Oker-Blom, C. (2005) 'Baculovirus entry into human hepatoma cells', *J Virol,* 79(24), 15452-9.

Matsumoto, N., Riley, S., Fraser, D., Al-Assaf, S., Ishimura, E., Wolever, T., Phillips, G. O. and Phillips, A. O. (2006) 'Butyrate modulates TGF-beta1 generation and function: potential renal benefit for Acacia(sen) SUPERGUM (gum arabic)?', *Kidney Int,* 69(2), 257-65.

Matthews, Q. L. and Curiel, D. T. (2007) 'Gene therapy: human germline genetic modifications--assessing the scientific, socioethical, and religious issues', *South Med J,* 100(1), 98-100.

McCord, J. M. and Fridovich, I. (1969) 'The utility of superoxide dismutase in studying free radical reactions. I. Radicals generated by the interaction of sulfite, dimethyl sulfoxide, and oxygen', *J Biol Chem,* 244(22), 6056-63.

McCormick, P. H., Chen, G., Tlerney, S., Kelly, C. J. and Bouchier-Hayes, D. J. (2003) 'Clinically relevant thermal preconditioning attenuates ischemia-reperfusion injury', *J Surg Res,* 109(1), 24-30.

McIntosh, A. H. and Ignoffo, C. M. (1989) 'Replication of Autographa californica nuclear polyhedrosis virus in five lepidopteran cell lines', *J. Invertebr. Pathol.,* 54, 97–102.

Mehta, M., Darling, R. C., Roddy, S. P., Ozsvath, K. J., Kreienberg, P. B., Paty, P. S., Chang, B. B., Resnikoff, M. and Shah, D. M. (2004) 'Outcome of concomitant renal artery reconstructions in patients with aortic aneurysm and occlusive disease', *Vascular,* 12(6), 381-6.

Meijer, K., de Vos, P. and Priebe, M. G. (2010) 'Butyrate and other short-chain fatty acids as modulators of immunity: what relevance for health?', *Curr Opin Clin Nutr Metab Care,* 13(6), 715-21.

Michalsky, R., Pfromm, P. H., Czermak, P., Sorensen, C. M. and Passarelli, A. L. (2008) 'Effects of temperature and shear force on infectivity of the baculovirus Autographa californica M nucleopolyhedrovirus', *J Virol Methods,* 153(2), 90-6.

Miller, L. K. (1997) *The baculoviruses.,* Plenum. Press. New York.

Miller, L. K. and Lu, A. (1997) The molecular basis of baculovirus host range*. The Baculoviruses*, Plenum Press, New York ed.

Miner, J. H. (2012) 'The glomerular basement membrane', *Exp Cell Res,* 318(9), 973-8.

Misra, S. (2013) 'Human gene therapy: a brief overview of the genetic revolution', *J Assoc Physicians India,* 61(2), 127-33.

Miyakawa, A. A., Dallan, L. A., Lacchini, S., Borin, T. F. and Krieger, J. E. (2008) 'Human saphenous vein organ culture under controlled hemodynamic conditions', *Clinics (Sao Paulo),* 63(5), 683-8.

Mizuno, M. and Yoshida, J. (1998) 'Improvement of transduction efficiency of recombinant adeno-associated virus vector by entrapment in multilamellar liposomes', *Jpn J Cancer Res,* 89(4), 352-4.

Moers, C., Smits, J. M., Maathuis, M. H., Treckmann, J., van Gelder, F., Napieralski, B. P., van Kasterop-Kutz, M., van der Heide, J. J., Squifflet, J. P., van Heurn, E., Kirste, G. R., Rahmel, A., Leuvenink, H. G., Paul, A., Pirenne, J. and Ploeg, R. J. (2009) 'Machine

perfusion or cold storage in deceased-donor kidney transplantation', *N Engl J Med,* 360(1), 7-19.

Mohan, C., Park, S. H., Chung, J. Y. and Lee, G. M. (2007) 'Effect of doxycycline-regulated protein disulfide isomerase expression on the specific productivity of recombinant CHO cells: thrombopoietin and antibody', *Biotechnol Bioeng,* 98(3), 611-5.

Monteiro, F., Carinhas, N., Carrondo, M. J., Bernal, V. and Alves, P. M. (2012) 'Toward system-level understanding of baculovirus-host cell interactions: from molecular fundamental studies to large-scale proteomics approaches', *Front Microbiol,* 3, 391.

Morris, P. J. (2004) 'Transplantation--a medical miracle of the 20th century', *N Engl J Med,* 351(26), 2678-80.

Murguía-Meca, F., Plata-Muñoz, J. J., Hitchman, R. B., Danquah, J. O., Hughes, D., Friend, P. J., Fuggle, S. V. and King, L. A. (2011) 'Baculovirus as delivery system for gene transfer during hypothermic organ preservation', *Transpl Int,* 24(8), 820-8.

Murphy, E. and Steenbergen, C. (2008) 'Mechanisms underlying acute protection from cardiac ischemia-reperfusion injury', *Physiol Rev,* 88(2), 581-609.

Murray, J. E., Tilney, N. L. and Wilson, R. E. (1976) 'Renal transplantation: a twenty-five year experience', *Ann Surg,* 184(5), 565-73.

Murry, C. E., Jennings, R. B. and Reimer, K. A. (1986) 'Preconditioning with ischemia: a delay of lethal cell injury in ischemic myocardium', *Circulation,* 74(5), 1124-36.

Muto, S. (2001) 'Potassium transport in the mammalian collecting duct', *Physiol Rev,* 81(1), 85-116.

Nahreini, P., AJ., H. and K, P. (2003) 'High-Yield Production of Recombinant Antibody Fragments in HEK-293 Cells Using SodiumButyrate', *BioTechniques,* 34, 968-972.

Nakhoul, N. and Batuman, V. (2011) 'Role of proximal tubules in the pathogenesis of kidney disease', *Contrib Nephrol,* 169, 37-50.

Namura, S., Zhu, J., Fink, K., Endres, M., Srinivasan, A., Tomaselli, K. J., Yuan, J. and Moskowitz, M. A. (1998) 'Activation and cleavage of caspase-3 in apoptosis induced by experimental cerebral ischemia', *J Neurosci,* 18(10), 3659-68.

Nanmoku, K., Kawano, M., Iwasaki, Y. and Ikenaka, K. (2003) 'Highly efficient gene transduction into the brain using high-titer retroviral vectors', *Dev Neurosci,* 25(2-4), 152-61.

Nath, K. A. and Norby, S. M. (2000) 'Reactive oxygen species and acute renal failure', *Am J Med,* 109(8), 665-78.

Ni, L., Li, T., Liu, B., Song, X., Yang, G., Wang, L., Miao, S. and Liu, C. (2013) 'The protective effect of Bcl-xl overexpression against oxidative stress-induced vascular endothelial cell injury and the role of the Akt/eNOS pathway', *Int J Mol Sci,* 14(11), 22149-62.

Nose, K. (2000) 'Role of reactive oxygen species in the regulation of physiological functions', *Biol Pharm Bull,* 23(8), 897-903.

Nudelman, A., Ruse, M., Aviram, A., Rabizadeh, E., Shaklai, M., Zimrah, Y. and Rephaeli, A. (1992) 'Novel anticancer prodrugs of butyric acid. 2', *J Med Chem,* 35(4), 687-94.

Obrig, T. G., Culp, W. J., McKeehan, W. L. and Hardesty, B. (1971) 'The mechanism by which cycloheximide and related glutarimide antibiotics inhibit peptide synthesis on reticulocyte ribosomes', *J Biol Chem,* 246(1), 174-81.

Okano, K., Vanarsdall, A. L., Mikhailov, V. S. and Rohrmann, G. F. (2006) 'Conserved molecular systems of the Baculoviridae', *Virology,* 344(1), 77-87.

Oliveira, J. V., de Brito, A. F., Braconi, C. T., de Melo Freire, C. C., Iamarino, A. and de Andrade Zanotto, P. M. (2013 Sep 4;) 'Modularity and evolutionary constraints in baculovirus gene regulatory network. *BMC Syst Biol.,* 7(87).

Oltvai, Z. N., Milliman, C. L. and Korsmeyer, S. J. (1993) 'Bcl-2 heterodimerizes in vivo with a conserved homolog, Bax, that accelerates programmed cell death', *Cell,* 74(4), 609-19.

Oomens, A. G. and Blissard, G. W. (1999) ' Requirement for GP64 to drive efficient budding of Autographa californica multicapsid nucleopolyhedrovirus.', *Virology,* 254, 297-314.

Ortiz, P. A., Hong, N. J., Plato, C. F., Varela, M. and Garvin, J. L. (2003) 'An in vivo method for adenovirus-mediated transduction of thick ascending limbs', *Kidney Int,* 63(3), 1141-9.

Ozbek, E. (2012) 'Induction of oxidative stress in kidney', *Int J Nephrol,* 2012, 465897.

O'Reilly DR, Miller LK and VA, L. (1994) 'Baculovirus Expression Vectors: A Laboratory Manual.' in, WH Freeman and Company; New York:

Ouma, G. O., Rodriguez, E., Muthumani, K., Weiner, D. B., Wilensky, R. L. and Mohler, E. R. (2014) 'In vivo electroporation of constitutively expressed HIF-1α plasmid DNA improves neovascularization in a mouse model of limb ischemia', *J Vasc Surg,* 59(3), 786-93.

Parajuli, N. and MacMillan-Crow, L. A. (2013) 'Role of reduced manganese superoxide dismutase in ischemia-reperfusion injury: a possible trigger for autophagy and mitochondrial biogenesis?', *Am J Physiol Renal Physiol,* 304(3), F257-67.

Parikh, S. V., Nagaraja, H. N., Hebert, L. and Rovin, B. H. (2014) 'Renal flare as a predictor of incident and progressive CKD in patients with lupus nephritis', *Clin J Am Soc Nephrol,* 9(2), 279-84.

Park, S. W., Kim, M., Kim, J. Y., Ham, A., Brown, K. M., Mori-Akiyama, Y., Ouellette, A. J., D'Agati, V. D. and Lee, H. T. (2012) 'Paneth cell-mediated multiorgan dysfunction after acute kidney injury', *J Immunol,* 189(11), 5421-33.

Passarelli, A. L. and Miller, L. K. (1993) 'Three baculovirus genes involved in late and very late gene expression: ie-1, ie-n, and lef-2', *J Virol,* 67(4), 2149-58.

Patterson, R. M., Selkirk, J. K. and Merrick, B. A. (1995) 'Baculovirus and insect cell gene expression: review of baculovirus biotechnology.', *Environ Health Perspect,* 103(7-8), 756-9.

Paul, A., Binsalamah, Z. M., Khan, A. A., Abbasia, S., Elias, C. B., Shum-Tim, D. and Prakash, S. (2011) 'A nanobiohybrid complex of recombinant baculovirus and Tat/DNA nanoparticles for delivery of Ang-1 transgene in myocardial infarction therapy', *Biomaterials,* 32(32), 8304-18.

Paul, A., Elias, C. B., Shum-Tim, D. and Prakash, S. (2013) 'Bioactive baculovirus nanohybrids for stent based rapid vascular re-endothelialization', *Sci Rep,* 3, 2366.

Paul, A., Hasan, A., Rodes, L., Sangaralingam, M. and Prakash, S. (2014) 'Bioengineered baculoviruses as new class of therapeutics using micro and nanotechnologies: principles, prospects and challenges', *Adv Drug Deliv Rev,* 71, 115-30.

Paul, A., Khan, A. A., Shum-Tim, D. and Prakash, S. (2010) 'BacMam virus transduced cardiomyoblasts can be used for myocardial transplantation using AP-PEG-A

microcapsules: molecular cloning, preparation, and in vitro analysis', *J Biomed Biotechnol,* 2010, 858094.

Paul, A., Nayan, M., Khan, A. A., Shum-Tim, D. and Prakash, S. (2012) 'Angiopoietin-1-expressing adipose stem cells genetically modified with baculovirus nanocomplex: investigation in rat heart with acute infarction', *Int J Nanomedicine,* 7, 663-82.

Pearson, M., Bjornson, R., Pearson, G. and Rohrmann, G. (1992) 'The Autographa californica baculovirus genome: evidence for multiple replication origins', *Science,* 257(5075), 1382-4.

Peng, Z. (2005) 'Current status of gendicine in China: recombinant human Ad-p53 agent for treatment of cancers', *Hum Gene Ther,* 16(9), 1016-27.

Peters, T. G., Shaver, T. R., Ames, J. E., Santiago-Delpin, E. A., Jones, K. W. and Blanton, J. W. (1995) 'Cold ischemia and outcome in 17,937 cadaveric kidney transplants', *Transplantation,* 59(2), 191-6.

Philipps, B., Rotmann, D., Wicki, M., Mayr, L. M. and Forstner, M. (2005) 'Time reduction and process optimization of the baculovirus expression system for more efficient recombinant protein production in insect cells', *Protein Expr Purif,* 42(1), 211-8.

Pisani, A., Sabbatini, M., Riccio, E., Rossano, R., Andreucci, M., Capasso, C., De Luca, V., Carginale, V., Bizzarri, M., Borrelli, A., Schiattarella, A., Santangelo, M. and Mancini, A. (2014) 'Effect of a recombinant manganese superoxide dismutase on prevention of contrast-induced acute kidney injury', *Clin Exp Nephrol,* 18(3), 424-31.

Plonsky, I., Cho, M. S., Oomens, A. G., Blissard, G. and Zimmerberg, J. (1999) 'An analysis of the role of the target membrane on the Gp64-induced fusion pore', *Virology,* 253(1), 65-76.

Ponticelli, C. (2014) 'Ischaemia-reperfusion injury: a major protagonist in kidney transplantation', *Nephrol Dial Transplant,* 29(6), 1134-1140.

Popov, S. G., Villasmil, R., Bernardi, J., Grene, E., Cardwell, J., Popova, T., Wu, A., Alibek, D., Bailey, C. and Alibek, K. (2002) 'Effect of Bacillus anthracis lethal toxin on human peripheral blood mononuclear cells', *FEBS Lett,* 527(1-3), 211-5.

Prachar, J., Hlubinová, K., Kovarík, A., Feldsamová, A. and Simkovic, D. (1988) 'Concentration of retroviruses by low-speed centrifugation', *Neoplasma,* 35(6), 651-5.

Prikhod'ko, E. A., Lu, A., Wilson, J. A. and Miller, L. K. (1999) 'In vivo and in vitro analysis of baculovirus ie-2 mutants.', *J Virol,* 73(3), 2460-8.

Qiao, Y. L., Qian, J. M., Wang, F. R., Ma, Z. Y. and Wang, Q. W. (2014) 'Butyrate protects liver against ischemia reperfusion injury by inhibiting nuclear factor kappa B activation in Kupffer cells', *J Surg Res,* 187(2), 653-9.

Quinlan, C. L., Perevoshchikova, I. V., Hey-Mogensen, M., Orr, A. L. and Brand, M. D. (2013) 'Sites of reactive oxygen species generation by mitochondria oxidizing different substrates', *Redox Biol,* 1(1), 304-12.

Radi, R., Cassina, A. and Hodara, R. (2002) 'Nitric oxide and peroxynitrite interactions with mitochondria', *Biol Chem,* 383(3-4), 401-9.

Rahman, N. A., Mori, K., Mizukami, M., Suzuki, T., Takahashi, N. and Ohyama, C. (2009) 'Role of peroxynitrite and recombinant human manganese superoxide dismutase in reducing ischemia-reperfusion renal tissue injury', *Transplant Proc,* 41(9), 3603-10.

Ramirez-Gordillo, D., Trujillo-Provencio, C., Knight, V. B. and Serrano, E. E. (2011) 'Optimization of gene delivery methods in Xenopus laevis kidney (A6) and Chinese hamster ovary (CHO) cell lines for heterologous expression of Xenopus inner ear genes', *In Vitro Cell Dev Biol Anim,* 47(9), 640-52.

Rashidi, A. (2006) 'Risk of diabetes in patients taking thiazide diuretics', *Mayo Clin Proc,* 81(12), 1637-8; author reply 1638.

Rodrigues, T., Carrondo, M. J., Alves, P. M. and Cruz, P. E. (2007) 'Purification of retroviral vectors for clinical application: biological implications and technological challenges', *J Biotechnol,* 127(3), 520-41.

Rodriguez, V. A., M.N, B. and P.D, G. (2012) 'Baculoviruses: Members of Integrated Pest Management Strategies', *Integrated Pest Management and Pest Control - Current and Future Tactics*.

Rogers, S., Lowenthal, A., Terheggen, H. G. and Columbo, J. P. (1973) 'Induction of arginase activity with the Shope papilloma virus in tissue culture cells from an argininemic patient', *J Exp Med,* 137(4), 1091-6.

Rohrmann, G. F. (1992) 'Baculovirus structural proteins.', *J Gen Virol,* 73 (Pt 4), 749-61.

Rohrmann, G. F. (2008) *Baculovirus molecular biology.* .

Rosenberg, S. A., Aebersold, P., Cornetta, K., Kasid, A., Morgan, R. A., Moen, R., Karson, E. M., Lotze, M. T., Yang, J. C. and Topalian, S. L. (1990) 'Gene transfer into humans--immunotherapy of patients with advanced melanoma, using tumor-infiltrating lymphocytes modified by retroviral gene transduction', *N Engl J Med,* 323(9), 570-8.

Rosenberg, S. A., Anderson, W. F., Blaese, M., Hwu, P., Yannelli, J. R., Yang, J. C., Topalian, S. L., Schwartzentruber, D. J., Weber, J. S. and Ettinghausen, S. E. (1993) 'The development of gene therapy for the treatment of cancer', *Ann Surg,* 218(4), 455-63; discussion 463-4.

Russell, R. L., Pearson, M. N. and Rohrmann, G. F. (1991) 'Immunoelectron microscopic examination of Orgyia pseudotsugata multicapsid nuclear polyhedrosis virus-infected Lymantria dispar cells: time course and localization of major polyhedron-associated proteins', *J Gen Virol,* 72 (Pt 2), 275-83.

Russell, W. C. and Kemp, G. D. (1995) 'Role of adenovirus structural components in the regulation of adenovirus infection', *Curr Top Microbiol Immunol,* 199 (Pt 1), 81-98.

Ryan, M. J., Johnson, G., Kirk, J., Fuerstenberg, S. M., Zager, R. A. and Torok-Storb, B. (1994) 'HK-2: an immortalized proximal tubule epithelial cell line from normal adult human kidney', *Kidney Int,* 45(1), 48-57.

Räty, J. K., Liimatainen, T., Huhtala, T., Kaikkonen, M. U., Airenne, K. J., Hakumäki, J. M., Närvänen, A. and Ylä-Herttuala, S. (2007) 'SPECT/CT imaging of baculovirus biodistribution in rat', *Gene Ther,* 14(12), 930-8.

Saba, H., Munusamy, S. and Macmillan-Crow, L. A. (2008) 'Cold preservation mediated renal injury: involvement of mitochondrial oxidative stress', *Ren Fail,* 30(2), 125-33.

Saikumar, P., Dong, Z., Weinberg, J. M. and Venkatachalam, M. A. (1998) 'Mechanisms of cell death in hypoxia/reoxygenation injury', *Oncogene,* 17(25), 3341-9.

Saito, T., Dojima, T., Toriyama, M. and Park, E. Y. (2002) 'The effect of cell cycle on GFPuv gene expression in the baculovirus expression system', *J Biotechnol,* 93(2), 121-9.

Salahudeen, A. K. and May, W. (2008) 'Reduction in cold ischemia time of renal allografts in the United States over the last decade', *Transplant Proc,* 40(5), 1285-9.

Sandig, V., Hofmann, C., Steinert, S., Jennings, G., Schlag, P. and Strauss, M. (1996) 'Gene transfer into hepatocytes and human liver tissue by baculovirus vectors', *Hum Gene Ther,* 7(16), 1937-45.

Sarkis, C., Serguera, C., Petres, S., Buchet, D., Ridet, J. L., Edelman, L. and Mallet, J. (2000) 'Efficient transduction of neural cells in vitro and in vivo by a baculovirus-derived vector', *Proc Natl Acad Sci U S A,* 97(26), 14638-43.

Schneider, S. and Klein, H. H. (2011) 'Preserved insulin secretion capacity and graft function of cryostored encapsulated rat islets', *Regul Pept,* 166(1-3), 135-8.

Schreiter, T., Marquitan, G., Darnell, M., Sowa, J. P., Bröcker-Preuss, M., Andersson, T. B., Baba, H. A., Furch, M., Arteel, G. E., Mathé, Z., Treckmann, J., Gerken, G., Gieseler, R. K. and Canbay, A. (2012) 'An ex vivo perfusion system emulating in vivo conditions in noncirrhotic and cirrhotic human liver', *J Pharmacol Exp Ther,* 342(3), 730-41.

Seifi, B., Kadkhodaee, M., Najafi, A. and Mahmoudi, A. (2014) 'Protection of liver as a remote organ after renal ischemia-reperfusion injury by renal ischemic postconditioning', *Int J Nephrol,* 2014, 120391.

Selzner, N., Boehnert, M. and Selzner, M. (2012) 'Preconditioning, postconditioning, and remote conditioning in solid organ transplantation: basic mechanisms and translational applications', *Transplant Rev (Orlando),* 26(2), 115-24.

Shen, H. C., Yeh, C. N., Chen, G. Y., Huang, S. F., Chen, C. Y., Chiu, Y. C. and Hu, Y. C. (2008) 'Sustained baculovirus-mediated expression in myogenic cells', *J Gene Med,* 10(11), 1190-7.

Sheridan, A. M. and Bonventre, J. V. (2001) 'Pathophysiology of ischemic acute renal failure', *Contrib Nephrol,* (132), 7-21.

Silva, D. G., Belini Junior, E., Carrocini, G. C., Torres, L. e. S., Ricci Júnior, O., Lobo, C. L., Bonini-Domingos, C. R. and de Almeida, E. A. (2013) 'Genetic and biochemical markers of hydroxyurea therapeutic response in sickle cell anemia', *BMC Med Genet,* 14, 108.

Smith, G. E., Summers, M. D. and Fraser, M. J. (1983) 'Production of human beta interferon in insect cells infected with a baculovirus expression vector', *Mol Cell Biol,* 3(12), 2156-65.

Steinman, H. M., Naik, V. R., Abernethy, J. L. and Hill, R. L. (1974) 'Bovine erythrocyte superoxide dismutase. Complete amino acid sequence', *J Biol Chem,* 249(22), 7326-38.

Stiegler, P., Sereinigg, M., Puntschart, A., Bradatsch, A., Seifert-Held, T., Wiederstein-Grasser, I., Leber, B., Stadelmeyer, E., Dandachi, N., Zelzer, S., Iberer, F. and

Stadlbauer, V. (2013) 'Oxidative stress and apoptosis in a pig model of brain death (BD) and living donation (LD)', *J Transl Med,* 11, 244.

Sugano, E., Tomita, H., Ishiguro, S., Abe, T. and Tamai, M. (2005) 'Establishment of effective methods for transducing genes into iris pigment epithelial cells by using adeno-associated virus type 2', *Invest Ophthalmol Vis Sci,* 46(9), 3341-8.

Sugano, M., Tsuchida, K., Hata, T. and Makino, N. (2005) 'RNA interference targeting SHP-1 attenuates myocardial infarction in rats', *FASEB J,* 19(14), 2054-6.

Summers, M. D. (2006) 'Milestones leading to the genetic engineering of baculoviruses as expression vector systems and viral pesticides', *Adv Virus Res,* 68, 3-73.

Summers, M. D. and Volkman, L. E. (1976) 'Comparison of biophysical and morphological properties of occluded and extracellular nonoccluded baculovirus from in vivo and in vitro host systems', *J Virol,* 17(3), 962-72.

Sun, X., Zhang, B., Hong, X., Zhang, X. and Kong, X. (2013) 'Histone deacetylase inhibitor, sodium butyrate, attenuates gentamicin-induced nephrotoxicity by increasing prohibitin protein expression in rats', *Eur J Pharmacol,* 707(1-3), 147-54.

Susa, D., Mitchell, J. R., Verweij, M., van de Ven, M., Roest, H., van den Engel, S., Bajema, I., Mangundap, K., Ijzermans, J. N., Hoeijmakers, J. H. and de Bruin, R. W. (2009) 'Congenital DNA repair deficiency results in protection against renal ischemia reperfusion injury in mice', *Aging Cell,* 8(2), 192-200.

Suzuki, T., Kobayashi, M., Isatsu, K., Nishihara, T., Aiuchi, T., Nakaya, K. and Hasegawa, K. (2004) 'Mechanisms involved in apoptosis of human macrophages induced by lipopolysaccharide from Actinobacillus actinomycetemcomitans in the presence of cycloheximide', *Infect Immun,* 72(4), 1856-65.

Swaney, W. P., Sorgi, F. L., Bahnson, A. B. and Barranger, J. A. (1997) 'The effect of cationic liposome pretreatment and centrifugation on retrovirus-mediated gene transfer', *Gene Ther,* 4(12), 1379-86.

Szeto, H. H., Liu, S., Soong, Y., Wu, D., Darrah, S. F., Cheng, F. Y., Zhao, Z., Ganger, M., Tow, C. Y. and Seshan, S. V. (2011) 'Mitochondria-targeted peptide accelerates ATP recovery and reduces ischemic kidney injury', *J Am Soc Nephrol,* 22(6), 1041-52.

Tanaka, T. and Takahara, S. (2010) '[Marginal - donor and recipient]', *Hinyokika Kiyo,* 56(8), 467-8.

Tang, X. C., Lu, H. R. and Ross, T. M. (2011) 'Baculovirus-produced influenza virus-like particles in mammalian cells protect mice from lethal influenza challenge', *Viral Immunol,* 24(4), 311-9.

Tani, H., Limn, C. K., Yap, C. C., Onishi, M., Nozaki, M., Nishimune, Y., Okahashi, N., Kitagawa, Y., Watanabe, R., Mochizuki, R., Moriishi, K. and Matsuura, Y. (2003) 'In vitro and in vivo gene delivery by recombinant baculoviruses', *J Virol,* 77(18), 9799-808.

Tani, H., Nishijima, M., Ushijima, H., Miyamura, T. and Matsuura, Y. (2001) 'Characterization of cell-surface determinants important for baculovirus infection', *Virology,* 279(1), 343-53.

Teixeira Neto, P. F., Gonçalves, R. P., Elias, D. B., de Araújo, C. P. and Magalhães, H. I. (2011) 'Analysis of oxidative status and biochemical parameters in adult patients with sickle cell anemia treated with hydroxyurea, Ceará, Brazil', *Rev Bras Hematol Hemoter,* 33(3), 207-10.

Temin, H. M. (1961) 'Mixed infection with two types of Rous sarcoma virus', *Virology,* 13, 158-63.

Tenenbaum, L., Hamdane, M., Pouzet, M., Avalosse, B., Stathopoulos, A., Jurysta, F., Rosenbaum, C., Hanemann, C. O., Levivier, M. and Velu, T. (1999) 'Cellular contaminants of adeno-associated virus vector stocks can enhance transduction', *Gene Ther,* 6(6), 1045-53.

Teng, C. Y., Chang, S. L., Tsai, M. F. and Wu, T. Y. (2013) 'A-synuclein and β-synuclein enhance secretion protein production in baculovirus expression vector system', *Appl Microbiol Biotechnol,* 97(9), 3875-84.

Thomas, R. and Sharifi, N. (2012) 'SOD mimetics: a novel class of androgen receptor inhibitors that suppresses castration-resistant growth of prostate cancer', *Mol Cancer Ther,* 11(1), 87-97.

Thomas, S. and Egée, S. (1998) 'Fish red blood cells: characteristics and physiological role of the membrane ion transporters', *Comp Biochem Physiol A Mol Integr Physiol,* 119(1), 79-86.

Tjia, S. T., zu Altenschildesche, G. M. and Doerfler, W. (1983) 'Autographa californica nuclear polyhedrosis virus (AcNPV) DNA does not persist in mass cultures of mammalian cells', *Virology,* 125(1), 107-17.

Toledo-Pereyra LH. (2010) 'Heart transplantation.', *J Invest Surg.,* 23(5), 1-5.

Trachootham, D., Lu, W., Ogasawara, M. A., Nilsa, R. D. and Huang, P. (2008) 'Redox regulation of cell survival', *Antioxid Redox Signal,* 10(8), 1343-74.

Transfiguracion, J., Jorio, H., Meghrous, J., Jacob, D. and Kamen, A. (2007) 'High yield purification of functional baculovirus vectors by size exclusion chromatography', *J Virol Methods,* 142(1-2), 21-8.

Transfiguracion, J., Mena, J. A., Aucoin, M. G. and Kamen, A. A. (2011) 'Development and validation of a HPLC method for the quantification of baculovirus particles', *J Chromatogr B Analyt Technol Biomed Life Sci,* 879(1), 61-8.

Triplett, J. W., Herring, B. P. and Pavalko, F. M. (2005) 'Adenoviral transgene expression enhanced by cotreatment with etoposide in cultured cells', *Biotechniques,* 39(6), 826, 828, 830, passim.

Usui, S., Oveson, B. C., Iwase, T., Lu, L., Lee, S. Y., Jo, Y. J., Wu, Z., Choi, E. Y., Samulski, R. J. and Campochiaro, P. A. (2011) 'Overexpression of SOD in retina: need for increase in H2O2-detoxifying enzyme in same cellular compartment', *Free Radic Biol Med,* 51(7), 1347-54.

Vail, P. V., Jay, D. L. and Hunter, D. K. (1971) 'Cross infectivity of nuclear polyhedrosis virus isolated from the alfalfa looper,*Autographa california.* ', *4th. Int. Coll. Insect Pathol.*, 297–304.

van der Wouden, E. A., Sandovici, M., Henning, R. H., de Zeeuw, D. and Deelman, L. E. (2004) 'Approaches and methods in gene therapy for kidney disease', *J Pharmacol Toxicol Methods,* 50(1), 13-24.

van Dorp, W. T., van Wieringen, P. A., Marselis-Jonges, E., Bruggeman, C. A., Daha, M. R., van Es, L. A. and van der Woude, F. (1993) 'Cytomegalovirus directly enhances MHC class I and intercellular adhesion molecule-1 expression on cultured proximal tubular epithelial cells', *Transplantation,* 55(6), 1367-71.

VandenDriessche, T., Thorrez, L., Naldini, L., Follenzi, A., Moons, L., Berneman, Z., Collen, D. and Chuah, M. K. (2002) 'Lentiviral vectors containing the human immunodeficiency virus type-1 central polypurine tract can efficiently transduce nondividing hepatocytes and antigen-presenting cells in vivo', *Blood,* 100(3), 813-22.

Vaughn, J. L., Goodwin, R. H., Tompkins, G. J. and McCawley, P. (1977) 'The establishment of two cell lines from the insect Spodoptera frugiperda (Lepidoptera; Noctuidae)', *In Vitro,* 13(4), 213-7.

Vaziri, N., Thuillier, R., Favreau, F. D., Eugene, M., Milin, S., Chatauret, N. P., Hauet, T. and Barrou, B. (2011) 'Analysis of machine perfusion benefits in kidney grafts: a preclinical study', *J Transl Med,* 9, 15.

Versteilen, A. M., Di Maggio, F., Leemreis, J. R., Groeneveld, A. B., Musters, R. J. and Sipkema, P. (2004) 'Molecular mechanisms of acute renal failure following ischemia/reperfusion', *Int J Artif Organs,* 27(12), 1019-29.

Vicente, T., Peixoto, C., Carrondo, M. J. and Alves, P. M. (2009) 'Purification of recombinant baculoviruses for gene therapy using membrane processes', *Gene Ther,* 16(6), 766-75.

Volkman, L. E. (1997) 'Nucleopolyhedrovirus interactions with their insect hosts.', *Adv Virus Res,* 48, 313-48.

Volkman, L. E. and Goldsmith, P. A. (1983) 'In Vitro Survey of Autographa californica Nuclear Polyhedrosis Virus Interaction with Nontarget Vertebrate Host Cells.', *Appl Environ Microbiol,* 45(3), 1085-93.

Wagener, O. E., Lieske, J. C. and Toback, F. G. (1995) 'Molecular and cell biology of acute renal failure: new therapeutic strategies', *New Horiz,* 3(4), 634-49.

Wang, P., Hammer, D. A. and Granados, R. R. (1997) 'Binding and fusion of Autographa californica nucleopolyhedrovirus to cultured insect cells', *J Gen Virol,* 78 (Pt 12), 3081-9.

Wang, S. and Balasundaram, G. (2010) 'Potential cancer gene therapy by baculoviral transduction', *Curr Gene Ther,* 10(3), 214-25.

Wang, Y., Jiang, Y. F., Huang, Q. F., Ge, G. L. and Cui, W. (2010) 'Neuroprotective effects of salvianolic acid B against oxygen-glucose deprivation/reperfusion damage in primary rat cortical neurons', *Chin Med J (Engl),* 123(24), 3612-9.

Warrell, R. P., He, L. Z., Richon, V., Calleja, E. and Pandolfi, P. P. (1998) 'Therapeutic targeting of transcription in acute promyelocytic leukemia by use of an inhibitor of histone deacetylase', *J Natl Cancer Inst,* 90(21), 1621-5.

Warrens, A. N., Birch, R., Collett, D., Daraktchiev, M., Dark, J. H., Galea, G., Gronow, K., Neuberger, J., Hilton, D., Whittle, I. R., Watson, C. J. and Advisory Committee on the

Safety of Blood, T. s. a. O., U. K. (2012) 'Advising potential recipients on the use of organs from donors with primary central nervous system tumors', *Transplantation,* 93(4), 348-53.

Washburn, J. O., Chan, E. Y., Volkman, L. E., Aumiller, J. J. and Jarvis, D. L. (2003) 'Early synthesis of budded virus envelope fusion protein GP64 enhances Autographa californica multicapsid nucleopolyhedrovirus virulence in orally infected Heliothis virescens', *J Virol,* 77(1), 280-90.

Watson, C. J. and Dark, J. H. (2012) 'Organ transplantation: historical perspective and current practice', *Br J Anaesth,* 108 Suppl 1, i29-42.

Watson, J. D. and Crick, F. H. (1953) 'Molecular structure of nucleic acids; a structure for deoxyribose nucleic acid', *Nature,* 171(4356), 737-8.

Weber, W., Weber, E., Geisse, S. and Memmert, K. (2002) 'Optimisation of protein expression and establishment of the Wave Bioreactor for Baculovirus/insect cell culture', *Cytotechnology,* 38(1-3), 77-85.

Wei, N., Yu, S. P., Gu, X., Taylor, T. M., Song, D., Liu, X. F. and Wei, L. (2013) 'Delayed intranasal delivery of hypoxic-preconditioned bone marrow mesenchymal stem cells enhanced cell homing and therapeutic benefits after ischemic stroke in mice', *Cell Transplant,* 22(6), 977-91.

Weinberg, J. M. (1991) 'The cell biology of ischemic renal injury', *Kidney Int,* 39(3), 476-500.

Weiss, D. J., Liggitt, D. and Clark, J. G. (1999) 'Histochemical discrimination of endogenous mammalian beta-galactosidase activity from that resulting from lac-Z gene expression', *Histochem J,* 31(4), 231-6.

Weissig, V. (2003) 'Mitochondrial-targeted drug and DNA delivery', *Crit Rev Ther Drug Carrier Syst,* 20(1), 1-62.

Wheeler, M. D., Katuna, M., Smutney, O. M., Froh, M., Dikalova, A., Mason, R. P., Samulski, R. J. and Thurman, R. G. (2001) 'Comparison of the effect of adenoviral delivery of three superoxide dismutase genes against hepatic ischemia-reperfusion injury', *Hum Gene Ther,* 12(18), 2167-77.

Whitt, M. A. and Manning, J. S. (1988) 'A phosphorylated 34-kDa protein and a subpopulation of polyhedrin are thiol linked to the carbohydrate layer surrounding a baculovirus occlusion body', *Virology,* 163(1), 33-42.

Whittaker, M. M. and Whittaker, J. W. (1998) 'A glutamate bridge is essential for dimer stability and metal selectivity in manganese superoxide dismutase', *J Biol Chem,* 273(35), 22188-93.

Wilkie, G. E., Stockdale, H. and Pirt, S. V. (1980) 'Chemically-defined media for production of insect cells and viruses in vitro', *Dev Biol Stand,* 46, 29-37.

Wirth, T., Parker, N. and Ylä-Herttuala, S. (2013) 'History of gene therapy', *Gene,* 525(2), 162-9.

Wirth, T., Samaranayake, H., Pikkarainen, J., Määttä, A. M. and Ylä-Herttuala, S. (2009) 'Clinical trials for glioblastoma multiforme using adenoviral vectors', *Curr Opin Mol Ther,* 11(5), 485-92.

Wolff, J. A. and Budker, V. (2005) 'The mechanism of naked DNA uptake and expression', *Adv Genet,* 54, 3-20.

Wright, S. H. (2005) 'Role of organic cation transporters in the renal handling of therapeutic agents and xenobiotics', *Toxicol Appl Pharmacol,* 204(3), 309-19.

Wu, C., Soh, K. Y. and Wang, S. (2007) 'Ion-exchange membrane chromatography method for rapid and efficient purification of recombinant baculovirus and baculovirus gp64 protein', *Hum Gene Ther,* 18(7), 665-72.

Wu, T. Y., Chen, Y. J., Teng, C. Y., Chen, W. S. and Villaflores, O. (2012) 'A bi-cistronic baculovirus expression vector for improved recombinant protein production', *Bioeng Bugs,* 3(2), 129-32.

Xie, J. and Guo, Q. (2006) 'Apoptosis antagonizing transcription factor protects renal tubule cells against oxidative damage and apoptosis induced by ischemia-reperfusion', *J Am Soc Nephrol,* 17(12), 3336-46.

Xie, J. and Guo, Q. (2007) 'Par-4 is a novel mediator of renal tubule cell death in models of ischemia-reperfusion injury', *Am J Physiol Renal Physiol,* 292(1), F107-15.

Xue, F., Wang, G., Pang, Z., Liu, C. and Liang, T. (2008) 'Protective effect of glutathione against liver warm ischemia-reperfusion injury in rats is associated with regulation of P-selectin and neutrophil infiltration', *Anat Rec (Hoboken),* 291(8), 1016-22.

Yamasowa, H., Shimizu, S., Inoue, T., Takaoka, M. and Matsumura, Y. (2005) 'Endothelial nitric oxide contributes to the renal protective effects of ischemic preconditioning', *J Pharmacol Exp Ther,* 312(1), 153-9.

Yan, Y., Du, J., Chen, T., Yi, M., Li, M., Wang, S., Li, C. M. and Hong, Y. (2009) 'Establishment of medakafish as a model for stem cell-based gene therapy: efficient gene delivery and potential chromosomal integration by baculoviral vectors', *Exp Cell Res,* 315(13), 2322-31.

Yang, B., Jain, S., Pawluczyk, I. Z., Imtiaz, S., Bowley, L., Ashra, S. Y. and Nicholson, M. L. (2005) 'Inflammation and caspase activation in long-term renal ischemia/reperfusion injury and immunosuppression in rats', *Kidney Int,* 68(5), 2050-67.

Yang, C. C., Lin, L. C., Wu, M. S., Chien, C. T. and Lai, M. K. (2009) 'Repetitive hypoxic preconditioning attenuates renal ischemia/reperfusion induced oxidative injury via upregulating HIF-1 alpha-dependent bcl-2 signaling', *Transplantation,* 88(11), 1251-60.

Yang, L., Humphreys, B. D. and Bonventre, J. V. (2011) 'Pathophysiology of acute kidney injury to chronic kidney disease: maladaptive repair', *Contrib Nephrol,* 174, 149-55.

Yang, Y., Lo, S. L., Yang, J., Goh, S. S., Wu, C., Feng, S. S. and Wang, S. (2009) 'Polyethylenimine coating to produce serum-resistant baculoviral vectors for in vivo gene delivery', *Biomaterials,* 30(29), 5767-74.

Yang, Y. W. and Hsieh, Y. C. (2001) 'Protamine sulfate enhances the transduction efficiency of recombinant adeno-associated virus-mediated gene delivery', *Pharm Res,* 18(7), 922-7.

Yard, B. A., Daha, M. R., Kooymans-Couthino, M., Bruijn, J. A., Paape, M. E., Schrama, E., van Es, L. A. and van der Woude, F. J. (1992) 'IL-1 alpha stimulated TNF alpha production by cultured human proximal tubular epithelial cells', *Kidney Int,* 42(2), 383-9.

Yassin, M. M., Harkin, D. W., Barros D'Sa, A. A., Halliday, M. I. and Rowlands, B. J. (2002) 'Lower limb ischemia-reperfusion injury triggers a systemic inflammatory response and multiple organ dysfunction', *World J Surg,* 26(1), 115-21.

Yeh, T. S., Fang, Y. H., Lu, C. H., Chiu, S. C., Yeh, C. L., Yen, T. C., Parfyonova, Y. and Hu, Y. C. (2014) 'Baculovirus-transduced, VEGF-expressing adipose-derived stem cell sheet for the treatment of myocardium infarction', *Biomaterials,* 35(1), 174-84.

Yin, H. Y., Zhou, X., Wu, H. F., Li, B. and Zhang, Y. F. (2010) 'Baculovirus vector-mediated transfer of NIS gene into colon tumor cells for radionuclide therapy', *World J Gastroenterol,* 16(42), 5367-74.

Yin, M., Wheeler, M. D., Connor, H. D., Zhong, Z., Bunzendahl, H., Dikalova, A., Samulski, R. J., Schoonhoven, R., Mason, R. P., Swenberg, J. A. and Thurman, R. G. (2001) 'Cu/Zn-superoxide dismutase gene attenuates ischemia-reperfusion injury in the rat kidney', *J Am Soc Nephrol,* 12(12), 2691-700.

Ylä-Herttuala, S. (2012) 'Endgame: glybera finally recommended for approval as the first gene therapy drug in the European union', *Mol Ther,* 20(10), 1831-2.

Yost, F. J. and Fridovich, I. (1973) 'An iron-containing superoxide dismutase from Escherichia coli', *J Biol Chem,* 248(14), 4905-8.

Yu, W. and Fang, H. (2007) 'Clinical trials with oncolytic adenovirus in China', *Curr Cancer Drug Targets,* 7(2), 141-8.

Yuan, H. J., Zhu, X. H., Luo, Q., Wu, Y. N., Kang, Y., Jiao, J. J., Gao, W. Z., Liu, Y. X. and Lou, J. S. (2012) 'Noninvasive delayed limb ischemic preconditioning in rats increases antioxidant activities in cerebral tissue during severe ischemia-reperfusion injury', *J Surg Res,* 174(1), 176-83.

Zanetti, M., Sato, J., Katusic, Z. S. and O'Brien, T. (2001) 'Gene transfer of superoxide dismutase isoforms reverses endothelial dysfunction in diabetic rabbit aorta', *Am J Physiol Heart Circ Physiol,* 280(6), H2516-23.

Zeng, J., Du, J., Lin, J., Bak, X. Y., Wu, C. and Wang, S. (2009) 'High-efficiency transient transduction of human embryonic stem cell-derived neurons with baculoviral vectors', *Mol Ther,* 17(9), 1585-93.

Zeng, J., Du, J., Zhao, Y., Palanisamy, N. and Wang, S. (2007) 'Baculoviral vector-mediated transient and stable transgene expression in human embryonic stem cells', *Stem Cells,* 25(4), 1055-61.

Zeng, J., Shahbazi, M., Wu, C., Toh, H. C. and Wang, S. (2012) 'Enhancing immunostimulatory function of human embryonic stem cell-derived dendritic cells by CD1d overexpression', *J Immunol,* 188(9), 4297-304.

Zhang, S., Wu, J., Wu, X., Xu, P., Tian, Y., Yi, M., Liu, X., Dong, X., Wolf, F., Li, C. and Huang, Q. (2012) 'Enhancement of rAAV2-mediated transgene expression in retina cells in vitro and in vivo by coadministration of low-dose chemotherapeutic drugs', *Invest Ophthalmol Vis Sci,* 53(6), 2675-84.

Zhu, X., Liu, B., Zhou, S., Chen, Y. R., Deng, Y., Zweier, J. L. and He, G. (2007) 'Ischemic preconditioning prevents in vivo hyperoxygenation in postischemic myocardium with preservation of mitochondrial oxygen consumption', *Am J Physiol Heart Circ Physiol,* 293(3), H1442-50.